VOLUME 37 SECOND SERIES NUMBER 8

APR 2

THE PHYSICAL REVIEW

A JOURNAL OF EXPERIMENTAL AND THEORETICAL PHYSICS

CONDUCTED BY

THE AMERICAN PHYSICAL SOCIETY

BOARD OF EDITORS

Managing Editor, JOHN T. TATE, University of Minnesota, Minneapolis
Assistant Editor, J. W. BUCHTA, University of Minnesota, Minneapolis
E. U. CONDON, C. J. DAVISSON, F. K. RICHTMYER, K. F. HERZFELD, A. W. HULL, F. W. LOOMIS, A. J. DEMPSTER, DAVID M. DENNISON, J. C. SLATER

APRIL 15, 1931

Diffraction of Hydrogen Atoms — THOMAS H. JOHNSON 847
Scattering of X-Rays from Gases — E. O. WOLLAN 862
Interaction of X-Rays with Bound Electrons — AUSTIN J. O'LEARY 873
Photoelectric Properties of Composite Surfaces at Various Temperatures and Potentials — DIMITER RAMADANOFF 884
Energy of Dissociation of Mercury Molecules — J. GIBSON WINANS 897
Properties of Some Zinc, Cadmium, and Mercury Bands — J. GIBSON WINANS 902
Perturbations and Predissociation in the S_2 Band Spectrum — ANDREW CHRISTY AND S. MEIRING NAUDÉ 903
Note on Modes of Spectograph Slit Irradiation — DONALD C. STOCKBARGER AND LAURENCE BURNS 920
Masses of O^{17} — HAROLD C. UREY 923
Propagation of Large Barkhausen Discontinuities — K. J. SIXTUS AND L. TONKS 930
Fermi-Dirac Statistics Applied to the Problem of Space Charge in Thermionic Emission — RUSSELL S. BARTLETT 959
Angular Distribution of Electrons Scattered by Mercury Vapor — J. M. PEARSON AND W. N. ARNQUIST 970
Electronic Velocities in the Positive Column of High Frequency Discharges — EGON HIEDEMANN 978
Electrical State of the Sun — ROSS GUNN 983
Surface Tension of Mercury — MARIE KERNAGHAN 990
Corrected Values for the Coefficient of Recombination of Gaseous Ions — OVERTON LUHR AND NORRIS E. BRADBURY 998
Letters to the Editor — 1001

Attempt to Measure the Energy of the Cosmic Electrons by Magnetic Deflection, *L. M. Mott-Smith*—1001; Transmission of Gases from 20 to 33a, *John Strong*—1003; Preliminary Report of the Application of the Photoelectric Cell to the Reading of Minima in a Magneto-Optic Method of Analysis, *Fred Allison, J. H. Christensen, and George V. Waldo*—1003; New Source of Active Nitrogen, *Joseph Kaplan*—1004; Zeeman Effect and Uncoupling Phenomena in Helium Bands, *John S. Millis*—1005; Alleged Production of Adsorbed Films on Tungsten by Active Nitrogen, *Irving Langmuir*—1006; Partial Absorption of X-Rays, *D. Coolidge and C. D. Cooksey*—1006; Absorption Spectrum of Bromine, *Waldon G. Brown*—1007.

Book Reviews — 1009

PROCEEDINGS OF THE AMERICAN PHYSICAL SOCIETY

New York Meeting, February 26 to 28, 1931; Minutes and Abstracts 1–49; Author Index — 1010

PUBLISHED BY THE AMERICAN PHYSICAL SOCIETY
EDITORIAL OFFICE: MINNEAPOLIS, MINN.

THE AMERICAN PHYSICAL SOCIETY

OFFICERS OF THE SOCIETY

President:	W. F. G. Swann	Bartol Research Foundation, Philadelphia, Pa.
Vice-President:	Paul D. Foote	The Gulf Companies, Pittsburgh, Pa.
Secretary:	W. L. Severinghaus	Columbia University, New York City
Treasurer:	G. B. Pegram	Columbia University, New York City
Editor:	John T. Tate	University of Minnesota, Minneapolis, Minn.
Local Secretary for the Pacific Coast:	L. B. Loeb	University of California, Berkeley, Calif.

THE PHYSICAL REVIEW

Published by the American Physical Society. Executive office: University of Minnesota, Minneapolis, Minn. Two volumes annually, twelve issues per volume.

First series. From July 1, 1893, to January 1, 1913, the Review was conducted by Edward L. Nicholas, Ernest Merritt and Frederick Bedell, with the financial support of Cornell University. The first four volumes were issued annually; subsequent volumes, semi-annually; thirty-five volumes in all.

Second series. On January 1, 1913, the Review was transferred to the American Physical Society as announced on the first page of the new series which was then begun. Since then it has been conducted by a Board of Editors elected by the Society. Semi-annual volumes begin in January and July. Since July 1, 1929, the Review has been issued twice a month.

Contributors are referred to page 2 of the advertisements for further information.

Annual subscription, throughout the Postal Union, $12.00 in advance.

General index, 1893-1920, $4.00, in advance.

Back Volumes, $9.00 per volume; Back Numbers, $1.50 per copy for issues prior to July 1, 1929 (Vols. 1-33), $.75 per copy for issues subsequent thereto. Postage is free if remittance accompanies order; otherwise postage is extra. No bound volumes can be supplied. The Review offers to purchase a limited number of First Series, Vol. 1, No. 1 (at $2.00 each); Second Series, Vol. 7, No. 1, January 1916; Vol. 7, No. 2, February 1916; Vol. 7, No. 4, April 1916; and Vol. 7, No. 5, May 1916 (at $2.00 each).

Advertisements. Rates will be supplied by the Editor on request. Copy for each number must be received at Minneapolis two weeks prior to the dates of issue; old copy is used until new copy is received. Send electrotypes direct to the printers, George Banta Publishing Co., Menasha, Wis.

Discount of ten per cent is allowed to members of the American Physical Society on purchase of back numbers.

Changes of Address and Complaints of failure to receive the Review, in the case of members of the Physical Society, should be addressed to the Treasurer; in the case of other subscribers, to the Editor. New copies can be sent free in response to complaint of non-delivery only if notice of non-delivery is received within three months of date of issue.

Editorial Correspondence should be addressed to the Physical Review, University of Minnesota, Minneapolis, Minn.

Entered at the post office at Menasha, Wis., as second class matter.
Acceptance for mailing at special rate of postage provided for in section 1103, Act of October 3, 1917, authorized September 6, 1926.

Second Series *April 15, 1931* *Vol. 37, No. 8*

THE
PHYSICAL REVIEW

DIFFRACTION OF HYDROGEN ATOMS

By Thomas H. Johnson
Bartol Research Foundation of the Franklin Institute
(Received March 11, 1931)

Abstract

Diffraction patterns of a beam of hydrogen atoms reflected from LiF.—Improved technique in the photography of the diffraction patterns produced by the reflection of a beam of hydrogen atoms from a crystal of lithium fluoride has resulted in more complete patterns than those previously described by the author. The observed patterns are those expected on the assumptions (1) that the incident beam contains the distribution of wave-lengths derived from the Maxwellian velocity distribution by the use of the de Broglie relation between wave-length and velocity, and (2) that the surface of the crystal constitutes an impenetrable square array of scattering points with the arrangement and spacing of the ions of a single type as known from x-ray measurements.

Wave-length distribution.—The intensity distributions in the diffraction patterns were measured, and were found to have maxima at positions in good agreement with those expected on the basis of the above assumptions.

Interpretation of relative intensities in the different orders.—The relative intensities in the observed orders are discussed in relation to the scattering coefficients of the two types of ions, and in relation to the dependence of the scattering coefficient on azimuth.

Diffraction by the secondary structure of the crystal.—A secondary spectrum is described, arising from a lattice of wide spacing the lines of which are parallel to the 100 cleaved edges of the crystal face.

IT HAS been well established for some time that the quantum mechanics correctly describes the motion of a free or a bound electron. Its success in the interpretation of band spectra has also shown that the motions of atomic nuclei within the molecule could be included in the theory, and because of this, it appeared almost certain that the new mechanics would be found correct in its description of the free motion of atoms and molecules. The comparatively recent experiments of Estermann and Stern[1] and of the author[2] were not disappointing in this regard for they have demonstrated that atoms and molecules of low atomic weight behave as predicted, in that they exhibit the properties of a wave radiation of wave-length $\lambda = h/mv$ in the plane-grating diffraction phenomena which appear when these are reflected from the surface of a crystal. These experiments are of interest not only because of their confirmation of the predictions of quantum mechanics, but also because

[1] Estermann and Stern, Zeits. f. Physik **61**, 95 (1930). O. Stern, Die Naturwissenschaften **17**, 391 (1929).

[2] T. H. Johnson, Phys. Rev. **35**, 1299 (1930).

they introduce the possibility of applying atom diffraction to investigations of the atomic constitution of surfaces. A beam of atomic hydrogen, for example, with ordinary thermal velocities, has a range of wave-lengths of the right magnitude for this purpose, centering around 1A, and the complete absence of penetration of these waves will insure that the effects observed arise entirely from the outermost atomic layer.

The first experiments demonstrating the diffraction of hydrogen atoms when reflected from a crystal of lithium fluoride were described in some detail in the Journal of the Franklin Institute.[3] The diffraction patterns which were photographed in that earlier work were of low intensity and they showed only a part of the complete structure which should have been produced by the array of ions on the surface of the crystal. Because of the low intensity in these earlier patterns, satisfactory intensity measurements were impossible, and only a rough comparison could be made between the observed distribution of wave-lengths and that predicted from the Maxwellian velocity distribution and the de Broglie relation between velocity and wave-length.

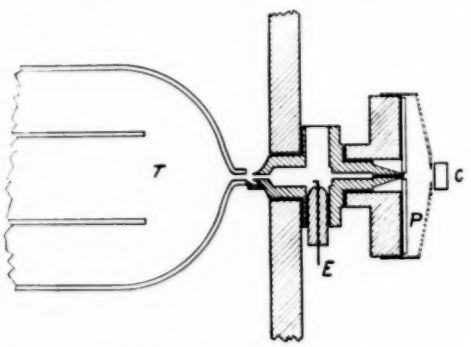

Fig. 1. Collimating system for normal incidence.

Recent improvements in the technique of obtaining photographic records of the diffraction patterns have overcome in large measure the deficiencies of the earlier work, and patterns of far greater intensity have been photographed which show all of the expected first-order branches. The intensity is now sufficient for the purposes of making photometric measurements of the wave-length distribution, and it has been possible to make some rough estimates of the relative intensities in the principle branches. In addition, some new features have been recorded which throw light upon the secondary structure of the crystal.

With the exception of a few modifications, the apparatus and the experimental procedure were the same as in the earlier work. A sharply defined beam of hydrogen atoms had its origin in a chamber T, Fig. 1, in which molecular hydrogen was dissociated by an electric discharge, and it was collimated by a series of tubes with suitable pumping systems for eliminating the excess gas. This beam was reflected from a freshly cleaved surface of a crystal (C) of lithium fluoride, and the reflected atoms were recorded on a plate (P)

[3] T. H. Johnson, Jour. Frank. Inst. **210**, 135 (1930).

coated with molybdenum oxide After an exposure the patterns recorded on the molybdenum oxide plate were made permanent by photographing in the usual way.

Since it is believed that atom diffraction may prove useful in studying the structure of surfaces a discussion of some of the technical features will be included for its interest to other investigators in this field.

Formation of the Beam

In designing a collimating system for the production of a molecular beam for use in diffraction experiments there are two requirements; the beam should be intense and it should be sufficiently sharp to resolve the effects sought. In the limit these demands are conflicting in that an increase in the sharpness of the beam results in a decrease in its intensity, and *vice versa*. Over the range of source chamber pressures which is of interest, the intensity of the beam, as regards its dependence on the configuration of the collimating system, is proportional to the area of the source aperture and inversely proportional to the square of the distance from the source to the point of detec-

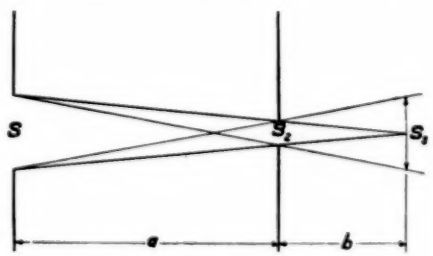

Fig. 2.

tion, and it is independent of the position and size of the collimating aperture as long as the point of detection is not occluded from any part of the source aperture. The sharpest beam, for a given intensity, may be obtained by making the collimating aperture a section of the cone of which the source aperture is the base, and the point of detection is the vertex. The linear dimensions (S_2, S_2') of the collimating aperture are therefore related to the corresponding dimensions (S_1, S_1') of the source aperture by

$$S_2 = S_1 b/(a + b), \tag{1}$$

where a and b are the distances indicated in Fig. 2. The corresponding dimensions of the cross-section of the beam at the point of detection are given by

$$S_3 = 2S_1 b/a. \tag{2}$$

Similar expressions also hold for the S' dimensions.

If a perfect reflector is placed a negligible distance behind the collimating aperture two reflected beams separated by an angle $\Delta\theta$ will be just resolved if their linear separation is equal to the beam width, i.e.

$$b\Delta\theta = 2S_1 b/a. \tag{3}$$

The resolving power of the collimating system, in the plane determined by S and the beam, defined as

$$R = 1/\Delta\theta = a/2S_1, \tag{4}$$

is independent of b and would remain unaffected by shortening this distance as much as permitted by convenience of construction.

The intensity I of the beam depends upon these dimensions of the collimating system in the manner

$$I \sim \frac{S_1 S_1'}{(a+b)^2} = \frac{aS_1'}{2R(a+b)^2} = \frac{a^2}{4RR'(a+b)^2}. \tag{5a, b}$$

From (5a) it is seen that, with fixed resolving power in one direction and fixed dimension S_1' normal to this direction, I has its greatest value, as regards its dependence on b when $b=0$, and, as regards its dependence on a, when $a=b$. If the resolving power is to be fixed in two dimensions, as, for example, would be the case with circular beams, (5b) shows that the intensity undergoes no variation with changes of the size of the collimating system, but it is inversely proportional to RR'.

Under the first of these conditions the greatest intensity is obtained with the collimating system as short as possible and the sizes of the apertures determined by (4) and (1) to yield the required resolving power.

The variation of beam-intensity with source-tube pressure is the next point to consider. The principles involved are not as clear in the case of atomic hydrogen beams as with other gases, for the degree of dissociation in the discharge tube depends, among other things, upon the pressure. With an incomplete understanding of discharge tube phenomena, considerations of this kind will be omitted and only the usual elements of the kinetic theory of gases will be taken into account.

On this basis the number of atoms leaving the source aperture in the direction of the beam is proportional to the pressure in the source chamber over the range of pressures for which "molecular flow" subsists. This number is diminished by collisions over the path a', between the source and the entrance to the collimating aperture, by the factor $e^{-a'/L}$ where L is the mean free path in this region. Since the speed of the diffusion pump which is used to eliminate the excess gas from the region between the first two apertures is approximately independent of the pressure, a constant ratio exists between the pressure within the source chamber (p) and that in the intermediate region, and L is inversely proportional to p. The intensity of the beam then varies with the pressure in the source chamber in the manner

$$I = Ape^{-p/p_0} \tag{6}$$

in which the constant p_0 is the pressure in the source chamber for which the intensity of the beam is a maximum. An expression of this form is in agreement with the observations on beam intensities in these experiments as well as with other published data, and with the apparatus used in these experi-

ments p_0 was found to be 0.3 mm. Corresponding to p_0, the intensity of the beam, from (6), is

$$I_0 = A p_0/e. \tag{7}$$

From the above considerations it may be seen that p_0 is proportional to the resistance of the source aperture, to the speed of the pumping system operating between the source and first collimating aperture, and inversely proportional to the path a' of the beam in this region, while the constant A is proportional to the ratio of the number of atoms which have the direction of the beam to the total emission from the source, and inversely proportional to the resistance of the source aperture. To realize a large value of I_0, a high speed pump and large connecting tubes were used at the first stage, the path a' was made as short as possible by the use of an auxiliary collimating tube (Fig. 1), and the source aperture was tubular in shape to produce a favorable directional distribution of the emitted atoms.

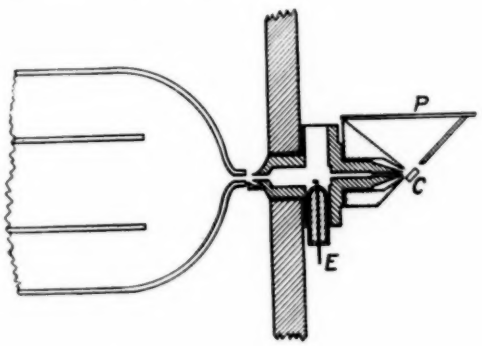

Fig. 3. Collimating system for 45° incidence.

Insofar as the directional distribution of the atoms emerging from the source aperture is unaffected by changes in its dimensions, the resolving power can be increased without affecting the intensity by diminishing the dimensions of the source aperture and simultaneously increasing the pressure in the source chamber so that the total number of atoms which emerge from the source aperture remains unchanged. A change of this character should leave the number of collisions in the intermediate chamber unaffected, for there the free path depends only on the rate at which gas is flowing in from the source chamber. This consideration therefore leads to the conclusion that the intensity can be increased, with fixed resolving power in *two* dimensions, by diminishing the size of the collimating system and simultaneously increasing the pressure in the source tube.

The collimating systems (Figs. 1 and 3) used in these experiments were constructed along the lines of these principles except that, in the arrangement for normal incidence, it was inconvenient to place the crystal directly in front of the last collimating aperture. The important dimensions are included in the following table.

Diameter of source tube	0.65 mm
Length of source tube	1.3 mm
Diameter of first collimating tube	0.67 mm
Diameter of second collimating tube	0.18 mm
Distance (a') from source tube to first collimating tube	1.0 mm
Distance (a) from source tube to far end of second collimating tube	24 mm
Distance (b) from end of second collimating tube to plate by way of specular reflection from the crystal at normal incidence	9 mm
Distance (b) for 45° incidence	10.5 mm

Elimination of High Energy Ions from the Atom Beam

One of the principal obstacles which stood in the way of the recording of intense patterns in the earlier work was the disintegration of the crystal surface by ion bombardment. Ions diffusing from the discharge chamber were

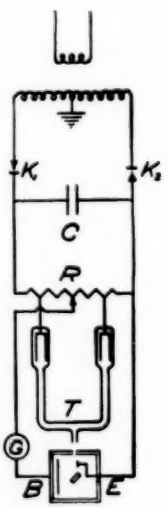

Fig. 4. Electrical connections.

subjected to a potential fall of the order of 5,000 volts between the center of the discharge and the observation chamber and some of these entered the beam and bombarded the crystal. The importance of their effect may be realized from the fact that, if unimpeded, the ion bombardment was sufficient to disintegrate the surface of the crystal in less than one minute to the extent of putting a stop to the regular reflection of atoms. The introduction of an electrode E (Figs. 4 & 1) to sweep the ions from the beam, materially improved the situation and exposures of three hours were feasible. There remained, however, a smaller number of neutral atoms of high energy in the beam which were formed in the first collimating tube by the neutralization of ions and these were not eliminated in this way. In the latest work, therefore, two additional precautions were taken. (1) The potential of the observation chamber was adjusted to be approximately the same as that of the center of

the discharge tube, so that ions diffusing from the source tube were accelerated as little as possible. (2) The remaining field between the center of the discharge and the entrance to the first collimating tube was made asymmetrical so that the ions were accelerated out of the line of the beam. The result of these precautions has been an almost complete elimination of the effects of bombardment with a resulting increase in the possible time of exposures to 24 hours or longer and a corresponding increase in the intensity of the patterns.

Fig. 4 is a diagram of the electrical circuit which was used to operate the discharge. A d.c. source of potential was supplied by a transformer and two kenetrons connected for half-wave rectification. This method of connecting the kenetrons had the advantage that the potential of the observation box, when adjusted to equal that of the center of the discharge, was close to the ground potential, and no trouble was experienced with leakage currents although the design of the apparatus made it inconvenient to insulate the box to withstand high voltages. To reduce the fluctuation of potential which took place during the cycle of alterations of the primary e.m.f., a condenser (C) having a capacity of 0.08 mf was used. A water resistance (R) served as a convenient potential divider and ballast resistance for the discharge. This was constructed of a series of four interconnected glass U-tubes, each 1.5 meters in length and 5 mm in diameter through which tap water was continuously circulated. This resistance could be varied in any of its parts by the insertion of wires into the arms of the U's, and it was adjusted so that no current was registered through the galvanometer (G).

General Darkening of the Detecting Plate

In the recording of faint patterns requiring long exposures it was necessary to exercise care to avoid a general over-all darkening of the molybdenum oxide detecting plate. A darkening of this character might have been produced by any one of three causes. (A) Atomic hydrogen, dissociated in the source chamber, might have been diffusely emitted from the collimating tube after scattering from its walls, and these might have reached the detecting plate either directly or after other reflections in the observation chamber. (B) Atomic hydrogen might have been formed in the observation chamber itself by electrons which were emitted either photoelectrically from the walls of the observation chamber or thermionically from the crystal holder and its heating unit, and which attained high velocities in the fields which surrounded the electrode E and its lead wire. (C) The most important cause of over-all darkening was the reduction of the molybdenum oxide by molecular hydrogen. This reaction can take place only if the molybdenum oxide is heated, but unless precautions were taken, the radiant heat from the crystal holder at the temperature used for degassing the surface of the crystal was sufficient to cause trouble.

Unquestionably some trouble had been experienced from cause (A) but this was rendered negligible by plating the inside walls of the collimating tubes with platinum black so that scattered atomic hydrogen was adsorbed until recombination to molecular hydrogen took place. The effects of (B) and

(C) were almost eliminated by protecting the detecting plate with a metal shield which completely surrounded it except for a small opening close to the crystal through which the reflected atoms entered. (See Figs. 1 and 3.) The inside and outside walls of this shield as well as the interior walls of the observation chamber were cleaned and freshly plated with platinum black before each exposure. To facilitate the cleaning of the interior of the observation chamber a copper lining was constructed which was easily removed, cleaned and plated.

Photographic Technique

The detecting plate consisted of either a "black-nickel" plated brass plate or a blackened photographic plate upon which was deposited a thin coating of molybdenum oxide formed by the oxidation of metallic molybdenum in an oxygen-gas flame. Since the blue reduced molybdenum oxide faded slowly when exposed to the air, the detecting plate was photographed as soon as possible after it was removed from the apparatus. The camera was of special construction and gave a 2.86 to 1 enlarged image. The plate was illuminated from the front by two 100 watt lamps placed beside the camera lens. To prevent fading of the pattern by reoxidation when exposed to the heat from these lamps, water filters were introduced between the lamps and the plate. A Wratten Aero No. 1 color filter was used in front of the camera lens to increase the photographic contrast between the white background and the blue pattern. The best reproductions of the patterns were obtained on Eastman Process plates with their D-9 developer.

Preparation of the Crystal

The crystals of lithium fluoride were grown from a melt by the method of Kyropolus,[4] which proved to be extremely simple and satisfactory. These crystals are of the simple cubic lattice, and they are cleavable along the 100 planes. From the lens shaped crystals which were grown in this way rectangular blocks 2 mm $\times$ 2 mm $\times$ 4 mm were cut, the faces of which were parallel to the cleavage planes. During an exposure one of these crystal blocks rested in a grove in a copper holder of which two types were used to realize the desired orientations. These holders contained heating coils of tungsten wire wound on mica and imbedded in alundum cement. After all other adjustments had been made the crystal was cleaved and mounted, and as quickly as possible the apparatus was evacuated. Without further treatment the freshly cleaved surface at the start was generally found to give a weak specularly reflected beam of the order of 1 percent of the incident beam. An initial heating at 500°C for about 3 min. with a subsequent cooling to room temperature increased the reflecting power to something of the order of 10 percent of the incident beam, but this again fell off in the course of an hour to very nearly nothing. If the temperature of the crystal was maintained steadily at about 300°C its reflecting power was higher and it persisted for a much longer period of time, but it was still helpful to heat the crystal at 500°C for a few minutes

[4] Kyropolus, Zeits. f. anorg. allgemein. Chem. **154,** 308 (1926).

at four or five hour intervals. With this procedure it has been possible to maintain a high reflecting power during 24 hour exposures with no apparent diminution. During the major part of the exposure it has been found best to maintain the crystal at as low a temperature as is possible without seriously interfering with its reflecting power, for at the higher temperatures, in addition to difficulties introduced by the heating of the detecting plate, there was some troublesome diffuse reflection which might have arisen from either or both of two causes. (1) The roughening of the surface by thermal agitation may have produced a diffuse blurring of the regularly reflected and the diffraction beams. (2) Adsorbed hydrogen atoms may have been re-emitted from the hot crystal in the monatomic state, although at low temperatures these remained on the crystal surface until recombination to molecular hydrogen had taken place.

The best explanation which can now be given of the continually diminishing reflecting power at low temperatures is that vapors from the picein wax, which sealed the many joints leading into the reflection chamber, gradually condensed on the crystal surface. To minimize this difficulty the concentration of this wax vapor was made as low as possible by the use of independently evacuated guard rings between the wax seals and the inside chamber. As further precautions against this vapor, a liquid-air-filled glass tube protruded into the observation chamber, and the inside walls were covered with an adsorbing layer of platinum black.

The Diffraction Patterns

For the purpose of demonstrating the principal features of the phenomenon of the diffraction of atoms, patterns were obtained by exposures with three different arrangements of the crystal and detecting plate. These will be referred to as (a) normal incidence (b) 45° incidence in the 110 azimuth and (c) 45° incidence in the 100 azimuth. In each case the patterns were those expected from the following two assumptions: (1) The distribution of wavelengths in the beam was that calculated from the Maxwellian velocity distribution by the use of the de Broglie relation, and (2) The diffraction grating was made up of scattering points arranged on the surface in a plane square array with a spacing d equal to the value 2.835A obtained by x-ray measurements for the distance between two adjacent ions of the same type. The principal axes of this array lie in the 110 azimuths and the angular positions (ϕ, θ) of the diffraction beams with respect to these axes can be correctly calculated from the plane cross-grating equations

$$\cos\theta_0 - \cos\theta = m\lambda/d \tag{8a}$$

$$\cos\phi_0 - \cos\phi = n\lambda/d \tag{8b}$$

in which m and n have the values $0, \pm 1$, etc.

Of the patterns which have been recorded, the most complete is that reproduced in Fig. 5 which was obtained with the crystal and the detecting plate arranged for normal incidence as is shown in Fig. 1. The specularly reflected

beam appears in the photograph at the center of the pattern superposed upon the hole drilled for the incident beam. The more intense dispersed branches of the pattern, which are reproduced in the vertical and horizontal directions, lie in the 110 azimuths of the crystal. These correspond to the four ways of assigning 0 and ± 1 to m and n in equations (8), and may be appropriately designated as (1, 0) beams. In addition to these, four other fainter beams are visible in the 100 azimuths corresponding to $n = \pm 1$, $m = \pm 1$. These will be designated as (1, 1) beams. The dispersion in these beams seems to be greater than that in the (1, 0) beams as would be expected since these may be considered as arising from a grating of the spacing $d/2^{1/2}$. The angular dimensions of the pattern may be judged from the fact that the distance from the crystal to the detecting plate, when increased in the ratio of the enlargement of the photograph, was 12.9 mm.

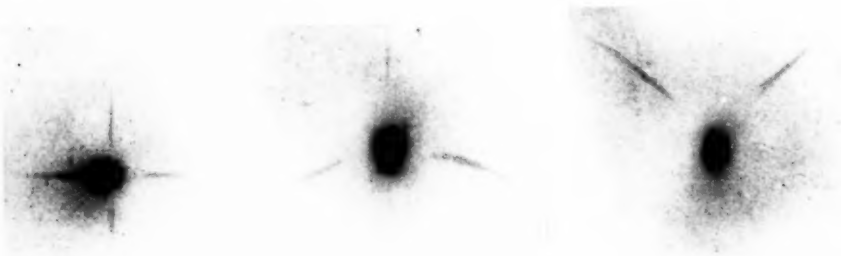

Fig. 5. Diffraction of hydrogen atoms reflected at normal incidence from an LiF crystal.
Fig. 6. Diffraction of hydrogen atoms reflected at 45° incidence in the 110 azimuth.
Fig. 7. Diffraction of hydrogen atoms reflected at 45° in the 100 azimuth.

A pattern produced by reflecting the beam at 45° incidence in the 110 azimuth is reproduced in Fig. 6. In this instance the arrangement of the crystal and detecting plate was that represented in Fig. 3. The (0, 0) specularly reflected beam again appears at the center of the pattern and the (1, 0) beams are now a straight line in the plane of incidence and a parabola symmetrically placed with respect to this line and intersecting it in the specularly reflected beam. If θ designates the angles measured from the rows of ions which are parallel to the plane of incidence, and ϕ those measured from the perpendicular rows, then the beam which is dispersed in the plane of incidence is represented by $m = +1$, $n = 0$ in equations (8). The two branches of the parabola, on the other hand correspond to $m = 0$ $n = \pm 1$. The straight branch in the plane of incidence on the lower side of the specular beam corresponding to $m = -1$, $n = 0$ might have been expected to appear but the dispersion was such that the most probable wave-length fell below the plane of the crystal, and, on account of the greater dispersion in this branch and the paucity of the wave distribution in the region of short wave-lengths, this branch was too faint to appear in the photograph.

The (1, 1) beams in this case take the form of two hyperbolae intersecting in the specular beam but these were perhaps too faint to be distinctly visible

in the reproduction. Unquestionably they could be brought out more intensely if a special effort were made.

The pattern at 45° incidence in the 100 azimuth (Fig. 7) was obtained with the same arrangement of Fig. 3, except that the crystal was rotated in its own plane 45° from its former position. The plane of incidence was in this case parallel and perpendicular to the cleaved edges of the crystal so that the principal axes of the surface lattice intersected the plane of incidence at angles of 45°. The (1, 0) branches of the pattern now appear as the two hyperbolic intercepts with the plane of the detecting plate of the two cones, $\theta = 60°$, and $\phi = 60°$. The branches which lie above the specular beam are intense but those lying between the specular beam and the plane of the crystal, although visible, are weak for the same reasons as were given in regard to the $n = 0$, $m = -1$ beam of Fig. 6. The (1, 1) beams in Fig. 7 should have the form of the (1, 0) beams of Fig. 6 except for greater dispersion but these were too faint to appear.

The Distribution of Wave-Lengths

Assuming the Maxwellian law for the distribution of velocities of the atoms per unit volume in the beam, the distribution in wave-lengths of the intensity of the atom waves falling on the crystal as predicted by the de Broglie relation is given by

$$dI/d\lambda = Ae^{-\lambda_0^2/\lambda^2}/\lambda^5 \tag{9}$$

in which λ_0 has the value $h/(2mkT)^{1/2}$. The expected distribution of intensity along the path s of a branch of the diffraction pattern is calculable from (9) by the relation

$$\frac{dI}{ds} = \frac{dI}{d\lambda}\frac{d\lambda}{d\theta}\frac{d\theta}{ds} \tag{10}$$

$d\lambda/d\theta$ may be obtained by differentiation of the grating equations (8) and $d\theta/ds$ is calculable from the geometry of the arrangement.

Since the intensity measurements were to be made with a densitometer the straight line patterns at normal incidence seemed at first sight to be the easiest to manipulate. A comparison of these patterns with those obtained at 45° incidence however showed that the latter were less obscured by diffuse radiation and for this reason were less subject to errors. To combine this advantage with ease of measurement it was decided to use a pattern obtained with the crystal oriented for 45° incidence in the 110 azimuth and a slightly different arrangement of the detecting plate as shown in Fig. 8. With this arrangement branches dispersed along the periphery of the 45° cone appeared on the detecting plate as a circle (Fig. 9) and this form of pattern was easily measured with a Koch and Goos densitometer by the use of a simple attachment constructed to give rotary motion. Besides its adaptation to measurement this pattern had two other great advantages. (1) All points of the circle were equally distant from the surface of the crystal and for this reason the general

darkening of the plate was distributed somewhat evenly. (2) The calculations were extremely simple and involved only the measurements of the angular positions ψ on the plate.

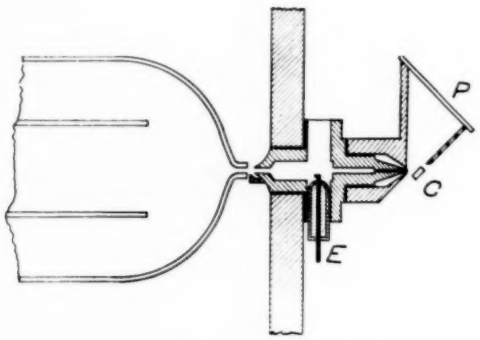

Fig. 8. Arrangement of plate holder for circular patterns.

The grating equation (8b) in this instance reduces to

$$\cos\phi = n\lambda/d \tag{11}$$

and the measured angle ψ of the circular pattern is related to ϕ by

$$\cos\phi = \sin\psi \sin 45°, \tag{12}$$

from which

$$dI/d\psi = A'e^{-2\lambda_0^2/d^2\sin^2\psi} \cos\psi/\sin^5\psi. \tag{13}$$

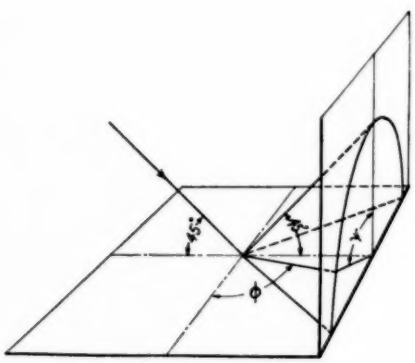

Fig. 9.

The angle ψ_0 of maximum intensity is found by equating to zero the derivative of the right hand member of (13) and it is given by

$$\cos^2\psi = -(2\lambda_0^2/d^2 - 3)/8 + [(2\lambda_0^2/d^2 - 3)^2/64 + \tfrac{1}{4}]^{1/2} \tag{14}$$

If it is assumed that the temperature of the source of the atom beam was

that of the water which circulated in a jacket surrounding the discharge tube[5] then

$$T = 300° K \qquad d = 2.835A$$
$$\lambda_0^2 = 3.13 \times (10)^{-16} \text{ cm}^2 \qquad \psi_0 = 32.7°.$$

Intensity measurements were made from the photographic negatives. As regards the position of maximum intensity this method of measurement would have been independent of the plate calibration were it not for the fact that the pattern was superposed upon a background of variable intensity in spite of the advantages of the arrangement for overcoming this trouble. In order to correct the measurements for this background intensity the plate was also measured along the circumference of a circle of slightly different diameter from that of the diffraction pattern itself, and this set of measurements was applied to the first set as corrections. A calibration of the densitometer deflection in terms of the intensity of an atom beam was obtained by exposing a separate plate in various places to the primary beam for successively increasing times so that a series of dark spots was formed which covered the intensity range of the patterns. This plate was photographed and developed under exactly the same conditions as pertained in the case of the plates which contained the patterns. Densitometer measurements then showed that the difference of the deflection produced by the center of one of the spots and that produced by the unexposed portions of the plate was very nearly proportional to the time of exposure of the spot. This fortunate coincidence led to the simple rule that the deflections of the densitometer could represent atom beam intensities if corrected by subtracting the deflection at an adjacent point of the background. Although this method of making intensity measurements cannot be regarded as possessing a high degree of reliability, as will be recognized by those familiar with the precautions necessary in ordinary photographic photometry, yet it led to surprisingly consistent results in good agreement with what was expected for the angle of maximum intensity. Eight corrected sets of measurements from plates made from three different molybdenum oxide originals gave a weighted mean value of $\psi_0 = 31.6°$ with a probable error of 2.2° as compared with the calculated value of 32.7°. This accuracy probably speaks more for the uniformity of the background than for the method of calibration and correction, and it is felt that a more reliable calibration must be devised before the photographic method can be used satisfactorily for precise intensity measurements.

Relative Intensities of the (1, 0) and (1, 1) Beams

Measurements of the relative intensities in different orders of x-ray spectra have been applied[6] to a determination of the relative scattering powers of the different atom species in the crystal. It is of interest to attempt the same thing using the different orders in the atomic diffraction patterns.

[5] From the work of J. B. Taylor, Phys. Rev. **29,** 309 (1927) this seems to be a reasonable assumption.

[6] W. H. Bragg and W. L. Bragg, X-rays and crystal structure, page 187, et seq.

Because of the overlapping of the 1, 0 and 2, 0 orders these beams are not well adapted to this purpose until more homogeneous velocities can be used, but it is interesting to compare the intensities in the 1, 0 and 1, 1 branches. In terms of the scattering powers U of the two ion types in the two directions, the ratio of the intensity of a (1, 1) beam of a particular wave-length to that of a (1, 0) beam of the same wave-length may be expressed, by the use of the principle of the superposition of amplitudes, as

$$I_{11}/I_{10} = (U_{11F} + U_{11Li})^2/(U_{10F} - U_{10Li})^2. \tag{15}$$

If the U's are assumed to be spherically symmetrical functions of space, i.e., $U_{11} = U_{10}$, the ratio U_F/U_{Li} can be determined from the measured ratio of intensities I_{11}/I_{10}.

In making the intensity measurements one must take account of the fact that the beams are not homogeneous in wave length but they contain a distribution (9) which is more highly dispersed in the (1, 1) than in the (1, 0) branches. The maximum of intensity on the plate in the (1,0) branches of the normal incidence patterns should fall, according to these considerations, at a distance S from the central spot equal to 0.408 l, where l is the distance between the crystal and the plate. The calculated position of maximum intensity in the (1, 1) branches is at $S = 0.589\ l$.

The ratio of intensities at these two points of maximum intensity is found from (9), (10) and (15) to be

$$\left(\frac{dI}{ds}\right)_{11} \Big/ \left(\frac{dI}{ds}\right)_{10} = (U_{Li} + U_F)^2/6.3(U_{Li} - U_F)^2. \tag{16}$$

The actual measurements carried out by means of the photometric technique described in the previous paragraph give a value of this ratio of about 1/6 with the possibility of an error of 100 percent or more arising not only in the unreliability of the method of calibration but also from the faintness of the 1, 1 branches. Although this inaccuracy of measurement renders a quantitative determination of U_{Li}/U_F impossible, the assumption of spherical symmetry of the U's leads to a small value of this ratio. The same conclusion results from a consideration of the great intensity in the 1, 0 orders where the contributions to the amplitude from the two ion types is 180° out of phase. From these measurements it is not necessary to conclude that the scattering power of an ion is definitely less in the 1,1 direction than in the 1,0 direction as Estermann and Stern found from the extremely small intensity which they observed in the (1,1) beams, although this conclusion would be necessary if a more accurate determination of the ratio (16) leads to a value greater than 1/6.

Diffraction by a Secondary Lattice of Wide Spacing

In addition to the spectra which have been described, arising from the surface array of ions, another type of spectrum of very low dispersion appeared on the plates. This type of spectrum was first noticed on a plate exposed at

45° incidence in the 100 azimuth where it appeared as a slight smearing of the specular beam in the plane of incidence. Later the same phenomenon was noticed on the plates exposed at 45° incidence in the 110 azimuth and in this case the spectra took the form of a blurred *X* extending out from the specular beam. These features may perhaps be distinguished in Figs. 6 and 7. An exposure at grazing incidence in the 100 azimuth increased the dispersion in this spectrum as shown in Fig. 10 but failed to separate the maximum of the

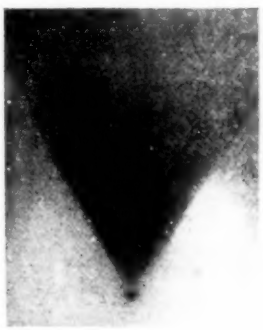

Fig. 10. Secondary structure spectrum at grazing incidence.

wave length distribution from the specular beam. It has been pointed out[7] that this spectrum indicates the existence of a secondary periodicity on the crystal surface parallel to the 100 planes in agreement with the theory of Zwicky.[8] Work is now under way to increase the resolving power in this spectrum with the hope of measuring the constant of the secondary lattice.

The writer wishes to take this opportunity to acknowledge his indebtedness to Mr. C. K. Boyer and Mr. M. A. Roesch, both of the Drexel Institute, who have assisted in this work.

[7] T. H. Johnson, Phys. Rev. **37,** 87 (1931).
[8] Zwicky, Helvetica Physica Acta III, 269 (1930).

SCATTERING OF X-RAYS FROM GASES

By E. O. Wollan
The University of Chicago

(Received February 18, 1931)

Abstract

Measurement of the intensity of scattering of x-rays by various gases has been made for scattering angles between 10° and 90°. Soller slits were used to get a well-defined scattering angle and matched filters of ZrO_2 and SrO were used to isolate the K_α lines of molybdenum. Intensity measurements have been made for hydrogen, helium, oxygen, neon and argon. All the measurements were put on the same scale by comparison of the intensity of scattering from the various gases with the scattering from hydrogen at 90°. This is equivalent to putting the intensities on an absolute scale since the scattering from hydrogen at 90° can be calculated with considerable certainty. Values of the structure factors for neon and argon were calculated and comparison made with those determined from wave mechanics for similar atoms.

Introduction

IN VIEW of Compton's[1] recent theory for determining the electron distributions in atoms from the angular distribution of intensity of x-rays scattered from monatomic gases it was thought desirable to get more complete experimental data.

Barrett[2] in 1928 published data for the scattering of x-rays from most of the gases included in this paper. He measured the intensity as a function of angle but no attempt was made to get absolute intensity measurements.

In the work reported here a more definite scattering angle has been obtained by the use of Soller slits, x-rays made homogeneous by the use of balanced filters have been used wherever the intensity permitted, and all the measurements have been put on the same scale by comparing the intensities from the various gases with that from hydrogen. This is equivalent to putting the intensity measurements on an absolute scale since the scattering from hydrogen at 90° can be calculated with considerable certainty.

Apparatus and Procedure

The set-up is shown in the diagram Fig. 1. A molybdenum target x-ray tube was operated at 40 kv peak and 35 m.a. with full-wave rectification. The tube was immersed in oil in a lead box fitted with a lead glass front. A small celluloid window within 2 mm of the tube transmitted the primary beam with only a small reduction in intensity due to the 2 mm of oil. This arrangement

[1] A. H. Compton, Phys. Rev. **35,** 925 (1930).

[2] C. S. Barrett, Phys. Rev. **32,** 22 (1928). Measurements of the relative scattering of hydrogen and Argon have been made by Herzog but not with homogeneous radiation. G. Herzog Helvetica Phys. Acta **2,** 169 (1929).

allowed the tube to be brought very near the spectrometer and the intensity was considerably greater than would have been possible with the tube in air.

The intensities were measured with an ionization chamber and a Compton electrometer with which currents of 5×10^{-15} amperes could be measured with a reproducibility of about five percent.

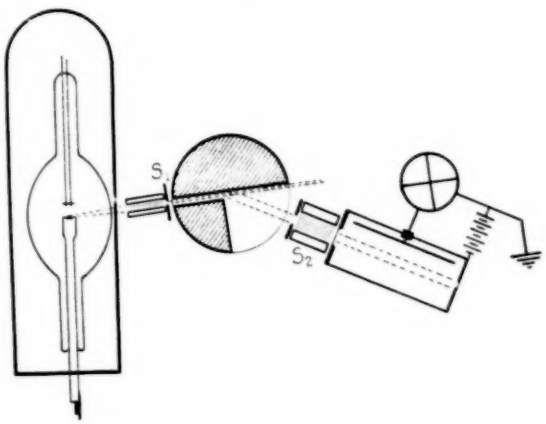

Fig. 1. Arrangement of apparatus.

The scattering chamber is shown in Fig. 2. It was made from a brass tube 5.5 inches in diameter, 3 inches high and having 1/8 inch walls. The top and bottom were 0.5 inch steel plates grooved and fitted with rubber gaskets and

Fig. 2. Scattering chamber.

held in position by three bolts as shown. The windows were of 0.7 mm celluloid 2 cm high. They were screwed down on rubber gaskets and picein wax used where it was found necessary. The base was fitted to the spectrometer table so it could be removed and replaced without affecting the readings. The top contains a gauge, an oxygen tank connection, a needle valve for the chamber and a side tube for evacuating the chamber and the leads. The chamber

was partially filled with sealing wax as shown in Fig. 1, and lined with lead. This cut the volume to about 250 cc and acted as a shield for the diffusely scattered x-rays.

The chamber was found to be very satisfactory as pressures of 200 pounds were used with a leak of only a few percent per week and the corrections for scattering from the evacuated chamber were almost negligible.

Reference to the diagram will show the arrangement of the chamber and the slit system. Soller slits were used to collimate the primary as well as the scattered beam. These slits allowed a maximum angular divergence of less than 2° in the horizontal plane. Slit S_1 was 3 mm wide and 1 cm high. Slit S_2 was 1 cm high and could be varied in width to 1.5 cm. Besides defining the

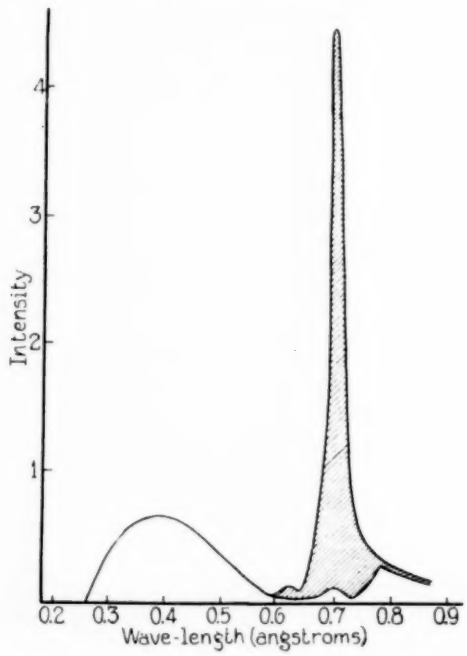

Fig. 3. Transmission through ZrO_2 and SrO filters.

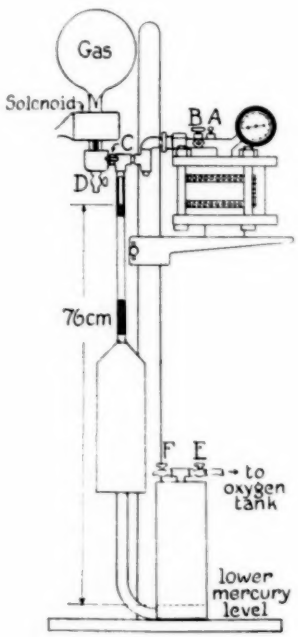

Fig. 4. High pressure mercury pump.

scattering angle the second slit served the additional purpose of determining the scattering volume. With this slit remaining constant the scattering volume was proportional to sin ϕ. The height of the slits S_1 and S_2 made the actual scattering angle slightly larger than indicated on the spectrometer circle. It was necessary to make correction for this on the readings between 10° and 30°.

The $K\alpha$ lines of molybdenum were separated out by the balanced filter method.[3] A filter of ZrO_2 containing about 0.025 gm per cm² was balanced by a filter of SrO so that less than five percent of the radiation corresponding to the difference of these filters lay outside of the range between the K critical absorption edges of Zr and Sr. A curve showing the transmission by these

[3] P. A. Ross, Phys. Rev. **28,** 425 (1926).

filters is shown in Fig. 3. The shaded portion represents the difference of the transmission by the two filters. The filters were additionally tested by measuring the absorption coefficient of aluminum which gave a straight line when log (I_0/I) was plotted against thickness. It is very important that these filters be well balanced so that reliable corrections for absorption can be made when elements like argon are compared with oxygen.

Since some of the gases were originally at atmospheric pressure it was necessary to construct a pump to put them into the chamber at the desired pressure. Fig. 4 shows the construction of the pump. The cylinders were of seamless steel tubing with welded bottoms and top and connecting tube. The rest was constructed mainly from iron pipes and connections. The vertical pipe was cut through at two places and a glass tube waxed inside to make the mercury level visible. With valve *B* closed and all the others open the system

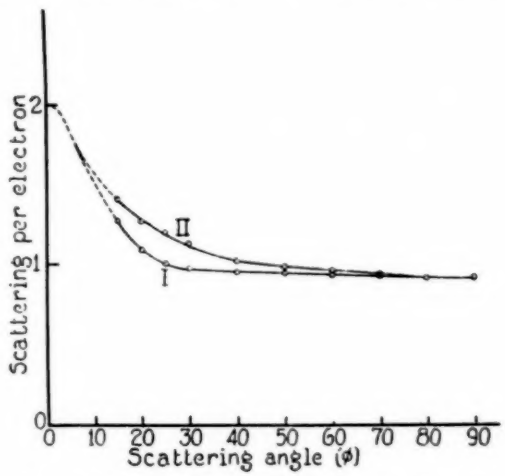

Fig. 5. Curve I hydrogen, Curve II helium.

could be evacuated through valve *D*. Closing valve *D* and breaking the tip in the glass container by means of the electromagnet, the gas expanded into the upper cylinder of the pump. By closing valves *C* and *F* the gas could be forced into the scattering chamber by applying the oxygen tank pressure at valve *E*. With repeated pumping it was necessary to draw the mercury back into the lower container by applying the vacuum pump at *F*.

Hydrogen

The hydrogen used in this experiment came from a tank especially prepared and analysed by Burdett Oxygen Company and found to have less than 0.1 percent oxygen and CO_2 and 0.07 percent water vapor by volume. After scattering measurements had been made on the gas the density was measured by weighing and no additional impurities were found to be present. The scattering chamber connected directly to the hydrogen tank, was evacuated together with all the leads, flushed out several times and filled to about 200 pounds pressure. It was then placed in position on the spectrometer table

and the scattered intensity measured from 10° to 90°. Even at 200 pounds pressure, however, it was necessary to use general radiation in place of the balanced filters. Curve I, Fig. 5 shows the scattering per electron corrected to $\lambda = 0.71$A plotted against ϕ. On the basis of the classical theory of scattering the value of $S \equiv I_s/ZI_e$ for hydrogen would be unity at 90°. The fact that practically all the intensity scattered at 90° from hydrogen is modified will make the experimental value at this angle slightly lower than unity. The Breit-Dirac relation may then be used

$$S_{\text{class}} = S_{\text{mod}} \{1 + \gamma \text{ vers } \phi\}^3. \quad (1)$$

Placing for 90° $S_{\text{class.}} = 1$, we have thus, $S \equiv S_{\text{mod.}} = (1+\gamma \text{ vers } 90°)^{-3}$. For $\lambda = 0.71$ A, γ vers $90° = 0.0243$, whence $S = 0.91$.

The data included in table I are all based on a value of S for hydrogen equal to 0.91 at 90°. To get the classical values of S Eq. (1) must be used.*

TABLE I. *Scattering per electron.* $\lambda = 0.71A$.

Angle	Hydrogen	Helium	Oxygen	Neon	Argon
10°			8.05	8.55	13.90
15°	1.27	1.45	4.90	6.87	10.65
20°	1.10	1.34	2.96	5.16	8.50
25°	1.03	1.27	2.00	3.85	6.35
30°	1.00	1.20	1.72	3.11	5.23
40°	0.98	1.08	1.43	2.04	4.15
50°	0.97	1.01	1.15	1.53	3.32
60°	0.95	0.97	1.04	1.32	2.74
70°	0.93	0.95	1.02	1.24	2.28
80°	0.92	0.92	1.01	1.18	2.10
90°	0.91	0.91	0.96	1.06	1.95

In so far as the scattering per electron from hydrogen is known, the scattering from other gases can be put on an absolute basis by comparison with it. Since the intensity of scattering from hydrogen is weak and difficult to measure it was first carefully compared with oxygen which was then used as a secondary standard of comparison.

COMPARISON OF OXYGEN AND HYDROGEN

Oxygen and hydrogen were compared several times at 90° using general radiation and pressures of about 200 lb/sq. in. for both gases. This involves a large correction for absorption for an unknown wave-length. To make this correction the intensity of scattering was plotted as a function of pressure. The decrease in scattering per gm at 200 lb/sq. in. over that at small pressures was taken as the absorption correction.

Comparison of hydrogen at 200 pounds pressure with oxygen at 40 pounds pressure, taking account of the difference in pressure and making only a very slight absorption correction, gave results in very close agreement with those of the first method.

* Equation (1) gives the classical value only when all the scattered radiation is modified. In the case of oxygen, neon and argon the unmodified radiation must also be considered. Compton (ref. 1) has shown how the classical value of S can be gotten in this case.

The hydrogen curve was corrected to a wave-length of 0.71A by a method shown by the curves of Fig. 6. The curves are: I, hydrogen with general radiation; II, oxygen with general radiation; and III, oxygen taken with $\lambda = 0.71$A and arbitrarily fitted to the other oxygen curve at 90°. From these curves the intensity of scattering from hydrogen for $\lambda = 0.71$A was determined.

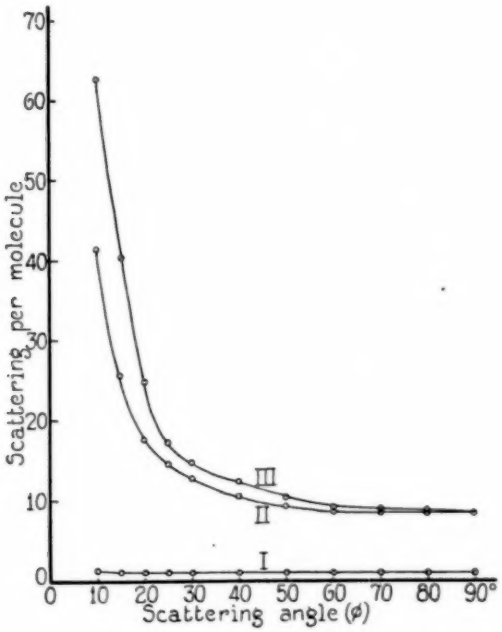

Fig. 6. Curve I hydrogen (general radiation), Curve II oxygen (general radiation), Curve III oxygen (filtered radiation, $\lambda = 0.71$A).

HELIUM

The helium came in liter containers at atmospheric pressure and was introduced into the chamber by means of the mercury pump described above. The pressure used was about 115 lb/sq. in. A number of sets of readings were taken and the intensity compared directly with hydrogen. The intensities of scattering from hydrogen and helium at 90° were found to be equal within the experimental error. Curve II, Fig. 5 shows the scattering per electron from helium corrected to $\lambda = 0.71$A in the same manner as for hydrogen.

In introducing the helium into the chamber about 0.9 percent of air by volume entered as an impurity. This was found to be the case by measurement of the density after the readings had been taken. Correction was of course made for this and would not lead to any appreciable error because the scattering from air could easily be measured. The data for hydrogen and helium are in very close agreement with the results obtained by Barrett. Although he obtained no excess scattering from hydrogen his data only extended to what corresponds to $\phi = 30°$ on the above curve.

Neon

Neon was also obtained in liter containers at atmospheric pressure and was put into the scattering chamber with the aid of the mercury pump.

The intensity measurements were made with filtered radiation and a number of sets of readings taken. In order not to have to evacuate and refill the chamber repeatedly, a sheet of celluloid was used for an intermediate comparison. Comparisons of the intensity from neon were made with the celluloid scatterer and then the chamber was evacuated and filled with oxygen and the comparisons with the celluloid scatterer again made. Corrections were made for the different absorption coefficients, and the results are shown in curve IV,

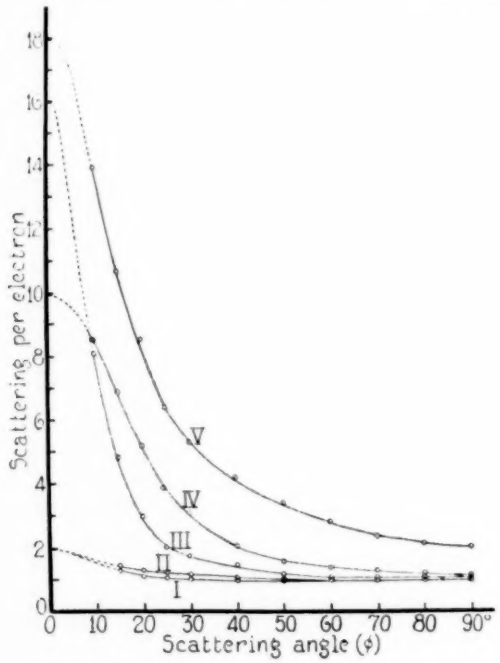

Fig. 7. λ=0.71A. Curve I hydrogen, Curve II helium, Curve III oxygen, Curve IV neon and Curve V argon.

Fig. 7. The scattering per electron from neon at 90° is very nearly that from oxygen. The neon curve begins to rise at larger angles than does the oxygen curve, a difference similar to that between hydrogen and helium.

Argon

The argon used in these measurements was obtained in a tank with about 0.3 percent impurity. The chamber could be readily filled to any desired pressure directly from the tank. This gas, however, presented greater difficulties than the other gases since its absorption coefficient is so much larger. Fig. 8 shows the relation between intensity and pressure for argon and oxygen. Curves I and II represent respectively the measured intensity from argon and oxygen; curves IV and III represent the values after correction for absorption

has been made. To make the corrections as small as possible and still get sufficient intensity from both oxygen and argon pressures of about 40 to 50 lb/sq. in. were used.

In the case of argon, the comparison of intensity with oxygen was done directly by taking a number of readings with one gas and then refilling the chamber with the other gas with the x-ray tube in operation during the process. Several of these comparisons were made and the pressures varied somewhat to make the absorption corrections more certain.

It is noticeable that in argon the scattering per electron is considerably larger than for the other gases. This would correspond to a greater electron density near the center of the argon atom.

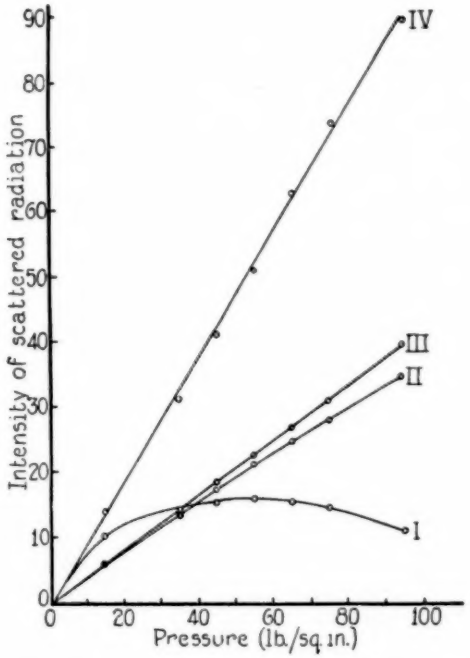

Fig. 8. Curves I and II represent respectively the measured intensity from argon and oxygen curves. Curves IV and III represent the values after correction for absorption has been made.

Errors

The largest errors involved in measuring the scattering per electron would probably be those of comparing the scattering from one gas with that of another. In the case of the comparison of the intensity of scattering from hydrogen with that from oxygen the probable error from the mean was about 1 percent. It is likely that there are other errors such as uncertainty of wavelength, measurement of pressure and corrections for absorption which would also amount to about 1 percent. This would mean that the scattering from oxygen would probably be correct to about 2 percent. In comparing neon and oxygen, considering the probable error already mentioned, the uncertainty

in the neon data would be of the order of 3 percent. In argon the large correction for absorption would probably increase the uncertainty to about 4 or 5 percent. In the case of hydrogen and helium the probable error of any point of the curve was about 2 percent.

Structure Factor

Calculation of the structure factors for neon and argon have been made from the relation given by Compton

$$F = Z\left\{\frac{S-1}{Z-1}\right\}^{1/2} \tag{2}$$

where S is the classical value of the scattering per electron, Z is the atomic number and F the structure factor. The values thus calculated are given in Table II. In order to make comparisons between these data and the structure

Table II. *Structure factor.*

ϕ	$\left(\frac{\sin \phi/2}{\lambda}\right)$	Neon		Argon	
		S_{class}	F	S_{class}	F
10°	0.123	8.55	9.16	13.90	15.63
15°	.190	6.87	8.08	10.65	13.53
20°	.245	5.16	6.80	8.50	11.93
25°	.306	3.86	5.64	6.36	10.10
30°	.365	3.12	4.86	5.26	9.00
40°	.482	2.06	3.43	4.17	7.77
50°	.596	1.56	2.49	3.35	6.69
60°	.704	1.37	2.02	2.79	5.84
70°	.808	1.30	1.80	2.34	5.06
80°	.905	1.26	1.70	2.18	4.72
90°	.995	1.17	1.37	2.05	4.49

factors calculated from crystalline reflection it is necessary to correct the latter for the effect of thermal agitation which does not affect the intensity of x-rays scattered from gases.

Some very interesting comparisons have been made by James and others[4,5] between the crystal reflection data at low temperatures and the structure factors calculated from Hartree's wave mechanics solution of the charge distribution in the K^+, Cl^- and Na^+ ions. Making temperature corrections and assuming the existence of zero point energy they get structure factor curves which are in good agreement with the theoretical curves.

The values of F from Table II are plotted in Figs. 9 and 10 together with F values from wave mechanics taken from the above mentioned papers.

In Fig. 9 the solid line represents the F curve for Na^+ calculated from wave mechanics and the broken line represents the F values for neon. From a consideration of equation (2) the reason for the apparently large inaccuracies in

[4] R. W. James and Brindley, Proc. Roy. Soc. **A121,** 155 (1928).
[5] R. W. James, I. Waller and D. R. Hartree, Proc. Roy. Soc. **A118,** 343 (1928).

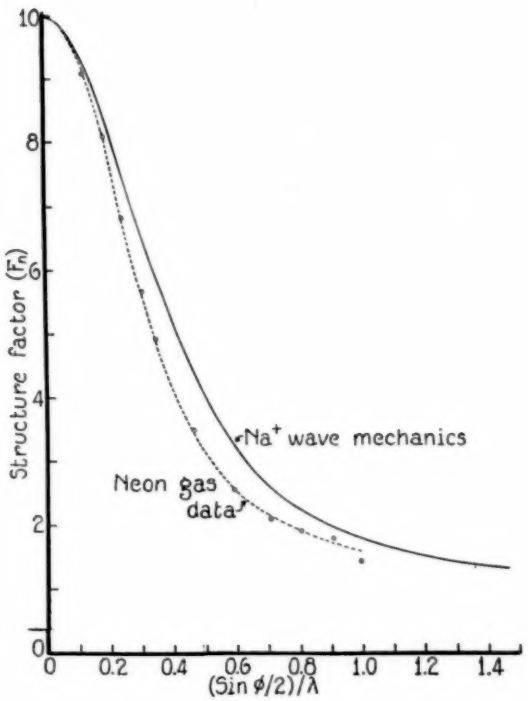
Structure factor (F_n)
10
8
6
4
2
0
0
0.2
0.4
0.6
0.8
1.0
1.2
1.4
$(\sin\phi/2)/\lambda$
Na^+ wave mechanics
Neon gas data

Fig. 9.

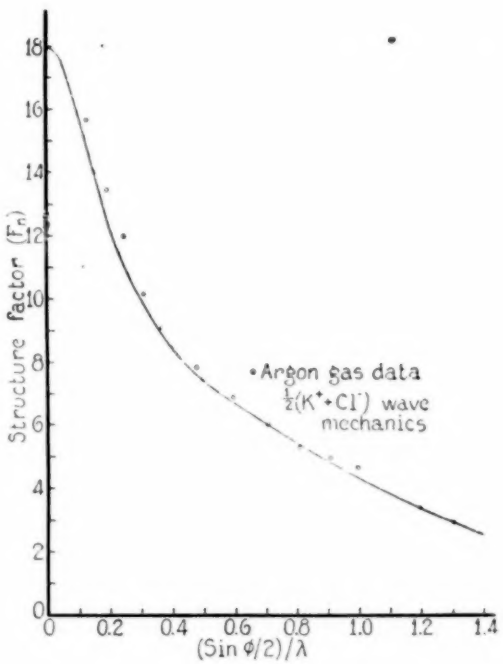
Structure factor (F_n)
18
16
14
12
10
8
6
4
2
0
0
0.2
0.4
0.6
0.8
1.0
1.2
1.4
$(\sin\phi/2)/\lambda$
Argon gas data
$\frac{1}{2}(K^+ + Cl^-)$ wave mechanics

Fig. 10.

the values of F when S is nearly equal to unity can be seen. For neon at $(\sin \phi/2)/\lambda = 1.00$ an error of 2 percent in S gives rise to an error of 9 percent in F.

A more significant comparison between theory and experiment is shown in Fig. 10. The curve represents the average of the F values for K^+ and Cl^- determined from wave mechanics. The circles give the F values from Table II for argon. The agreement is seen to be very satisfactory.

As has recently been shown by Compton[6] a comparison of these data with that determined from reflection from a crystal of KCl and corrected to 0°K gives a good experimental check of the existence of zero point energy.

Conclusion

These data furnish a significant check of Compton's recent theory of the intensity of x-rays scattered from gases and the use of these data for the determination of electron distribution in atoms. The agreement between the F curves of argon and those determined from wave mechanics and also from crystal reflection should give more confidence in the use of these methods for determining the distribution of charge in the atom.

A comparison of the F curves determined by these three methods is also a further check on the existence of zero point energy.

Calculation of the electron distribution curves from these data are now in progress.

In conclusion the author wishes to express his appreciation to Professor A. H. Compton, who suggested this problem, for his continued assistance in its solution.

[6] A. H. Compton, Phys. Rev. **37**, 104 (1931).

INTERACTION OF X-RAYS WITH BOUND ELECTRONS

By Austin J. O'Leary
Columbia University

(Received February 28, 1931)

Abstract

I. Change of wave-length of scattered x-rays. A previous analysis of scattered x-rays in this laboratory by means of the double crystal spectrometer showed fine structure in both the unmodified and modified lines. These fine structure lines were interpreted as being due to absorption of an amount of energy equal to the binding energy of the electrons in the scattering substance. Since then, other experimenters have failed to observe this phenomenon in scattered x-rays. The earlier work has been repeated using measuring apparatus having greater stability and sensitivity but with experimental conditions for producing the scattered radiation as nearly as possible like those of the earlier experiments. No fine structure was found though a line of intensity greater than 10 percent of molybdenum $K\alpha_1$ unmodified could have been detected.

II. Change of wave-length without scattering. A change of wave-length ascribed to this type of phenomenon without scattering has been reported by B. B. Ray and R. C. Majumdar. A number of experiments have been performed in an attempt to detect a change of wave-length of this type due to partial absorption of molybdenum $K\alpha_1$ and copper $K\alpha_{1,2}$ characteristic rays in the K-level of carbon. No indication of a modified line was found though a line of smaller intensity than that of the lines reported could have been detected. Two possible sources, other than a change of wave-length, are suggested which may give rise to lines of the type reported.

I. Change of Wave-Length of Scattered X-Rays

Discussion. Spectroscopic analyses have in general shown that when monochromatic x-rays are scattered by matter, the scattered radiation consists of two wave-lengths.[1] An unmodified line appears, having the same wave-length as the incident radiation and a modified line for which the wave-length separation from the unmodified is given by the Compton theory of scattering by free electrons and is

$$\delta\lambda = h/mc(1 - \cos\phi) \tag{1}$$

where h is Planck's constant, m the mass of an electron, c the velocity of light and ϕ the angle of scattering. A theory of scattering by bound electrons was proposed by A. H. Compton[1] in 1924. For the special case in which the recoil electron has zero kinetic energy, the theory predicts wave-length changes given by

$$\delta\lambda = \frac{\lambda^2}{\lambda_s - \lambda} \tag{2}$$

where λ is the wave-length of the incident radiation and λ_s the critical absorption wave-length of the level from which the bound electron is ejected.

[1] A. H. Compton, X-Rays and Electrons, Chapt. IX.

An analysis of scattered x-rays in this laboratory by means of the double crystal spectrometer which gave greater resolution than was hitherto possible with the single crystal methods, gave results which indicated fine structure in both the unmodified[2] and modified[3] lines. The change of wave-length for the fine structure lines found in the unmodified characteristic molybdenum $K\alpha_1$ x-rays scattered at 90° by carbon, beryllium, and aluminum, agreed with that given by Eq. (2). In the case of beryllium, an "anti-Stokes" line was observed but no line in the position of $K\alpha_1$. Similar fine structure lines were reported in the modified radiation scattered by carbon at 155° and beryllium 163°, the wave-length change being given by

$$\delta\lambda = h/mc(1 - \cos\phi) + \frac{\lambda^2}{\lambda_s - \lambda} \tag{3}$$

except that using the estimated angle of scattering, ϕ, the constant h/mc was found to be about 9 percent less than the theoretical value. These fine structure lines were no broader than in the unmodified in spite of the large divergence in ϕ.

Since then, Ehrenberg,[4] Coster,[5] and Kast,[6] using single crystal spectrographic methods failed to observe this reported phenomenon. More recently, the question of scattered radiation was investigated by Bearden,[7] and Gingrich,[8] using double crystal spectrometers without finding any indication of fine structure. Bearden analyzed copper $K\alpha_{1,2}$ and silver $K\alpha_{1,2}$ scattered by graphite and aluminum, and Gingrich, molybdenum $K\alpha_{1,2}$ scattered by graphite. They each observed the $K\alpha_{1,2}$ modified lines and found the wave-length separation from the unmodified to be accurately given by Eq. (1), the constant h/mc agreeing with the theoretical value within experimental error.

About the same time, the author repeated the earlier work done in this laboratory using measuring apparatus having greater stability and sensitivity but with experimental conditions for producing the scattered radiation as nearly as possible like those of the earlier work. A brief description of the experiments is given in the following.

Apparatus and method. A double crystal spectrometer of the type developed here, with both crystals set for first order reflection, was used to analyze the scattered radiation. Two slits, 43 cm apart, 15 mm high, and 7 mm wide, defined the direction of the scattered beam with a third slit between the crystals. Power was supplied at 125 volts and 500 cycles to a three kilowatt oil-immersed transformer and the high potential current rectified by means of two kenotrons and a large condenser. The voltage was read on an electrostatic voltmeter.

[2] B. Davis and D. P. Mitchell, Phys. Rev. **32,** 331 (1928); D. P. Mitchell, Phys. Rev. **33,** 871 (1929).

[3] B. Davis and H. Purks, Phys. Rev. **34,** 1 (1929).

[4] Ehrenberg, Zeits. f. Physik **53,** 234 (1929).

[5] Coster, Nature **123,** 642 (1929).

[6] Kast, Zeits. f. Physik **58,** 519 (1929).

[7] J. A. Bearden, Phys. Rev. **36,** 791 (1930).

[8] N. S. Gingrich, Phys. Rev. **36,** 1050 (1930).

The ionization chamber consisted of two aluminum cylinders, 10 cm long and 4 cm in diameter, one at positive and the other at negative potential, suspended inside a grounded brass box. The central collecting rods in each were connected together and to the lead from the insulated quadrants of the electrometer. There are thus two ionization chambers connected so that the ionization currents in the two are in opposite directions and tend to balance each other. The leak in each chamber due to natural ionization was almost zero. To minimize the irregularity in the electric field produced by the grounded case, an aluminum cap was placed over the end of each cylinder with a window 2 cm high and 1 cm wide corresponding to a similar pair of windows in the grounded case. The x-ray beam entered one window while in front of the other was placed a small radio-active source behind a shutter. The chamber was filled with methyl bromide to absorb the rays.

The sensitivity of the electrometer was 11,000 mm per volt at 1 meter. The capacity of the system as measured with a string electrometer was 38 e.s.u. distributed as follows: 10 e.s.u. each for the ionization chamber and electrometer with the remaining 18 e.s.u. in the shielded lead wires between the two.

The method of measurement was as follows. The shutter was adjusted until the ionization current produced by the radium source just balanced that due to the background radiation. Rocking curves of the unmodified $K\alpha_{1,2}$ scattered rays were taken by timing the drift over a definite part of the scale. The width at half maximum of these curves was always between 20 and 25 seconds. Then a careful search was made to detect the existence of any other lines by insulating the grounding key for a definite time, say 10 minutes, for each setting of the second crystal and noting the drift if any during that time. Compensation for large backgrounds is unsatisfactory but for the small amount of background radiation present in these experiments, the method proved quite successful. The stability of the system was remarkably good, the drift from the zero position never being greater than 3 divisions during the 10 minutes for each reading.

Scattering from carbon at 90°. A cylindrical tube 6.5 cm in diameter with a molybdenum target was placed just out of line of the slits so that no radiation scattered by the glass could pass through. The tube operated steadily at 62 milliamperes and 45 kilo-volts. Both graphite and paraffin blocks were used to scatter the x-rays and were placed along side of the tube so that the average angle of scattering was about 90° with a fairly large divergence. When paraffin was used, a stream of cold air was blown against it continuously to keep it from being melted by the heat from the tube. In no case was there any indication of a line other than the unmodified $K\alpha_{1,2}$ lines though the method was sufficiently sensitive to detect a line of intensity greater than 10 percent of the unmodified $K\alpha_1$ line. With the radium source removed, readings were taken with and without the carbon, everything else remaining the same. The ionization current was zero with the carbon removed, showing that all the x-rays entering the ionization chamber came from the carbon.

Carbon at 150°, beryllium 154°. A tube was built with molybdenum target and graphite scattering element inside as closely similar as possible to the tube used in the original investigation[3] of fine structure in the Compton effect. The focal spot was 5 mm wide and 9 mm long and faced a small graphite block supported about 2 cm from the center of the spot. This gave a large divergence in scattering angle, the average being about 150° with a plus or minus divergence of about 15°. A similar tube had a beryllium scattering element with an estimated scattering angle of $154° \pm 18$. The anode in each tube was tilted sufficiently toward the scattering block to insure against any possibility of direct radiation from the molybdenum target and was out of line of the slits so that no radiation from the copper anode itself could come through. This was checked by a photographic method. Curves for the $K\alpha_{1,2}$ lines scattered by graphite were similar to those found for 90° scattering, with no indication of fine structure. An unmodified line of very small intensity was observed from beryllium with no indication of an "anti-Stokes" line. A curve for the modified radiation was not taken in either case but a search was made in the position where the fine structure lines were originally observed without finding any indication of them. The modified radiation apparently formed a very broad hump as would be expected from the divergence in scattering angle.

II. Change of Wave-Length without Scattering

Discussion. A change of wave-length ascribed to this type of phenomenon has been reported by B. B. Ray[9] at zero angle of scattering, his conclusion being that a change of wave-length of x-rays on traversing matter does occur but without change of direction. He passed x-rays from a metal tube with tungsten filament through carbon soot and air and photographed the transmitted radiation with a Siegbahn spectrograph with calcite crystal. Besides the lines to be expected, several broad and diffuse lines appeared each time on the photographic plate and were interpreted as being due to a change of wave-length of the characteristic lines caused by absorption of an amount of energy equal to that necessary to raise an electron from the K-levels of carbon, nitrogen, and oxygen, to a higher level or remove them from the atom with zero velocity. Lines due to a similar absorption in the L-levels would be expected but could not have been detected with the apparatus. A variety of characteristic wave-lengths was used, all showing the same effect. R. C. Majumdar,[10] working in the same laboratory, has reported a similar effect due to partial absorption of characteristic x-rays in the L_1 level of aluminum.

The following considerations indicate the factors which are important in testing the existence of this phenomenon in the presence of continuous radiation. Suppose monochromatic radiation of frequency ν, and intensity I, falls on a thickness of matter d. Assuming the particular type of absorption mentioned above, the amount of radiation emerging from the matter with

[9] B. B. Ray, Nature **125,** 746 and 856 (1930); Nature **126,** 399 (1930); Zeits. f. Physik **66,** 261 (1930).

[10] R. C. Majumdar, Nature **127,** 92 (1931).

modified frequency $\nu' = (\nu - \nu_k)$ where ν_k is the critical absorption frequency of the K-level, would be:

$$I' = kIe^{-\mu' d}\left\{\frac{e^{(\mu'-\mu)d} - 1}{\mu' - \mu}\right\} \tag{4}$$

where μ is the linear absorption coefficient for radiation of frequency ν, μ' that for radiation of frequency ν' and k the linear absorption coefficient for this particular type of absorption in the K-level. The absorption due to modification of the frequency ν' itself has been neglected. Taking $\mu = \mu'$, which is approximately true, (4) reduces to

$$I' = kIde^{-\mu d}. \tag{5}$$

This is a maximum for $d = 1/\mu$ which would be the optimum thickness to use if no continuous radiation were present but this is not the case in the experiments under discussion. The continous radiation is absorbed in the usual way though it is not affected to any extent by the type of absorption under consideration and if I_1 is the incident intensity of the continuous in the region of frequency ν', then its intensity on emerging is $I_1 e^{-\mu d}$. Thus the ratio R, of the modified line to the background in its neighbourhood, which determines the contrast on the photographic plate is:

$$R = kdI/I_1 \tag{6}$$

and is directly proportional to the ratio I/I_1 and the mass of absorbing material. Conversely, knowing the amount of absorption produced by the absorbing material and the ratios I/I_1 and R, one gets the ratio of the intensity of an observed modified line, or of one which might be observed, to the intensity o the incident radiation producing it. This is given by

$$\frac{I'}{I} = R \cdot \frac{1}{I/I_1} \cdot e^{-\mu d}. \tag{7}$$

To test the existence of this phenomenon, the following requirements should be observed:

(1). The mass of material producing the effect should be as large as possible. This is, of course, limited by the time of exposure and the intensity of the radiation.

(2). The ratio I/I_1 should as far as possible be a maximum. This is determined for the most part by the operating voltage which should be high since the ratio increases with the voltage. Impurities in the target reduce this ratio and also extraneous scattered radiation if the plate is not properly shielded.

(3). To eliminate errors, photographs should be taken with and without the absorbing material in place before concluding that any lines observed are produced by its presence.

When a fixed crystal method is used, with a single narrow slit to give resolution and the x-ray beam having the necessary divergence in angle for

reflection of different wave-lengths, each wave-length comes from a different part of the target and errors may arise if the distribution of intensity over the target is not uniform. A pin-hole and a narrow-slit photograph of the target of one of the x-ray tubes with coil filaments used in this laboratory is shown in Fig. 1 and shows clearly the image of the filament coils on the target. Similar photographs of the targets of many other tubes were taken and showed widely different patterns, the particular distribution of intensity depending on the shape and position of the filament, filament cup, and anode. In no case was the distribution of intensity uniform. After reflection of the x-rays from a crystal, the characteristic lines appear on a background having the same pattern as that given by a narrow slit photograph of the target. If the distance from the narrow slit to the photographic plate is short enough, in comparison with the distance to the target, lines, not much broader than the characteristic lines, might appear on the plate and be erroneously interpreted. The tube used by Ray was of the heated filament type and it is possible that the lines observed by him, in every case broad and diffuse, were really due to lines in the target which accidentally appeared in a position where they might be given the interpretation he gave them. Also if the narrow slit is not close to the crystal, each wave-length is reflected from a different part of the crystal and there is the possibility of error due to imperfections in the crystal face. No statement was made as to whether or not photographs were taken with and without the absorbing material in place or other precautions taken to eliminate the possibility of such errors.

In the discussion Ray has assumed, without explaining how he arrived at the figure, that the intensity of the new lines, as compared with that of the primary, is only of the order of one in 400 or 500. However his photographs show that the intensity of these new lines above the background is at least as intense as the background (i.e. $R \geq 1$) and since the ratio of the intensity of the primary line to the background (I/I_1) is not likely greater than 50, Eq. (7) requires that the amount of absorbing material must have been sufficient to absorb 90 percent of the incident rays. The mass of absorbing material has not been given but it is unlikely that the amount of nitrogen and oxygen in which the rays were absorbed, was sufficient to produce this amount of absorption. In such case, the intensity of these lines, as compared with that of the primary, would be greater than that given above.

The experiments described in the following were carried out in an attempt to observe a change of wave-length of this type due to partial absorption of molybdenum $K\alpha_1$ and copper $K\alpha_{1,2}$ characteristic rays in the K-level of carbon.

Absorption of molybdenum Kα_1 in carbon. The change of wave-length predicted for x-rays which suffer absorption of the type considered was given by Eq. (2). For molybdenum $K\alpha_1$ absorbed in the carbon K-level this change would be about 11X.U. The modified wave-length would have a reflection angle from a calcite crystal 6.5 minutes greater than Mo$K\alpha_1$.

An x-ray tube with molybdenum target, thin glass window, and line focus, was operated at 25 milliamperes and 52 kilovolts peak voltage. Two slits,

0.05 mm wide and 76 cm apart, defined the x-ray beam. A calcite crystal mounted on a spectrometer table with a crystal rocking device reflected the rays to a photographic plate, placed at a distance of 2.4 meters and carefully

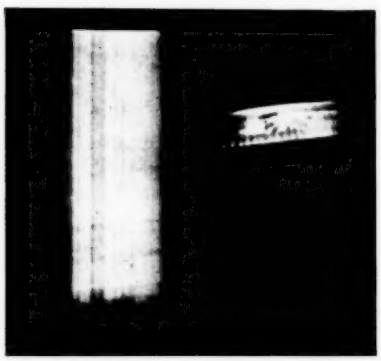

Fig. 1. Pinhole and narrow slit photograph of the target of an x-ray tube with coil filament showing the image of the filament coils on the target.

shielded from scattered radiation. This formed a system with high resolving power. The $K\alpha_1$ and $K\alpha_2$ lines were separated by a distance of 3.5 mm on the plate. Compressed lamp black was used to absorb the x-rays and was placed

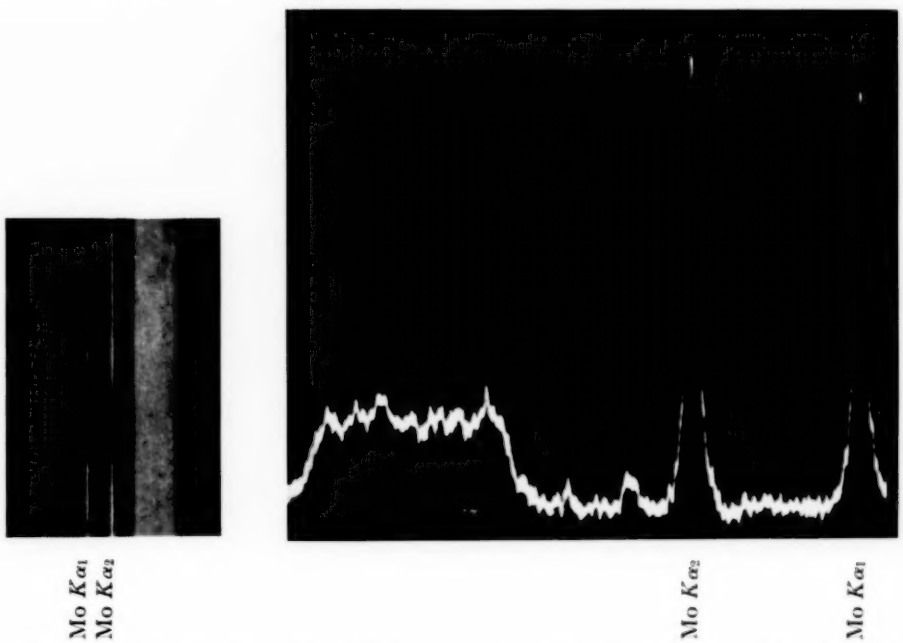

Fig. 2. Photograph taken with molybdenum target, carbon absorbing material and crystal rocking device to reflect radiation in the neighborhood of a line which would be produced if Mo$K\alpha_1$ were partly absorbed in the K-level of carbon.

Fig. 3. Microphotometer curve of one of the plates similar to that shown in Fig. 2.

in front of the slit nearest the tube. It was found experimentally that the lamp black absorbed 85 percent of Mo$K\alpha_1$ and that the ratio I/I_1 was 57.

After the crystal had been adjusted and the positions for reflection of $K\alpha_1$ and $K\alpha_2$ carefully determined, the method of procedure was as follows: With the carbon in place, short exposures of $K\alpha_1$ and $K\alpha_2$ were taken to give two reference lines on the plate. $K\alpha_1$ was usually exposed for about 15 minutes and $K\alpha_2$ 30 minutes so that the two lines would have approximately the same intensity. The crystal was then turned through an angle of 6.5 minutes from the setting for $K\alpha_1$ and the crystal rocking device set so that the crystal was rocked over a range of 4 minutes, covering 2 minutes on each side of this central position. Exposures were then taken for periods between 65 and 95 hours.

One of the photographs is shown in Fig. 2. The plates were projected on a screen under high magnification and microphotometer curves of two plates were taken but in no case was there any indication of a modified line. One of the microphotometer curves is shown in Fig. 3. A line of intensity 50 percent greater than the intensity of the background could easily have been observed. By Eq. (7), the intensity of such a line, as compared with that of the incident primary radiation, is one in 750.

The double crystal spectrometer was also used in a search for this modified wave-length. Direct radiation from a molybdenum tube, operating at 7 milliamperes and 37 kilovolts, was passed through the compressed lamp black. The ratio I/I_1 in this case was 75 and a line of intensity 15 percent greater than the continuous radiation could easily have been detected but no indication of such a line was found. In this case then, the intensity of a line that could have been observed as compared with that of the primary is, by equation (7), one in 3000.

Absorption of copper K$\alpha_{1,2}$ in carbon. The change of wave-length predicted for copper $K\alpha_1$, undergoing this particular type of absorption in the K-level of carbon, is about 55 X.U. and the reflection angle from a calcite crystal for this modified wave-length would be 33 minutes greater than for $K\alpha_1$. In this experiment the crystal rocking method was not used. Pin-hole and narrow slit photographs of two tubes with copper targets showed them to be unsuitable for a fixed crystal method. One target however showed a band of uniform intensity which was suitable for the purpose provided the rest of the target was blocked out. This was done by means of two slits 20 cm apart. The slit nearest the lead box was 0.04 mm wide and the width of the other slit and the position of the tube, were adjusted until the radiation coming through formed a beam of uniform intensity with a divergence of about 44 minutes.

The tube was operated at 30 milliamperes and 52 kilovolts peak voltage. The carbon used was a uniform slab of graphite of a thickness which absorbed 70 percent of the $K\alpha$ rays. It was interposed in the beam at the slit nearest the tube. The photographic plate was placed 75 cm from the crystal and was carefuly shielded so that no radiation could strike it except that from the crystal.

The central positions of the crystal for reflection of $K\beta$ and $K\alpha_{1,2}$ were determined. Then with the graphite in position short exposures were taken of $K\beta$ and $K\alpha_{1,2}$ and a 24-hour exposure taken with the crystal set at an angle 33 minutes greater than the central position for reflection of $K\alpha_1$. Photographs were also taken without the graphite in place and were exactly similar to those taken with. In no case was there any indication of a line. The method was however not entirely satisfactory since each wave-length was reflected from a slightly different portion of the crystal and the band on the plate was somewhat patchy due to imperfections in the crystal face. One of these photographs is shown in Fig. 4.

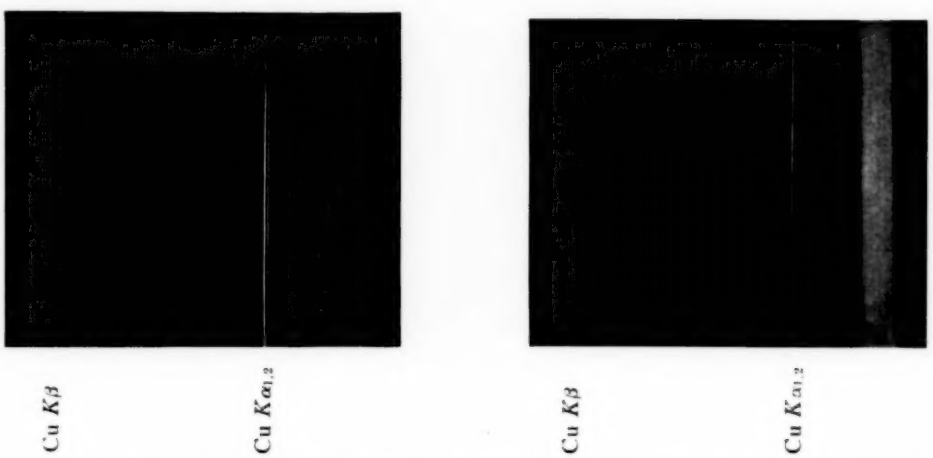

Fig. 4. Photograph with carbon absorbing material and fixed crystal, using the radiation from only that portion of a copper target which gave uniform intensity. Narrow slit was 25 cm from crystal.

Fig. 5. Photograph similar to that shown in Fig. 4 except that narrow slit was close to crystal.

This objectionable feature was eliminated from the next set of photographs. The slit nearest the tube was reduced in size to 0.04 mm. In order that the divergence in angle from the small portion of the target giving uniform intensity, be large enough to give a band of the desired width on the photographic plate, the distance between slits was reduced to 5 cm and the tube moved up as close to the opening in the lead box as safety would permit. The width of the slit nearest the tube, and the position of the tube, were adjusted until the radiation coming through was only that from the portion of the target which gave uniform intensity. The short distance between slits made this difficult but it was finally accomplished. The divergence in angle of the beam was this time about 28 minutes. Each wave-length was reflected from closely the same part of the crystal and conditions were very favorable for observing a modified line.

Photographs were taken with and without the carbon in place as an added precaution against error, the time of exposure varying between 20 and 35 hours. One of the photographs is shown in Fig. 5. A microphotometer curve

of the band on the same plate is shown in Fig. 6. In every case the band was perfectly uniform with no indication of a line. A line of intensity of the order of one in 800, as compared with that of the primary, could easily have been detected.

Another set of photographs was taken using the radiation from the whole target. The distance from the narrow slit to the tube was small enough in comparison with the distance to the plate that any lines in the focal spot

Fig. 6. Microphotometer curve of band on plate shown in Fig. 5.

would appear broad enough on the plate that they would not be confused with the characteristic lines. One of the photographs is reproduced in Fig. 7. On the original, three broad and diffuse lines can clearly be seen in the position marked X due to lines in the focal spot which might cause error, were not their true origin known. The tungsten lines are due to evaporation from the filament and the nickel lines from the nickel used in spot welding the

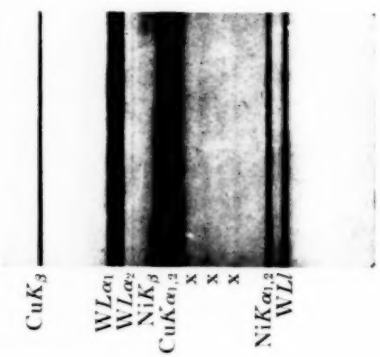

Fig. 7. Photograph taken with fixed crystal, no absorbing material, and narrow slit close to crystal, using radiation from the whole copper target. Three broad and diffuse lines due to lines in the target are marked by an X.

filament cup. Photographs were again taken with the carbon absorbing material in place and showed no indication of a modified line due to absorption.

III. Summary of Results

An analysis, by means of the double crystal spectrometer, of characteristic molybdenum $K\alpha_1$ x-rays scattered by carbon and beryllium, has failed to show

the existence of fine structure lines due to absorption of an amount of energy equal to the binding energy of the electrons in the scattering substance. The method was sufficiently sensitive to detect a line of intensity greater than 10 percent of molybdenum $K\alpha_1$ unmodified. This is in agreement with the results of all other experimenters since the fine structure was first reported.

An analysis of x-rays transmitted through carbon has failed to show a similar change of wave-length without scattering, as certain lines observed by Ray and Majumdar were interpreted. For molybdenum $K\alpha_1$ absorbed in carbon, a line of intensity of the order of 1 in 750, as compared with the intensity of the incident primary radiation, could have been detected with the single crystal method, and a line of the order of only 1 in 3000 with the double crystal spectrometer. For copper $K\alpha_{1,2}$ absorbed in carbon, a line of the order of 1 in 800 could have been detected. In discussing his results, Ray assumed that the intensity of the new lines as compared with the intensity of the primary, was of the order of 1 in 400 or 500. Thus the present experiments were sufficiently sensitive to detect a line of considerably less intensity. Two possible sources are suggested which may give rise to lines similar to those observed by Ray and ascribed to this absorption phenomenon.

In conclusion, the author wishes to express his indebtedness to Professor Bergen Davis for his interest in this work and for full privileges in his laboratory, and to the authorities of Columbia for a University Fellowship.

PHOTOELECTRIC PROPERTIES OF COMPOSITE SURFACES AT VARIOUS TEMPERATURES AND POTENTIALS

By Dimiter Ramadanoff
Department of Physics, Cornell University, Ithaca, New York

Abstract

Experiments designed to determine the variation of photoelectric current with temperature and plate potential for barium photoelectric cells are described. The technique used in making the cells is also given. A new method, employing interrupted illumination, a transformer coupled amplifier and a cathode ray oscillography, is developed for measuring the photoelectric current. In this way the thermionic current and currents of slow response are completely eliminated and only the a.c. component of the photo-current is amplified.

Experimental results. With constant plate voltage the photoelectric current increases gradually with temperature and at about 600°C is nearly twice as large as the current at room temperature. As the temperature however is raised from 600°C to 750°C the increase in photoelectric current for steady illumination is 100-fold while for interrupted illumination it is only 17-fold. The smaller increase in the latter case may be explained in view of the elimination of all sluggish currents produced by light in some secondary way. While the two curves for steady and interrupted illumination are similar in appearance, the latter has a maximum at 560°C which resembles very much a resonance peak.

The increase or decrease in photoelectric sensitivity with temperature for composite surfaces consisting of barium and oxygen on platinum may be explained by the diffusion of barium or oxygen on the surface. The increase in saturation voltage of the potential-current curves with temperature may likewise be explained by an increase in the contact potential brought about by a change in the work function.

Introduction

THE variation of photoelectric current with temperature for both oxides and pure metals has been studied by a number of investigators. Merritt[1] found that the photoelectric current obtained by illuminating the oxide-coated filaments of Western Electric audion bulbs increased in some instances 1400 times as the temperature of the filament was raised from that of the room to dull red heat. Large increases of photoelectric current with temperature for filaments coated with various oxides were also reported by Koppius,[2] Crew,[3] Berger,[4] Newbury,[5] and others. Similarly for pure metals Du Bridge[6] and Warner[7] using platinum and tungsten respectively have measured an increase in the photoelectric current with temperature. In all of these

[1] E. Merritt, Phys. Rev. **17,** 525 (1921).
[2] O. Koppius, Phys. Rev. **18,** 443 (1921).
[3] W. H. Crew, Phys. Rev. **28,** 1265 (1926).
[4] C. E. Berger, Phys. Rev. **34,** 1566 (1929).
[5] K. Newbury, Phys. Rev. **34,** 1418 (1929).
[6] Du Bridge, Phys. Rev. **29,** 451 (1927).
[7] A. H. Warner, Phys. Rev. **33,** 815 (1929).

instances however, both the oxide-coated and the pure metal filaments were poor photoelectric and good thermionic emittors and consequently a number of difficulties were encountered. The photoelectric current at room temperatures was small, while at the higher temperatures the thermionic current was large and in most cases masked the whole photoelectric phenomenon. Moreover in the investigations referred to the photoelectric current was measured with no regard to time response, for which Lawrence and Beams[8] have reported a value of 3×10^{-9} second. Sluggish currents which may have been present with the photoelectric current are attributed to the true photo-current. In this connection Bodemann,[9] who has studied the photoelectric emission from filaments coated with the oxides of Ba and Ca at various temperatures, has named the increase in photoelectric current with temperature "addition current." This "addition current" he explained as due to the action of light on the negative space charge adjacent to the cathode. According to this view the "addition current" is to be regarded as nothing else than an increase in the thermionic current. Such currents however should be expected to have considerable time lag and are hardly to be regarded as true photoelectric currents.

The present investigation was undertaken for the purpose of studying the variation of the photoelectric current with temperature for barium photoelectric cells with both continuous and interrupted illumination. The barium cells were constructed in a manner similar to that described by Case.[10,11] It was felt by the author that the barium cells were particularly suited for the study of the above mentioned phenomena not only because they were remarkably sensitive to ordinary visible light, but also because Case[10] has already observed a 100-fold increase in the photoelectric current as the temperature of the cell was raised to just under dull red heat. The determination of the variation of the photoelectric current with temperature with and after eliminating all sluggish currents with rapidly interrupted illumination and proper filter circuits, forms the chief endeavour of this investigation.

Apparatus

a. Vacuum system. The vacuum system consists of two liquid air traps, a two-stage mercury diffusion pump and a Cenco oil pump. No stopcocks were used on the high vacuum side. The McLeod gauge which was made entirely of glass is sealed between the liquid air traps and the mercury diffusion pump. The high vacuum side was made as short as possible with tubing of large diameter. Pyrex glass was used for the whole system and for convenience it was mounted on a rigid metal frame. This latter arrangement permitted a complete torching of the entire high vacuum side before the photoelectric cells were made.

[8] Lawrence and Beams, Phys. Rev. **32,** 478 (1928).
[9] E. Bodemann, Ann. d. Physik **3,** 614 (1929).
[10] T. W. Case, Phys. Rev. **17,** 398 (1921).
[11] T. W. Case, Proc. Am. Electrochem. Soc. **39,** 423 (1921).

b. Photoelectric cells. In the experiments to be described later several cells of slightly different construction were used. The most photoelectric typical cells are shown in Fig. 1 and Fig. 2. The glass of the cell in Fig. 1 is made of Pyrex and quartz joined together by means of a graded seal. No cement joints were used at any time with the photocells. In this particular cell the anode F consists of an oxide-coated Western Electric filament which was spot-welded to two tungsten leads. A thin platinum strip P, about 3 mm wide and 2.5 cm long, was similarly welded to another pair of tungsten leads, and served as cathode. These latter leads were made of two different sizes of tungsten wire. The finer leads were so selected as to reduce the cooling at the ends of the platinum strip which was heated by passing a current through it

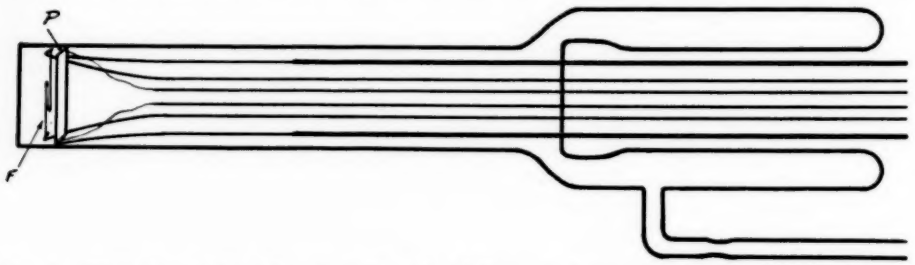

Fig. 1. Diagram of photoelectric cell made of Pyrex and quartz joined with a graded seal.

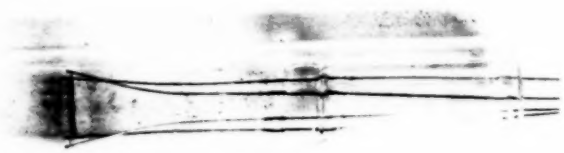

Fig. 2. Photograph of a typical photoelectric cell made entirely of Pyrex glass.

from a storage battery. Provision was made to measure the potential drop across the platinum strip in order to determine its temperature. For this purpose two fine platinum filaments were welded across the plate and the center pair of tungsten leads. All tungsten wires were sealed directly through the Pyrex.

No efforts were spared in thoroughly outgassing the cells before the photosensitive material was deposited. Three electric ovens were used to bake out photocells together with the traps and the few centimeters of adjoining tubing. The temperature of the ovens was kept constant at 550°C for more than 24 hours. In the meantime the McLeod gauge and the remaining glass on the high vacuum side were thoroughly torched. During the bake out, the filament F and the plate P were heated several times to yellowish-red colour.

Great care was also used in preventing any mercury vapor from getting into the cell. While the cell and the trap next to it were kept at 550°C, the oven of the second trap was removed and liquid air applied. Liquid air was then applied to the next trap, and finally the oven of the cell was removed. In making some of the cells a charcoal trap immersed in liquid air was used next to the cell to improve the vacuum still further. In most cases however the burning of thoriated tungsten filaments was found to be most satisfactory. With all these precautions taken, the pressure was not greater than 10^{-7} mm of Hg.

During the process of making the photoelectric cells the functions of the electrodes are reversed. The filament F is heated to a temperature of about 1100°C or more and is used as a source of thermionic current. At the same time the platinum strip P is used as anode and its potential with respect to the filament is gradually increased to 400 volts or more. For several minutes the thermionic current is very small, but as soon as the filament is "activated" or "broken down," the thermionic current increases greatly and the plate voltage and filament temperature have to be reduced until the emission current is limited to a safe value. Then by varying the plate voltage from 200 to 700 volts for various filament temperatures a condition is finally reached when barium or oxygen, or both begin to evaporate from the filament and deposit on the plate. Soon the plate becomes coated with a very thin layer of deposit which has a brownish appearance. The plate so coated is remarkably sensitive to light and is used as the emittor of photoelectrons, while the filament serves as collector. That the evaporated material is barium and oxygen on platinum seems very likely in view of the recent work of Becker[12] who found that metallic barium evaporates from an activated oxide-coated filament if the temperature is not too high and if the emission current is small. He also found that oxygen evaporates if the temperature is high enough and if the thermionic current is limited not by space charge but by emission. Since the conditions under which the photoelectric cells were made correspond to those described by Becker it seems very likely that oxygen and barium evaporated either simultaneously or consecutively. In such a case one would expect the sensitivity of the cell to vary, in analogy with the thermionic emission, with the relative position of barium and oxygen with respect to the platinum. As will be seen later this seems to be the case in most of the experiments. If the oxide-coated filament is heated during the making of the cell to a very high temperature barium oxide evaporates. A cell which was made in this way gave no measurable current with the sensitive galvanometer in use.

At the present time there seem to be two different opinions as to the mechanism of production of barium from an oxide-coated filament. One view maintains that the oxide dissociates by a thermal reaction, while the other view favors the production of barium through electrolysis of the oxide. In this connection it may be of interest to mention that a photoelectric cell can be made by merely heating the oxide-coated filament i.e. without applying

[12] J. A. Becker, Phys. Rev. **34,** 1323 (1929).

any voltage. Under this condition however the "breaking down" of the filament is rather slow and the temperature to which the filament should be heated is much higher. The result is that mostly barium oxide evaporates and the cell so made is rather insensitive to light.

The filaments of most of the photoelectric cells were coated with oxide by rubbing barium nitrate crystals on a red hot platinum-iridium ribbon, or by dipping the ribbon several times in a solution of barium nitrate. These filaments were more desirable than the commercial type because the oxide coating consisted mostly of barium oxide with traces of strontium and calcium oxides. The photoelectric cells which were made with these filaments were sensitive, not only to the ultraviolet light but also to visible light. This latter feature was particularly desirable because it made the use of the quartz mercury arc unnecessary.

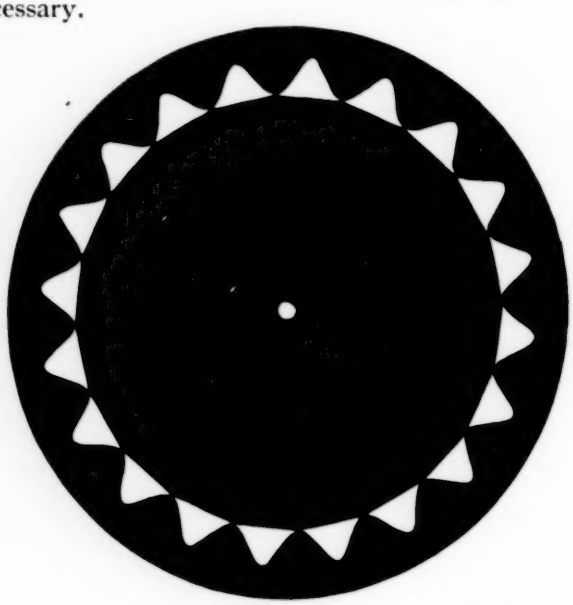

Fig. 3. Disk used to interrupt the light falling on the photoelectric cell.

It was found best to make the photocells after they are sealed off. If a cell is made while on the pumps its sensitivity decreases considerably in the course of time. This shows how detrimental traces of gases are to the sensitive material.

c. Source of illumination. As already mentioned the cells which were made with the Western Electric oxide-coated filaments were sensitive only to the ultraviolet light and therefore a quartz mercury arc was used for a light source. In all cases the total radiation from the light was allowed to fall on the cell. The intensity of the light remained remarkably constant after the lamp had reached its operating temperature.

[13] For a detailed description of the disk, the amplifier and their use in connection with the photoelectric cells and the cathode-ray oscillograph see: "A Method of Studying the Effect of Temperature on Photoelectric Currents," D. Ramadanoff, R. S. I. **1**, 768 (1930).

For the interrupted illumination[13] an incandescent lamp was used. The filament of a 500-watt projection lamp was focused on the platinum strip of the cell. Between the cell and the source were situated a water cell, a shutter, and a revolving disk. The disk shown in Fig. 3 has twenty holes around its periphery. The shape of the holes is of the form $y=\sin^2 x$. It is easy to see that the light passing through these holes, as the disk revolves at constant speed, will vary sinusoidally and will give approximately a sinusoidal photoelectric current superimposed on a d.c. current. Each hole of the disk gives a complete cycle of the a.c. wave.

d. Measuring instruments and method. The photoelectric current was measured with two different sets of apparatus both of which are shown diagrammatically in Fig. 4 and Fig. 5. Two galvanometers having current sensitivities of 2.96×10^{-10} and 3.4×10^{-9} respectively were used. The difference

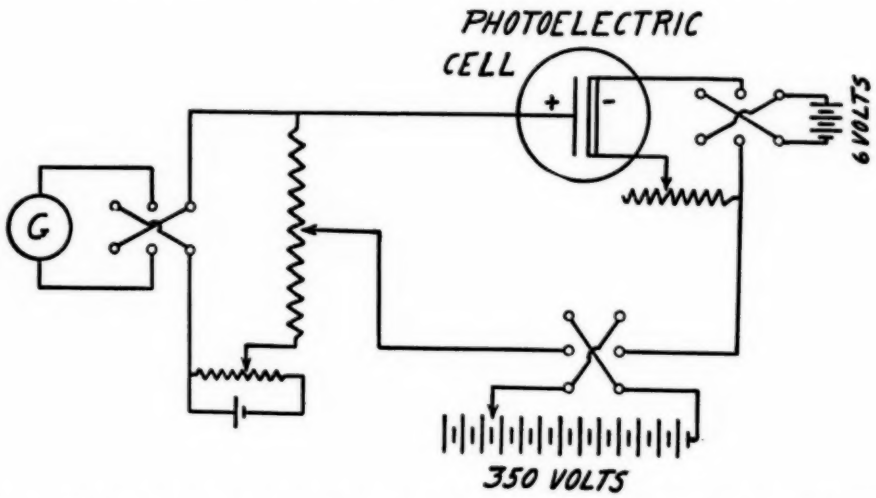

Fig. 4. Circuit diagram of photoelectric cell and galvanometer used to measure the current produced by steady illumination.

in the galvanometer deflections obtained with the light on and off were recorded as true photoelectric currents. In most cases the thermionic current was not balanced because the photoelectric current was large and was read with no difficulty. One of the photoelectric cells which was used in the experiments gave 0.592 μa saturation current with the plate cold, when the light from 150-watt lamp was focussed on the cell. It is evident from the brief description of the circuit that with the galvanometer only the total current due to light can be measured. Sluggish currents which may be due to light in some secondary way cannot be distinguished from the true photocurrents which are characterized by a very short time response.

The circuit in Fig. 5 was designed to eliminate the thermionic current and any sluggish currents which may be present, and to amplify only the true photocurrents.[13] After two stages of amplification the current is impressed on one pair of plates of a "Bedell-Reich Stabilized Oscilloscope," a visual cath-

ode-ray oscillograph. The deflections of the cathode spot indicate on the fluorescent screen not only the wave shape of the current but also its magnitude. From measurements of the amplitude of the voltage wave the photocurrent can easily be determined. A photograph of the a.c. wave as it appeared on the screen is shown in Fig. 6. In this particular case a disk with circular holes was used and therefore the wave shape of the photoelectric current is not sinusoidal.

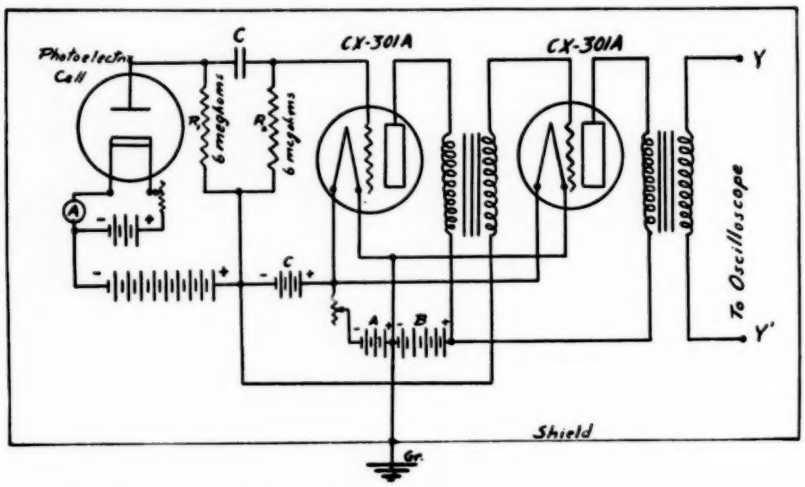

Fig. 5. Circuit diagram of photoelectric cell, amplifier and cathode-ray oscillograph used to measure the current produced by interrupted illumination.

The temperature of the photoelectric material was varied by passing various currents through the strip. By measuring the potential drop across the platinum strip, it was possible to determine its change in resistance and therefore its temperature. At the higher temperatures an optical pyrometer was used as a check. During the photoelectric measurements the heating cur-

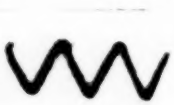

Fig. 6. Photograph of a.c. wave as it appeared on fluorescent screen.

rent was not interrupted since it was found that the oscilloscope deflections were the same whether the heating current was on or off provided that the temperature of the strip did not change when the photoelectric current was measured. The oscilloscope was particularly useful for eliminating this difficulty since the response of the cathode spot is practically instantaneous. Such an observation would have been impossible with the ordinary galvanometer or electrometer. It is of interest to notice that this result is contrary to the hypothesis of Shenstone[14] who suggested that the change in photoelec-

[14] A. G. Shenstone, Phil. Mag. **45**, 918 (1923).

tric sensitivity was due to changes in the metal which were produced by the current flowing through it.

Experimental Results

A. Measurements made with galvanometer*

a. Potential-current saturation curves. Fig. 7 shows the variation of photoelectric current with potential applied between the electrodes when the light intensity is kept constant and the photoelectric surface is at room temperature. The low saturation potential and the reproducibility of the photoelectric current with both increasing and decreasing potentials is typical of all photoelectric cells used in the experiments. This latter feature is clearly indicated on the curve with large and small circles, the large circles being used for increasing potentials.** It is also easy to see from this curve that the

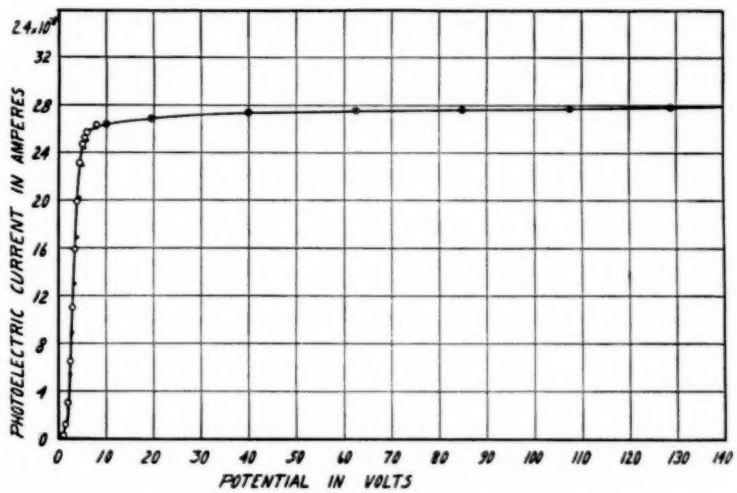

Fig. 7.

photoelectric current saturates as well as can be expected of a cell with a composite surface. In the experiments the plate potential was increased to 300 volts which is about 40 times the saturation potential and produces a gradient between the electrodes of more than 1000 volts per cm. But even at these high potentials the photoelectric current remained substantially constant.

In Fig. 8 is shown a family of saturation curves for constant illumination and for different temperatures of the photoelectric surface. The values of the photoelectric current for increasing and for decreasing potentials are so closely identical that they are represented by single curves. The thermionic current at the temperatures at which the curves were obtained was either small or zero. The saturation potential of all three curves increases with

* Under this heading the photoelectric current is defined as the difference in galvanometer deflections with the light on and off. In all cases the total radiation from the lamp was used.

** This notation is used for all curves.

temperature, i.e., the saturation points are shifted to the right. This experimental evidence is just the opposite of what has been reported by Crew[3] who found that the saturation potential decreases as the temperature of the photoelectric surface is increased. That the shift should be as in Fig. 8 is evident from the fact that the contact difference of potential changes with a change in the work function. If the thermionic current however is large and the emission is limited by space charge then the increase in saturation potential with temperature will be greater and will be due partly to the increased space charge.

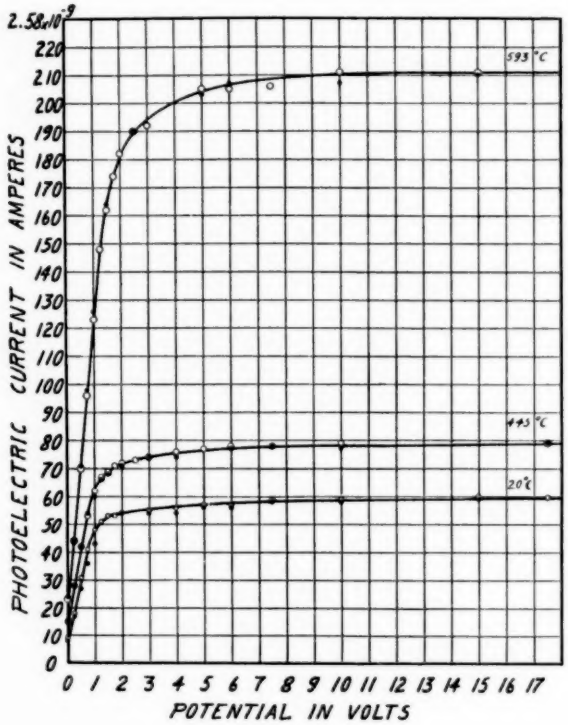

Fig. 8.

From the curve in Fig. 8 it is also evident that the photoelectric current increases with temperature. This increase in emission can be accounted for qualitatively by the relative position of barium and oxygen with respect to the platinum. The experiments which were performed to obtain these and other curves seem to indicate that the decrease in activity of the photoelectric material at room temperature is due to the negatively charged oxygen ions which have diffused to the surface on top of the barium layer. Since the photoelectrons come from the barium the strong surface field of the oxygen will tend to hinder the emission. But as the temperature of the plate is increased, more and more barium diffuses to the surface and exchanges place with the oxygen. Beyond this point any further increase in temperature

should not increase the emission. As will be seen later temperature-current curves were obtained which tend to show that this is probably the case.

Another possible explanation is that the light acts not only on the barium layer but also on the negative adsorbed oxygen ions and changes them to neutral atoms. Under this condition the photoelectric and thermionic emission will increase with light. In this connection Bodemann[9] seems to maintain that the total increase in the photoelectric emission with temperature is due to the action of light on the negative space charge and he calls this increased current "addition current," which in reality is nothing else than an increase in the thermionic current. It is hard to believe however that the total increase in current due to light is thermionic, because currents which are produced indirectly by the action of light on a negative space charge

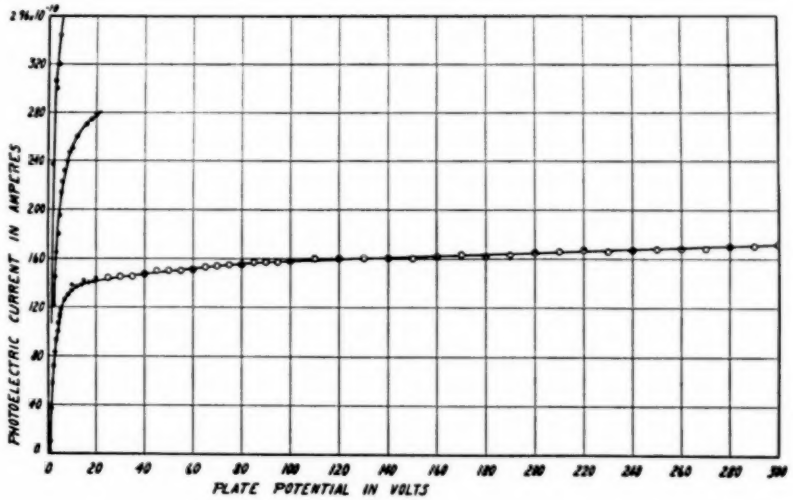

Fig. 9.

should be expected to have considerable time lag. As will be seen later experiments were performed to prove this point by the use of rapidly interrupted illumination.

A group of saturation curves which in all respects are similar to those in Fig. 8 are shown in Fig. 9. These curves however were obtained with a different photoelectric cell the anode of which was built in the form of a squirrel cage by welding fine thoriated tungsten wires on two nickel rings. The filament wires were spaced two mm apart and could be heated to incandescence by passing current from one ring to the other. In this way the anode served not only as collector but also as a "getter."

b. Variation of photoelectric current with temperature at constant plate potential. The curve in Fig. 10 brings out many interesting points which were not evident from the previous curves. In spite of the fact that this curve was taken when the total radiation of the mercury arc shone on the cell, its general appearance has a striking resemblance to the curves reported by War-

ner[7] for pure tungsten with monochromatic illumination. The curve shows that at 800°C the photoelectric current reaches saturation and is at this temperature about 100 times greater than the photoelectric current at room temperature. The fact that the emission increases only slightly until a temperature of 600°C is reached, seemingly confirms the hypothesis that the increased activity is due to the diffusion of barium to the surface. It is particularly significant, in view of the low melting point of barium (850°C), that the greatest increase in photoelectric current occurs between the temperatures of 600°C and 750°C.

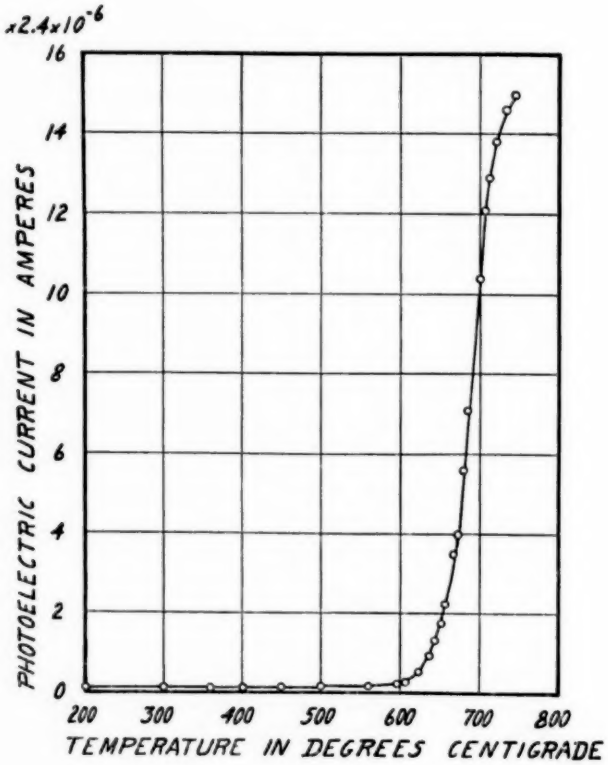

Fig. 10.

B. MEASUREMENTS MADE WITH CATHODE RAY OSCILLOGRAPH

a. Variation of photoelectric current with temperature at constant plate potential. In this group of experiments three photoelectric cells were tested and found to exhibit the same general characteristic. The curve in Fig. 11 was obtained by varying the light intensity sinusoidally with a frequency of 1000 cycles per second. The thermionic current, the d.c. component of the fluctuating photoelectric current, and all sluggish currents were completely filtered out. Only the a.c. component of the photoelectric current was allowed to pass through the amplifier. The sluggish currents were noticeable in the measurements only when the frequency of the interrupted light was

reduced to a few cycles per second. The data for the curve in Fig. 11 were obtained by measuring the amplitude of the a.c. wave on the fluorescent screen of the cathode ray tube. This curve is very similar to that shown in Fig. 10 except that the maximum and minimum values differ by a factor of 16 instead of 100. The peak at 560°C suggests a resonance phenomenon and was reproducible with both increasing and decreasing temperatures as shown by the large and small circles on the curve. The curve further shows that the optimum emission occurs at 750°C. Above this temperature the photoelectric emission decreases gradually. This decrease may be caused either by the diffusion of more barium ions which increase the surface concentration be-

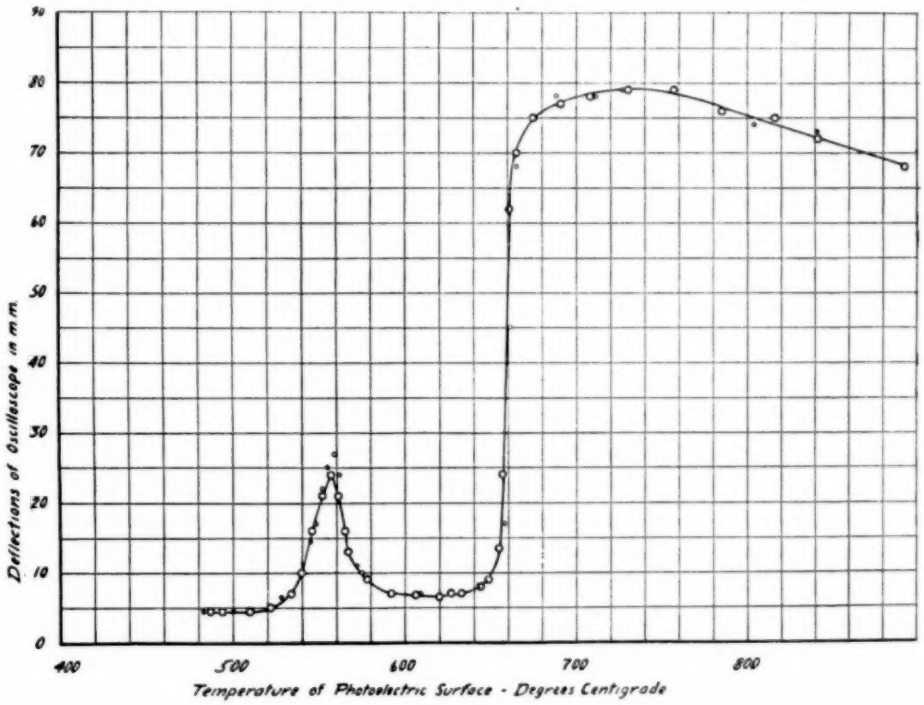

Fig. 11.

yond that necessary for the optimum emission, or else by the reappearance of oxygen ions. It is doubtful if this decrease is caused by the evaporation of barium or oxygen ions since thin adsorbed layers will adhere to the platinum surface at high temperatures much better than thick, heavy coatings.

It is of interest to obtain potential-current curves as in Fig. 8 and Fig. 9 with interrupted illumination. It is of particular interest to determine what effect the sluggish currents will have upon the long wave-length limit of the photoelectric surface used. At the present time the apparatus is not sensitive enough to permit such measurements.

Discussion

The increase in photoelectric emission with temperature from composite surfaces containing barium and oxygen on platinum cannot be explained

satisfactorily by surface gas contamination. The activity of such surfaces depends not only on the surface concentration of metallic barium and oxygen, but also on the relative position of the two. It is unlikely that the thin adsorbed layers of oxygen and barium will leave the surface without using very high temperatures which will distill off the photoelectric material and ruin the cell. Most of the oxygen on the surface due to its strong electron affinity is negatively charged. The barium which diffuses on the surface at the higher temperatures changes the intensity and the distribution of the surface fields and as a result changes the work function. This change in work function produces a change in the contact differences of potential which manifests itself in an increase of the saturation potential with temperature if the thermionic current is small. When large thermionic current limited by space charge is present the increase in saturation potential with temperature is caused also by the increase in space charge.

Any increase in thermionic current which may be caused by the heat rays of the light source or by the influence of the light alone in some secondary way should not be regarded as a true photoelectric current. The experiments with the oscillograph show definitely that part of the increased emission due to light at the higher temperatures is not caused by such secondary effects but is due to an increase in the photoelectric current. This finding is contrary to the results obtained by Bodemann. The increased photoelectric current is independent of the frequency of light interruptions for the range used from 500 to 1000 cycles per second.

The author is deeply indebted to Professor Ernest Merritt for suggesting the problem and for his many valuable suggestions and helpful criticism, and to Professor Frederic Bedell for his general interest in this investigation and for providing the Oscilloscope and other facilities in connection with the work. He also gratefully acknowledges the benefits derived from discussions with Dr. J. A. Becker and Professor H. A. Barton. For the construction of the glass apparatus thanks are due to Mr. H. W. Banta.

THE ENERGY OF DISSOCIATION OF MERCURY MOLECULES

By J. Gibson Winans
Department of Physics, University of Wisconsin
(Received March 5, 1931)

Abstract

The absorption spectrum of mercury vapor in the Schumann region showed three apparently continuous bands with maxima at wave-lengths 1849, 1808, and 1692. The 1849 and 1692 bands appeared without the 1808 band in the emission from an electrodeless discharge through mercury vapor. The absorption spectrum in the region 1900–1804 is correlated with a pair of potential energy curves for Hg_2. From these curves, the energy of dissociation of Hg_2 is 0.15 volts.

Introduction

THE problem of the energy of dissociation of mercury molecules is particularly interesting because, as far as chemical evidence is concerned, mercury molecules do not exist. For example c_p/c_v for mercury vapor is 1.666, the value for a purely monatomic gas. Also the molecular weight of mercury vapor equals that of liquid mercury.[1] Nevertheless mercury molecules exist in both the excited and unexcited states as evidenced by the presence of bands in the absorption and emission spectra of mercury vapor.[2]

The binding force between two mercury atoms must be similar to that between two helium atoms since both have a closed outer shell containing two paired s electrons. So far three types of binding for diatomic molecules have been proposed; ionic as in NaCl, exchange forces as in H_2, and polarization or van der Waal's forces. The binding between neutral mercury atoms can not be ionic, and Heitler and London[3] have shown that the exchange forces between helium-like atoms must be repulsive if the Pauli exclusion principle holds. There remain only the polarization forces to hold the mercury molecule together. The analysis of Eisenschitz and London[4] has shown that the polarization forces may, at large separations be greater than the exchange forces and produce a definite equilibrium when the exchange forces are repulsive. Mercury molecules are probably of this type.

Values for the energy of dissociation of mercury molecules have been obtained by Koernicke[5] and Mrozowski.[6] Koernicke, following the work of Franck and Grotrian,[7] measured the change in total intensity of the mercury

[1] Summary by J. W. Mellor, Treatise on Inorganic and Theoretical Chemistry, vol. 4, p. 766.

[2] R. W. Wood, Astphys. J. **26,** 41 (1907); Rayleigh, Proc. Roy. Soc. **A116,** 702 (1927); F. L. Mohler and H. R. Moore, J.O.S.A. **15,** 74 (1927).

[3] W. Heitler and F. London, Zeits. f. Physik **44,** 455 (1927).

[4] R. Eisenschitz and F. London, Zeits. f. Physik **60,** 515 (1930).

[5] E. Koernicke, Zeits. f. Physik **33,** 219 (1925).

[6] S. Mrozowski, Zeits. f. Physik **55,** 338 (1929).

[7] J. Franck and W. Grotrian, Zeits. f. Tech. Physik **3,** 194 (1922).

band at 2540 with superheating and calculated the energy of dissociation of Hg_2 as 1.4 kg. cal./mol. or 0.06 volts. Mrozowski measured the total intensity of fluorescence in mercury vapor at different positions along the direction of the exciting light. He obtained the absorption coefficient of saturated mercury vapor at different temperatures for several exciting wave-lengths. Assuming this coefficient proportional to the number of Hg_2 molecules, he calculated D for Hg_2 as 17 kg. cal./mol. Koernicke's and Mrozowski's values differ by a factor 12. The two methods will be discussed in detail in a later paper.

The results of the present investigation give a value for D for Hg_2 which lies between the two above mentioned but is quite different from either. The method is the same as that used to obtain D for Zn_2 and Cd_2.[8] The value of D comes from an interpretation of the absorption region in the vicinity of the resonance line 1^1S-2^1P. This line comes at wave-length 1849 for mercury.

Apparatus and Procedure

The absorption spectrum of mercury in the region 3000–1550 was photographed with a small vacuum fluorite spectrograph on Schumann plates. The absorption cell, shown in Fig. 1, was made of fused quartz. The windows were

Fig. 1.

very thin to give increased transparency and hemispherical in shape to withstand atmospheric pressure. The cell was heated in an electric furnace. A hydrogen discharge tube served as a source of continuous light.

For photographing the emission spectrum of mercury, the cell of Fig. 1 was waxed to a tube leading to the spectrograph, a wire wrapped around each end, one wire grounded and the other connected to a low-voltage Tesla coil (leak chaser). When the tube was heated by a bunsen burner, a brilliant mercury discharge was obtained. CO bands from a discharge through air were used as standards for wave-length measurements.[9]

Results

The absorption spectra taken with increasing pressures of mercury vapor (Fig. 2) show first the atomic line 1849 which broadens rapidly, then a continuous band with a maximum intensity at 1808 A (Fig. 2 No. 1) and finally another continuous band with maximum at 1692 (Fig. 2, No. 2), Fig 3 is a microphotometer record of Fig. 2 showing the 1692 band. Fig. 2, No. 2 shows how, at increased pressure the 1808 band is broadened principally toward

[8] J. G. Winans, Phil. Mag. **7**, 555 (1929).

[9] T. Lyman, Astrophys. J. **23**, 204 (1906); "The Spectroscopy of the Extreme Ultraviolet," p. 114.

longer wave-lengths and the absorption region surrounding 1849 broadened toward shorter wave-lengths as far as the 1808 band but no farther, and toward longer wave-lengths beyond 2200 A. The lack of intensity below 1690 in No. 1 Fig. 2 was due to short exposure and not to absorption.

Fig. 2.

Fig. 3.

In the emission spectrum from the electrodeless discharge (Fig. 2, No. 3), the band surrounding 1849 and the one at 1692 were observed but not the one at 1808. The distribution of intensity in the 1692 band was the same in emission and absorption (Fig. 3).

TABLE I.

Description	Wave-length	Vacuum wave-number
Absorption maximum	1691.4	59123
Emission maximum	1692.1	59097
average	1691.8	59110
Absorption maximum	1808.0	55311
*Short wave limit	1804.2	55427

* The wave-length was measured at the point where the photographic blackening from the source had been reduced to one half.

Table I gives a summary of results. Wave-lengths previously given (Phys. Rev. **36**, 1020(1930) should be corrected to agree with Table I.

DISCUSSION

The continuous bands at 1808 and 1692 do not coincide with atomic transitions and are observed only at pressures much greater than that needed to show the atomic line 1^1S-2^1P. They are therefore attributed to molecules of mercury and these molecules are assumed to be diatomic. The characteristics of these bands as described above can be correlated with a set of potential energy curves for the Hg_2 molecule.

The band at 1808 was observed in absorption but not in emission in the electrodeless discharge. In the spectra of atoms, absorption lines are sometimes missing in emission because they are absorbed by the vapor surrounding the source. This can not be the case for the 1808 band; since, from the

order of appearance of the bands with increasing pressure, the absorption coefficient of the missing band 1808 lies between that of the two bands at 1849 and 1692, both of which were observed in emission. A probable reason for the non-appearance of 1808 in emission is that the Hg_2 molecule is dissociated upon absorption of this wave-length. If this is true, the curves of potential energy as a function of nuclear separation must have definite relative positions. According to the Franck-Condon principle, the nuclei of a molecule do not change their separation appreciably during an electron transition. If curves of potential energy and nuclear separation are plotted for the excited and normal molecule, allowed transitions are represented by vertical lines connecting the two curves. For interpreting absorption spectra, one assumes a Boltzmann distribution of molecules in the vibrational states of the normal molecule, so that the lowest vibrational state with 1/2 quantum of energy is the most thickly populated. The most intense part of an absorption band should be represented by vertical lines through the points of the normal mole-

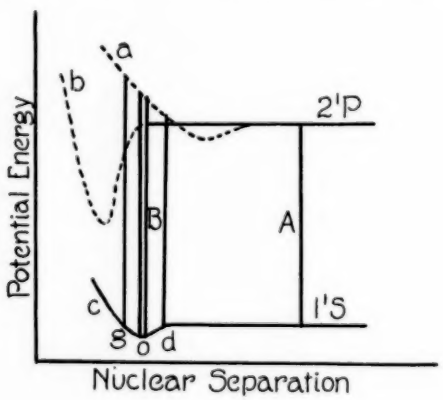

Fig. 4.

cule curve, corresponding to this lowest energy. If absorption of the 1808 band results in dissociation of an Hg_2 molecule, the potential energy curves must have relative positions like either *c* and *a* or like *c* and *b* in Fig. 4. If positions *c* and *a* are correct, after absorption of 1808, (transition B) the nuclei find themselves with sufficient potential energy to dissociate into one excited and one normal atom. This is the usual interpretation given to a photo-chemical dissociation. If curves *c* and *b* are correct, the nuclei simply lose all attraction for each other upon absorption of 1808, and find themselves free to drift apart. In either case the band 1808 should be observed in absorption but not in emission.

If the original assumption that absorption of 1808 means dissociation is correct, it is not difficult to decide which of the two relative positions shown in Fig. 4 must be right. From analogy with He_2, which is found to exist only when excited, the energy of binding in the excited mercury molecule is probably greater than that in the normal molecule. In practically all molecules which have been studied, greater energy of binding is associated with

smaller nuclear separation at the minimum of the potential energy curve, so that curves *c* and *b* should be required for Hg_2. If curves *c* and *a* were correct, with increase of pressure and temperature and corresponding increase in the number of normal molecules in higher vibrational states, the 1808 band (*B*, Fig. 4) should broaden toward both longer and shorter wave-lengths corresponding to transitions from points *g* and *d*. This does not agree with the observation that the 1808 band broadened almost entirely toward longer wave-lengths. On curve *c* and *b*, however, we see that 1808 represents the longest vertical distance between the two curves and absorption from points *g* and *d* would give a broadening toward longer wave-lengths only.

Further we can also explain the very interesting fact that the absorption region surrounding 1849 reaches a short wave limit coinciding with that for the 1808 band, but reaches no definite long wave limit. Consider two mercury atoms making a collision. Their mutual potential energy would follow the curve for the normal mercury molecule (estimated as curve *c*, Fig. 4). If they absorbed light during a collision, the energy absorbed would correspond to vertical lines between the two potential energy curves of Hg_2, and since they come to rest at point *g*, Fig. 4, and move more slowly at point *d* than at *o*, the positions *g* and *d* would be more probable positions for the absorption of light. This would represent wave-lengths slightly greater and slightly less than that of the atomic absorption line 1849. Now suppose the number of colliding atoms which absorb light to be greatly increased, one should observe absorption from points *c* and *o*. This would mean a continuous broadening of the 1849 line toward both longer and shorter wave-lengths but it would reach a limit on the short wave side coinciding with the limit for the 1808 band. This exactly describes what was observed. Of course, it is not sure that the short wave limit of 1849 exactly coincides with that of 1808 since the observed limit comes from a superposition of both. It is, however, significant that the 1849 band does not broaden beyond 1804 on the short wave side but broadens beyond 2200 on the long wave side.

We have correlated a set of curves such as *b* and *c*, Fig. 4, with three observations; the appearance of 1808 in absorption but not in emission, the broadening of the 1808 band toward longer wave-lengths with pressure, and the peculiar broadening of the 1849 band with pressure.

From Fig. 4 it is easily seen that the energy of dissociation of the normal molecule is simply the difference in energy between the 1849 and the 1808 bands. This gives *D* for Hg_2 equal to 0.15 volts or 3.5 kg. cal./mol. This value is three times Koernicke's value and one-third of Mrozowski's. The three methods will be compared and discussed in a later paper.

PROPERTIES OF SOME ZINC, CADMIUM, AND MERCURY BANDS

By J. Gibson Winans
University of Wisconsin

(Received March 16, 1931)

Abstract
Zinc bands at wave-lengths 2139, 2064, and 2002 are shown to resemble the corresponding bands of cadmium and mercury in emission as well as in absorption.

THE absorption spectra of zinc, cadmium, and mercury each show three corresponding continuous bands which may be called A, B, and C. The wave-lengths at the maxima are given in Table I. It has been shown[1] that

Table I.

	A	B	C
Zinc	2139	2064	2002
Cadmium	2288	2212	2114
Mercury	1849	1808	1692

for cadmium and mercury the bands A and C appear in emission in an electrodeless discharge but not the band B. The present experiment was undertaken to see if the same thing were true for the zinc bands.

A quartz tube was evacuated and sealed off after having had some zinc distilled into it. Nicrome wires wrapped around the ends served as external electrodes. One electrode was grounded and the other attached to a small Tesla coil (leak chaser). When the tube was heated by blow torches to give a stream of zinc vapor through the tube, a bright discharge was obtained. In stagnant vapor the discharge was very weak. This may have been the result of impurities as observed by Wood and Voss[2] in mercury vapor. Spectra were photographed with nitrogen flowing through the spectrograph to eliminate oxygen.

The resulting discharge through zinc vapor showed band A with great intensity and with the maximum reversed, and showed also band C. No trace of band B was observed. These observations are the same as those on the corresponding bands for Cd and Hg.[1] An interpretation for one set of these bands will apply to all since the bands are shown to have the same properties. One interpretation[1] gives energies of dissociation of zinc, cadmium, and mercury molecules of 0.24, 0.20, and 0.15 volts respectively.

There was observed only one difference in the behavior of these bands relative to each other for the various elements. In the absorption spectra, the zinc bands B and C appeared with increasing pressure at practically the same pressure; the cadmium band C required about 1.7 times that required for band B, and the mercury band C needed about 5 times as much pressure as the mercury band B for equal intensities. This does not affect the interpretation given to the bands but it may indicate an interesting change in properties of similar elements with increasing atomic weights.

[1] Winans, Phil Mag. **7**, 555 (1929); Phys. Rev. **37**, 897 (1931).
[2] R. W. Wood and V. Voss, Jour. Frank. Inst. **205**, 486 (1928).

PERTURBATIONS AND PREDISSOCIATION IN THE S_2 BAND SPECTRUM

By Andrew Christy and S. Meiring Naudé
Ryerson Physical Laboratory, University of Chicago

(Received February 27, 1931)

Abstract

The S_2 bands belonging to the $^3\Sigma_u^- \leftrightarrow {}^3\Sigma_g^-$ transition have been photographed with relatively large dispersion in absorption and in emission between λ3500 and λ2400. Several perturbations have been found in the vibrational levels of the excited $^3\Sigma_u^-$ state. These became apparent when the quantum assignment of the band heads were determined. The following revised equation was found to fit the unperturbed heads:

$$\nu = 32250.9 + 429.5(v'+1/2) - 2.75(v'+1/2)^2 - 727.4(v''+1/2) + 2.91(v''+1/2)^2$$

Weak bands were observed (mainly in absorption) about 20 cm^{-1} to the violet of the heads in the $v''=0$ progression. These bands are believed to be due to another system. Perturbations of about $+17$ cm^{-1} have been found in the heads of the bands with $v'=0, 2, 4$, which are presumably due to perturbations of the rotational levels near the band heads by another electronic state or perturbations in the $U(r)$ curve of the $^3\Sigma_u^-$ state. Perturbations found in the levels with $v'>9$ are attributed to a $^3\Pi_u$ state which causes predissociation in these bands.

Predissociation. This phenomenon is discussed in terms of the Franck-Condon principle of transition probabilities. It is shown that the $^3\Pi_u$ continuous state which causes predissociation must intersect the $U(r)$ curve of the $^3\Sigma_u^-$ state at two points giving the two observed regions of predissociation. The relative transition probabilities for the radiationless jump in the two regions are discussed.

Dissociation. The energies of dissociation of the lower and upper states are found to be 4.45 and 2.07 volts. This gives 1.6 volts as the separation of the ^3P and ^1D states of the S atom.

I. Introduction

THE S_2 bands which extend from λ6000 to λ2300 have been studied by various investigators.[1] Rosen,[2] who gave the first quantum analysis of these bands, found that the band heads could be represented by the equation:[3]

$$\nu = 32290 + 427.1(v'+\tfrac{1}{2}) - 2.7(v'+\tfrac{1}{2})^2 - 727.4(v''+\tfrac{1}{2}) + 2.91(v''+\tfrac{1}{2})^2. \quad (1)$$

For this analysis he had a relatively small dispersion (1 mm = 300 cm^{-1} in the ultraviolet) at his disposal.

[1] J. J. Graham, Proc. Roy. Soc. **A84,** 311 (1911); J. J. Dobbie and J. J. Fox, Proc. Roy. Soc. **A95,** 484 (1919); V. Henri and M. C. Teves, C. R. **179,** 1156 (1924); J. C. McLennan, I. Walerstein, H. G. Smith, Phil. Mag. **3,** 390 (1927); and the references given in this paper.

[2] (a) B. Rosen, Zeits. f. Physik **43,** 106 (1927); (b) ibid. **48,** 545 (1928); (c) ibid. **52,** 16 (1928).

[3] This equation is the same as that given by Rosen except that the quantum numbers have been changed from n to $(v+1/2)$.

There are large discrepancies in the combination differences[4] $\Delta G(v+\frac{1}{2})$ given by Rosen (cf. Table 15 of reference 2a) which should be the same within experimental error for any one row or column of his table. It may be concluded, therefore, either that his experimental errors were very large, which is possible since his dispersion was very small, or that the assignment of the vibrational quantum numbers to at least some of the heads, was wrong. The latter alternative is not so impossible as it may appear, since with larger dispersion in the present work it was found that many of the heads which Rosen measured as one, consist of groups of two or more heads. Furthermore, in the region above λ2900 the spectrum is so complicated due to overlapping, as can be seen from our plates, that the heads with $v' < 8$ all may have been assigned incorrectly. Therefore it became necessary for us to determine the correct assignment of the band heads before proceeding with the rotational analysis of the bands. The latter has already been published[5] and will be referred to here as I.

In the course of this investigation it was found that the irregularities in the $\Delta G(v+\frac{1}{2})$ values given by Rosen were due partly to an incorrect assignment of some of the band heads and partly to numerous perturbations in the vibrational levels of the upper state. The perturbations are larger than any that have been observed in the band systems of other molecules and therefore need special consideration.

The phenomenon of predissociation which Henri[6] found to occur in the S_2 bands, has also been studied in relation to the vibrational analysis. The interpretation of this phenomenon as it is observed in these bands differs from that given by other investigators.

II. Experimental Procedure

Since absorption spectra obtained at different temperatures offer the best means of studying the vibrational analysis, especially of the upper electronic state, a quartz absorption cell, having a length of 5 cm and a diameter of 2.5 cm was used. The cell was first baked out and sufficient distilled sulphur was added to give a vapor pressure of 12 mm[7] at 450°C. The cell was heated electrically. Since the amount of sulphur in the cell remained constant throughout the investigation, the vapour pressure of the sulphur within the cell (above 450°C) was proportional to the temperature.

A hydrogen tube was used as continuous source.[8]

[4] $\Delta G(v+1/2) = G(v+1) - G(v)$ where $G = E_v/hc$ (cf. R. S. Mulliken, Phys. Rev. **36,** 623, 625 (1930)).

[5] S. M. Naudé and A. Christy, Phys. Rev. **37,** 490 (1931).

[6] V. Henri, Structure des Molecules, Paris 1925; V. Henri and M. C. Teves, Nature **114,** 894 (1924).

[7] V. Henri (see Symposium of the Faraday Soc. on Molecular Spectra and Molecular Structure, Sept. 1929, p. 765) used 0.1 mg of sulphur in a 16 cc quartz tube at 600°C which gave him about the same S_2 vapour pressure.

[8] The hydrogen tube used has been described previously: S. M. Naudé, Phys. Rev. **36,** 333 (1930).

The region between λ3500 and λ2400 was studied in absorption. The absorption plates were taken with an E1 Hilger spectrograph giving a dispersion varying from 1 mm = 7.7A at λ3500 to 1 mm = 2.3A at λ2400, as well as in the first order of the 21 foot Rowland grating, giving a dispersion of 2.6A per mm. Eastman 33 plates were used. The iron and copper arcs were used as comparison spectra, the wave-lengths of which were taken from Kayser's "Hauptlinien" and Shenstone's work,[9] respectively. The copper arc was used mainly in the region below λ2800 since the iron lines are very weak and too numerous in this region to serve as standards.

The wave-lengths of the band heads on the plates obtained with the E1 spectrograph were calculated with Hartmann's formula. The measurements of the band heads obtained with both instruments agreed within experimental error. This error was relatively large (about 2 cm^{-1}), because the band heads are not very well defined owing to their characteristic rotational structure. Below λ2792.8 the heads are fuzzy due to predissociation which increases the error in this region to 5 $cm.^{-1}$ Below λ2615 the heads become very diffuse making the experimental error as large as 10 $cm.^{-1}$

The S_2 spectrum was studied in emission in the region between λ3500 and λ2400. The spectrum was excited by means of a Geissler tube described in I. The plates were taken in the first order of the 21-foot grating. Iron standard wave-lengths were used as comparison spectrum.

III. Description of the Plates

Fig. 1a is a reproduction of the bands obtained in absorption. When the absorption tube is heated to about 450°C the maximum absorption occurs in the region between λ2741 and λ2799. Plates were also taken with the absorption cell at about 600°C and 750°C. With higher temperatures the maximum absorption is shifted to longer wave-lengths as is to be expected. For temperatures of the cell below 400°C (i.e., below the boiling point of sulphur) no bands appeared in absorption in the region investigated. In emission the maximum intensity lies in the region between λ3000 and λ3500. In this region the band heads are not clearly defined owing to the great amount of overlapping. This overlapping causes many clusters of lines to be formed on the plates in this region which are not easily distinguishable from heads. These intensity relations, both in absorption and in emission, can be understood with the help of the potential energy curve obtained from the vibrational and rotational analyses given in section VII below.

Below λ2792.8 (cf. Fig. 1b) the absorption bands become diffuse. As can be seen from the plate, there are two regions in which the bands are diffuse to a different degree: first, between λ2792.8 and λ2615 and secondly between λ2615 and λ2440. The bands in the latter region are more diffuse than those in the former. In addition there seems to be a continuous absorption in the second region which reaches a maximum at λ2549. Although indications of the rotational structure reappear below λ2440 (cf. Fig. 1d) the bands are still more diffuse than in the first region.

[9] A. G. Shenstone, Phys. Rev. **28,** 449 (1926).

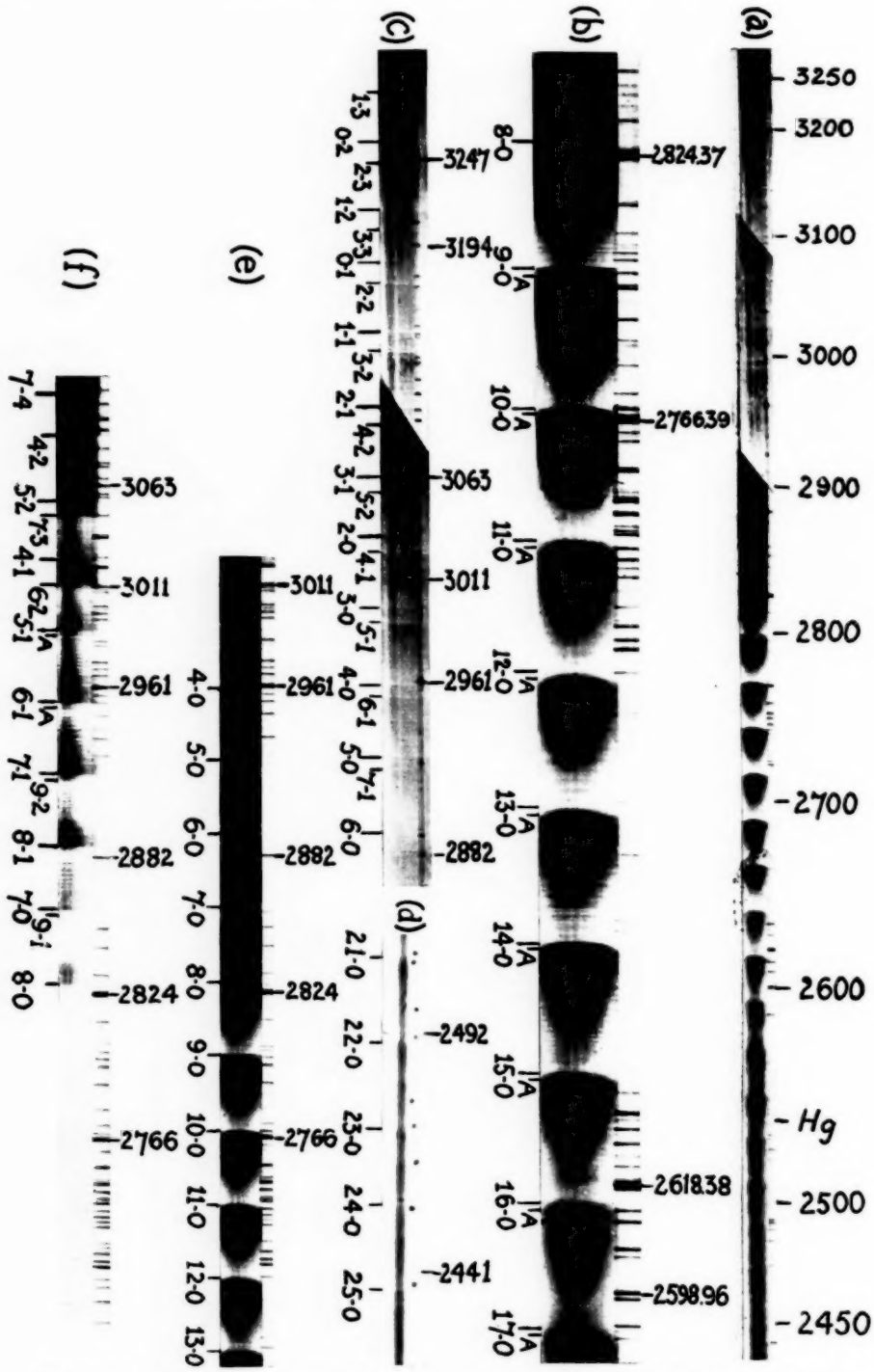

Fig. 1. (a) S_2 spectrum investigated in absorption. (b) Part of (a) showing the first region of predissociation between λ2792.8 and λ2615.0 and the first band of the second region below λ2615. (c) Absorption spectrum obtained with sulphur cell at about 750°C. (d) Bands of the second region of predissociation showing indications of rotational structure. (e) Absorption spectrum obtained with sulphur cell at about 450°C. (f) Emission spectrum of S_2.

By comparing (e) and (f) one sees that the bands which become diffuse in absorption due to predissociation do not appear in emission.

Accompanying the strong heads in absorption and about 20 cm^{-1} to the violet of these lie a number of faint heads indicated by "*A*" in Fig. 1b. These heads Henri and Teves[6] evidently accounted for as *R* heads, the strong heads being supposed to be formed by *Q* branches. It has been shown in I that the main system of bands is due to a $^3\Sigma^-_u \rightarrow {}^3\Sigma^-_g$ transition. Furthermore, the authors have found that no *Q* branches appear in these bands. Therefore the weak heads are probably due to a different electronic transition.

IV. The Vibrational Analysis

The band heads obtained in absorption can be arranged now as shown in Table IA. One would expect the bands which appear at the lowest temperature in absorption to correspond mainly to those having $v''=0$. Hence the band heads which were measured on the plates corresponding to the cell temperature of about 450°C can be assigned to transitions for which $v''=0$ and $v''=1$, the former being much more intense. These bands lie within zone (1) (cf. Table IA). When the temperature of the cell was raised to about 600°C, the band heads with $v''=1$ became more intense and in addition the band heads for which $v''=2$ appeared. These bands lie within zone (2). Similarly at about 750°C the bands for which $v''=3$ appear in absorption as well as a few for which $v''=4$ and 5. These bands lie within zone (3).[10,11] Most of these bands are indicated in Fig. 1c and 1e.

The consistent values of $\Delta G(v+\frac{1}{2})$ for any one column and row in Table IA prove the correctness of the assignment of vibrational quantum numbers to the various heads as brought out by changing the temperature of the absorption cell. Table IA reveals a number of irregularities in the values of $\Delta G(v'+\frac{1}{2})$ which will be discussed in section V. One would expect the $\Delta G(v'+\frac{1}{2})$ values to decrease regularly as v' increases. As is clear from Table IA, however, these values vary irregularly as v' increases.

The band heads measured on the plates taken in emission in the region λ3500 to λ2800 are given in Table IB. Most of the band heads observed in emission agree within experimental error with the absorption values. It is seen from Table IB that all the bands observed in emission have $v'<10$.

The values of the vibrational constants ω_e and $\omega_e x_e$ given by Rosen[2a] are essentially correct. He obtained the vibrational constants ω_e'' and $\omega_e'' x_e''$ of the lower state from the progression having $v'=3$ which was excited in fluorescence by the mercury line λ3132A = 31922 $cm.^{-1}$. Further he derived the vibrational constants ω_e' and $\omega_e' x_e'$ for the upper state mainly from the absorption bands having $v'>4$. However, most of the heads with $v'>7$ measured by him are the weaker heads of the bands designated as *A* bands (cf. section III) which are discussed later. The differences between the weaker and the stronger heads are approximately constant (20 cm^{-1}) and hence the value

[10] For the higher temperatures the absorption in the region between λ2800 and λ2600 becomes complete.

[11] By adding more sulphur to the absorption cell and increasing the temperature it would be possible to obtain the bands having $v''>4$ in absorption. This was not carried out as the above results were sufficient for our present purpose.

TABLE I. *Band heads of the* $^3\Sigma_u^- \longleftrightarrow {}^3\Sigma_g^-$ *system.*
A. Absorption

v'' / v'	0	1	2	3	4	5	Mean ΔG $(v'+\frac{1}{2})$
0		31399	30681	29974	29271	28577	
		402	407	408			405.7
1	39525	31801	31088	30382			
	433	436	435	434			434.5
2	32958	32237	31523	30816			
	400	398	396 2	393			398.3
3	33358	32635	31919	31209		3	
	422	421	422	418			421.6
4	33780	33056	32341	31627			
	384 1	385	385				384.7
5	34164	33441	32726				
	399	400					399.5
6	34563	33841			31717		
	391	388	2		392		389.5
7	34954	34233			32109		
	385	386					385.5
8	35339	34619		3			
	374	373					373.5
9	35713	34992					
	388	389					388.5
10	36101	35381					
	368	371 1					369.5
11	36472	35749					
	356	360					358.0
12	36828	36109					
	366	366					366
13	37194	36475					
	356	357					356.5
14	37550	36828					
	346						346.0
15	37896						
	333						333.0
16	38229						
	326						326.0
17	38555						
	330						330.0
18	38885						
	336	1					336.0
19	39221						
	316						316.0
20	39537	38832					
	310	303					310.0
21	39847	39135					
	292	290					292.0
22	40139						
	310	309					310.0
23	40449	39734					
	260	255					260.0
24	40709						
	301	297					301.0
25	41010	40286					
	269	268					
26	41279						269.0
		270					270.0
27		40284					
		277					277.0
28		41001					

In obtaining the mean value of $\Delta G(v'+\frac{1}{2})$, we have considered the accuracy of the measured band heads.

TABLE I. *B. Emission*

v' \ v''	0	1	2	3	4	5	6
0					29275		
					402		
1				30381	29677		
				437			
2			31527	30818			
			394	393			
3		32634	31921	31214?			29123
		422	420				
4		33056	32341	31628		30231	
		384	386				
5		33440	32727		31315		
		402	404		402		
6	34563	33842	33131		31717	31019	
	392	393			389		
7	34955	34235		32812	32106		30717
	385	383					385
8	35340	34618				31796	31102
		370					
9		34988	34269				

of ω_v derived from them is essentially correct. The dispersion used by Rosen was not sufficient to resolve these heads, and furthermore, when the vapour pressure of the sulphur in the absorption tube is increased, the weak heads become completely absorbed, and consequently one is liable to measure these as the main heads as Rosen apparently has done. This can be seen by comparing our assignment of vibrational quantum numbers to the various band heads with that of Rosen as is done in Table II. For wave-lengths greater

TABLE II. *Comparison of assignment of vibration quantum numbers to band heads*

Present		Rosen		Present		Rosen	
$v'-v''$	ν	$v'-v''$	ν	$v'-v''$	ν	$v'-v''$	ν
7–1	34233	7–1	34237	13–0	37194	13–0	37210
6–0	34563	6–0	34589	A	37214		
8–1	34619			14–0	37550	14–0	37550
7–0	34954	7–0	34970	A	37569		
9–1	34992			15–0	37896	15–0	37900
8–0	35339	8–0	35358	A	37915		
A	35358			16–0	38229	16–0	38240
9–0	35713	9–0	35720	A	38247		
A	35733			17–0	38555	17–0	38580
10–0	36101	10–0	36110	A	38885		
A	36123			18–0	38885	18–0	38910
11–0	36472	11–0	36480	A	38911		
A	36496			19–0	39221	19–0	39240
12–0	36828			A	39250		
A	36851	12–0	36850				

Note: The bracketed heads have been measured as one by Rosen.

than λ2926 the absorption spectrum becomes complicated and consequently Rosen's results become less trustworthy. In this region it is impossible to correlate our results with those given by him. Owing to these errors in Rosen's assignment the vibrational constants of the upper state as well as ν_e should be changed as follows:

$$\nu_e = 32250.9 + 429.5(v' + \tfrac{1}{2}) - 2.75(v' + \tfrac{1}{2})^2 - 727.4(v'' + \tfrac{1}{2}) + 2.91(v'' + \tfrac{1}{2})^2. \quad (2)$$

The above mentioned faint absorption heads (cf. section III) which lie about 20 cm^{-1} to the violet of the $v'' = 0$ progression, have been observed only next to the main band heads having v' ranging from 8 to 20. Some of these heads are indicated by A in Fig. 1b. A few more weak heads have been found to appear in absorption and a few in emission which seem to belong to the same electronic transition as those marked A. These band heads are tabulated in Table III which gives a possible arrangement. This arrangement, however, is uncertain, since no more heads can be found, as they are relatively

TABLE III. *The A System of bands of S_2*

	33476″	37214
	33879″	37569
	34269′	37908
35358	34640?	38249
35733		38577
36123		38911
36496	35794	39248
36851		39555

NOTE: (″) These band heads have been found in both emission and absorption.
(′) Found only in emission. All the other heads have been observed only in absorption.
(?) Doubtful value.
The band heads are arranged in this manner in order to show the parallelism between these heads and those of the $^3\Sigma^-_u \leftarrow {}^3\Sigma^-_g$ system.

weak compared with the bands of the main system and are overlapped by these bands. It is therefore impossible to determine whether the upper or the lower state is common to these two systems. This might be decided in case a series of experiments were performed in which the temperature in the cell was comparatively low and the pressure was increased gradually. In addition to these two systems of bands a large number of heads have been observed above λ3500 which appear in emission. A special study of these bands, if possible with a low temperature source such as active nitrogen which would diminish the excessive overlapping of the bands, should be made in order to determine whether or not they belong to the $^3\Sigma_u^- \rightarrow {}^3\Sigma_g^-$ transition.

V. PERTURBATIONS

In the great majority of band systems which have been analyzed thus far the vibrational combination difference $\Delta G(v+\frac{1}{2})$ has been found to decrease regularly as the vibrational quantum number increases.[12] If in Table IA we compare the mean $\Delta G(v'+\frac{1}{2})$ values, we see that perturbations must

[12] It was observed by G. Nakamura in the NaH bands (Zeits. f. Physik **59**, 218 (1930)) and by T. Hori in the LiH bands (Zeits. f. Physik **62**, 352 (1930)) that the $\Delta G(v'+1/2)$ values, instead of decreasing with v', increase up to a certain value of v' and then decrease regularly. W. Weizel (Zeits. f. Physik **60**, 599 (1930)) showed that this may be accounted for by uncoupling of the $p\sigma$ and $s\sigma$ electrons.

be present in the vibrational levels of the upper $^3\Sigma^-_u$ state. This is shown more strikingly if one compares the observed and calculated energy levels as shown in Table IV. The calculated values were obtained by passing the best graph through the observed $\Delta G(v'+\frac{1}{2})$ values, and then adjusting the value of the calculated $v'=0$ level until the best fit was obtained with the

TABLE IV. *Calculated and observed energy values of the vibrational levels for the $^3\Sigma_u^-$ (upper) state of the system.*

v'	o	c	$o-c$	v'	o	c	$o-c$
0	32120.0	32002.0	+18.0	12	36828.8	827.0	+ 1.8
1	32525.7	526.0	− 0.3	13	37194.8	37185.0	+ 9.8
2	32960.2	944.5	+15.7	14	37550.3	537.5	+12.8
3	33358.5	33357.5	+ 1.0	15	37896.3	884.5	+11.8
4	33780.1	765.0	+15.1	16	38229.3	38226.0	+ 3.3
5	34614.8	34167.0	− 2.2	17	38555.5	560.0	− 6.7
6	34564.3	563.5	+ 0.8	18	38885.3	890.5	− 7.2
7	34953.8	954.5	− 0.7	19	39221.3	39215.5	+ 3.6
8	35339.3	35340.0	− 0.7	20	39537.3	535.0	+ 0.3
9	35712.8	720.0	− 7.2	21	39847.3	849.0	− 1.7
10	36101.3	36094.5	+ 6.8	22	40139.3	40157.5	−18.2
11	36470.8	463.5	+ 7.3	23	40449.3	460.5	−11.2

NOTE: Our measurements below the 23←0 bands are very inaccurate, hence no comparison can be made for $v'>23$. In considering the o-c values it must be remembered that the experimental error for the bands having $v'<9$ is about 2 cm^{-1} and for $v'>9$ probably greater (cf. section II).

experimental values. It is seen that the o-c values for $v'=7$ and 8 are zero within the experimental error. We know from I that the rotational levels for $v'=7$ and 8 are normal, whereas those for $v'=9$ are perturbed. From Table IV we see also that the vibrational levels $v'=7$ and 8 are normal and $v'=9$ seems to be displaced. It appears that the levels with $v'=0, 2, 4$ are perturbed by about +17 cm^{-1}. From $v'>9$ predissociation begins and it appears that practically all these levels are perturbed in varying degree. The perturbations for $v'=0, 2, 4$ as obtained by measuring the heads of the bands, might be due either to perturbations of the rotational lines near the heads or to perturbations of the vibrational levels.

Johnson and Asundi[13] found that in the Cameron CO bands all band heads with $v'=1$ are displaced by 4.2 cm.$^{-1}$ Rosenthal and Jenkins[14] showed that all the rotational lines near the heads of these bands are perturbed, all the lines being displaced in the same direction, thus giving a displacement of the head and consequently an apparent displacement of the vibrational level. In the CN bands Rosenthal and Jenkins[15] showed that the perturbations of the rotational lines occurring in some of these bands are due to the fact that certain rotational levels of the upper state have energies approximately equal

[13] R. C. Johnson and R. K. Asundi, Proc. Roy. Soc. **A123**, 560 (1929).
[14] J. Rosenthal and F. A. Jenkins, Proc. Nat. Acad. of Sciences **15**, 896 (1929).
[15] J. Rosenthal and F. A. Jenkins, Proc. Nat. Acad. of Sciences **15**, 382 (1929).

to the rotational levels of another state with the result that the two sets of levels are mutually perturbed, as we would expect from Kronig's theory.[16,17]

It may be that the perturbations of the S_2 band heads for $v'=0, 1, 2, 4$ are of the same type, i.e. that all the rotational lines near the band heads are displaced in the same direction and that, consequently, the heads are displaced by about $+17$ cm.$^{-1}$ But in order that the alternate vibrational levels might be perturbed, we must assume the presence of another state having an ω which is approximately twice that of the $^3\Sigma_u^-$ state. If such a state were present, we would expect transitions between this and the normal state of the molecule. It may be, however, that some of the emission bands are due to such a transition.

The observed perturbations of the band heads with $v'=0, 2, 4$ may, be due to perturbations of the vibrational levels. In this case one would expect the $U(r)$ curve to be irregular and not a smooth curve as it seems to be for the electronic states of most other molecules. A similar type of perturbation to that observed in S_2 has been found by Jevons[18] in the bands of CS, where the band heads having $v'=1, 2, 4$ were found to be displaced in the same way, the maximum displacement of the CS band heads being 7.4 cm^{-1} as compared with $+18$ cm^{-1} for S_2. Moreover, by comparing the observed displacements of the R and Q heads from their calculated positions,[19] Jevons concluded that the observed perturbations were due to perturbations of the vibrational levels.

Whether this type of perturbation as observed in the S_2 bands is due to rotational or vibrational perturbations or to a superposition of both can only be determined by studying the rotational structure of the S_2 bands having $v'=0, 2, 4$ with reference to the unperturbed bands. Owing to the great amount of overlapping of those bands in the S_2 spectrum, this study is impossible unless some other type of excitation (active nitrogen or fluorescence) will excite fewer and less extensive bands, and consequently give less overlapping. Although still difficult, this study may be carried out in the CS bands.[20]

The perturbation present in the vibrational levels for $v'>9$ may be due to the continuous state which causes predissociation and which is discussed in the next section. Although the probable error in the measurement of these diffuse bands ($v'>9$) is large (cf. section II), consequently making it difficult to interpret correctly the observed minus calculated values, it may be pointed

[16] R. de L. Kronig, Zeits. f. Physik **50,** 347 (1928).

[17] But cf. H. H. Hyman and C. R. Jeppesen, Nature **125,** 462 (1930) and R. T. Birge and C. R. Jeppesen, Nature **125,** 463 (1930). These investigators have found a perturbation in the $v''=0$ level of the normal state of H_2, where presumably there could not be another interacting state present.

[18] W. Jevons, Proc. Roy. Soc. **A117,** 351 (1927–1928).

[19] If both the R and Q heads were displaced by the same amount, one might attribute this displacement to a perturbation of the vibrational level. If, however, the two heads were displaced by different amounts, this displacement might be due to the perturbation of the rotational levels. Cf. also references 13 and 14.

[20] This investigation has been started by one of the authors (S.M.N.).

out that, whereas the level $v'=9$ seems to be displaced downwards, those above the intersecting curve ($v'=10-16$) seem to be displaced upwards which suggests some interaction between the corresponding $U(r)$ curves.

We know according to I from our rotational analysis of the 9–1 and 9–2 bands that the rotational levels of the $v'=9$ level are perturbed. In these bands we have found that the mean value of B_9' obtained from the Δ_2F_9' graph is larger than the B_7' and B_8'.[21] The fact that B_9' obtained from lower values of K is less than the values obtained from higher values of K (the factor $8D_vK^3$ has been considered) seems to indicate that the perturbation increases with K.

VI. Predissociation*

It has been remarked in a previous section of this paper that there are two regions in this spectrum where the bands are diffuse. As can be seen from Fig. Ib the absorption bands are sharp[22] up to λ2799.1 ($v'=9$, $v''=0$).[23] To the violet of this point they become at first more and more diffuse, the maximum diffuseness being at about λ2741.0 (11←0) As we proceed toward shorter wave-lengths the bands become sharper. At 2615.0 (16←0) the bands suddenly become much more diffuse, the maximum diffuseness of the second region being at λ2549.0 (19←0). From this point on the bands become less diffuse. Although the spectrum has been photographed down to λ2400, the bands below λ2492 are no sharper than those between λ2792 and λ2615, as can be seen from Fig. Id. In the first region of predissociation (λ2799–λ2615), the bands although diffuse, still preserve some of their rotational structure, the diffuse lines merging into definite groups (cf. Fig. 1b). In the second region (λ2615 – λ2435) the bands are completely diffuse, all group structure disappearing.

All the bands which are diffuse in absorption fail to appear on our emission plates (cf. Figs. 1e and 1f and also Table I).[24] No bands were observed in emission with $v'=10$, although the exposures were long enough to photograph these had their intensity been one tenth of that of the others. The non-appearance of these bands may be ascribed primarily to the small life time of the molecule in the vibrational levels of the $^3\Sigma_u^-$ state with $v'>9$, due to the transitions from these levels to those of another state with subsequent dissociation. The non-appearance of the 9→0 band may be explained by the fact that the transition probability from $v'=9$ to $v''=0$ is small. The

[21] $B_v=B_e-\alpha_e(v+1/2)$. Hence B_v should decrease as v increases.

* The authors appreciate the discussions with Drs. J. L. Dunham and Carl Eckart about points brought up in this section.

[22] When we use the expressions: bands are "sharp" or "diffuse," we actually mean that the rotational lines of the bands are sharp or diffuse.

[23] V. Henri gave λ2792.4 as the wave-length at which the bands become diffuse (cf. reference 6). However, the band at λ2792.4 (2792.8 according to our measurements) does not belong to the main system, i.e. $^3\Sigma^- - ^3\Sigma_g^-$, but to a weaker group of bands which are designated here as A bands and are given in Table IV. As will be shown in section VII, this wave-length has no special meaning.

[24] This fact was independently observed by H. H. van Iddekinge, Nature **125**, 858 (1930).

transition probability for $v'>9$ to $v''=0$ is still smaller, hence these bands would be weak even if predissociation was not present.

Various investigators[25,26,27] have given explanations of the predissociation, which occurs in this spectrum. Franck[25] showed that if we assume two intersecting curves as in Fig. 2A, we may expect transitions to take place at the point b with immediate dissociation of the molecule. The theoretical explanation based on wave mechanics, as given by Kronig[26] involves the same basic principles as those used by Franck. Kronig showed that the selection rules for radiationless transitions are $\Delta\Lambda=\pm1, 0$; $\Delta\Sigma$ or $\Delta S=0$; $\Delta J=0$; and that transition can occur only between two $+$(or$-$) rotational levels belonging to two electronic states that are both g or both u.[28] [It may be pointed out that the ordinary transition rules are $\Delta\Lambda=\pm1, 0$; $\Delta\Sigma$ or $\Delta S=0$; $\Delta J=0, \pm1$; $+$(or$-$) levels to $-$(or$+$) levels and g(or u) to u(or g) states (if equal atoms)]. The probability of a radiationless transition is proportional to $J^2/(E)^{1/2}$.[29] E is the energy difference between any level of the $^3\Sigma_u^-$ state and the line $b\,b'$, b' being the dissociation energy of state a. The above formula would indicate that no transition is possible between the two intersecting curves below b. Hence we would expect predissociation to begin sharply and then decrease gradually as we reach the vibrational levels above the point b. However, in both the first and second region, predissociation begins suddenly and increases gradually to a maximum before it decreases.

The explanation given by Herzberg[27] for the observed predissociation in the S_2 bands is a further development of Franck's principle. According to Herzberg curve a[30] cuts the $^3\Sigma_u^-$ curve at two points, c and b, as in Fig. 2B, corresponding to the two regions of predissociation. He points out that the bands of the second region may be more diffuse, first because in this region the bands will be overlapped by the continuum[31] due to $^3\Sigma_g^-\leftarrow a$, and secondly, because at c the probability of predissociation will be greater, for at

[25] J. Franck and H. Sponer, Nachricht Gesellschaft d. Wiss. Göttingen, Math.-Phys. Klasse, p. 241 (1928); K. F. Bonhoeffer and L. Farkas, Zeits. Phys. Chem. **134,** 337 (1927).

[26] R. de L. Kronig, Zeits. f. Physik **50,** 347 (1928); **62,** 300 (1930).

[27] G. Herzberg, Zeits. f. Physik **61,** 604 (1930).

[28] The last rule as formulated by Kronig (cf. Zeits. f. Physik **62,** 300 (1930)) is symmetrical to symmetrical, and antisymmetrical to antisymmetrical states. The $+$ and the $-$ levels here referred to are the "gerade" (g) and "ungerade" (u) rotational levels of Kronig (cf. Zeits. f. Physik **50,** 351 (1928)) and Mulliken (cf. Phys. Rev. **36,** 617 (1930). The g and u used here refer to the "gerade" and "ungerade" electronic states of Hund as Π_u, Σ_g, Σ_u, etc. (cf. Zeits. f. Physik **51,** 759 (1928)).

[29] The J^2 term in Kronig's formula enters only when the transition involves $\Delta\Lambda=\pm1$. For a transition for which $\Delta\Lambda=0$, the probability is independent of J. The dependence on J would indicate that within any diffuse band, the rotational lines would become more diffuse as we go away from the origin. The probability essentially depends upon J and not on J^2 since $J^2/(E)^{1/2}\propto J$. It is difficult to determine from our results whether or not the lines within a band become more diffuse as we go away from the origin.

[30] Herzberg points out that curve a may or may not have a minimum. His explanation fits either case equally well.

[31] Fig. 3 shows that the most probable transition from the lower vibrational levels of the $^3\Sigma_g^-$ state is to the left of the upper curves.

this point the radiationless transition may occur before it is necessary for the molecule to complete half a vibration as it would at point *b*. It is highly improbable, however, that the overlapping continuum will make the bands appear more diffuse than they actually are. Furthermore, since the frequency of vibration is much larger than that of rotation, the fact that the molecule will have to complete half a vibration at *b* and not at *c* before it dissociates, can have no appreciable effect on the relative probability of predissociation of the bands in the two regions.

The first idea which suggests itself is that there may be two curves intersecting the $^3\Sigma_u^-$ curve, giving the two regions of predissociation. It may be well, therefore, to consider here the various possible states which may be present. It has been shown by us[5] that the main system of bands which show predissociation is due to a $^3\Sigma_u^- \leftarrow ^3\Sigma_g^-$ transition, $^3\Sigma_g^-$ being the lower state. By a comparison with the Schumann-Runge bands of O_2 (cf. also section VII), one would expect the $^3\Sigma_g^-$ of S_2 to dissociate into two ^3P atoms, and the excited state, $^3\sum_u^-$, into one ^3P and one ^1D atom. It is evident also from the $U(r)$ curves that the states which cause predissociation must dissociate into two normal atoms. By applying the results of Wigner and Witmer,[32] one finds that the molecular electronic states resulting from similar atoms both in a ^3P state are the following: $^1\Delta_g$, $^1\Pi_g$, $^1\Pi_u$, $^1\Sigma_g^+$, $^1\Sigma_g^-$, $^1\Sigma_u^-$, $^3\Delta_u$, $^3\Pi_u$, $^3\Pi_g$, $^3\Sigma_u^+$, $^3\Sigma_u^+$, $^3\Sigma_g^-$, $^5\Delta_g$, $^5\Pi_g$, $^5\Pi_u$, $^5\Sigma_g^+$, $^5\Sigma_g^+$, $^5\Sigma_u^-$. The state or states causing predissociation (curve *a* in Fig. 2B or Fig. 2C) must be among the above. But according to the rules given by Kronig[16] for a radiationless transition, the only state in the above list which can interact with a $^3\Sigma_u^-$ state is a $^3\Pi_u$ state. Hence the state which causes predissociation must be a $^3\Pi_u$ state and must intersect the $^3\Sigma_u^-$ at two points as Herzberg assumed.[27] However, we have still to explain why the bands in the second region corresponding to *c* are more diffuse than those in the first.

It may be shown that Kronig's formula does not apply to the region *c*. In deriving his formula,[33] he assumed that the nuclear momentum of the molecule in state *a* (here identified as a $^3\Pi_u$ state) is constant. That is, he was dealing only with the flat portion of the curve, line *b b'* of Fig. 2A. If, however, the curve has no minimum[34] as in Fig. 2C the momentum will not be constant near either of the points *b* or *c*.[35]

[32] E. Wigner and E. E. Witmer, Zeits. f. Physik **51**, 859 (1928).

[33] Kronig took as the wave function of state *a* an oscillatory function with a constant period, i.e., constant momentum.

[34] The $^3\Pi_u$ state may have a very shallow minimum. If it had a sharp minimum we would expect to find discrete bands either in emission or absorption due to a $^3\Pi_u \longleftrightarrow ^3\Sigma_g^-$ transition. No such bands have been found although there is a region of weak continuous absorption beginning at about λ2600 which may be ascribed to this transition. The group of bands designated in this paper as *A* bands are not due to this transition, for they are found in absorption after the point *c* has been passed.

[35] Since the $^3\Pi_u$ intersects the $^3\Sigma_g^-$ curve at *c*, we will have to suppose that although the interaction between the two atoms forming the $^3\Pi_u$ state is almost zero for very small distances of internuclear separation, when this distance is made still smaller, the repulsion between the two atoms is smaller than that in state $^3\Sigma_u^-$. (This will be the case if the electronic configuration of the $^3\Pi_u$ state resembles the united atom more closely than that of the $^3\Sigma_u^-$ state.)

In the tentative explanation given here we shall make use of the Franck-Condon theory[35] of transition probabilities between the two states $^3\Sigma_u^-$ and

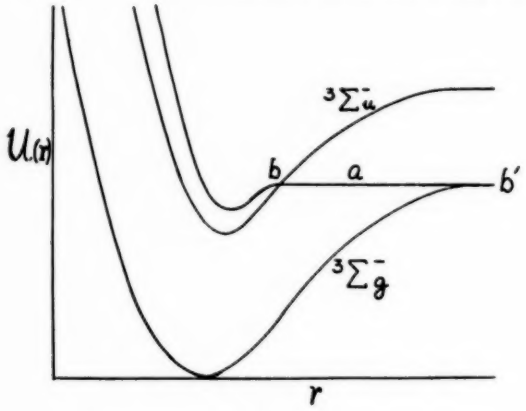

Fig. 2A

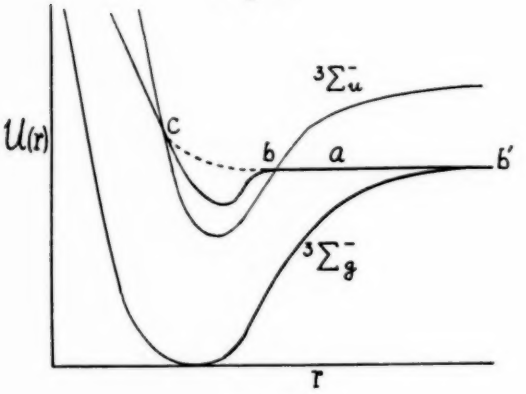

Fig. 2B

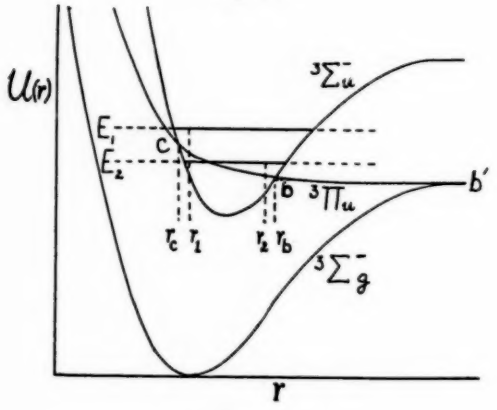

Fig. 2C

$^3\Pi_u$. According to this theory the probability of a transition is greatest when

[35] E. U. Condon, Phys. Rev. **28**, 1182 (1926).

the nuclear separation as well as the momentum remain unchanged during the transition. Since the slopes of the two intersecting curves are more nearly alike at the point c than at b, and furthermore remain closer together at the former point than at the latter, a transition from a discrete vibrational level whose energy is near that of c to the continous curve will involve a very much smaller change in the nuclear separation at this point than at the point b. The ratio of the nuclear momenta in the neighbourhood of the two points is approximately the same in both cases. This can be seen from Fig. 2C. If we take two discrete vibrational levels E_1 and E_2 so that $E_1-c=E_2-b$, and consider the points on E_1 and E_2 having zero nuclear momentum it is quite evident that the difference of the nuclear separation for the former is much less than for the latter. For two other points on E_1 and E_2 having nuclear separations r_1 and r_2 so that $r_1-r_c=r_b-r_2$ the ratios of the nuclear momenta in the former case will be about the same as in the latter. Hence the probability of the predissociation at the former point will be greater (therefore the rotational lines more diffuse) than at the latter point. Furthermore, since the two curves remain closer together near c, i.e. the second region of predissociation, we would expect more bands to be diffuse in the second region of predissociation than in the first. Finally, from the above explanation we would expect that, in both regions of predissociation, the bands tend to become more diffuse as we approach the points of intersection from either side.[37] These phenomena are exactly what we observed.

It has been stated in a previous section that the overlapping continuum reaches a maximum at λ2549. This maximum could not be due entirely to transitions between the $^3\Sigma_g^-$ and the $^3\Pi_u$ states, for according to Fig. 3, the maximum probability of this transition should occur at λ2662. We have also seen that the band at λ2549 (19←0) is the most diffuse band in this spectrum. Hence the overlapping continuum at this point must be due to the fact that the rotational levels for the $v'=19$ are so diffuse as to be practically continuous.

For a quantum mechanical formulation of the results obtained by application of the Franck-Condon principle, we would make the step by step conversion from one to the other exactly as Condon has done for ordinary transitions.[38] One sees that the overlapping of the wave functions of the two states ($^3\Sigma_u^-$ and $^3\Pi_u$) is greater at c than at b since the internuclear distances (with zero nuclear momentum) on both curves are nearer the same in the neighborhood of the former point than of the latter. Therefore the two waves will tend to reenforce each other more at c than at b, giving a greater transition probability in the neighborhood of c.

[37] L. A. Turner (Am. Phys. Soc. Meeting, New York, Feb. 1931, Paper No. 12) refers to two types of predissociation. In one the broadening of the lines sets in suddenly at a definite wavelength and in the other it sets in gradually. The former is the type discussed by Kronig (cf. Fig. 2A) and is also approximated at point b of Fig. 2C. According to our interpretation the continuous curve at point b has almost the value of dissociation. Hence at this point one would expect the broadening of the lines to set in more suddenly than at point c.

[38] E. U. Condon, Phys. Rev. **32,** 858 (1928), also Condon and Morse, Quantum Mechanics, pp. 168–170.

In the above discussion we were concerned mainly with the $^3\Sigma_u^- \longleftrightarrow {}^3\Sigma_g^-$ bands. The other system of bands which we have designated as A bands shows exactly similar characteristics. Whenever a band of the main system is diffuse the corresponding A band is also diffuse.

While this paper was being written Asundi[39] reported that in the presence of argon at high pressures, he was able to photograph the bands in emission

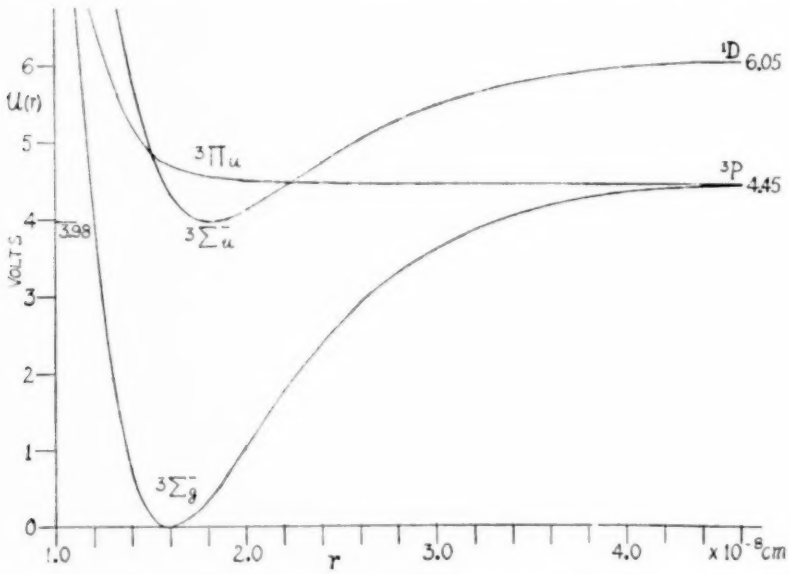

Fig. 3. Potential energy curves of the known states of the S_2 molecule. The $^3\Sigma^-_g$ and $^3\Sigma^-_u$ curves have been drawn using Morse's equation.

beyond the first limit of predissociation. If the mechanism of predissociation given by all thus far is correct, it is difficult to see what effect the presence of argon could have except that of increasing the population of the levels with $v' > 9$. Thus, although dissociation does take place there are still sufficient molecules present in these states to emit the bands with sufficient intensity to be observed.

VII. Heats of Dissociation

In our previous paper[5] we showed that the main system of S_2 bands is due to a $^3\Sigma_u^- \longleftrightarrow {}^3\Sigma_g^-$ transition, and is analogous to the Schumann-Runge bands of O_2. We should, therefore, expect the normal $^3\Sigma_g^-$ state of S_2 to dissociate into two ^3P atoms just as in the case of O_2, and similarly the upper state $^3\Sigma_u^-$ to dissociate into a ^3P and a ^1D atom.

From the graph $\omega_e : v$ for the $^3\Sigma_u^-$ state we obtain by linear extrapolation 2.07 volts for the heat of dissociation D' of this state.[40] Hence the total energy required to excite the molecule into the $^3\Sigma_u^-$ state and to dissociate it is:

$$\nu_e + D' = 3.98 + 2.07 = 6.05 \text{ volts}.$$

[39] R. K. Asundi, Nature **127**, 93 (1931).

[40] Of the 2.07 volts the energy is known up to 1.01 volts and the rest is extrapolated.

The $^3\Pi_u$ level which causes the predissociation must also dissociate into two ^3P atoms, since there is no other possible atomic state between the ^3P and ^1D states. From the description of the phenomenon of predissociation as observed in these bands given in section VI it is clear that the rotational lines of the bands, are sharp up to λ2792.8 where they begin to become diffuse. The rotational lines immediately below λ2792.8 which are diffuse in absorption correspond to transitions from the higher rotational levels in $v''=0$ to the corresponding levels of $v'=10$. These lines are diffuse because the rotational levels of $v'=10$ have energies which lie in the continuous energy range of the $^3\Pi_u$ curve (i.e. $>D''$). Since the lines near the head of the 10–0 band ($\nu=36101$ cm^{-1}) also are diffuse the energies of these lines are greater than D''. The head of the 9–0 band is sharp so that its energy is less than D''. In I, moreover, it was shown that the rotational lines of the 9–1 and 9–2 bands could be followed to $K\approx 30$. The line having $K\approx 30$ corresponds to an energy 35713 cm$^{-1}+B_9K(K+1)\approx 36000$ cm^{-1}. This energy must be less than D'' otherwise the rotational lines could not have been observed in emission. D'' must therefore lie between 36000 and 36100 cm.$^{-1}$ Therefore $D''=4.45\pm 0.01$ volts.[41] This value is in good agreement with the chemical value 103600 cal $=4.5$ volt obtained by Budde.[42] By extrapolation of th ω_e:v graph for the $^3\Sigma_g^-$ state we ought to obtain the same value for its energy of dissociation D''. But, as in the case of O_2, this extrapolation leads to a value of D'' which lies above the correct values for S_2 as obtained from predissociation.[43]

Using the values of r_e' and r_e'' given in I and the values of ν_e, D' and D'' obtained above, we are able to draw the potential energy curves of the $^3\Sigma_g^-$ and $^3\Sigma_u^-$ states of S_2 using Morse's equation,[44] (see Fig. 3). Assuming the $^3\Pi_u$ curve to intersect the $^3\Sigma^-{}_u$ curve at about $v'=19$ and $v'=11$ according to section VI and to give two ^3P atoms, we may draw this curve as shown in Fig. 3.

According to the above results the separation of the ^1D and ^3P atomic states must be $6.05-4.45=1.60$ volts. The value of this separation for O as given by Frerichs[45] is 1.95 volt and the corresponding separations in the Se and Te atoms as determined by McLennan and Crawford[46] are 1.2 and 1.3 volts. By interpolating we obtain 1.6 ± 0.1 volts for S which is in good agreement with the value given above;

The authors wish to thank Professor R. S. Mulliken for his interest and criticism in connection with this work.

[41] G. Herzberg, Zeits. f. Physik **61,** 604 (1930) lays great stress on the fact that one can obtain only a maximum value of the energy of dissociation from predissociation data. From our interpretation of the phenomenon it is clear that a fairly accurate determination is possible for S_2.

[42] Budde, Zeits. f. Analyt. Chem. **78,** 169 (1912).

[43] The linear extrapolation in this case will be very inaccurate as it is much greater than in the $^3\Sigma_u^-$ state.

[44] P. M. Morse, Phys. Rev. **34,** 57 (1929).

[45] R. Frerichs, Phys. Rev. **36,** 398 (1930).

[46] J. C. McLennan and M. F. Crawford, Nature **124,** 874 (1929).

NOTE ON MODES OF SPECTROGRAPH SLIT IRRADIATION

DONALD C. STOCKBARGER AND LAURENCE BURNS
RADIATION MEASUREMENTS LABORATORY
MASSACHUSETTS INSTITUTE OF TECHNOLOGY

(Received February 26, 1931)

ABSTRACT

The mercury lines, 3650–63, have been photographed with very approximately coherent slit irradiation and with a number of different slit-widths. Maximum sharpness and resolution were obtained when the slit-width had a rather critical value. Multiple lines appeared when a multiple of the critical slit-width was used. Diffraction patterns appeared between the lines when the slit was made narrower than the critical value. A more detailed account of the research, of which this is but a small part, will appear later.

THE recent appearance of a mathematical paper by van Cittert[1] has prompted us to publish a small portion of the experimental results which we are accumulating in our study of spectrograph slit irradiation. Although the work has been in progress for nearly a year we do not feel justified in attempting to treat the subject in a general way until the entire program has been covered. The results presented will serve, therefore, merely as an indication of what we are finding, viz., that the width and shape of a line image are influenced to a large degree by the mode of slit irradiation.

We were led to undertake the research by difficulties encountered during the past few years in connection with such things as line absorption and intensity measurements. Evidently others have experienced similar difficulties.[2] Sometimes photographed lines appeared to have absorption cores when there were no assignable reasons for self-reversal. In one instance several lines seemed to suffer a shift of wave-length so great that no known agencies could account for it. Although the false effects could be eliminated usually through adjustment of the optical system, we felt that a systematic investigation should be made in order to remove the necessity for cut-and-try methods. Practically no help was found in the literature.

Van Cittert treats the two special cases, coherent and noncoherent monochromatic irradiation, in some detail and draws conclusions in regard to a few intermediate modes such as would be met in practice. Wadsworth[3] and Schuster[4] had already treated the completely noncoherent case but, as van Cittert suggests, a self-radiant slit which is sufficiently narrow is practically

[1] P. H. van Cittert, Zeits. f. Physik **65,** 547 (1930).

[2] Shenstone, Phys. Rev. **34,** 726 (1929).

[3] Wadsworth, Ast. Jour. **1,** 52 (1895); ibid. **3,** 170 and 321 (1896); ibid. **4,** 54 (1896); Phil. Mag. **43,** 317 (1897).

[4] Schuster, Ency. Brit. Article on Spectroscopy; Ast. Jour. **21,** 197 (1905).

unattainable. Approximately noncoherent irradiation can be realized through the use of a very broad source or by imaging a source on the slit with a very large condenser lens. Departure from noncoherency of irradiation may lead to narrower lines but it can also seriously affect their shapes. In ordinary prac-

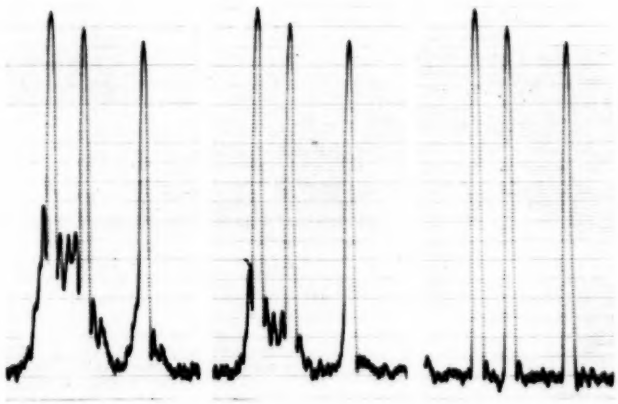

Fig. 1. Slit 2.5 divisions. Note the pronounced diffraction background.
Fig. 2. Slit 3.5 divisions.
Fig. 3. Slit 4.5 divisions. Sharpness and resolution appear to be best with this slit width.

tice this departure may be considerable. For every mode of slit irradiation there exists a slit-width which should not be exceeded. This width being measured in wave-lengths, the correct setting for one spectral region is incorrect for another.

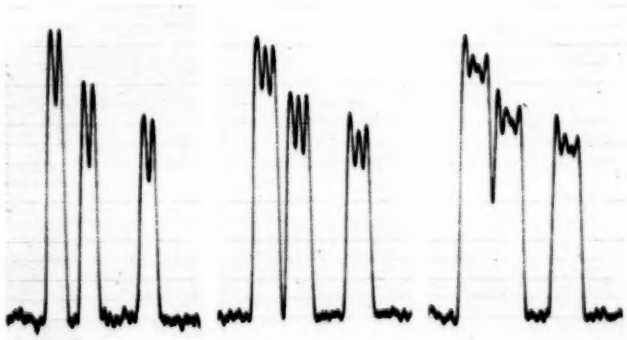

Fig. 4. Slit 9.5 divisions.
Fig. 5. Slit 12.5 divisions.
Fig. 6. Slit 14.5 divisions.

In general, we find our experimental results to be in qualitative agreement with van Cittert's mathematical analysis. We are including intermediate modes of irradiation, however, and consequently are finding different orders of effects and some effects not mentioned in his paper.

In the example selected for this note, the source was a low pressure quartz mercury arc placed 2.25 meters from the slit of a Hilger E2 quartz spectrograph. To narrow the beam of radiation an opaque screen with a window, about one centimeter in diameter, was mounted 25 cm in front of the arc. The arc and screen were carefully adjusted in position so that the radiation passed through the center of the collimator lens. This mode of irradiation, which approached the coherent case, was of such a nature that pronounced diffraction effects were observed, but it was not an extreme case. The 3650–63 lines were photographed with different slit-widths, and then the plates were examined with the aid of a recording microphotometer.

Figs. 1–10 show that maximum sharpness and resolution of the lines were obtained when the width had a rather critical value, viz., 4.5 divisions on the drum. At multiples of the critical width the lines tended to appear equally

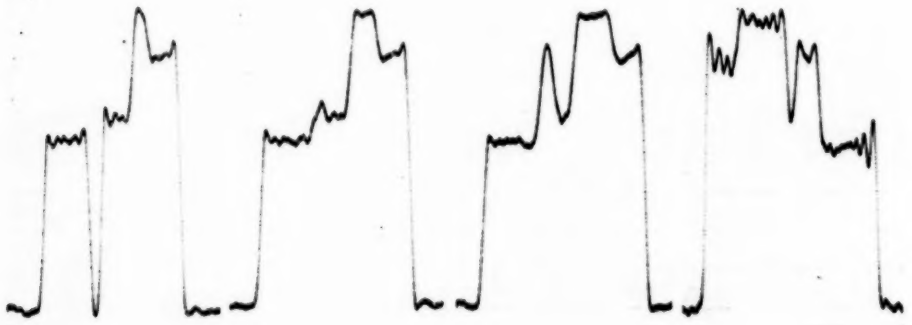

Fig. 7. Slit 21.5 divisions.
Fig. 8. Slit 26.5 divisions.
Fig. 9. Slit 31.5 divisions.
Fig. 10. Slit 36.5 divisions.

multiple, e.g., a doubling occurred at twice the critical slit-width. For widths between multiples of the critical value the diffraction patterns were not as regular. The lines were often well resolved even when they appeared to be multiple. Below the critical width, however, the spaces between the lines were filled with a diffraction background of considerable density.

Evidently accurate estimates of the relative intensities would be difficult to make in some of the cases illustrated, either through measurement of areas or from reading maximum densities. Furthermore, very misleading information concerning true line shapes could easily be got from an examination of the images. The minima due to doubling might be misinterpreted as an indication of reversal. In extreme cases the diffraction patterns might even suggest fine structure.

We plan to present in much greater detail in a forthcoming paper the results of similar studies made with a number of modes of slit irradiation. Some of these modes give rise to doubling or trebling with wide separations between components.

THE MASSES OF O^{17}[1]

By Harold C. Urey
Department of Chemistry, Columbia University

(Received March 9, 1931)

Abstract

The rest mass of O^{17} is calculated from the known rest masses of N^{14}, He^4, and H^1 and the masses due to the kinetic energies of He^4, H^1, and O^{17} as determined by Blackett and Harkins in the transmutation reaction $N^{14}+He^4 \rightarrow O^{17}+H^1$. The only assumptions involved are that the conservation of momentum and of mass-energy holds in these reactions. The masses secured in this way from seven sets of data do not agree within the probable limits of error for the experimental data. It is suggested that this is due either to the formation of O^{17} atoms of different masses and energies in this reaction or to the emission of gamma-rays during the collision. The former of these predicts discontinuous energy levels while the latter would probably cause the rest mass of O^{17} as calculated here to vary continuously. The relation of this calculation to the experiments of Bothe and Pose on the ranges of H particles from boron and aluminum is discussed.

BLACKETT[2] and Harkins and his coworkers[3] have reported the presence of anomalous forked cloud tracks when α particles from thorium C and C′ bombard nitrogen gas in a Wilson cloud-tract apparatus. These forked tracks consist of the usual α-particle track up to the point of the fork; beyond this point there is one heavy track due to a heavy atom and one thin track having all the characteristics of the tracks of high speed hydrogen particles. These forked tracks are anomalous in that the kinetic energy is not conserved. Blackett has given a critical discussion of these tracks and shows that the range of the heavier secondary track is consistent with the assumption that it has an atomic number of 8 and a mass somewhere between 12 and 20 atomic weight units. It seems certain that only two particles are produced as a result of the collision between the α-particle and the nitrogen nucleus because only two tracks result and because these two tracks and the original α-particle track lie in one plane. The approximate conservation of mass requires that the heavy particle produced have an approximate atomic weight of 17 and thus that it be O^{17}. The subsequent discovery of this nucleus in atmospheric oxygen increases our confidence in the correctness of this conclusion.

These authors have secured the velocities of the He^4, O^{17}, and H^1 nuclei (that of N^{14} is zero) and using Aston's values for the rest masses of He^4, N^{14} and H^1, it is possible to calculate the rest mass of O^{17} assuming the conserva-

[1] This paper is Contribution 653 of the Department of Chemistry, Columbia University, New York, N. Y.

[2] P. M. S. Blackett, Proc. Roy. Soc. **107A**, 349 (1925).

[3] W. D. Harkins, and H. A. Shadduck, Zeits. f. Physik **50**, 99 (1928); W. D. Harkins, and A. E. Schuh, Phys. Rev. **35**, 809 (1930).

tion of mass and energy. The mass of O^{17} is then easily seen to be given by

$$M_O = [M_{He}(1 - v_{He}^2/c^2)^{-1/2} + M_N - M_H(1 - v_H^2/c^2)^{-1/2}](1 - v_O^2/c^2)^{1/2}, \quad (1)$$

where $M_O M_{He}$, M_N and M_H are the rest masses of the corresponding atoms in atomic weight units ($O^{16} = 16$) and v_{He}, v_H and v_O the corresponding velocities. The velocities v_H and v_O are calculated from the angles between the direction of the original α-particle track and the directions of the oxygen and hydrogen tracks using the formulae

$$v_O = \frac{M_{He}}{M_O} v_{He} \frac{\sin \psi}{\sin (\psi + \omega)}, \quad v_H = \frac{M_{He}}{M_O} v_{He} \frac{\sin \omega}{\sin (\psi + \omega)}, \quad (2)$$

where ψ and ω are the angles between the α-particle track and the hydrogen and oxygen tracks, respectively. These formulae follow if the law of conservation of momentum holds for these collisions. The velocity of the α-particle is secured from the remaining range of the α-particle at the point of collision by using the well-known relation between range and velocity, $R = kv^3$.

Blackett used $M_{He} = 4$, $M_H = 1$ and $M_O = 17$ in calculating the values of v_O and v_H and did not correct for the change of mass with velocity. Harkins probably used the rest nuclear masses (not the atomic masses) but did not correct for the change of mass with velocity. In making the calculations for M_O, $M_{He} = 4.00107$, $M_H = 1.00723$, $M_O = 17$ have been used in securing preliminary values for v_{He} v_H, v_O and M_O. Using these results values for $M_{He}(1 - v_{He}^2/c^2)^{-1/2}$, $M_H(1 - v_H^2/c^2)^{-1/2}$ and $M_O(1 - v_O^2/c^2)^{-1/2}$ were secured which were then used in repeating the entire calculation in order to correct for the change of mass with velocity and to use only the rest masses of the nuclei and not those of the atoms. These corrections changed the values of M_O by nearly a constant amount of 0.0007 at weight units and did not change the variations in M_O appreciably.

The probable errors in this calculation can be estimated more readily by expanding (1) in the form

$$M_O = M_{He} + M_N - M_H + \frac{1}{2} M_{He} \frac{v_{He}^2}{c^2} - \frac{1}{2} M_H \frac{v_H^2}{c^2} - \frac{1}{2}(M_{He} + M_N - M_H) \frac{v_O^2}{c^2} + \frac{3}{8} M_{He} \frac{v_{He}^4}{c^4} - \frac{3}{8} M_H \frac{v_H^4}{c^4} + \cdots. \quad (3)$$

Then substituting the values of (2) in (3) and neglecting the terms in v^4_{He} and v^4_H, we secure

$$M_O = M_{He} + M_N - M_H + \frac{1}{2} M_{He} \frac{v_{He}^2}{c^2} - \frac{1}{2} \frac{M_{He}^2}{M_H} \frac{v_{He}^2}{c^2} \cdot \frac{\sin^2 \omega}{\sin^2 (\psi + \omega)} - \frac{1}{2} \frac{M_{He}^2 (M_{He} + M_N - M_H)}{M_O^2} \frac{v_{He}^2}{c^2} \frac{\sin^2 \psi}{\sin^2 (\psi + \omega)}.$$

In the last term M_O can be set approximately equal to $M_{He}+M_N-M_H$ since this term is small and the equation then becomes

$$M_O = M_{He} + M_N - M_H + \frac{1}{2} M_{He} \frac{v_{He}^2}{c^2} \left(1 - \frac{M_{He}}{M_H} \frac{\sin^2 \omega}{\sin^2 (\omega + \psi)} - \frac{M_{He}}{M_{He} + M_N - M_H} \frac{\sin^2 \psi}{\sin^2 (\psi + \omega)} \right). \tag{4}$$

From this it is easily seen that the errors in the rest masses of He, N, and H introduce the same error in each calculation and that this is approximately Aston's error in the rest mass of N,[14] namely $\sim$0.0028 atomic weight units and that the error in the energy of the α-particle only affects the small quantity $M_O-M_{He}-M_N+M_H$. An error of one percent in the energy of the α-particle makes an error of only a few units in the fifth decimal place as will be seen below. A study of the effects of errors in ω and ψ on the mass shows that the error in ω is by far the more important because it is a small angle in the case of all the forked tracks measured by Blackett and because M_{He}/M_H ($=\sim 4$) is much larger than $M_{He}/(M_{He}+M_N-M_H)$ ($=\sim 0.235$) so that the error in the second term within the parenthesis of Eq. (4) is the important one. Blackett estimates his mean error of measurement of angles[4] as about 10′ providing the tracks are not curved and the angles are not near 90°, i.e., less than 75°. These conditions are fulfilled in the case of ω for every case except one in which the tracks are curved. The least laborious way for calculating this error was found to be a repetition of the calculation of M_O using $\omega+10'$ instead of ω throughout. The probable error in M_O is then taken as

$$\Delta M_O = (\Delta M_1^2 + \Delta M_2^2)^{1/2}$$

where ΔM_O is the probable error of M_O and ΔM_1 and ΔM_2 are the errors produced by a one percent error in the energy of the α-particle and an error of 10′ in ω, respectively.

The probable errors in Harkins' measurements cannot be estimated. The

TABLE I. *Atomic weights of* O^{17} *with that of* O^{16} *taken as 16.*

Author	M_O(nucleus)	M_O(atom)	$\Delta M_1 \times 10^5$	$\Delta M_2 \times 10^5$	$\Delta M_O \times 10^5$
B4	17.00067	17.00504	2.7	7.1	7.6
B7*	16.99965	17.00402(?)	1.6	7.1	7.3(?)
B1	16.99927	17.00364	1.3	6.0	6.1
B5	16.99893	17.00330	0.9	7.2	7.3
B3	16.99863	17.00300	0.6	6.6	6.6
B6	16.99857	17.00294	0.6	27.7	27.7
B2	16.99698	17.00135	1.0	8.3	8.4
Preliminary Mean	16.99895	17.00332			
Harkins and Schuh	17.0007	17.0050	?	?	

* The measurements are in doubt because the tracks are curved.

[4] P. M. S. Blackett, Proc. Roy. Soc. **103A,** 62 (1923).

track observed by Harkins and Shadduck[5] is difficult to explain because both ω and ψ are obtuse angles so that the conservation of momentum is impossible and thus Eqs. (2) cannot apply, while the angles between the tracks are not reported in the case of the track observed by Harkins and Schuh.

The results of the calculations are listed in the Table I. Column 1 contains a symbol, B1, etc., indicating the first track of Blackett, etc. Altogether the data are complete for seven tracks.

Discussion of Results

It is evident that the total variation of the calculated masses of O^{17} is very much greater than any reasonable estimate of the experimental errors. The lowest value is 0.00197 below the mean. It would be impossible to make a sufficient error in the kinetic energy of the α-particle to account for this error, for in order that this lowest value should agree with the 17.00300 value it would be necessary to assume that the energy of the α-particle was about 1/6 of that actually used in the calculation. The error in the measurement of ω necessary to account for this difference would be about 4°. Yet the track meets all of Blackett's requirements and the published track appears to be distinct and capable of exact measurement. The largest value is 0.00172 above the average. The angle ψ in this case is 78°52′ and thus difficult to measure according to Blackett, but errors in this angle will make only small errors in M_O and thus there is no reason to believe that the mass calculated from this track is in error. Thus the conclusion that these values of the mass of O^{17} do not agree within experimental error seems justified and the preliminary average is not permissible.

The following ways of accounting for the discrepancies may be considered:

1. The oxygen atoms formed may not have the same mass and energy and the mass differences measure the energy-level differences of the O^{17} nucleus. If this is the case, one would expect γ-rays to be emitted by the O^{17} nucleus very soon after the collision.

2. γ-rays may be emitted during the collision process.

A descision between these possibilities is not possible on the basis of these experiments, nor, in fact, on that of the experiments of Bothe[6] and Pose[7] who have shown that the ranges of the H particles produced when α particles of uniform range bombard boron and aluminum respectively fall in discontinuous groups. The second assumption is the one usually assumed by workers in this field. I choose, however, to use the first, for it is more nearly in accord with the well established interpretation of collision phenomena of the external electron shells. Moreover, the time of collision is of the order of mag-

[5] The figure drawn by these authors does not agree with the angles reported but the writer has been unable to reproduce their values for the velocities of O^{17} and H^1 by assuming different ways of defining the scattering angles.

[6] W. Bothe, Zeits. f. Physik **63,** 381 (1930).

[7] H. Pose, Zeits. f. Physik **64,** 1 (1930).

nitude of 10^{-21} sec. while the probability of emission of a quantum from the nucleus should be about 10^{15} so that the emission of a quantum during the collision is relatively improbable. The calculations in either case are subject to about the same errors due to neglect of the momentum of the quantum. An estimate of these errors can be made easily for the calculations as made here.

It is likely that the γ-ray quantum would be emitted within $\sim 10^{-15}$ seconds after the collision.[8] During this time the O^{17} nucleus would move a distance equal to the diameter of one atom and thus the angle between the track of the excited O^{17} nucleus and the original α-particle track would not be the observed angle used in deriving equations (2), since the momentum of the quantum would deflect the track of O^{17}. To see how large an error this would make we shall consider the B4 track and assume that a quantum having energy equivalent to 0.00369 atomic weight units is emitted. This should give the greatest possible error. If this quantum were emitted in a direction parallel to the direction of the O^{17} nucleus, no change in the angle ω would result and thus no error be made in the calculation. If it were emitted perpendicular to the approximate plane of the three tracks, only a slight error would be made since the angle between the O^{17} and α-particle tracks would be changed but slightly. Finally if it were emitted in a direction perpendicular to the O^{17} track and in the plane of the three tracks, a maximum displacement of the O^{17} track would result. This angle is given by the relation

$$M_O v_O \sin(\Delta\omega) = 0.00369c$$

or

$$\Delta\omega \backsimeq \frac{0.00369 \times 3 \times 10^{10}}{17 \times .454 \times 10^{9}} = 0.014 \text{ radians} = 50'.$$

A comparison with the calculated errors in M_O assuming an error of 10′ in the measurement of ω shows that the maximum error possible in the B4 case is about ± 0.00038. The error cannot be this large in any other case for the quantum cannot be as large as the quantum assumed here unless the rest mass of O^{17} is considerably less than 17.00135 which does not appear likely. Thus the actual spacings of the energy levels may be uncertain due to this effect by not more than 10 percent of their total separations from the lowest level. If the B2 collision does not produce a normal O^{17} nucleus, the maximum uncertainty increases in approximately direct proportion to the excitation energy and the uncertainty remains the same fraction of the excitation energy. The probable error would certainly be less, for the quantum may be emitted in a more favorable direction and the total excitation energy may not be emitted at the same time or in the same direction. The largest atomic

[8] The probability of emission of a quantum is proportional to $\nu^3 a^2$ where ν is the frequency and a a length of the dimensions of the emitting system. Taking ν equal to about 10^5 times the frequencies emitted by atoms and a equal to 10^{-4} of the diameter of an atom, we see that this probability will be 10^7 times that of an atom which is known to be $\backsim 10^8$.

weight difference of 0.00369 is equivalent to 0.00358A or 3.4×10^6 electron-volts.

Altogether these estimates of possible errors lead to the conclusion that the B1, B5, B3, and B6 values may all be due to one energy level but that B4 and B2 are due to the formation of O^{17} nuclei of different masses. Finally the B7 track may be disregarded because of the uncertainty arising from the curved tracks. Three masses separated by about equal differences are indicated by the data as shown in Table II. The data are too meager and

TABLE II.

Track	M_o	Av. M_o	ΔM_o
B4	17.00504	17.00504	
B1	17.00364		>0.00182
B5	17.00330	17.00322	
B3	17.00300		
B6	17.00294		>0.00187
B2	17.00135	17.00135	

the uncertainty to great to regard these differences as certain, but equally spaced vibration levels due to a proton (or neutron) vibrating relative to an O^{16} residue of the O^{17} nucleus immediately comes to mind as a possibility.

Bothe's and Pose's experiments showing discontinuous ranges of H particles agree with the assumption of discrete energy levels in the heavier nucleus as they have indicated.[9] If the range of the α-particles is uniform as was the case in their experiments, and if the energy of the heavier nucleus is small as compared with that of the hydrogen nucleus, discrete ranges of H particles will occur, the higher range particles occurring when a nucleus of low energy is formed. These conditions are not fulfilled by Blackett's data for the energy of the α-particles are not sufficiently uniform. It is of interest, however, to note the rough agreement between this data and the data of these authors. Table III shows the atomic weight of O^{17} as calculated, the kinetic energies

TABLE III.

Track	M_o	E_{He} $\times10^{+3}$	E_0 $\times10^{+3}$	E_H $\times10^{+3}$	v_H $\times10^{-9}$	R_H(cm)
B4	17.00504	8.35	1.94	4.30	2.58	17.2
B7	17.00402	8.64	1.08	5.95	3.25	34.3
B1	17.00364	7.63	0.98	5.40	3.09	29.5
B5	17.00330	7.45	1.90	4.65	2.87	23.6
B3	17.00300	6.96	1.72	4.64	2.87	23.6
B6	17.00294	8.70	3.15	4.49	2.64	18.4
B2	17.00135	8.28	1.55	7.78	3.71	51.1

of the α-particle, and of the H and O^{17} nuclei, the velocity of the H nucleus and its range in air calculated from the formula, $R_H/R_{He}=v^3_H/v^3_{He}$. The

[9] E. Rutherford and J. Chadwick, Proc. Camb. Phil. Soc. **25,** 186 (1929) conclude that the variation of Blackett's data is outside experimental limits of error, but do not calculate the masses of O^{17} as is done here.

kinetic energies are expressed in atomic weight units per gram molecule (at. wt. of $O^{16}=16$). The energy of the O^{17} nucleus is considerably smaller than that of the hydrogen nucleus except in the case of the B6 track. The shortest range H nucleus is indeed that of the B4 track and the longest that of the B2 track as expected. The irregularities of the ranges as compared to the calculated masses of O^{17} can be seen to be due to the variations in the kinetic energies of the α-particles or of the O^{17} nucleus.

Bothe and Becker[10] have detected the emission of γ-rays from lighter elements during the disruption of the nucleus in agreement with the expectations of this calculation and the interpretation of the results. They report, however, that the γ-radiation in the case of nitrogen gas bombarded with α-particles from polonium is very weak. This does not contradict the prediction of γ-rays in the collisions observed by Blackett, for they are all due to α-particles of considerably longer range (6.24 to 7.79 cm) than those from polonium.

On the basis of this calculation the atomic weight of O^{17} cannot be greater than the minimum value calculated, namely, 17.00135 ± 0.0028 if the atomic weight of O^{16} is taken as 16.000.

[10] W. Bothe, and H. Becker, Zeits. f. Physik **66,** 289 (1930).

PROPAGATION OF LARGE BARKHAUSEN DISCONTINUITIES

By K. J. Sixtus and L. Tonks
General Electric Company, Schenectady, New York

(Received February 28, 1931)

Abstract

Large Barkhausen discontinuities have previously been observed by Forrer and by Preisach in nickel wires and hard-drawn wires of the nickel-iron series respectively under stress. A prediction that these discontinuities occur in form of a propagation along the wire, starting at a nucleus, has now been substantiated. In the experiments an additional local field was used to start the propagation at a definite point on the wire, which was in a uniform magnetic field, and the velocity was determined by measuring the short time interval elapsing between the passage through two search coils around the wire. With a fixed value of tension on the wire, the velocity v was found to vary approximately linearly with the applied uniform field H, so that $v=A(H-H_0)$. A is the slope of the velocity-field characteristic and H_0 is called the *critical field*. Measured velocities range from 500 to 40,000 cm sec^{-1}. H_0 varies with composition, amount of cold working, and with the stress applied to the wire. Increasing tension reduces the critical field over the greater part of the Ni-Fe alloy composition range. The behavior of H_0 with increasing and decreasing tension shows the presence of elastic hysteresis. A is nearly constant for changes in tension, in diameter of wire, for composition of wire, and is the same for a strip. Its value is approximately 25,000 cm sec^{-1} gauss^{-1}.

The existence of eddy currents limits the speed with which magnetism can penetrate the wire. A rough calculation of this time gives values in the neighborhood of 10^{-2} sec. Thus a discontinuity travelling at 10^4 cm per sec. occupies a length of some 100 cm on the wire. This was substantiated both by measurements of the peak voltage induced in a search coil and by oscillograms taken of the induced voltage. The observed passage times agree well with the theoretical penetration times.

The constancy of the v-H slope for wires of different diameters is believed to indicate that the velocity depends upon surface phenomena rather than volume phenomena. The velocity would thus be determined by conditions existing near the front edge of the discontinuity where the penetration is still slight. The critical field is believed to represent a threshold value of magnetic field which must be exceeded at all points of the wire before reversal of magnetism can occur. The excess of the impressed field over the critical is nullified during propagation by the fields arising from the eddy currents. A possible picture of the discontinuity is one in which the reversal occurs within a minute distance of an approximately conical surface in the wire, the edge of the base of the cone forming the front of the wave.

The explanation advanced by Preisach for the asymmetric hysteresis loops found if one limit of the magnetization cycle was reduced has been extended. In this case magnetic inhomogeneities act as nuclei. Mechanical distortion introduces inhomogeneities of another type which also lead to the very easy formation of a nucleus. The phenomena found with torsion are more complicated than for tension. In some cases the slope of the v-H lines shows appreciable variation with direction of twist. The results of tests with various compositions of the nickel-iron series are described using both tension and torsion, but no new relations to other properties of these alloys can be given so far. Identifying H_0 with coercive field, R. Becker's theory has been compared with our results. It appears that in most cases increased elastic tension and increased cold working stresses shift H_0 in opposite directions.

1. Large Barkhausen Discontinuities

SINCE the discovery of the Barkhausen effect, it has been a well-established fact that a great part of the change in induction in a ferromagnetic when subjected to a varying field, is made up of discontinuous changes. These ordinary discontinuities can only be observed after amplification and are not detectable by the ballistic method. Large discontinuities were first observed by Forrer[1] in 1926 in the hysteresis loop of a strained nickel wire. Later Preisach[2] showed that wires of Ni-Fe alloys under the influence of any stress (tension, torsion, bending) gave large discontinuities in a longitudinal field. In some cases these discontinuities were equal to almost the whole change in induction between saturation in the two directions.

If one tries to picture the manner in which such a magnetization discontinuity occurs, one is struck by the difficulty of accounting for a simultaneous reversal in the whole length of a fine wire. This consideration led Langmuir to predict that the magnetization first reversed at one point in the wire, forming a nucleus, and that the two boundaries which were thus formed then travelled along the wire with a finite velocity which probably depended on the magnetic field strength and the elastic strain. This prediction has been well substantiated by the experiments which will be described in what follows. A preliminary report of this work has appeared in the Phys. Rev. **35,** 1441 (1930).

2. The Propagation of Magnetization

Several investigations on the propagation of magnetic waves have been carried out.[3] The method used has been the same in all cases. An iron wire or bar was subjected to an alternating magnetic field at one point and the phase shift and maximum value of induction a certain distance away were measured. Zenneck[4] proposed a theory for the observed effects, based on the assumption of eddy currents as a determining factor, and postulated the equivalence of electric and magnetic waves propagating along a ferromagnetic conductor. But the velocities corresponding to the observed phase shifts differed within a wide range (10^3 to 10^5 cm/sec), the whole phenomenon appeared to be very complex, and no effort was made to relate theory and experiment to each other.

The problem appears simpler in the case of the propagation of a single discontinuity, particularly a 100 percent discontinuity, by which is meant one in which the reversal of saturation is complete. In such a case we are dealing with a medium of finite conductivity and permeability unity but capable of reversing its magnetization at a point under a certain critical local condition.

[1] M. R. Forrer, Journ. de Physique [VI] **7,** 109 (1926).

[2] F. Preisach, Ann. d. Physik **3,** 737 (1929).

[3] A. Oberbeck, Ann. d. Physik **21,** 672 (1884); **22,** 73 (1884). H. A. Perkins, Amer. Jour Sci. **18,** 165 (1904). Lyle and Baldwin, Phil. Mag. **12,** 433 (1906). C. V. Drysdale, Electrician **67,** 95 (1911).

[4] T. Zenneck, Ann. d. Physik **9,** 497 (1902).

This local condition is defined by two variables, the state of elastic strain and the magnetizing force.

It was thought that general energy considerations might enable us to make an attack on this problem. A change of intensity of magnetization ΔI in a field H represents an available energy density of $H\Delta I$. This must at least exceed the energy dissipated by the eddy currents accompanying the magnetization wave.[5] These losses can be estimated as follows. The whole change of magnetization intensity, ΔI, is assumed to occur in a

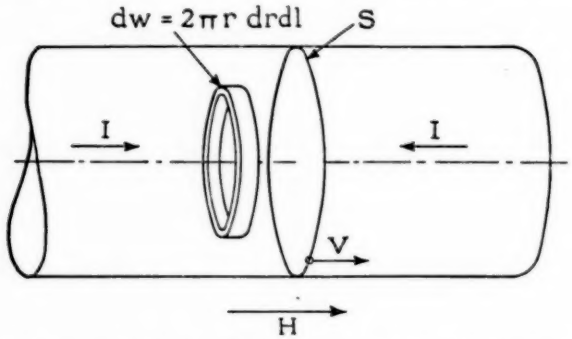

Fig. 1. Illustrating the induction of eddy currents by a moving magnetic discontinuity.

thin plane slab, S, moving with velocity v as shown in Fig. 1. The time integral of the e.m.f. induced in an annular volume dw of radius r will be that due to the change in flux, $\Delta\phi$, inside that ring, that is,

$$\int F dt = \Delta\phi/c = \pi r^2 \cdot 4\pi\Delta I/c \tag{1}$$

where F is the e.m.f. induced in dw and c is the ratio of units. The chief contribution to this integral will occur while the discontinuity is within a distance of dw which is comparable with its radius r. Accordingly, instead of $\int F dt$, where F is the e.m.f., we may write $F\Delta t$, approximately, where $\Delta t = 2r/v$. Applying this to Eq. (1), we have

$$F = 2\pi^2 r v \Delta I/c. \tag{2}$$

Since F is acting for a time Δt the eddy current loss in dw is $F^2\Delta t dr dl/2\pi r\rho$ where ρ is the specific resistance. Combining with Eq. (2) and integratting, the energy loss per unit length of wire of diameter a is found to be $E = (4/3)\pi^3 a^3 v(\Delta I)^2/\rho c^2$. The magnetic energy available is $E_m = \pi a^2 H\Delta I$. Equating the two we find for the velocity

$$v = (3/4\pi^2)\rho c^2 H/a\Delta I \tag{3A}$$

in magnetic units or

$$v = 0.76 \times 10^8 \rho H/a\Delta I \tag{3B}$$

in practical units.

[5] This reasoning obviously neglects any elastic energy changes which may occur.

Another calculation based on what appeared to be a less favorable hypothesis at the time was made by Dr. H. Poritzky. The assumption that the magnetization change occupies a length, λ, of the wire, long compared to a, gives

$$\Delta t = \lambda/v.$$

Reasoning as before, it follows that

$$v = (1/2\pi^2)\rho c^2 H\lambda/a^2\Delta I \tag{4A}$$

in magnetic units, or

$$v = 0.51 \times 10^8 \rho H\lambda/a^2\Delta I \tag{4B}$$

in pratical units for this case.

3. Apparatus

Theory of method. In measuring rectangular hysteresis loops of the same type as published by Preisach, it was noticed that the field strength at which the large discontinuity occurred, which will be called the *starting field*, was variable within a few percent in successive experiments. Since the occurrence

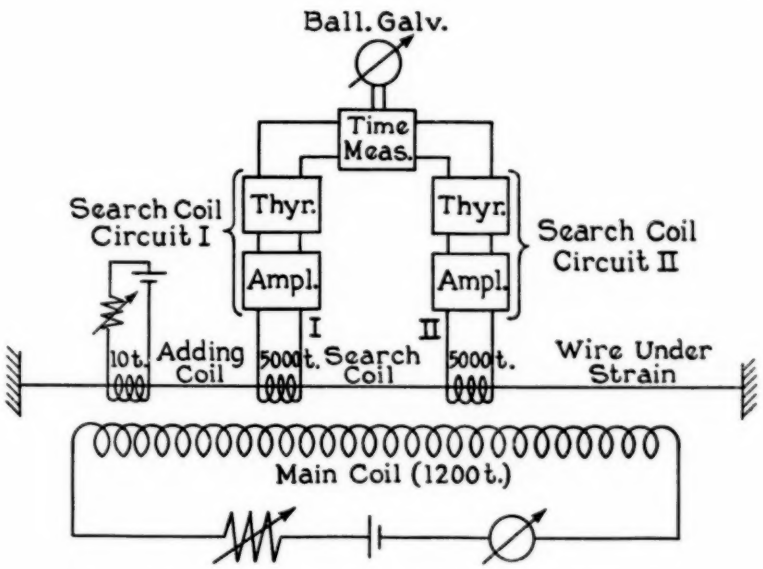

Fig. 2. Schematic diagram of circuit for velocity measurements.

of the large discontinuity depends upon the spontaneous formation of a nucleus, as described in Section 1, this erratic behavior can either mean that one nucleus was itself starting erratically or that different points along the wire were acting as nuclei. To control the creation of a nucleus an "artificial nucleus" was made by locally increasing the field strength by means of a current through a small magnetizing coil which created a local adding field. If then the homogeneous field, which will be called the *main field*, was set at a value

below the starting field, the large discontinuity could be initiated by applying the local adding field. The change in magnetization then begins at this point and propagates into the homogeneous part of the field where its velocity can be determined in the following way. If we place two search coils around the wire at a known separation, the discontinuity in travelling along the wire will produce successive voltage surges in these coils. If their time interval be measured, the velocity can be calculated.

Design of apparatus. The main field (Fig. 2) was furnished by a helix of 65.5 cm length containing 1200 turns of copper wire of 0.051 cm diameter, wound on a glass tube. Thus the uniform part of the field is given by $H = 23.0\, i$ (i being the magnetizing current in amperes). The decrease in H 23 cm from the middle of the coil is 0.5 percent. At first a liquid resistance allowing continuous variation of current was used, but later on a slide-wire resistance was found to give a sufficiently gradual variation.

The wire under investigation was held in the axis of the coil and could be subjected to tension or torsion or both in the same way as described by Preisach. The tension was read by a spring balance and the twist by a pointer connected to the wire. The wire was surrounded by a capillary glass tube so as to permit its easy replacement with the search coils in place.

Each search coil consisted of 5000 turns of copper wire of 0.008 cm diameter. Since the length of the winding was 0.65 cm and the inner and outer diameters were 0.4 and 1.8 cm respectively, the voltage induced in them could not be proportional to the change in flux in one point on the wire, but gave an average over a distance comparable with the outer diameter (i.e., approximately 2 cm). The coils were wound on hard rubber spools and could be moved separately along the capillary tube by means of strings connected to them, and their positions could be read by pointers fastened to the strings and sliding along a scale. In most cases their separation was kept at 20 cm, each being 10 cm from the center of the main field.

The additional local field was produced by a coil of 10 turns of copper wire of 0.051 cm diameter, wound on a spool which was also movable along the wire. Generally the adding coil was placed at a distance of 24 cm from the middle of the main field.

Time-measuring arrangement. For measuring the time interval between the voltage impulses induced in the two search coils by the passing discontinuity, a vacuum tube device (Fig. 3) was built. This system, which is similar to the one used by Turner for his Kallirotron amplifier,[6] has two stable states of current distribution, if voltages and resistances are properly adjusted. In State 1, plate current is flowing only in Tube I and there is no measurable plate current in Tube II; in State 2, current is flowing only in Tube II and there is no current in Tube I. To explain this let us assume that both tubes carry current. If a negative voltage impulse is now applied to the first grid, the plate current in Tube I decreases and in turn reduces the potential drop in R_I, which makes Grid II more positive. The plate current in II there-

[6] L. B. Turner, Radio Review 1, 317 (1920).

fore rises, causing an increasing potential drop in R_{II}, and since this drop furnishes the grid bias for Tube I the grid voltage in I becomes still more negative. This cumulative action proceeds until practically no current is flowing in I, while the plate current in II has its full value. The current may now be shifted back to Tube I by applying a sufficient negative voltage to the grid of Tube II. Since the minimum value required increases as the resistances R_I and R_{II} are increased, the sensitivity of the circuit is under control. Two UX-112A tubes were used.

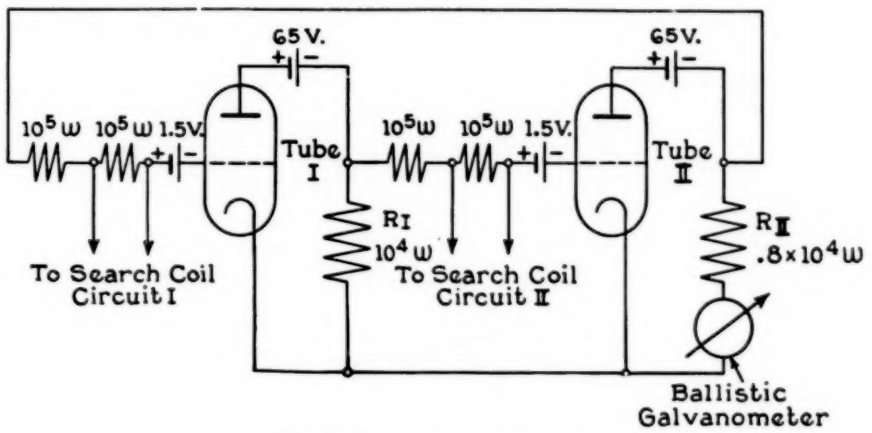

Fig. 3. Time-measuring circuit.

In making a time interval measurement this circuit was put into State 1 and a negative voltage impulse excited by Search Coil I was applied to the grid of Tube I. This shifts the current over to Tube II. After a time interval t the impulse from Search Coil II impressed on the second grid stops the current in Tube II. Thus the quantity of electricity which has passed through Tube II is a measure of the time t between the impulses. This quantity was measured by a ballistic galvanometer so that t was given by

$$i_P t = C\theta \tag{5}$$

where i_P is the plate current, C the ballistic constant of the galvanometer, and θ its deflection.

This relation was checked by means of a pendulum which opened two contacts in succession. Each contact was joined in series with a battery and the primary of a transformer, and the secondaries were connected respectively to the grids of Tubes I and II of the timing circuit. The opening of the contacts thus produced voltage impulses on the grids. The pendulum was calibrated by using a known condenser discharging through a known resistance. The time interval found from the pendulum calibration agreed with those calculated from Eq. (5). This means that the shift of the current from one tube to the other occurs in a time short compared with the time intervals to be measured.

The negative voltage impulse applied to tube I had to exceed a certain

minimum value (for given voltages and resistances in the timing circuit) but if it were too large, the current, after shifting to II, failed to return with the negative impulse on II. Thus it was necessary to keep the impulses within a certain range. The timing circuit was so adjusted that impulses of 1 volt operated it, and this voltage was obtained independently of the magnitude of the voltage induced in a search coil in the following way: The impulse from each search coil was amplified by a two-stage resistance-coupled amplifier whose output was impressed on the grid of a thyratron[7] as shown in Fig. 4. The sudden rise of plate current, from 0 to 100 m.a. in the present circuit, being independent of the voltage impressed on the grid, always gives the same voltage of approximately 1v. across the secondary of the transformer in

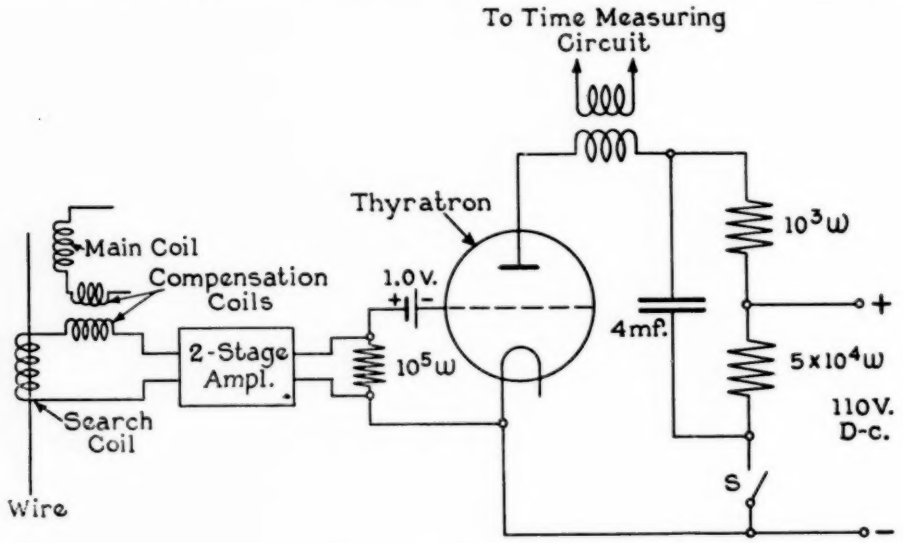

Fig. 4. Thyratron relay.

the plate circuit. The 4-μf condenser and 50,000-ohm resistance made it possible to stop the discharge in the thyratron by simply closing the switch S. thus setting the circuit for the next impulse.

The maximum voltages induced in the 5000 turn search coils were of the order of 0.1 v. The amplification of the amplifiers used was about 120. As the grid bias of the thyratrons was so adjusted that positive impulses of about 1 v. would start the discharge, both thyratrons were started before the voltage impulse reached its maximum (See oscillograms Figs. 11 and 12). The whole

[7] A thyratron is a three element tube containing a small amount of mercury. The cathode of the one used was oxide coated. In a thyratron which is initially carrying no current, current does not start to flow as long as the grid potential is less than a certain value. As soon as the grid voltage exceeds this critical value, however, the full plate current begins to flow, and from this moment on the grid has no further influence on this current. By using a proper value of grid bias this tube can be used as a relay, as in Fig. 4, or as a peak voltmeter. See: A. W. Hull, Hot-Cathode Thyratrons, Gen. Elec. Rev. **32,** 213, (1929) and **32,** 390 (1929); A. W. Hull and I. Langmuir, Proc. Nat. Acad. Sci., March 1929; A. W. Hull, Trans. A.I.E.E. **47,** 753 (1928).

arrangement, it was found, worked satisfactorily down to time intervals of 0.5×10^{-3} sec, since all time constants were kept as low as possible.

Hysteresis loops. Hysteresis loops were taken with the magnetizing coil and one search coil (Fig. 2). The latter was connected to a ballistic galvanometer (Leeds and Northrup Type HS No. 2285d) with a sensitivity as used of 1425 Maxwell/Sc. div. and a period of 30 sec. The direct effect of the magnetizing coil on the search coil was compensated as usual by a mutual inductance.

4. Velocity Measurements

Composition and treatment of specimens. The wires used in our experiments were made from ingots of electrolytic nickel and Armco iron plus 0.25 percent manganese to make the alloy ductile. The ingots were swaged and then drawn down to 0.10 cm diameter, sometimes to 0.076 cm, with annealing. From this diameter the wires were cold drawn to 0.038 cm. The per-

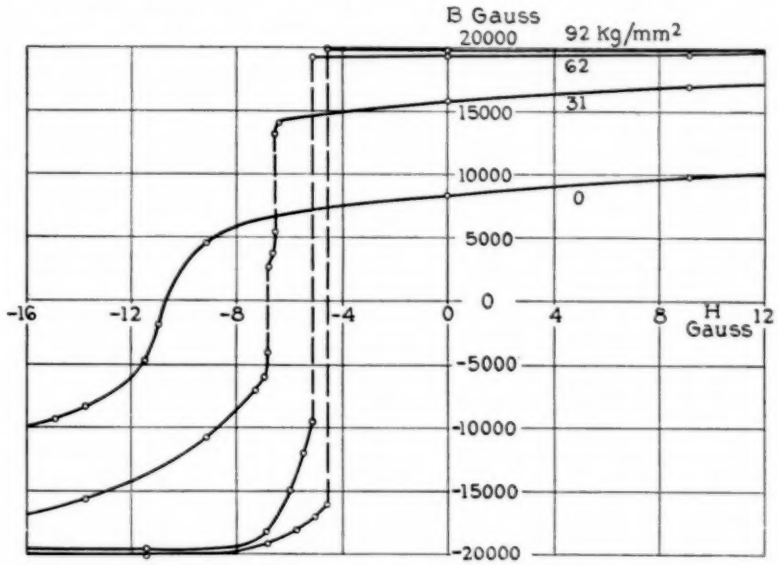

Fig. 5. Hysteresis loops for a wire under different tensions. Wire of 0.038 cm diameter from ingot No. 32, 15 percent Ni-Fe (only half of the total loop is shown).

centage of Ni was determined for each wire investigated by chemical analysis. In this section we shall deal mainly with alloys of between 10 and 20 percent Ni since these show the phenomena of propagation very markedly. In Section 11 the results with wires of other compositions will be considered briefly.

The wires were aged by stretching them for about 1 hour with loads near to the elastic limit, because more consistent results were obtained in this way. The aging load was never exceeded by the tensions used in the course of an experiment. Incidentally, in these hard drawn wires the breaking point lies only slightly beyond the elastic limit.

Effect of tension on hysteresis loops. Fig. 5 shows hysteresis loops for a wire of 15 percent Ni Fe and 0.038 cm diameter (cold drawn from 0.076 cm)

under different tensions. These loops are of the same type as the ones observed by Preisach. With no load only the ordinary Barkhausen discontinuities occur and these cannot be detected by the galvanometer. With rising tension the formation of large discontinuities begins until with high tension a great part of the whole change between negative and positive saturation occurs in one single discontinuity. The maximum magnetizing field was in all cases 34.5 gauss. The curves show that for increasing tension the remanence

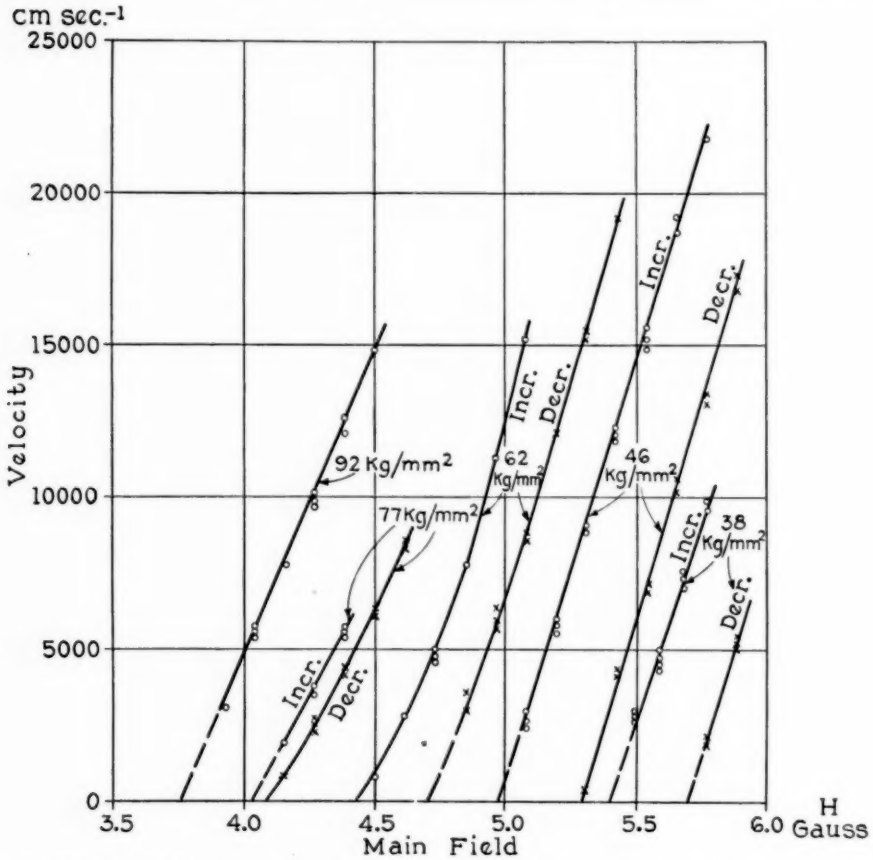

Fig. 6. Velocity-field curves for a wire under different tensions. Wire of 0.038 cm diameter from ingot No. 14, 14 percent Ni-Fe.

increases until it equals 100 percent saturation as exactly as we could measure. The coercive field on the other hand is reduced by increasing tension.

Velocity measurements. A complete set of velocity measurements covered both variation of tension and of magnetic field. This was accomplished by finding the relation of velocity to field at each of a series of values of tension. In this series the tension was increased from zero to a maximum and then decreased again. At any one tension the starting field (see Section 3) was determined so that it might serve as an upper limit to the fields which could be used in the velocity determinations The main field was then set at a value be-

low this, and the propagation was started by sending a current through the adding coil. The velocity of propagation was obtained from the throw of the ballistic galvanometer in the timing circuit and the known separation of the coils.

The results for a wire, 14 percent Ni-Fe, 0.038 diameter, are given in Fig. 6 for several values of tension between 38 and 92 kg/mm², the range in which large discontinuities were found. These curves exhibit some very striking features. They are, except in two cases, straight lines and are approximately parallel to each other. The higher the tension the further are the curves shifted to lower field strengths. The failure of the curves taken with decreasing tension (marked "Decr.") to coincide with the curves taken with increasing tension (marked "Incr.") shows the presence of elastic hysteresis which was observed directly by stress-strain measurements. When the wire which had undergone the stress cycle described was allowed to "rest" without tension for an hour, it reverted almost completely to its original condition, so that approximately the same cycle could be reproduced.

Observations of velocity were made down to velocities as low as possible but in many cases the experimental points could not be measured below 1000 cm/sec. In this neighborhood the discontinuity, after passing the first coil, often failed to reach the second one. In view of the linearity of the curves it is quite reasonable to suppose that the failure to propagate at low velocities does not arise from any inherent limitation in the mechanism of propagation but rather from irregularities in the wire which, influencing relatively small portions of the material, are unable to affect seriously a discontinuity propagating under more favorable conditions. For this reason the curves have been extrapolated to zero velocity, and the intercept with the H-axis has been interpreted as the limiting field in which propagation at a velocity approaching zero would occur in an ideal wire. This field will be called the *critical field* and will be designated by H_0.

The behavior of the v-H curves with respect to the elastic hysteresis mentioned is peculiar in that the successive curves with decreasing tension instead of lagging with respect to the "Incr." curves, as they would if H_0 were a function of elongation, show the opposite behavior. This could be due to two types of response in the wire, one an immediate elastic response, and the other a slower and limited plastic yield. A lowering of H_0 by the elastic strain combined with an increase of H_0 with plastic deformation would account for the phenomenon observed. (See Section 12).

Judging from their general character, the curves may best be represented by an empirical formula of the type

$$v = A(H - H_0) \tag{6}$$

where v is the velocity of propagation, and A is the slope of the line which was within 25 percent of a value of 25,000 cm sec^{-1} gauss^{-1}.

When the velocity was measured over subdivisions of the usual 20 cm and over other portions of the wire still within the uniform 46 cm of field, this

velocity was found to be always the same for the same conditions in the cases where the v-H characteristics were straight lines. When these characteristics were curved, however, the velocity showed some variation. This suggests that the curvature arises in some way from a variation in the state of the wire along its length.

One of the cases in which the characteristics showed the greatest curvature was that of the wire whose hysteresis loops were shown in Fig. 5. These characteristics are reproduced in Fig. 7 as an example of the greatest deviation from the simple relations usually found.

The above tests were originally made with a view to testing the constancy of the velocity of propagation. Another test consisted of varying the position and intensity of the adding field. It was found that for a certain position of

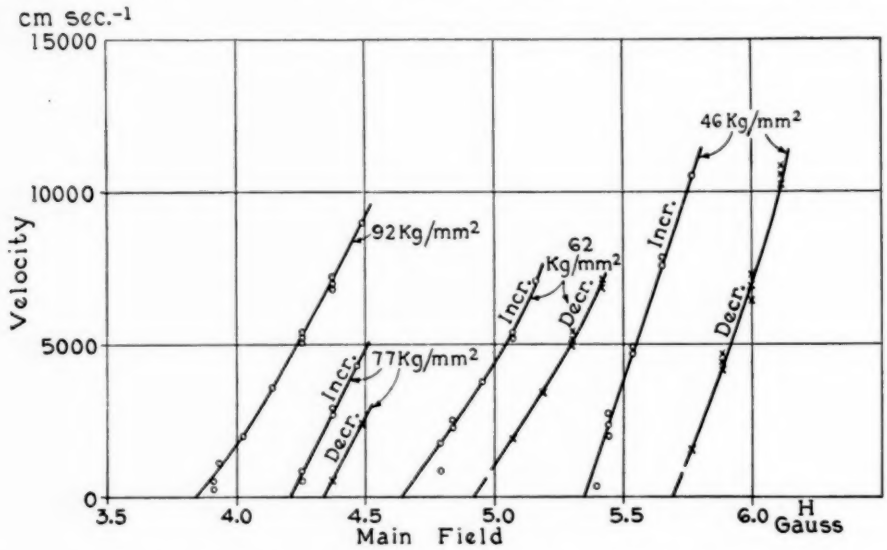

Fig. 7. Velocity-field curves for a wire under different tensions. Wire of 0.038 cm diameter from ingot No. 32, 15 percent Ni-Fe.

the adding coil a certain minimum current was required to start the discontinuity, but that this minimum varied in successive trials. The average of this minimum at each of several successive points along the wire was found to vary considerably, exhibiting maxima and minima even in the homogeneous part of the field. The velocity of propagation was independent of both position and magnitude of adding field as long as this field did not add to the uniform field between the search coils appreciably.

The magnitude of the discontinuity is nearly constant over the homogeneous part of the field; only at very low velocities do large differences at different points appear. Since large differences at the same point in successive trials were also found, we can only conclude that the behavior is erratic at low velocities.

It is significant to note that the general effect of the aging process referred

to at the beginning of this section is to increase the critical field but to leave the slope of the characteristic in most cases unchanged. This suggests that while the critical field depends on the strain state of the wire, the slope depends on other factors.

5. Comparison of Experiments and the Eddy-Current Theory

It is now possible to make a direct comparison of the velocities appearing in Fig. 6 with those calculated from the eddy current formulas derived in Section 2. For 15 percent Ni-Fe $\rho = 30 \times 10^{-6}$ ohm cm and using an average value of H of 5 gauss and an average value of ΔI of 2400, Eq. (3B) gives $v = 250$ cm sec^{-1} compared to velocities well exceeding 10^4 cm sec^{-1} in many cases. A discrepancy in the other direction might well have been explained on the basis that the magnetic energy was only partially available for conversion into eddy currents. Eq. (4B), however, permits of velocities greater than those given by Eq. (3B) roughly in the ratio that λ exceeds a. Actually, the observed velocity of 10^4 cm sec^{-1} would require a ratio $\lambda/a = 60$. But how could a transition 60 times as thick as the diameter of its front characterize the definite self-propagating phenomenon we were observing?

At least, the formulas gave experimental hints and also served to emphasize certain features of the velocity-field characteristics. We have already remarked that these characteristics do not pass through the origin so that v is not proportional to H. This might be an indication that, for some reason, the magnetic energy available is not $H\Delta I$ but $(H - H_0)\Delta I$ so that on this hypothesis

$$v = 0.51 \times 10^8 \rho\lambda(H - H_0)/a^2\Delta I \tag{7}$$

On the other hand, such reasoning would increase λ/a over ten-fold since $H - H_0$ is some 0.4 gauss compared to the 5 gauss assumed for H at $v = 10^4$ cm sec^{-1}.

A comparison of velocity-field slopes with ΔI (or ΔB as in Fig. 8) shows no such correspondence as indicated by Eq. (3B) and a check of slope against wire diameter gave the values of slope shown in Fig. 9. The wires used were of 10 percent Ni-Fe and were cold drawn from 0.102 cm to the different diameters. Over a three-fold range of diameters, namely, from 0.020 to 0.061 cm the observed slopes, taken for one wire at different tensions or for different wires, lie scattered in the range 2 to 3×10^4 cm sec^{-1} gauss^{-1}, and show no evidence of an increase in slope with a decrease in diameter. The 0.071 cm diameter slope is probably not comparable with the rest because the magnitude of the discontinuity gradually decreased as it proceeded along the wire.

The successively smaller wires have been subjected to successively greater amounts of cold working thus raising the question as to how comparable the results can be on this account. It has been pointed out, however, (Section 4) that the aging process has a marked effect on the critical field but almost none on the v-H slope. And later it will be seen that annealing wires of various diameters, succeeded by cold drawing to a uniform size, again yields specimens having different values of H_0 but approximately equal v-H slopes. Thus the

differences in cold working are probably of no significance as regards our present conclusions.

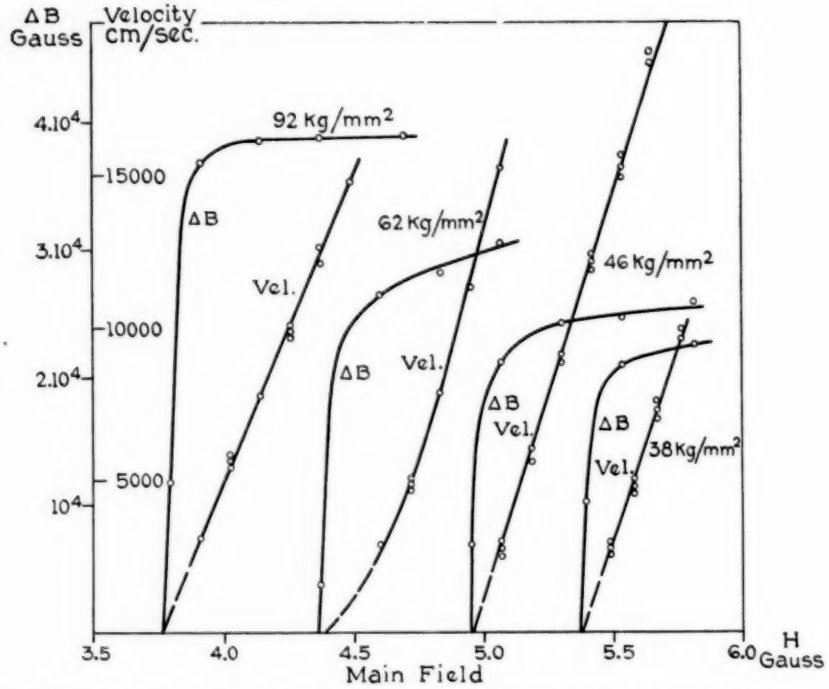

Fig. 8. Magnitude of the discontinuity and velocity as functions of field and tension. Wire of 0.038 cm diameter from ingot No. 14, 14 percent Ni-Fe.

The evidence against the eddy-current theory which we considered to be most convincing was given by the following experiment. A wire of 0.254 mm

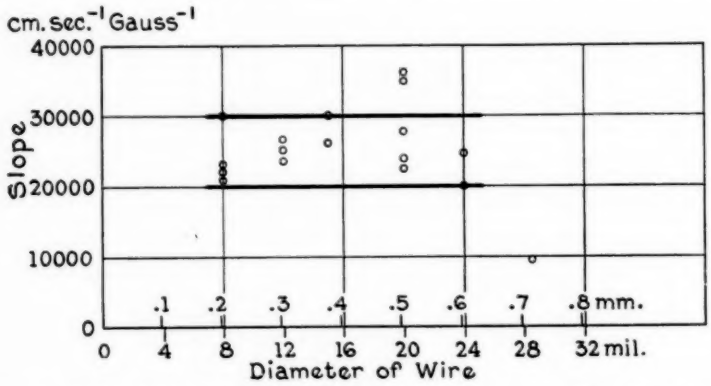

Fig. 9. Slope of velocity-field curves for wires of different diameters. Wires from ingot No. 24, 10 percent Ni-Fe.

diameter was rolled down to a strip 0.076 mm thick and 0.53 mm wide. Although the influence of eddy currents is, of course, reduced considerably in

comparison with the round wire, the v-H slopes measured for the strip fall in the same range as the slopes found for wires.

At this stage in the investigation we found ourselves in the position of observing magnetic discontinuities travelling with such high velocities that for the phenomenon to be energetically possible this "discontinuity" must occupy a length on the wire of at least 60 times and perhaps 750 times (if energy available is $(H-H_0)\Delta I$) the wire radius. The proof that this actually occurs is a result of the measurements on the voltage induced in the search coils and of the oscillograms of the wave shape which are described in the next two sections.

6. Voltage Measurements

We have already mentioned the fact that the voltages induced in the search coils are of the order of several tenths of one volt, but we should expect much higher voltages on the basis of a plane wave front. Let us make the assumption that the total change in flux, $\Delta\phi = 47$ lines (for a change in induction of $\Delta\phi = 40{,}000$ gauss) in a 0.038 cm wire, produces a voltage in the coil during the time Δt, which the jump needs to travel a distance equal to the diameter (2 cm) of the coil. That will give us an average value of voltage to be expected, and the maximum voltage might be much higher than this. Now $v = 10^{-8} n\Delta\phi/\Delta t$ where v is the voltage induced in a coil of n turns. Taking $n = 5000$, and $\Delta t = 2\times 10^{-4}$ sec (for a velocity of 10,000 cm/sec), we obtain 11.8 volts as a lower limit for the peak voltage. The existence of any such voltages would have rendered the use of amplifiers in the original velocity measurements entirely unnecessary. It therefore became of interest to eliminate this large discrepancy by direct voltage measurements.

In our determinations a thyratron circuit, similar to the one shown in Fig. 4, was used as a peak voltmeter. By adjusting the grid bias in several trials, a bias value was found at which the single impulse just started the discharge. The difference between the known critical voltage and the applied bias is the peak voltage of that impulse. The voltage induced in a 200-turn search coil was amplified by two screen-grid stages, giving a uniform amplification of 120 in the frequency range between 30 and 10^4 cycles/sec. While a single search coil permits the measurement of the voltage peak only, it was thought that two search coils with variable separation and connected in series-opposition would allow a rough determination of the wave shape itself to be made simply by plotting the observed peak voltage against coil separation. A more detailed analysis made after numerous measurements had been taken shows that this experiment would give the same apparent wave-front shape for a variety of actual shapes.

Thus in Fig. 10 the shape of the curves which were obtained in this way is roughly that to be expected from the method used, leaving as significant features only the voltage maximum attained and the least separation of the coils which gives that maximum. The former yields the maximum rate of change of flux, the latter the distance from wave front to this point in the wave.

The curves of Fig. 10 depict measurements made with different values of main field, that is, with different velocities. Over a 3-fold range of velocities the maximum is seen to come between 4 and 6 cm from the beginning, and the plot to the right shows that the peak voltage is proportional to the velocity. This indicates that the discontinuity retains an approximately constant shape as its velocity changes.

Although the two-coil method fails to give the wave shape near the wave front it is reliable beyond the voltage maximum. This region was explored by connecting the coils in series-addition (the negative peak voltage with the series-opposition connection could also have been used) but as the oscillograms taken subsequently cover the same range in greater detail these results will not be given.

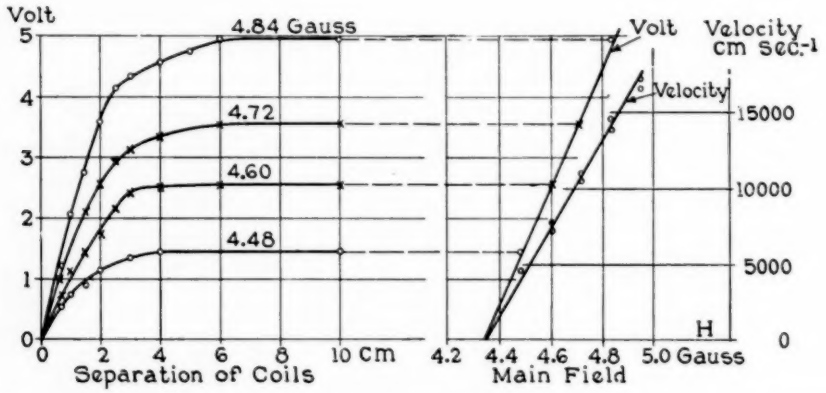

Fig. 10. Amplified peak voltage induced by the discontinuity in two search coils connected in series-opposition. Voltage amplification 120 times. Wire of 0.038 cm diameter from ingot No. 14, 14 percent Ni-Fe.

A comparison between the voltages induced in two coils of 200 and 5000 turns, respectively, was made to make sure that the internal capacity of the coils was not reducing the coil voltages. The ratio of voltages found, namely, $0.023/0.59 = 0.039$, so nearly checks the turn ratio as to prove that any such effect is negligible in these experiments.

7. Oscillograms

Further information concerning the nature of the discontinuity was obtained from oscillograms of the voltage induced in a search coil. The circuit connections were made in this order: 5000-turn search coil to high resistance potentiometer to amplifier to oscillograph. The potentiometer was used to obtain a suitable oscillograph deflection in each case. The amplifier had 3-resistance-coupled stages. The oscillograph was of the Blondel type. The vibrator used to reproduce the voltage had a sensitivity of 1.45 m.a./mm and a natural frequency of 1000 cycles/sec. Figs. 11 and 12 show the amplified voltage wave superimposed on the plate current of the last tube for a wire of 14 percent Ni-Fe and 0.038 cm diameter under a tension of 92 kg/mm^2. In

Fig. 11 the discontinuity is traveling at a rate of 17,000 cm sec^{-1} in a field of 4.25 gauss, in Fig. 12 the velocity is 7000 cm sec^{-1} in a field of 3.91 gauss. We note the steep rise of the voltage and the long tail with many irregularities. But in interpreting these curves we have to bear in mind that the resolution of the method is limited by three factors. First, there is the limited space resolution of the search coil, a factor also present in the method employed in Section 6. It has already been estimated that this limit is of the order of 2 cm for the 5000-turn coil used. But of more importance here is the second factor, the limited time resolution of the oscillograph vibrator. The maximum in

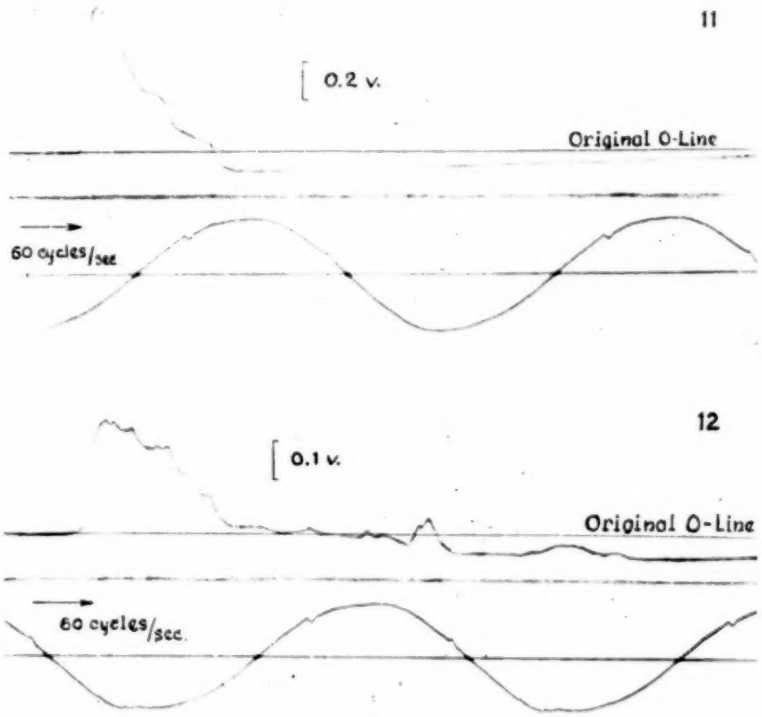

Figs. 11 and 12. Amplified voltage induced in a 5000-turn search coil by the discontinuity. Velocities: Fig. 11, 17,000 cm sec^{-1} (see Table I, Osc. No. 29); Fig. 12, 7000 cm sec^{-1} (see Table I, Osc. No. 28).

Fig. 11 occurs only 0.68×10^{-3} sec after the beginning of the deflection. Since the period of the vibrator is 10^{-3} sec, the oscillograms can give us no useful information concerning the fore-part of the wave.

The two factors mentioned are of little importance as regards the general shape of the tail of the wave, but here the third factor enters, the fact that the voltage surge produces a charge on every inter-stage condenser, which discharges comparatively slowly. This appears in the zero shift occurring in the oscillograms. In this connection it is interesting to note that the peak voltages were about 25 percent lower than those found in the preceding section, undoubtedly on account of the second factor.

The area under the oscillogram curve is proportional to the total change in flux through the search coil. The area when measured (allowing in any reasonable way for zero shift) gave a value of flux change only a few percent less than that found ballistically, Section 3. Thus the third factor can be estimated with fair accuracy.

It is essential to know which features of the wave are characteristic of a propagating discontinuity in general and which arise from special local conditions. Successive oscillograms at the same point are identical except for small variations in the details. Oscillograms taken at different points along the wire show greater variation in the minor discontinuities, but the total

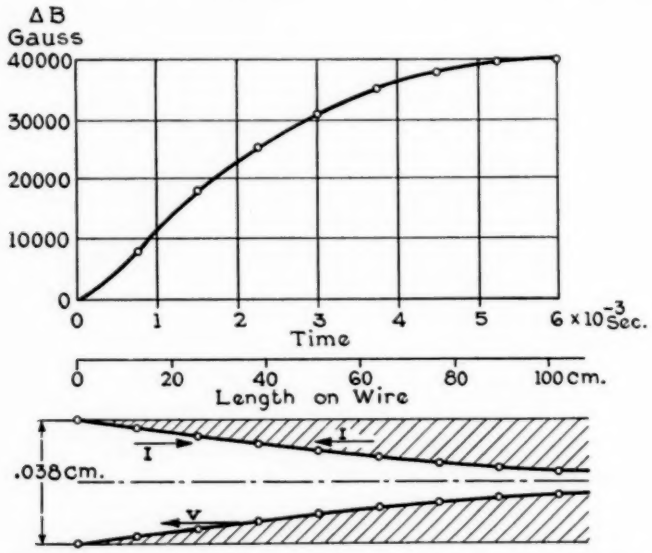

Fig. 13. Change of induction with time (upper part) and penetration of induction into the wire. (The shaded area represents the portion of the wire which has changed direction of magnetization). The radial dimensions are magnified 675 times with respect to the axial dimensions.

duration of the wave and for the most part the main structure, involving perhaps two or three major peaks, are preserved.[8] The main structure is unaltered if the main field is changed so that the wave velocity is different.

Incidentally, the oscillograph was used to obtain a check on the velocity measurements made with the timing circuit by recording the impulse from the two search coils connected in series at a known separation. The agreement was exact.

Since the integral of the voltage curve from its beginning gives the total flux change in the wire up to the corresponding time, an oscillogram enables us to plot this flux as a function of distance along the wire if we make use of the known velocity. In addition to the plot of the integral in Fig. 13, we have

[8] In the single experiment made, the voltage maximum decreased with distance travelled by 20 percent in the central 20 cm of the main field, although ballistic measurements have shown in general that the magnitude of the whole discontinuity remains unchanged.

shown the change as progressing from the surface of the wire inward, assuming that each element of the wire completely reverses magnetization instantaneously.[9] The existence of eddy currents definitely requires that the progress of the change shall be inward, and the instantaneous reversal is plausible if a quantum phenomenon is involved.

Such an analysis applied to the oscillogram of Fig. 11 gives Fig. 13. In this particular case the jump was 97 percent of saturation reversal, and as shown, the 3 percent deficiency has been localized at the axis of the wire. The justification for this is not clear-cut but has some basis in the consideration that the orienting forces are probably least at the axis.

The most striking feature is the experimental demonstration of the fact that the wave occupies a length of some 100 cm in the 0.038 cm wire, a length of the same order of magnitude as calculated in discussing Eq. (7). The comparison of experiment with theory will, however, be based on time of passage rather than length of discontinuity for two reasons. First, because the oscillograph measures time directly and second because the formulas developed in Section 2, being based fundamentally on skin-effect considerations have to do with the time required for a magnetic field to penetrate to a certain depth. They are not concerned with conditions at other points relatively large distances away. On this basis, the only possible interpretation of these formulas is in terms of the time required for the change at a single cross-section to complete itself. Eq. (3) has been definitely found to be inapplicable. Eq. (4), as modified in Eq. (7), gives for this time,

$$\delta t = \lambda/v = 1.96 \times 10^{-8} a^2 \Delta I/\rho(H - H_0) \tag{8}$$

Table I sets forth our most representative comparisons between the directly observed times required for the discontinuity to pass (Column 5) and

TABLE I. *Comparison between the experimental and calculated times of penetration.*

Osc. No.	Main Field Gauss	ΔI Gauss	Velocity cm sec^{-1}	Time δt in 10^{-3} sec. Exp.	Calc.	Ratio $\delta t_{exp}/\delta t_{calc}$	Length λ cm
18	4.48	1740	4000	13.5	4.0	3.4	54
11	4.60	2110	7400	11.1	2.5	4.4	81
14	4.72	2250	10700	6.2	1.8	3.4	66
15	4.84	2300	14000	4.8	1.4	3.4	66
48	4.48	1740	4000	18.7	4.0	4.7	79
49	4.60	2110	7400	9.4	2.5	3.8	70
50	4.72	2250	10700	10.2	1.8	5.7	109
51	4.84	2300	14000	6.6	1.4	4.7	92
28	3.91	3240	7000	22.5	4.2	5.4	157
29	4.25	3240	17000	6.0	1.7	3.5	102

Nos. 28 and 29 are taken with 92 kg/mm^2 tension (H_0=3.68 gauss), the rest with 62 kg/mm^2 (H_0=4.35 gauss).

the times calculated from Eq. (8) (Column 6). The small numerical value of the ratio of these two (Column 7) constitutes a satisfactory check in view of the manner of deriving Eq. (7), and the constancy of this ratio for velocity

[9] In this connection see Section 8.

ratios of 3.5 to 1 lends strong support to the fundamental correctness of the calculation. Unfortunately, simultaneous velocity and oscillograph measurements on wires of other diameters have not been made so that the dependence of δt on a has not yet been checked.

The question as to whether the whole hysteresis loss is an eddy-current loss or whether appreciable transfer to heat occurs through magnetostrictive vibrations, quantum transitions, and possibly other mechanisms, has never been conclusively answered. The present results, however, furnish a very strong indication that at least for large Barkhausen discontinuities only a small fraction $(H-H_0)/H$ of the magnetic loss goes into eddy currents.

The possibility presents itself that the remaining energy appears as magnetostrictive energy. An experiment in which we tried to detect either a momentary or permanent change in length of the wire accompanying a reversal gave a negative result. The accuracy was not quite good enough, however, to be able to reject this hypothesis definitely.

In view of the large penetration times found by us, it becomes of some interest to inquire just what Preisach (reference 2, p. 778) was measuring when he detected harmonics to 10^7 cycles/sec in a stretched wire subjected to a 6000 cycle magnetizing field. It is impossible to say conclusively in the absence of definite data, but it may be pointed out that in 0.5×10^{-7} sec. 0.01 cm of wire surface to either side of a nucleus can reverse by propagation and that the increase of field in that time interval may well cause a large number of magnetic elements to reverse spontaneously, thereby becoming nuclei. The combination of propagation and nucleus formation may easily cause the reversal of an appreciable fraction of the surface of the wire during this time. On this basis the reversal time of a nucleus or any small portion of the wire may be far less than the minimum fixed by Preisach's experiment.

8. The Nature of the Discontinuity

Experiments have enabled us to outline roughly the flux distribution in the discontinuity, Fig. 13, and an eddy-current theory has been advanced which gives the penetration time. The only results, however, so far obtained which throw the slightest light on the longitudinal velocity are those which show that the slopes of the v-H curves for different size wires and even for the strip are all approximately the same. This indicates that the velocity, which corresponds to a given $H-H_0$, being independent of cross-section, is determined only by conditions existing within a small distance of the surface. Since the front edge of the wave lies in the surface, we have been led to the view that the forces at the wave edge determine the velocity, the rest of the wave penetrating the wire as fast as eddy currents allow. It seems plausible to assume that the force required to reverse an element of the wire is H_0 itself or is directly related to it. On such a basis a too-rapid progress of the wave would either give rise to eddy currents or alter the wave configuration near the front in such a way as to reduce the force at the wave front below the minimum reversing value. In this case no new elements could reverse until eddy

currents had decreased or later portions of the wave had advanced sufficiently to reestablish the minimum field.

Any theory must take cognizance of the electromagnetic field set up by the discontinuity. As a solution of Maxwell's equations for the discontinuity shown in Fig. 13, travelling at a high velocity, seems to be extremely complicated at the best, the attempt might be made to disentangle the various factors for the simpler case of very low velocities. As a first step we shall assume as an approximation that the shape of the wave is independent of velocity in the experimental range and remains constant in the limit as $v \to 0$. It may then be possible to make a first order calculation of magnetic field arising from eddy currents for low velocity and assume that this remains valid at the highest velocities measured. The proportionality of peak voltage to velocity and the approximate shape constancy found by experiment themselves strongly suggest that first order effects are the important ones.

Let us tentatively assume that Fig. 13 indicates the nature of a discontinuity travelling from right to left with magnetization reversing from positive to negative. Both unchanged and reversed portions of the medium present north poles to the wave front with the result that it is a surface of magnetic charge of pole strength m per unit area, m being given by

$$m = \Delta I dy/dx \tag{9}$$

where y is the depth of the discontinuity below the wire surface at a distance x back from the front edge. This distribution of magnetism, supposed stationary, gives rise to an almost radial magnetic field from the discontinuity surface outward. An approximate calculation of this field can be made on the assumption that $y \propto x$. For the 100 cm discontinuity in the 0.038 cm wire with ΔI equal to 3240, Eq. (9) gives

$$m \sim 3240 \times 0.019/100 = 0.62$$

whence the radial field near the front edge is

$$H_r = 4\pi m = 8 \text{ gauss}.$$

A field of this magnitude would not allow the elements which are completing their reversal to align themselves axially, but a little consideration will show that their deviation from axial alignment need be very little in order to annihilate the internal poles. Referring to Fig. 14 showing the discontinuity FF' travelling with velocity v, it is readily seen that if the intensity of I_2 in the reversed domains forms the same angle with FF' as the original intensity I_1, there is no pole development in the wire. The angle β, being twice α, will thus be about $2 \times 0.019/100 = 3.8 \times 10^{-4}$ radians which is a negligible deviation from perfect alignment. Finally, this deviated I_2 can be joined to the axial I_2 which is supposed to exist when the discontinuity has completely passed with a discrepancy only of the order of $(3.8 \times 10^{-4})^2$.

In this representation the reversal of intensity occurs within a distance equal to the thickness of a domain, but it is also possible to picture the transition as being much less abrupt. The one condition to be fulfilled, established

by the requirement that no internal poles develop, is that the intensity of magnetization be solenoidal throughout the wire, or, mathematically, that $\nabla \cdot I = 0$. This means, of course, that we can imagine tubes of intensity drawn in the wire and that all poles develop on the surface. A little consideration

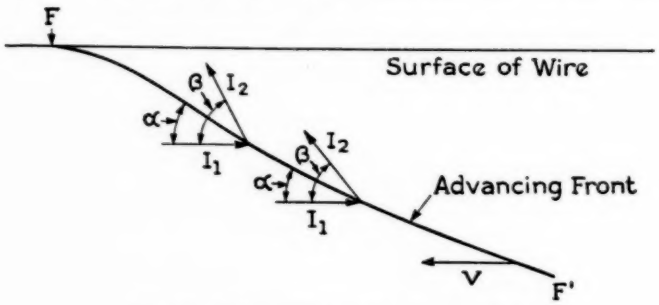

Fig. 14. Compensation of internal poles.

shows that this surface distribution of pole strength is given by the oscillograms. Fig. 15a shows two possible configurations of intensity tubes for an iron-nickel strip with idealized surface distribution. Only half the strip is shown. As represented, the tubes are of equal strength and therefore terminate at the surface in equal poles as given by equal partial areas under the

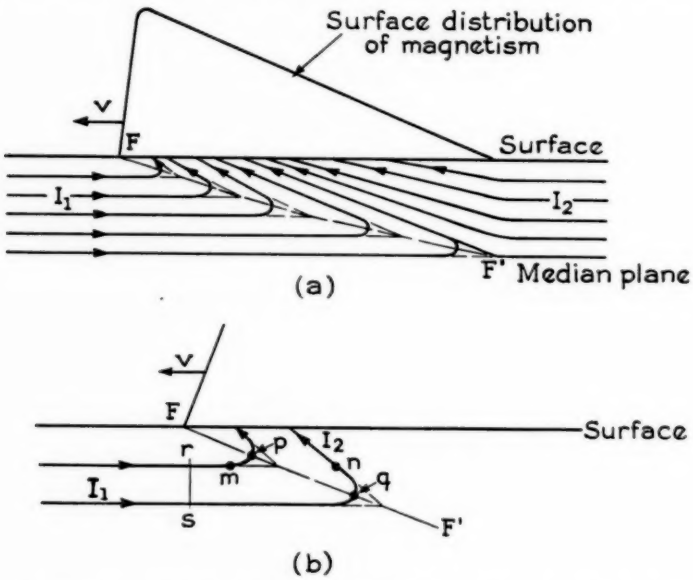

Fig. 15. a. Possible configuration of lines of intensity in a strip. b. Detail of reversal region.

distribution-of-magnetism curve. I_1 can join I_2 either via the sharp dashed bend or via the smooth curve. The former corresponds to Fig. 14, the latter to a more gradual transition.

The interesting feature of this transition is that it cannot occur as a uniform progression. Referring to Fig. 15b, which gives the detail of Fig. 15a, it

is seen that such a progression would mean a continually increasing rotation of I from domain to domain in going from m to n. This in turn would require that the intensity of all domains along pq be parallel. Now it is evident that a tube of intensity expands between rs and pq, both of which represent surfaces normal to the tube. Since I is solenoidal, I at pq must be less than I at rs, which is incompatible with detailed parallelism of the domains. But if we abandon the idea of uniform progression and suppose that as the reversal region mn begins to traverse any small volume (large compared to a domain) certain of the domains scattered throughout it reverse before others, then no such inconsistency arises.

The representation of the discontinuity just given has only been recently devised and no calculation of the fields arising from eddy currents in the neighborhood of the front edge has been made. It seems quite possible, however, that they may be comparable with $H-H_0$. In that case we shall have reached the simple viewpoint that the excess magnetic field over H_0 is just that necessary to overcome the opposing eddy current field.

The velocity would thus be dependent upon the surface magnetization in the neighborhood of the wave front, the length λ of the discontinuity is in turn the product of this velocity and the calculable penetration time δt. Both λ and ΔI, as well as a, then fix the average pole strength of the surface. But what in turn establishes the surface distribution of magnetism? That must probably await a detailed solution.

9. The Effect of Inhomogeneities in the Wire

Magnetic inhomogeneities. The magnetic and mechanical uniformity of the wire is of utmost importance with respect to large Barkhausen discontinuities. The importance of the first factor has been pointed out by Preisach in the experiment in which he varied the limits of the hysteresis cycle. We now look at it from a new viewpoint reached through our knowledge concerning the propagation. In all the preceding experiments the cycle of magnetization was carried as far as ± 34.5 gauss. Later we performed an experiment somewhat similar to Preisach's. In successive cycles the positive field strength limit was decreased as indicated in Fig. 16. On the negative side the limit was always at 34.5 gauss. We note that reduction of the maximum field on the positive side reduces both starting field and the magnetization change at the succeeding jump. In the limiting case, if the maximum positive field used is that required to cause the jump, the succeeding negative starting field is little less than the critical field for this wire.

The explanation for this lies in the following. The usually small change in induction which occurs after a large discontinuity is irreversible and contains smaller Barkhausen discontinuities. Thus in not carrying the cycle to saturation on the positive side, we have failed to turn a number of elementary magnets into the positive direction. These particles set up fields in the negative direction and thus act as nuclei where a discontinuity may start. The bigger such a nucleus is, i.e., the higher the field it produces, the lower the starting field which we have to apply in order to start propagation. We should expect

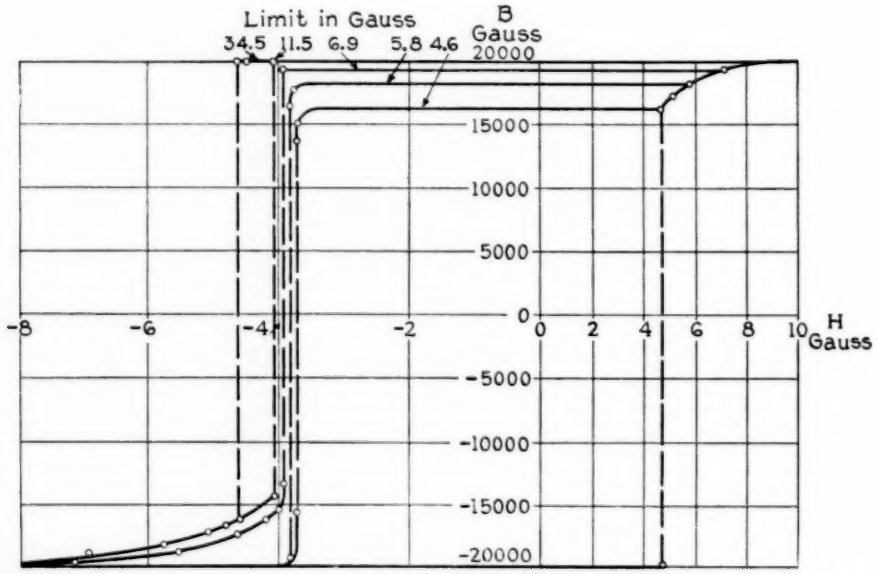

Fig. 16. Effect of varying one limit of the hysteresis loop. Wire of 0.038 cm diameter from ingot No. 32, 15 percent Ni-Fe.

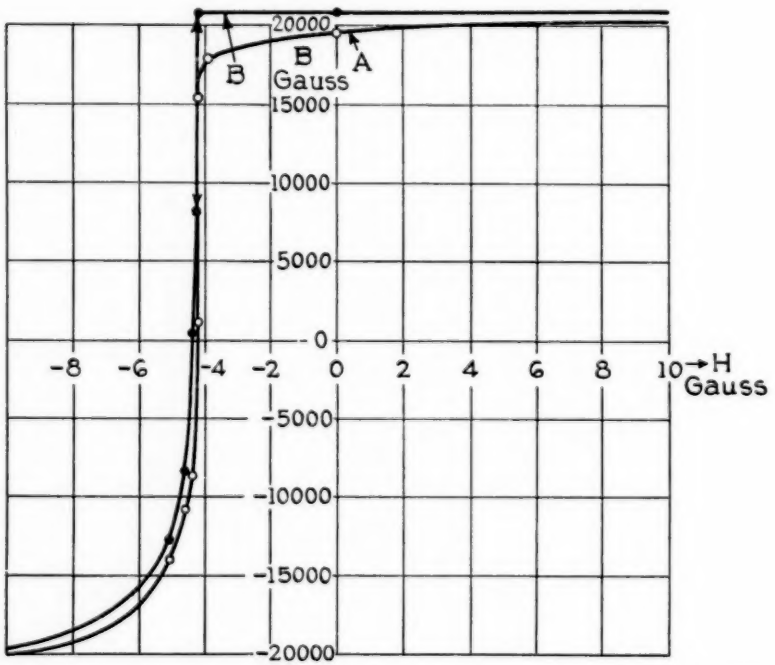

Fig. 17. Influence of a bend in the wire. A. Apparent hysteresis loop of the bent portion. B. Hysteresis loop of unbent portion.

that the starting field could never be less than the critical field, since we found this to be the lower field limit for propagation. In experiment this expectation was not quite confirmed since the lowest observed starting field in some cases was lower than the critical field. But the deviation in no case amounted to more than a few percent.

Mechanical inhomogeneities. In a special case the range of field strength, within which propagation could be observed in a 14 percent Ni-Fe wire of 0.038 cm diameter and under 62 kg/mm^2 tension was found to be 4.25 to 4.65 gauss. This wire was bent in its middle to a semicircle of 2.5 mm radius (the wire being strained far beyond its elastic limit in doing this), was then straightened out again and was finally put under the same tension as before. After this treatment the starting field coincided with the critical field at 4.25 gauss so that propagation could not be obtained. This behavior can be explained by the fact that the bent part has a magnetization curve different from the rest of the wire as shown by curves *A* and *B* of Fig. 17. Curve *A* was taken in the usual way with a search coil placed at the bent portion of the wire. The hysteresis curve so obtained gives a change of induction just below the starting field which is even less than the actual because of the flux leakage arising from the shortness of the bent portion. Thus when the critical field of the normal wire is reached, a considerable part of the bent portion has already changed magnetization and again those elementary particles, which point in the field direction, act as nuclei to start propagation.

Another example of the same type of phenomenon is the fact that hand-drawn wires have starting fields which lie only slightly above the critical field. The irregularity of hand drawing undoubtedly creates "weak nuclei" just as the bending did. Since a low starting field makes it impossible to measure the higher speeds of propagation, machine drawn wires were used in all experiments.

In all but one early experiment the wire projected from both ends of the magnetizing coil so that it extended into regions of comparatively low field strength. In that experiment, however, a short wire terminating within the homogeneous part of the field was used. This wire was clamped to copper wires with brass fastenings and was put under tension. The ends of the wire where it was clamped were not under the same strain as the middle part. Accordingly they did not have rectangular hysteresis loops and acted as weak nuclei.

From these experiments we can conclude that the upper limit of the propagation range is fixed by the non-homogeneity of the wire. The greatest range observed extended from 3.20 to 4.75 gauss in the case of a 14 percent Ni-Fe wire under combined tension and torsion. To the higher field value there corresponded a velocity of 40,000 cm sec^{-1}, which is the highest one measured so far.

10. Torsion

Preisach obtained great discontinuities in magnetization also when he applied torsion to a wire. In this case, too, we found that the magnetization

propagated in the same way as in the case of tension. We also observed a parallel shift of the velocity field lines to the left for increased twist in the range between 8 and 20 percent Ni-Fe, but we obtained much greater variations with respect to slope than in the case of tension. Fig. 18 taken for a 0.038 cm, 25 percent Ni-Fe wire shows this behavior very clearly. For this particular wire it made a great difference whether the twist was applied clockwise or counter-clockwise and if tension was added still another slope was found. All these curves were perfectly reproducible which shows that the

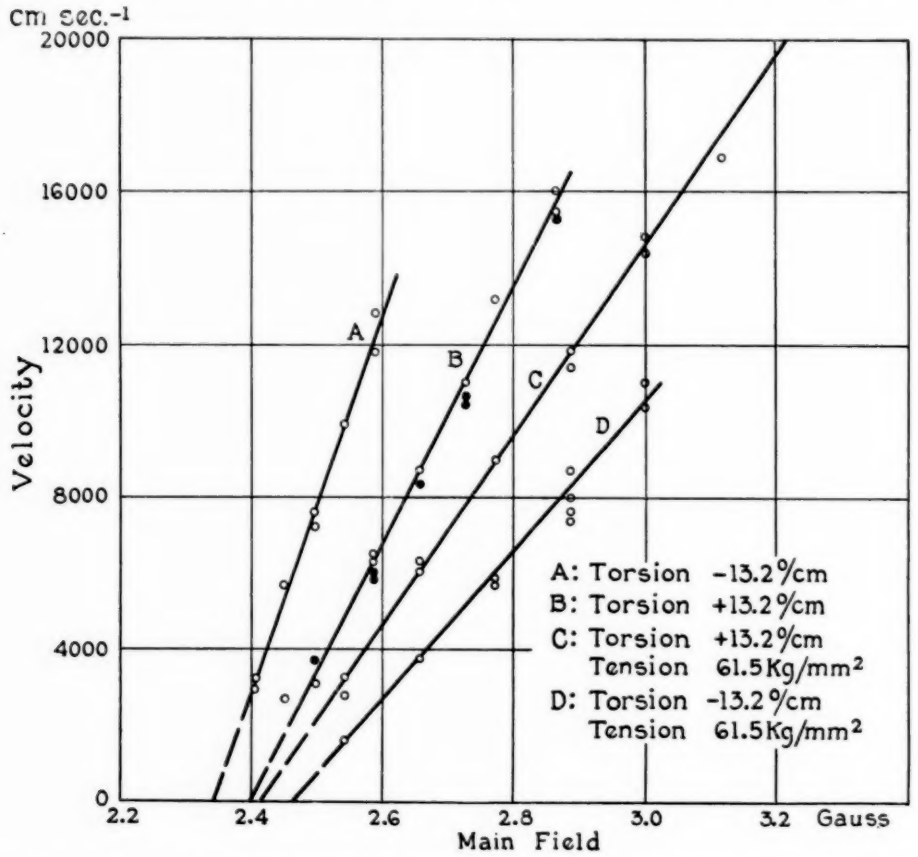

Fig. 18. Velocity-field curves for torsion and combined tension and torsion. Wire of 0.038 cm diameter from ingot No. 19, 25 percent Ni-Fe. The black dots represent check points.

strains were elastic. (The black dots in Fig. 18 were taken after the direction of applied torsion had been changed several times.) As another wire from the same lot did not exhibit this dependence of slope on direction of twist, it is probable that internal strains have an important influence on the slope in the case of torsion. More work on wires having different strain distributions has to be done before the observed effects can be explained.

The data for these cases are insufficient as yet for checking the application of Eq. (7).

11. Wires of Different Composition

Nickel iron wires of 3, 5, 8, 10, 12, 14, 15, 20, 25, 35, 40, 55, 60, 78, 80, 90 and 100 percent nickel content have been examined. We were able to obtain large discontinuities (i.e., of more than 80 percent of the double saturation value) with *tension* only in the ranges 8 to 25 percent and 55 to 78 percent.[10] From 5 percent down and from 80 percent up no large discontinuities could be observed and with 35 and 40 percent only small jumps of about 1/10 of the double saturation value appeared under tension. These jumps were very erratic and probably only included a short length of wire at a time so that velocity measurements with these compositions were impossible. Throughout the remainder of the range the v-H slope did not deviate much from an average value of 25000 cm sec^{-1} $gauss^{-1}$, but the effect of tension on the critical field varied profoundly. Between 8 and 20 and at 78 percent increasing tension reduced the critical field H_0, but at 55 and 60 percent it increased H_0. At 25 percent there was a pronounced reversal in the dependence of H_0 on tension. Up to a certain value of tension H_0 increased with increasing tension; after passing this value the critical field decreased again.

Torsion produced large discontinuities over the entire range between 8 and 100 percent Ni-Fe, and the great variations in v-H slope already mentioned as existing in the 8 to 20 percent interval were found to be present over this wider range, varying between the values 10^4 and 6×10^4 cm sec^{-1} $gauss^{-1}$. There were no simple relations between either composition or amount of twist and critical field. The v-H characteristics were occasionally curved, but no more frequently than in the case of tension.

No experiments have been carried out on the propagation in wires under an elastic bending force.

12. The Critical Field

Some of our experimental results allow comparison with a theory recently advanced by R. Becker[11] which has already been applied successfully to the case of nickel under tension.[12] Becker introduces the close and important relation between the magnetic and elastic state of materials by the assumption that the direction of magnetization in each Weiss domain is determined by the stress tensor in that domain in the absence of an external field. The theory enables him to derive hysteresis loops for these districts for different initial angles between magnetization and applied field.

For the limiting case of anti-parallelism between magnetization and field, this theory yields a rectangular hysteresis loop for which the coercive field is given by

$$H_C = 8SAI_m$$

[10] Preisach (p. 755) has already pointed out that the upper limit coincides with the composition at which magnetostriction and accordingly the effect of tension on magnetization change sign.

[11] R. Becker, Zeits. f. Physik **62,** 253 (1930).

[12] R. Becker and M. Kersten, Zeits. f. Physik **64,** 660 (1930).

where $S \sim 1$ is a factor calculated from magnetostriction, A is the elastic deformation of the domain and I_m is the saturation intensity of magnetization. With exact antiparallelism, however, the force couple exerted by the impressed field is zero, with the consequence that the domain may conceivably retain its position of unstable equilibrium even for values of H exceeding H_C. It is interesting that the Ni-Fe wire as a whole exhibits this behavior. On this basis the critical field H_0 is to be identified with the coercive field H_C, while the somewhat erratic starting field corresponds to the indeterminate field at which the equilibrium of the Weiss domain may be destroyed.

As a matter of fact, the wire only approximates to a single Weiss domain, both because of the peaks evident in the oscillograms and because of the fact that for fields only slightly greater than H_0 the reversal of the wire is incomplete (as may be seen in Fig. 8), indicating that the coercive force for certain portions of the wire exceeds H_0. It is possible that the ΔI vs H curves in

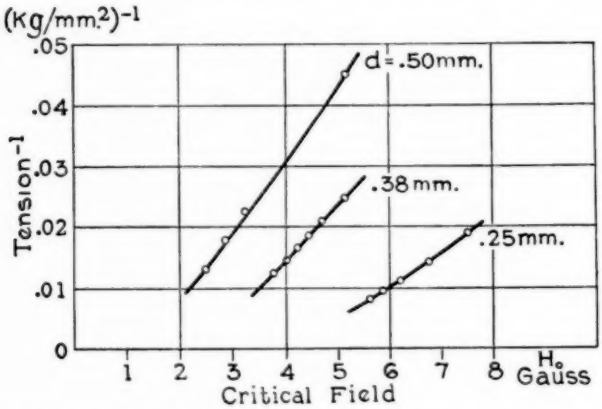

Fig. 19. Critical field for wires of different diameter. All Wires cold drawn from annealed wire 0.102 cm diameter from ingot No. 14, 14 percent Ni-Fe.

that figure give the proportion of the wire for which H exceeds the coercive field.

Becker's formula, when applied to our conditions, yields values more than 10 times higher than those observed by us and predicts in the case of iron and low nickel-iron alloys for which S is positive, an increase in H_C with increasing elastic deformation A. In our experiments with Ni-Fe wires of 8 to 20 percent nickel content, we observed just the opposite relation. This is shown clearly by Fig. 19 in which the reciprocal of tension is plotted vs. the critical field for different diameters. In a certain range of tensions we obtain almost a linear relation between $1/T$ and H_0! In his second article Becker recognizes this difficulty.

Fig. 19 allows of one other comparison with experiments made by Becker and Kersten. The critical fields obtained for wires of different diameter for the same stress are quite different. Since all wires were cold drawn from 0.102 cm, the explanation lies in the different amounts of cold working the wires have suffered. The more cold working, the greater are the internal strains,

and the higher the coercive force. In their experiments with nickel wires Becker and Kersten are able to obliterate differences in internal strain conditions entirely by application of high tension and they can account for this satisfactorily by assuming that hard drawing produces only longitudinal strains in the wire whose influence disappears in the limiting case of high applied tension.

In our case, however, this does not occur, for even with tension near to the breaking point, the coercive forces are still considerably different for wires subjected to different amounts of cold working. This is illustrated by

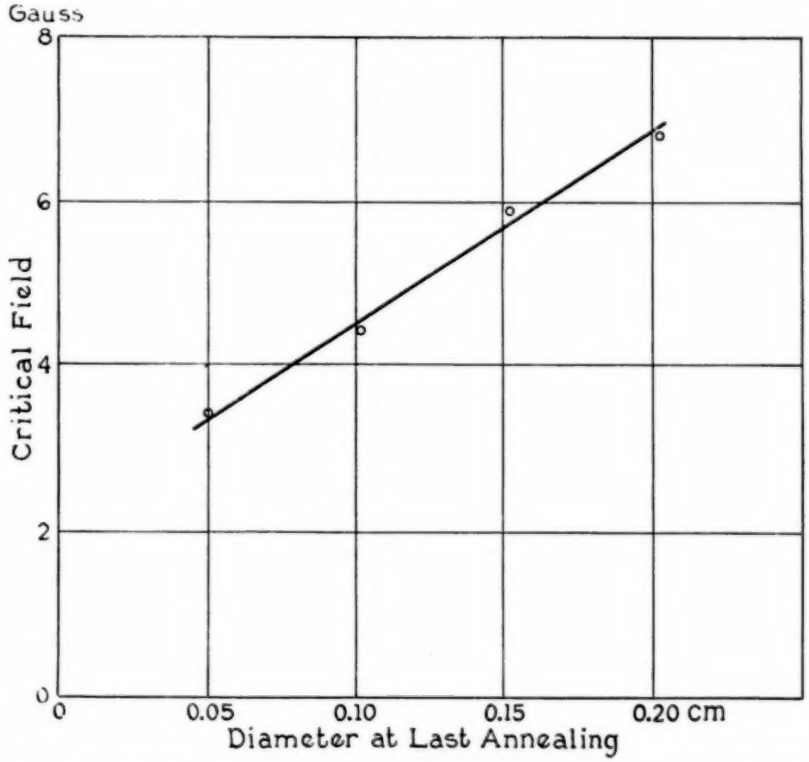

Fig. 20. Critical field at 62 kg/mm² tension for wires with different amounts of cold working. All wires of 0.038 cm diameter from ingot No. 22, 20 percent Ni-Fe.

Fig. 20 which shows the critical field for wires of 0.038 cm diameter annealed at the diameters shown and then cold-drawn. Even with 62 kg/mm² tension, the coercive force varies between 3.3 and 6.8 gauss. It may well be that radial and associated ring strains introduced by cold working play an important role in determining the coercive force. On the other hand, Becker and Kersten's results on stretched Ni wires where only continuous and reversible changes are present show that any radial strains can be neglected. Further investigation of propagation in thin strips may give additional information regarding the role of strains in this connection, as the strain structure is probably much simpler in rolled strips than in drawn wires.

Among the various possibilities which present themselves for extending this work we intend to refine the oscillographic method further and to use that method on different sized wires and strips and also on composite strips (strips with a surface layer only of Ni-Fe) with the hope of obtaining a more detailed picture of the magnetic discontinuity. We also intend to examine the effect of temperature change both on nucleus formation and propagation velocity.

We appreciate the interest which Professor R. Becker has shown in this work, and we wish to express our gratitude to Dr. I. Langmuir who, as we have said, not only foresaw the magnetic propagation, but has also given many suggestions and much advice.

FERMI-DIRAC STATISTICS APPLIED TO THE PROBLEM OF SPACE CHARGE IN THERMIONIC EMISSION

By Russell S. Bartlett
Yale University

(Received March 2, 1931)

Abstract

This paper develops mathematically the state of an electron gas in equilibrium with a plane electrode when the electron gas obeys the Fermi-Dirac rather than the classical distribution law. For a part of the range of integration graphical methods were found necessary, but fortunately a change of variable leads to a solution, shown graphically, which is independent of the temperature and of the nature of the emitting electrode. Thus a single graphical integration can be applied to any emitting surface at any temperature, giving the density, electric intensity, and potential at any desired distance from the surface. A simple extension of the theory makes possible the calculation of the thermionic current between plane electrodes. Numerical examples are given, and the validity of the asumptions is discussed briefly.

WHEN Schottky[1] first proposed that the thermionic work function could be explained by the attraction of an escaping electron to its electric image in the surface, he discussed at some length the possible effects of space charge and "structure effects," and finally concluded that other forces were small compared to the image force. Recently Waterman and the author[2] have questioned this conclusion, and have suggested that, at least under certain conditions, possibly always, space charge and structure effects are more important than the image force.

Schottky, assuming the image force to be correct, and assuming a Maxwell distribution of electron velocities, was able from measured electron emission currents to calculate the concentrations of the electron atmosphere at all points outside the metal and found it so rarefied that space charge could be neglected. This extension of the image force from a region out from the surface where it can be confirmed experimentally down towards the surface through a region where it could not be expected to be valid appears to be unjustifiable. The alternative treatment by space charge analysis, which is to be developed in this paper, is certainly not free from criticism. In particular, it is necessary to apply Poisson's equation to an electron gas, thus assuming a continuous distribution of electricity which certainly does not exist. On the other hand it would appear, as is pointed out in a previous paper by Waterman and the author, that the choice of suitable statistics may in part avoid that difficulty. In any case the space charge method of attack seems justified close to the surface where the image force certainly breaks down. In order to

[1] Schottky, Phys. Zeits. **15,** 872 (1914).
[2] Bartlett and Waterman, Phys. Rev. [2] **37,** 279 (1931).

shed more light on this question certain calculations have been carried out, assuming that the electron concentration is controlled by space charge alone.

Equilibrium. Classical Distribution Law

After the manner of Fry,[3] Langmuir,[4] and others, consider a stream of electrons emerging from an infinite plane electrode with initial velocities distributed according to some law. The electrons outside the surface of the electrode will induce a charge on the electrode tending to draw the electrons back to it. There will be a potential distribution outside the metal surface through which the electrons move, those with higher initial velocities normal to the surface getting further out before they are turned back.

With no external field and no neighboring electrode, we may write an expression for the charge density at any point in potential space.

$$\rho = 2\epsilon \int_{(2V\epsilon/m)^{1/2}}^{\infty} \frac{f(v_0)}{v} dv_0 \tag{1}$$

where $f(v_0)dv_0$ gives the number of electrons emerging from the surface per square cm with initial velocities normal to the surface lying between v_0 and v_0+dv_0, while v represents the normal velocities of these electrons at the point in question. Clearly

$$v_0^2 - v^2 = \frac{2V\epsilon}{m}. \tag{2}$$

Using Poisson's equation we get

$$\frac{d^2V}{dx^2} = -4\pi\rho = -8\pi\epsilon \int_{(2V\epsilon/m)^{1/2}}^{\infty} \frac{f(v_0)}{v} dv_0. \tag{3}$$

Multiplying both sides by $2\,dV/dx$ and integrating in the usual manner gives

$$\left(\frac{dV}{dx}\right)^2 = 16\pi m \int_{(2V\epsilon/m)^{1/2}}^{\infty} v f(v_0) dv_0. \tag{4}$$

We cannot proceed further without knowing the distribution law of velocities expressed in $f(v_0)$. For the classical case

$$f(v_0) = n_0 \frac{mv_0}{kT} e^{-mv_0^2/2kT} \text{ or } f(v_0) = N_0 \left(\frac{m}{2\pi kT}\right)^{1/2} v_0 e^{-mv_0^2/2kT}, \tag{5}$$

where n_0 is the number of electrons passing through a square centimeter of the surface per second, and N_0 is the number of electrons per unit volume at the surface. Then

$$\left(\frac{dV}{dx}\right)^2 = 16\pi m N_0 \left(\frac{m}{2\pi kT}\right)^{1/2} \int_{(2V\epsilon/m)^{1/2}}^{\infty} v v_0 e^{-mv_0^2/2kT} dv_0. \tag{6}$$

[3] Fry, Phys. Rev. [2] **17**, 441 (1921).
[4] Langmuir, Phys. Rev. [2] **21**, 419 (1923).

Changing the variable to v gives

$$\left(\frac{dV}{dx}\right)^2 = 16\pi m N_0 \left(\frac{m}{2\pi kT}\right)^{1/2} \int_0^\infty v^2 e^{-mv^2/2kT - V\epsilon/kT} dv \tag{7}$$
$$= 8\pi N_0 kT e^{-\epsilon V/kT}$$

since the integral is a well known form having the value $\frac{1}{4}(8\pi k^3T^3/m^3)^{1/2}$.

Taking the square root and performing the next step in the integration gives

$$x = \left(\frac{kT}{\pi N_0}\right)^{1/2} \frac{1}{2\epsilon} e^{\epsilon V/2kT}. \tag{8}$$

The first boundary condition requires that V and x shall approach infinity together as dV/dx approaches zero, and this is satisfied by the above equations. The second condition specifies that at the surface the number of free electrons per cubic centimeter has a fixed value, in this case N_0. That requires that the surface of the metal shall be at x_0 given by

$$x_0 = \left(\frac{kT}{\pi N_0}\right)^{1/2} \frac{1}{2\epsilon}. \tag{9}$$

Combining Eqs. (1) and (5) and integrating at once gives Boltzmann's equation

$$N = N_0 e^{-\epsilon V/kT}. \tag{10}$$

We could, in fact, have arrived at Eq. (8) by combining (10) with Poisson's equation. But (10) is of interest now in that, combined with (8) it gives us the concentration at various distances from the surface. The quantities V, dV/dx, x, and N are so related that as soon as we have fixed one all the others may be determined from various combinations of Eqs. (7), (8), and (10). It is also seen that a different metal, with a different electron concentration at the surface, could be handled by the same equations with an appropriate value of x_0 at the surface.

Equilibrium. Fermi-Dirac Distribution Law

If in Eqs. (1) and (4) we replace the classical expression for $f(v_0)$ by that obtained from Fermi-Dirac statistics, the problem becomes much more complicated.

Now

$$f(v_0) = \frac{2\pi kTGm^2}{h^3} v_0 \log\left(A_0 e^{-mv_0^2/2kT} + 1\right) \tag{11}$$

where A is a measure of the degeneracy of the electron gas. This gives us instead of (1) and (4) the following.

$$N = \frac{4\pi kTGm^2}{h^3} \int_{(2V\epsilon/m)^{1/2}}^\infty \frac{v_0}{v} \log\left(A_0 e^{-mv_0^2/2kT} + 1\right) dv_0 \tag{12}$$

and

$$\left(\frac{dV}{dx}\right)^2 = 32\pi^2 kTG\left(\frac{m}{h}\right)^3 \int_{(2V\epsilon/m)^{1/2}}^{\infty} vv_0 \log\,(A_0 e^{-mv_0^2/2kT} + 1)dv_0. \quad (13)$$

Making the change of variable from v_0 to v gives

$$N = \frac{4\pi kTGm^2}{h^3} \int_0^{\infty} \log\,(Ae^{-mv^2/2kT} + 1)dv \quad (14)$$

where

$$A = A_0 e^{-\epsilon V/kT}$$

and

$$\left(\frac{dV}{dx}\right)^2 = 32\pi^2 kTG\left(\frac{m}{h}\right)^3 \int_0^{\infty} v^2 \log\,(Ae^{-mv^2/2kT} + 1)dv. \quad (15)$$

Since the evaluation of these integrals is rather complicated, it will be convenient to make certain substitutions.

Let

$$\frac{mv^2}{2kT} = u^2.$$

Let

$$f(A) = \int_0^{\infty} \log\,(Ae^{-u^2} + 1)du$$

and

$$g(A) = \int_0^{\infty} u^2 \log\,(Ae^{-u^2} + 1)du.$$

Then

$$N = \frac{2\pi G(2mkT)^{3/2}}{h^3} f(A) \quad (16)$$

and

$$\left(\frac{dV}{dx}\right)^2 = \frac{16\pi^2 Gm^{3/2}(2kT)^{5/2}}{h^3} g(A). \quad (17)$$

For the case where $A < 1$ the solution is fairly simple. Expanding the log $(Ae^{-u^2}+1)\,du$ we get

$$f(A) = \int_0^{\infty} [Ae^{-u^2} - \tfrac{1}{2}A^2e^{-2u^2} + \tfrac{1}{3}A^3e^{-3u^2} \cdots]du \quad (18)$$

and

$$g(A) = \int_0^{\infty} [Au^2e^{-u^2} - \tfrac{1}{2}A^2u^2e^{-2u^2} + \tfrac{1}{3}A^3u^2e^{-3u} \cdots]du. \quad (19)$$

The integrals involved are ordinary probability integrals. Hence

$$f(A) = \tfrac{1}{2}(\pi)^{1/2}[A - A^2/2^{3/2} + A^3/3^{3/2} \cdots] \tag{20}$$

$$g(A) = \tfrac{1}{4}(\pi)^{1/2}[A - A^2/2^{5/2} + A^3/3^{5/2} \cdots]. \tag{21}$$

Further, for the case where $A \ll 1$ we get the usual Boltzmann relation that $N = N_0 e^{-\epsilon V/kT}$. When the gas is not classical the Boltzmann relation becomes $A = A_0 e^{-\epsilon V/kT}$, as Waterman has found from a different point of view.

When $A > 1$ the solution becomes more difficult since the expansion used above is not valid over the total range of integration. It is necessary to divide the range of integration into two parts, for which Ae^{-u^2} is less than or greater than unity. Then

$$f(A) = \int_0^{(\log A)^{1/2}} \log [Ae^{-u^2}]du + \int_0^{(\log A)^{1/2}} \log [e^{u^2}/A + 1]du + \int_{(\log A)^{1/2}}^{\infty} \log [Ae^{-u^2} + 1]du \tag{22}$$

and

$$g(A) = \int_0^{(\log A)^{1/2}} u^2 \log [Ae^{-u^2}]du + \int_0^{(\log A)^{1/2}} u^2 \log [e^{u^2}/A + 1]du + \int_{(\log A)^{1/2}}^{\infty} u^2 \log [Ae^{-u^2} + 1]du. \tag{23}$$

If $A \gg 1$ (i.e., the electron gas completely degenerate) the first term is the only one of consequence.

This first term can be integrated directly to give

$$f(A) = 2/3(\log A)^{3/2} \tag{24}$$

$$g(A) = 2/15(\log A)^{5/2} \tag{25}$$

And finally by means of series expansion and integration by parts, involving steps of questionable rigor but justified by the result, one obtains

$$f(A) = \frac{2}{3}(\log A)^{3/2}\left[1 + \frac{\pi^2}{8(\log A)^2} + \frac{7\pi^4}{640(\log A)^4} + \frac{31\pi^6}{6144(\log A)^6} + \frac{4191\pi^8}{5 \times 2^{16}(\log A)^8} \cdots\right] \tag{26}$$

$$g(A) = \frac{2}{15}(\log A)^{5/2}\left[1 + \frac{5\pi^2}{8(\log A)^2} - \frac{7\pi^4}{384(\log A)^4} - \frac{155\pi^6}{43008(\log A)^6} - \frac{381\pi^8}{2^{16}(\log A)^8} \cdots\right] \tag{27}$$

where these series, though not convergent, may be used for large values of A, and have been checked by graphical integration.

In the Sommerfeld-Fermi-Dirac statistics, the number of particles per unit volume and the energy per unit volume are expressed in terms of two

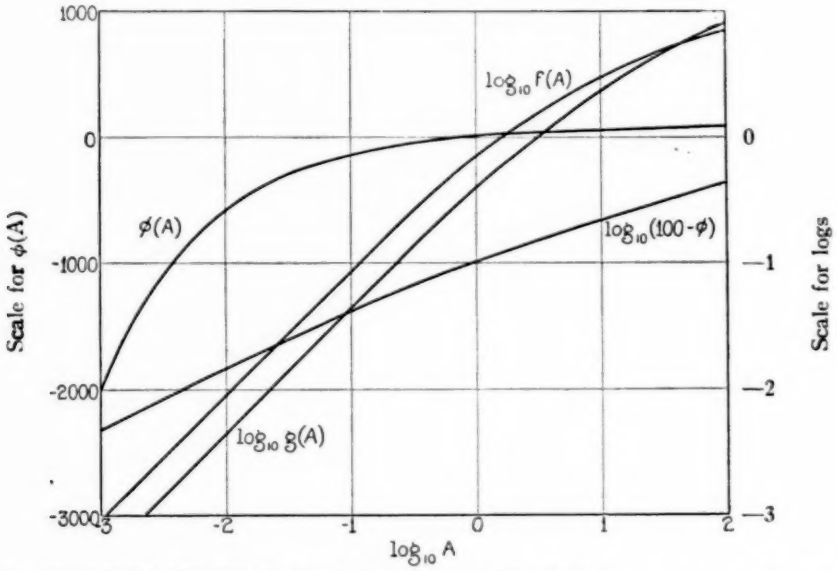

Fig. 1. $N=5.4830\times10^{16}\ T^{3/2}f(A)/\text{cm}^3\ E=1843.9\ T^{5/4}[g(A)]^{1/2}$ volts/cm. $X=2.1631\times10^{-9}\ \phi(A)/T^{1/4}$ cm. $V=1.9851\times10^{-4}\ T\log_{10}A$ volts.

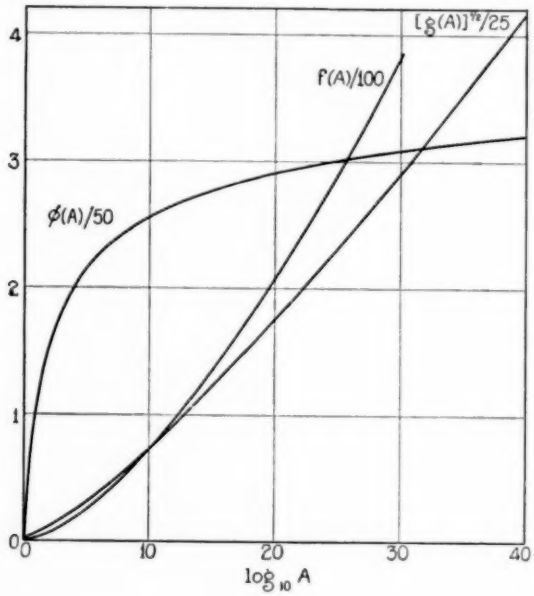

Fig. 2.

functions $F(A)$ and $G(A)$. It turns out that $f(A)$ as used above is equal to $\pi^{1/2}/2\cdot F(A)$, while $g(A)=\pi^{1/2}/4\cdot G(A)$, thus confirming the results of the questionable steps mentioned above.

We now have expressions for $f(A)$ and $g(A)$, hence for N and $(dV/dx)^2$ over four regions, completely degenerate, less degenerate, approaching classical, and completely classical. The two extremes are handled by exact expressions, the intermediate regions by series, and there is a region between for which neither series is valid. $f(A)$ and $g(A)$ have been evaluated graphically for this intermediate region. Numerical results of this graphical integration and of the series expansions are given in Figs. 1, 2 thus covering the regions between the exact expressions for completely degenerate and completely classical states.

For the degenerate state $N=4\pi G(2mkT)^{3/2}/3h^3\cdot(\log A)^{3/2}$ and for the classical state $N=G(2\pi mkT)^{3/2}/h^3\cdot A$. For intermediate states $N=2\pi G(2mkT)^{3/2}/h^3\cdot f(A)$ where $f(A)$ for any value of A may be found from the figures.

Further for the degenerate state

$$\left(\frac{dV}{dx}\right)^2 = 32\pi^2 G m^{3/2}(2kT)^{5/2}/15h^3\cdot[\log(A_0 e^{-eV/kT})]^{5/2}.$$

Taking the square root of both sides and integrating directly gives

$$x = \frac{15^{1/2}h^{3/2}}{2^{7/4}\pi G^{1/2}m^{3/4}(kT)^{1/4}\epsilon}\log A^{-1/4}. \tag{28}$$

For the classical state

$$\left(\frac{dV}{dx}\right)^2 = \frac{4Gm^{3/2}(2\pi kT)^{5/2}}{h^3}A_0 e^{-eV/kT}.$$

This also may be integrated directly to give

$$x = \frac{h^{3/2}}{2^{5/4}G^{1/2}m^{3/4}\pi^{5/4}(kT)^{1/4}\epsilon}\cdot A^{-1/2}. \tag{29}$$

For the intermediate region graphical integration is required, since there is no exact solution. It is seen that

$$\frac{dV}{dx} = \text{const}\,(g(A))^{1/2} = \text{const}\,(g(A_0 e^{-eV/kT}))^{1/2}.$$

Since values for the expression under the radical have been tabulated as a function of A, easily convertible to a function of V, it is possible to perform a graphical integration. To simplify the arithmetical work this has been done to give a new function $\phi(A)$ proportional to x, values for which are given in Figs. 1 and 2.

$f(A)$, $g(A)$, and $\phi(A)$ are perfectly general functions, independent of temperature and of the nature of the electron emitter. The coefficients of these functions in the various equations take care of the effect of temperature. The curves in Fig. 1 show these functions plotted against A. The origin at log $A=0$ is purely arbitrary. In effect there is no origin, or better, perhaps, each particular problem provides its own origin, fixed by the conditions of the sur-

face. In practice it is convenient to consider distances and potential differences from x_1, V_1 corresponding to A_1, to x_2, V_2, corresponding to A_2. The formulae below together with the tables cover the entire range of an electron gas.

$$V(\text{volts}) = 300kT/\epsilon \cdot \log A = 690.8kT/\epsilon \cdot \log_{10} A = 1.9851 \times 10^{-4} T \log_{10} A \tag{30}$$

$$N = 2\pi G(2mkT)^{3/2}/h^3 \cdot f(A) = 5.4830 \times 10^{15} T^{3/2} f(A) \tag{31}$$

$$A \gg 1 \quad N = 4\pi G(2mkT)^{3/2}/3h^3 \cdot (\log A)^{3/2} = 1.2772 \times 10^{16} T^{3/2} (\log_{10} A)^{3/2} \tag{32}$$

$$A \ll 1 \quad N = G(2\pi mkT)^{3/2}/h^3 \cdot A = 4.8591 \times 10^{15} T^{3/2} A \tag{33}$$

$$E = 2^{13/4}\pi G^{1/2} m^{3/4} (kT)^{5/4}/h^{3/2} \cdot [g(A)]^{1/2} \text{E.S.U/cm} = 1843.9 T^{5/4} [g(A)]^{1/2} \text{ volts/cm} \tag{34}$$

$$A \gg 1 \quad E = 2^{15/4}\pi G^{1/2} m^{3/4} (kT)^{5/4}/15^{1/2} h^{3/2} \cdot (\log A)^{5/4} = 1909.8 T^{5/4} (\log_{10} A)^{5/4} \text{ volts/cm} \tag{35}$$

$$A \ll 1 \quad E = 2^{9/4}\pi^{5/4} G^{1/2} m^{3/4} (kT)^{5/4}/h^{3/2} \cdot A^{1/2} = 1227.4 T^{5/4} A^{1/2} \text{ volts/cm} \tag{36}$$

$$x = h^{3/2} \times 0.046052/2^{13/4}\pi G^{1/2} m^{3/4} (kT)^{1/4} \epsilon \cdot \phi(A) \text{ cm} = 2.1631 \times 10^{-9} \phi(A)/T^{1/4} \text{ cm} \tag{37}$$

$$A \gg 1 \quad x = 15^{1/2} h^{3/2}/2^{7/4}\pi G^{1/2} m^{3/4} (kT)^{1/4} \epsilon \cdot (\log A)^{-1/4} = 4.1770 \times 10^{-7}/T^{1/4} \cdot (\log_{10} A)^{-1/4} \text{ cm} \tag{38}$$

$$A \ll 1 \quad x = h^{3/2}/2^{5/4} G^{1/2} m^{3/4} \pi^{5/4} (kT)^{1/4} \epsilon \cdot A^{-1/2} = 1.4112 \times 10^{-7}/T^{1/4} \cdot A^{-1/2} \text{ cm}. \tag{39}$$

A small additive correction is necessary to join different regions. This may easily be calculated, but has been omitted here to avoid further complications.

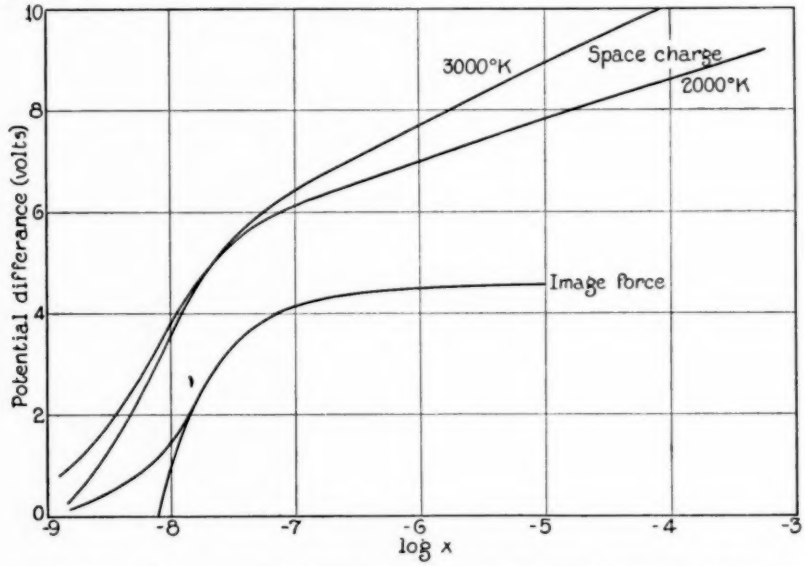

Fig. 3. Height of potential barrier at different distances from the surfaces.

If then N is known for any point, A, V, x, and E may be found from these formulae used in conjunction with the figures. And as soon as one of these is fixed for another point, all the others may be found. The separation of the points in space and in potential is found by subtracting the V's and x's for the two points. Figs. 3, 4 give some characteristic results for various conditions.

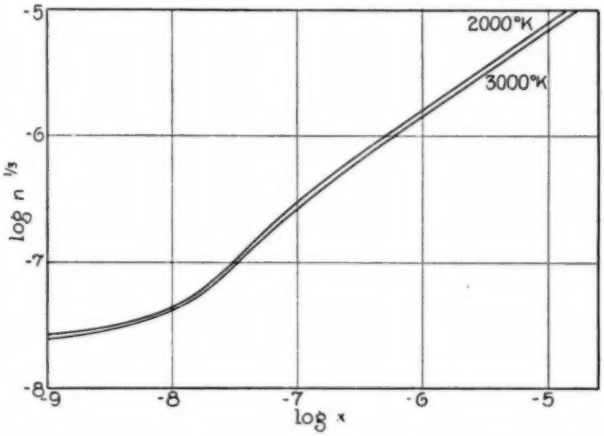

Fig. 4. Distances between electrons at different distances from the surface.

Current to the Anode

The analysis just given applies to the case of no current, effectively an equilibrium case, though it was considered from the point of view of emerging and returning streams. Fortunately it is possible to take advantage of earlier work by Fry and Langmuir in going over to the case where a current is flowing from the hot cathode. In Langmuir's paper two variables are defined

$$\xi = 4(\pi/2kT)^{3/4}m^{1/4}(\epsilon i)^{1/2}(x - x_m) \tag{40}$$

$$\eta = \epsilon(V - V_m)/kT. \tag{41}$$

It is easily seen that $\eta = \log A - \log A_m$ in our notation. Now the current passing a potential barrier V is given by

$$i = 2\pi\epsilon kTGm^2/h^3 \cdot \int_{(2V\epsilon/m)^{1/2}}^{\infty} u \log (A_0 e^{-mu^2/2kT} + 1)du \tag{42}$$

$$i = 2\pi Gm\epsilon(kT)^2/h^3 \cdot A_0 e^{-\epsilon V/kT} = 2\pi Gm\epsilon(kT)^2/h^3 \cdot A \tag{43}$$

provided $A_0 e^{-\epsilon V/kT} < 1$.

If this value of i is put into the expression for ξ above we get

$$\xi = 2^{9/4}\pi^{5/4}(kT)^{1/4}m^{3/4}\epsilon A_0^{1/2}e^{-\epsilon V/kT}(x - x_m)/h^{3/2} \tag{44}$$

from which it appears that $\xi = 0.046052\pi^{1/4}/2^{3/4} \cdot \phi(A) \cdot A^{1/2}$ with similar relations beyond the range of $\phi(A)$. Thus it is possible to apply the Langmuir Fry analysis to this case if a little care is exercised, using the relation $\xi = \xi_1 A_0^{1/2} e^{-\epsilon V/2kT} = \xi_1 A^{1/2}$.

The Langmuir-Fry analysis assumes electrons streaming out from the electrode with velocities according to Maxwell's distribution law. Of these the highest velocity electrons escape completely, so that the returning stream consists of only a part of the Maxwellian distribution. Now in thermionic emission the currents are generally so small that the loss of electrons to the returning stream is of no consequence close to the electrode where the distribution is no longer classical. In the region where the loss of electrons is of consequence, the distribution is classical or so nearly so that the Langmuir-Fry analysis can be joined to mine as indicated without serious error.

Illustration of the Method of Calculation

Let us take the case of an emitter at 3000°K.

$N_0 = 6.2 \times 10^{22}$ (tungsten) Parallel plane electrodes 1 cm apart.
From the figures $\log A_s = 9.534$ $A_s = A$ at surface
Arbitrarily $\log A_m = -3.0000$ $A_m = A$ at potential minimum
A simple calculation gives i corresponding to A_m as 3.612×10^{-4} amps/cm^2
From the figures $\phi(A_s) = 126.59$ $\phi(A_m) = 2002.06$
Using equation (45) $\xi_{1m} = 43.399$ $\cdot \xi_{1s} = -2.744$ $\xi_1 = 46.143$
Multiplying by $A^{1/2}$ gives $\xi = 1.4592$
To this we add 1.1397 to fit classical to Fermi,
giving ξ_1' (from surface to potential minimum) $= 2.5989$
From 40 or 44 $\xi' = 43.041$
so that ξ_2' (from potential minimum to collecting electrode) $= 40.442$
From tables of Langmuir, extended to cover some cases dealt with here,
$\eta_2 = 87.49$ (from potential minimum to collecting electrode.)
η(total) $= 74.96$ $V = 19.387$ from equation 41
Repetition of this process for a series of values of A_m leads to the results given in Fig. 5.

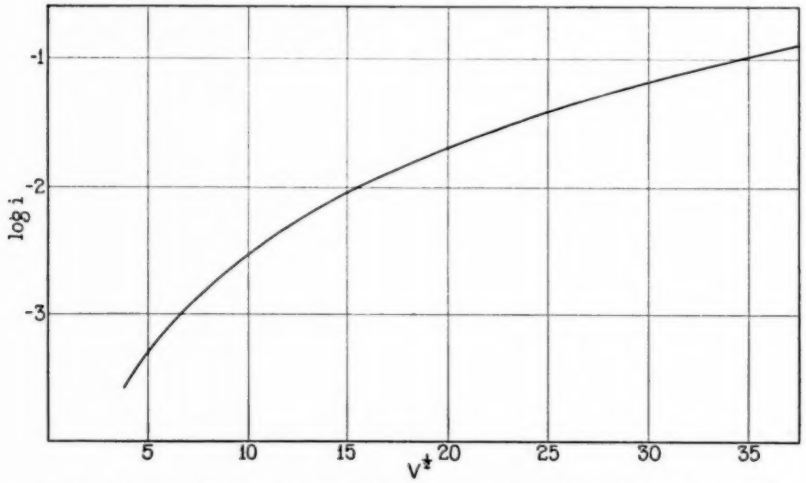

Fig. 5. Current from emitter at 3000° to parallel electrode 1 cm distant for different accelerating potentials.

Discussion of Results

Fig. 3, showing the height of the potential barrier at various distances from the surface, for tungsten, $N_0 = 6.2 \times 10^{22}/\text{cm}^3$ is interesting in that it shows a value for the work function much larger than that conventionally accepted, this larger value being necessary to nullify the effect of the zero-point energy of a highly concentrated electron gas.

Fig. 4 shows in effect the average distance between electrons as a function of distance from the surface. The distance between electrons is comparable with the distance from the surface at a point so close that the image force is meaningless, and slightly further out it is seen that an electron is further from the surface than its nearest neighbor, showing that space charge is certainly important.

When considering the calculations shown in Fig. 5, it should be remembered that the calculations were carried out for plane parallel electrodes, whereas experiments have almost invariably used coaxial cylinders. The rapid change of space charge outward radially from a fine wire would naturally lead to different results. In order to test this question, an attempt is now being made to reproduce experimentally the conditions here treated theoretically.

There are two more questions of importance that must be recognized here. In the first place, the calculated electric field at the surface is so large that a great reduction of electron concentration within the surface should result from the very large surface charge. Just what effect this might have on the case of a current cannot be predicted. The calculations for the equilibrium case are still valid, if one chooses a proper electron concentration at the surface. A second question, of course, is that of the validity of Poisson's equation. It seems to the author that probably this calculation is reasonably close to the truth in regions where the concentrations of electrons is large. But at considerable distances from the surface, where the concentration is low, the approximation to the truth cannot be as good. It is for this reason that for the calculation of emission currents the electrodes were chosen so close together. Also for this reason results are not given for currents at lower temperatures. This particular problem will be investigated further.

In conclusion the author wishes to thank Professor A. T. Waterman for many helpful discussions of the problem.

THE ANGULAR DISTRIBUTION OF ELECTRONS SCATTERED BY MERCURY VAPOR

By J. M. Pearson and W. N. Arnquist
Norman Bridge Laboratory, California Institute of Technology

(Received February 27, 1931)

Abstract

Instead of using pressures of the order of 10^{-2} mm the apparatus described is designed for pressures in the range 10^{-3} to 10^{-4} mm. Heavy primary current densities are used to afford measurable scattered currents, and high angle scattering is found to be more easily measurable. It is found that the angular distribution curves for electrons scattered by mercury are not monotonic functions of the angle of scattering. For a given energy of incident electrons the curve passes through a minimum, the angular position of which depends upon the energy.

I. Scheme of Experiment

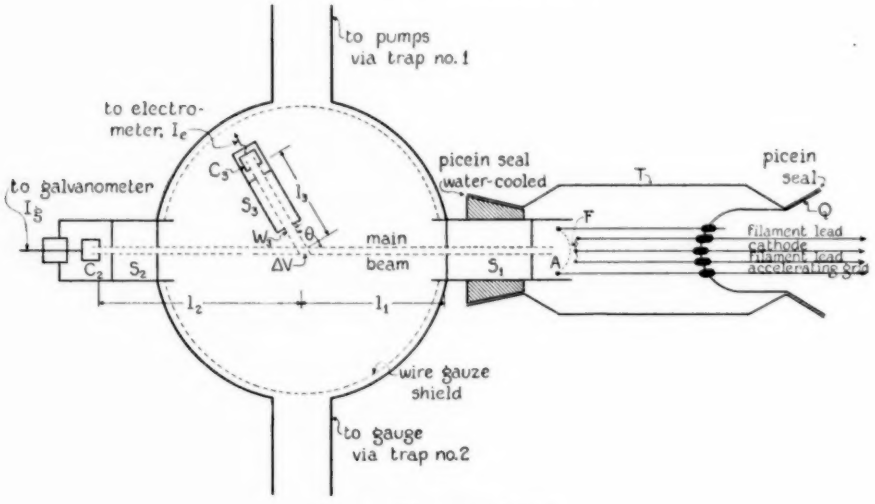

Fig. 1. Diagram of tube.

THE principles of design of this type of apparatus are well enough known so that it will be necessary here to point out only the salient features.

The tube is constructed of brass. It is 15 cm in diameter, and shaped as in Fig. 1. Electrons are accelerated from the tungsten filament F (supplied at the center-tap), through the grid A, and retarded between the grid A and the first of the collimating slits S_1.

The circuits are so arranged that the entire enclosure is maintained at ground potential. The electron beam passes diametrically across the chamber to the slits S_2, and through these to the Faraday cage C_2.

The axis of the main beam is oriented to be parallel to the horizontal com-

ponent of the earth's field, which is carefully neutralized by one set of large Helmholtz coils. A magnetic pendulum was used to determine the necessary current.

Slits S_1 and S_2 are optically aligned, and by means of another pair of large Helmholtz coils the vertical component of the magnetic field in the apparatus is adjusted until the main beam is received on C_2. By changing the current in the latter coils the beam can be moved back and forth across the slits S_2. This affords a means of measurement of the divergence of the beam.

Electrons scattered from the main beam are collected principally by the walls of the chamber, which are made more absorbing by the use of the copper gauze as shown.

A portion of the electrons scattered at an angle θ in the center of the apparatus, pass through the slits S_3 and reach C_3. The axis of collimation of slits S_3 passes always through the center of the apparatus as θ is varied. See Fig. 2 for a vertical section.

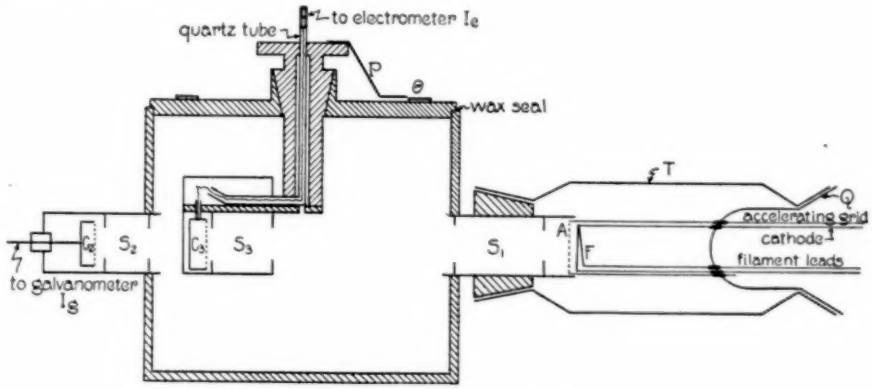

Fig. 2. Vertical section of tube.

Slits S_3 and cage C_3 are mounted in the lid on a movable, central, stem with a tapered joint as shown. A pointer P reads the angle θ, on a scale engraved on the lid.

Slits S_1 and S_2 are 10 mm long. Slits S_3 are 8 mm long. The spacings and widths are so adjusted that, with length considered, 90 percent of the electrons passing any pair of slits is contained within an angle of $\pm 1.5°$ of the central axis of that pair.

Other details such as accessibility of the filament or of the chamber, are explained by the figures.

The electric circuits are shown in Fig. 3.

II. Theory of Apparatus

Let ΔV be the volume of the intersection of the paths of collimation of S_1 and S_3. Let p be the gas pressure in mm Hg; α the coefficient of scattering in the expression,

$$I = I_0 \exp(-\alpha p x).$$

Let I be the current in amperes, at the point "x" measured along the main beam from ΔV; I_0 the main beam current entering ΔV; l_2 the distance from C_2 to ΔV; l_3 the distance from C_3 to ΔV (constant). Let $f(\theta)d\theta$ be the probability under given conditions that a scattered electron will be deflected between the angles θ and $\theta+d\theta$.

At any point x in the beam passing ΔV we have the current

$$I = I_0 \exp(-\alpha p x). \tag{1}$$

So in the distance dx

$$dI = -\alpha p I_0 \exp(-\alpha p x)dx. \tag{2}$$

$-dI$, is therefore the scattered current in the distance dx.

Let us consider now the current we can hope to receive on C_3 at the angle θ. Let I_s be the current scattered in ΔV; w_3 the width of slits S_3. Then

$$I_s = -dI = \alpha p I_0 \exp(-\alpha p x)dx = \alpha p I_0 w_3/\sin\theta.$$

since $x=0$ at ΔV and $dx=w_3/\sin\theta$. Hence the fraction of I_s that is scattered between θ and $\theta+d\theta$ is given by

$$I_s f(\theta)d\theta = \frac{\alpha p I_0 w_3 f(\theta)}{\sin\theta}d\theta. \tag{3}$$

Of this current only a fraction, K_3, will reach C_3 because of slits S_3. The current is also attenuated by scattering along the path of length l_3 from ΔV to C_3. So the current, I_e, received on C_3 is

$$I_e = \frac{\alpha p I_0 w_3 f(\theta) K_3}{\sin\theta}d\theta \exp(-\alpha p l_3). \tag{4}$$

Consider next the current received on C_2: because of the slits S_2 only a fraction, K_2, of the incident main beam will reach C_2. The beam is also attenuated by scattering along the path of length l_2. Hence the current, I_g, received on C_2 is

$$I_g = I_0 K_2 \exp(-\alpha p l_2). \tag{5}$$

If we divide (4) by (5) we eliminate I_0:

$$\frac{I_e}{I_g} = \frac{\alpha p K_3}{K_2} w_3 \frac{f(\theta)}{\sin\theta}d\theta \exp(\alpha p[l_2 - l_3]).$$

so that

$$f(\theta) = \frac{K_2 \exp(-\alpha p[l_2 - l_3])}{K_3 \alpha p d\theta w_3}\frac{I_e}{I_g}\sin\theta.$$

$$f(\theta) = K\frac{I_e}{I_g}\sin\theta \tag{6}$$

where

$$K = \frac{K_2 \exp(-\alpha p[l_2 - l_3])}{K_3 \alpha p d\theta w_3}.$$

The value of K is constant so long as one set of conditions is constant, since $d\theta$, K_2, K_3, l_2, and l_3, are all functions of a fixed geometry. The K's seem to depend upon the electron speed, and upon the condition of equilibrium of the apparatus. This is probably because the condition of the slit surfaces depends upon the bombardment they receive. During a given run, if the apparatus has previously been brought to equilibrium, K will remain quite constant. However, when the apparatus has been out of equilibrium between runs, K will vary by as much as a factor of 5.

It follows that by measuring I_e, I_g, and θ, the value of $f(\theta)/K$ can be calculated as a function of θ.

It is noted that the current I_e received by C_3,

$$I_e = \frac{\alpha p I_0 w_3 K_3 f(\theta) d\theta}{\sin\theta} \exp(-\alpha p l_3)$$

goes to zero for high pressures because of the exponent, and to zero for low pressures because of the factor p. However it goes to zero much more slowly

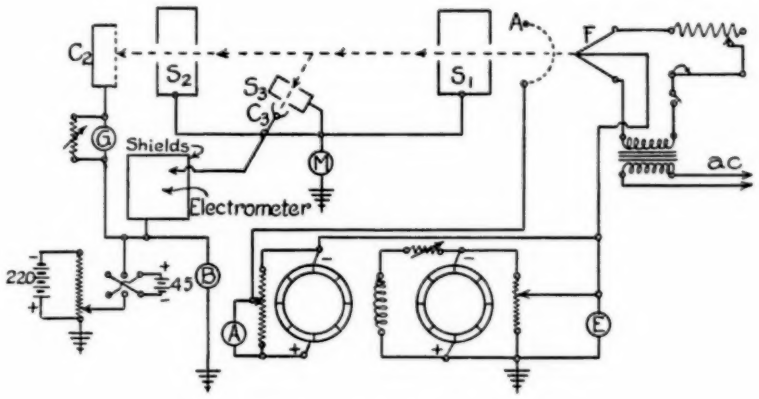

Fig. 3. Diagram of electrical arrangement.

on the low pressure than on the high pressure side of its maximum. This is fortunate since the maximum lies at such a high pressure that the condition of "single" scattering is not satisfied in an apparatus of practical dimensions.

In using lower pressures if the product pI_0 is kept constant, I_e can be maintained at a readable value.

I_e was measured by a "null" circuit using a modified Dolezalek electrometer.[1]

From the experimental values of α, and the dimensions of this apparatus, the mean free path of an electron is about the diameter of the apparatus at $p = 10^{-3}$ mm Hg. Thus at the pressure used ($1.8 \cdot 10^{-4}$mm) the condition for single collision scattering is well satisfied.

[1] J. M. Pearson, Journ. Op. Soc. 19, 6, p. 371.

In order to obtain the intensities of main beam desired some concessions had to be made in the voltage distribution of the electrons. Coated, equipotential, low temperature cathodes were tried, but were short lived owing to the heavy positive ion bombardment. Heavy tungsten was finally used, with a center-tap through which to supply the space current.

Studies were made of the voltage distribution of the electrons received on the Faraday cages. Two things were discovered, namely: (1) that the electrons were distributed over a range of 3 volts at E; and (2) that the cages were inefficient electron collectors. This was made evident by the fact that the electron current was cut off by a bias as much as 20 volts less than E, in vacuum, when the bias was applied to the cage. If however, the bias was applied to a grid somewhat ahead of C_2 (not shown), the cut-off bias was the same as E. This indicated that a deeper cage was necessary, or at least that an assisting gradient towards the cage was necessary.

Because of this low resolving power both at the collectors and at the filament, inelastic electrons were not resolved from the elastic electrons.

The currents received on C_2 are of the order of microamperes, and are measured by a suitably shunted wall galvanometer "G" (Fig. 3).

III. Manipulation

The apparatus is manipulated as follows:

(1). After several hours of pumping the filament is lit and the slits are bombarded. Liquid air is maintained on both traps. (see Fig. 4.) From two to five hours generally suffices to reach a state of equilibrium.

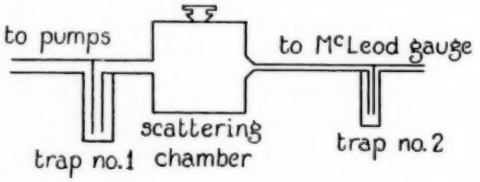

Fig. 4. Scattering chamber and connecting traps.

(2). When equilibrium is reached, an ice bath, vigorously agitated, is substituted for the liquid air on trap No. 1. Liquid air is maintained on trap No. 2, on the other side, connected to the chamber through a long tube. Thus after another lapse of hours the mercury vapor pressure inside the chamber becomes stable at very close to $1.8 \cdot 10^{-4}$ mm Hg.

(3). With the magnetic field neutralized and the values of the accelerating and retarding potentials adjusted, two sets of simultaneous readings of I_e and I_g are made at each setting of θ. When these pairs of readings check to ± 5 percent at each point, the run is accepted. Otherwise the apparatus is considered to be out of equilibrium.

In order to eliminate the effects of the positive ions that are collected due to the negative bias on the cages, readings are first taken with a low bias and

then with a high bias so that the difference of the readings gives the electron current. The positives are usually of the order of one-tenth the strength of the electrons. The biases used are marked on the curves.

IV. Results

The curves of Figs. 5 to 9 give a graphic summary of the results obtained. Of special interest is the fact that the curves are not monotonic, but behave as though the scattering were negligible at a certain angle for each electron energy. That these phenomena are associated with the mercury is attested by the fact that other gases (air, for instance, in thise case) gave monotonic scattering curves. In a vacuum (as in (1), manipulations,) no scattering is found at all.

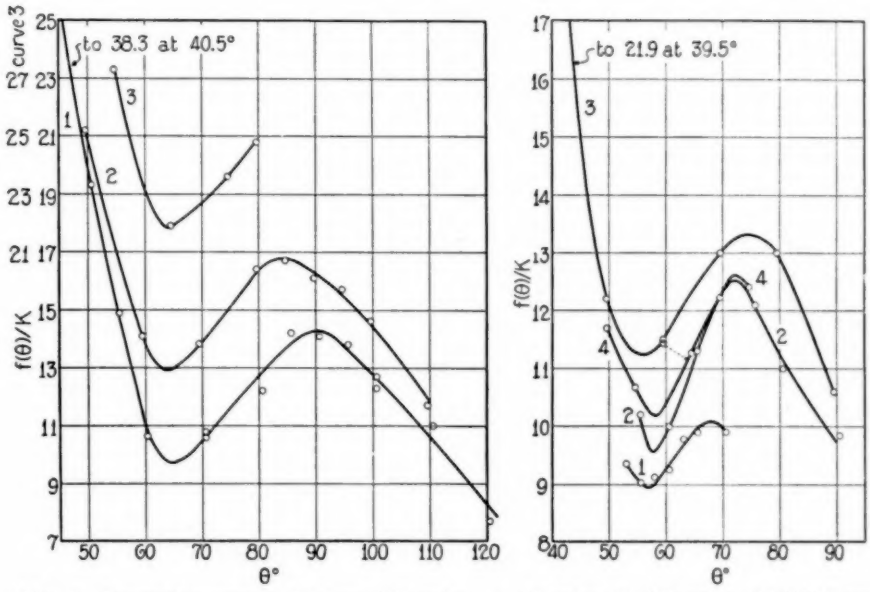

Fig. 5. Scattering curves. Energy, 100 volts. *A*, 95 volts; *E*, 100 volts; *M*, 0.007 amp.; *B*, −75, −102 volts. Curve 1, positive angles; Curve 2, negative angles taken several hours later; Curve 3, negative angles taken several days later.

Fig. 6. Scattering curves, Energy 125 volts. *A*, 165 volts; *E*, 125 volts; *M*, 0.0058 amp.; *B*, −100, −126 volts. Curve 1, positive angles; Curve 2, positive angles taken later; Curve 3, negative angles taken next day; Curve 4, negative angles taken two hours later.

An interesting relationship is presented by the last curve, where the cotangents of the positions of the minima are plotted with the energies. However, lacking a theoretical interpretation this relation may be fortuitous.

For energies less than 100 electron-volts the main beam currents become unmanageably small, while above 200 electron-volts the minima are concealed in the steep part of the curve.

That these minima have not been reported before is perhaps due to the high angles at which they occur. In this case the use of high primary currents makes measurements at the higher angles comparatively easy.

The apparatus can also be used to check the scattering at low angles, and the results fit Langmuir's[2] empirical equation very well:

$$f(\theta) = f(\theta)_{\theta=0} \exp(-\theta^2/\theta_0^2).$$

The experimental points found fit best when $\theta_0 = 12.7°$ at 150 electron-volts energy.

Langmuir finds that for Arnot's[3] curve for 82 volt electrons, $\theta_0 = 11.3°$ is the best value.

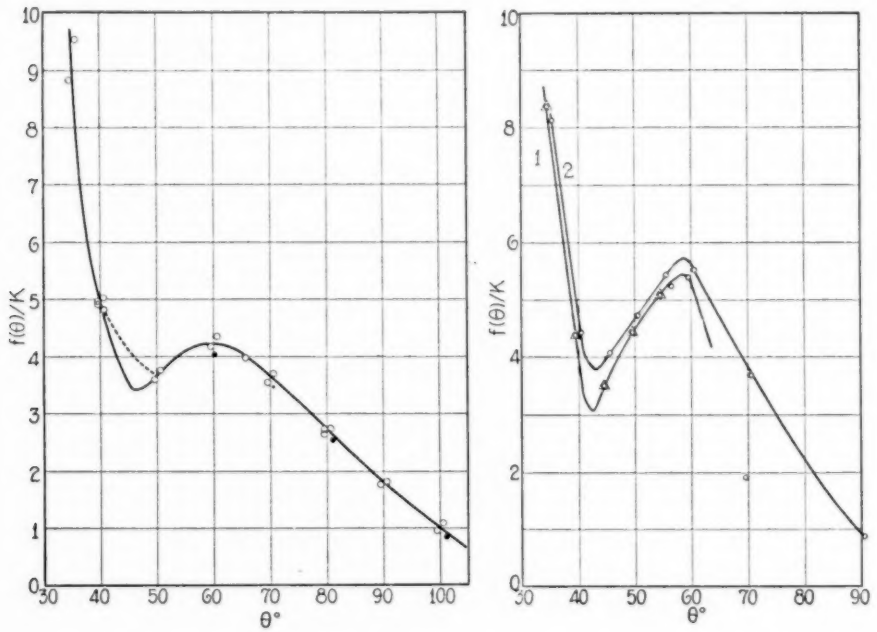

Fig. 7. Scattering curves. Energy 150 volts. *A*, 190 volts; *E*, 150 volts; *M*, 0.006 amp.; *B*, −120, −150 volts. Positive and negative angles read in succession. The solid dots are check points taken later.

Fig. 8. Scattering curves. Energy 175 volts. *A*, 210 volts; *E*, 175 volts; *M*, 0.007 amp.; *B*, −140, −180 volts. Curve 1, negative angles; Curve 2 positive angles taken later. The triangles are check points on negative angles taken two days later.

Some objections to measurements made at small angles can be offered in that the resolving power is somewhat diminished at small angles because of the slit length. Further investigations may justify a correction for this effect.

It is the authors' intention to present these data as being more of a preliminary than of a final nature. Improvements and simplifications which will follow from further work with this type of apparatus, will undoubtedly make for greater precision. At present, the loci of the minima are probably not determined better than $\pm 1.5°$.

[2] K. T. Compton, Irving Langmuir, Revs. Mod. Phys. **2**, 123 (1930).
[3] F. L. Arnot, Proc. Roy. Soc. **A125**, 660 (1929).

In conclusion the authors wish to express their appreciation and indebtedness to Dr. R A. Millikan for his continued interest and advice in this work. We should like to thank also the members of the laboratory shops for their care and skill in constructing the apparatus.

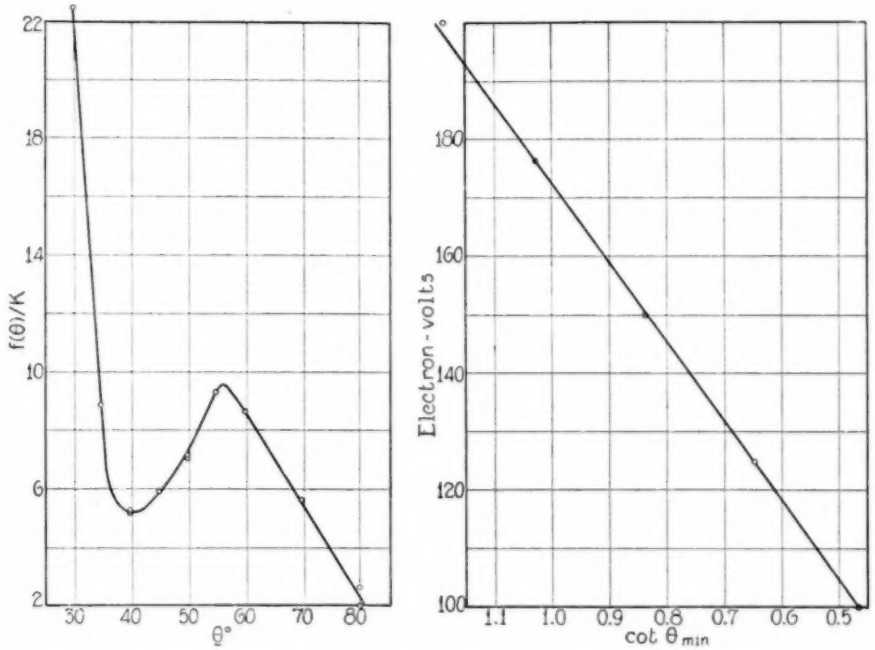

Fig. 9. Scattering curves. Energy 200 volts. *A*, 258 volts; *E*. 200 volts; *M*, 0.006 amp.; *B*, −160, −200 volts. Readings made at different times with apparatus out of equilibrium in meantime.

Fig. 10. Variation of the cotangent of the angle of minimum scattering with electron energy.

Energy	θ_{min}	Weight
100 volts	65	3
125	57	3
150	50	7
175	44	3
200	40	1

ELECTRONIC VELOCITIES IN THE POSITIVE COLUMN OF HIGH FREQUENCY DISCHARGES

By Egon Hiedemann
Physikalisches Institut
Universität Köln

(Received March 9, 1931)

Abstract

Theoretical discussion of the mechanics of individual electrons in the positive column of high frequency discharges with special consideration of the effect of elastic impacts proves that small mean values of the electric force do not prohibit the production of electrons of sufficient velocity to excite or even ionize gas molecules.

IN A recent paper Charles J. Brasefield[1] has published measurements of the potential drop at the electrodes and the electric force in the positive column of high frequency discharges in mercury, helium, and neon for different gas pressures and frequencies of oscillation. The procedure of measuring the electric force in the positive column was the same as that used by the author.[2] and others in earlier work on high frequency discharges. It consisted in measuring the total voltage between the electrodes for various distances of the electrodes and a given current. The mean electric force of the positive column can then be calculated in the known manner, if one assumes that the drop in potential at the electrodes is, for a given current, independent of the separation of the electrodes.

Discussing his interesting results Brasefield concluded that "these results showed that in general, the magnitude of the electric force was too small to produce electrons whose velocity would be sufficient to ionize or excite the gas." This statement would be of the greatest importance for the theory of the positive column in high frequency discharges if it were the only reasonable inference to be drawn from the experimental results. But an explanation, and a very plausible one, may be obtained by calculations similar to those given by the author for a similar problem in an earlier paper.[3]

In order to look clearly into this matter it is necessary to give the experimental results, the calculations and the proposed solution of the problem in essential detail.

Brasefield, as others, observed that for a given current and a given frequency there exists an optimum pressure at which the conductivity is a maximum. The electric force at this gas pressure and at gas pressures near to it is very small. He then calculates the electric force necessary to give an electron the ionizing velocity in an electric field alternating with high fre-

[1] Charles J. Brasefield, Phys. Rev. **37**, 82 (1931).
[2] E. Hiedemann, Verh. D. Phys. Ges. (3) **7**, 47 (1926); Ann. d. Physik **85**, 649 (1928).
[3] L. Ebeler and E. Hiedemann, Ann. d. Physik (5) **5**, 625 (1930).

quency. His calculation gives values for the necessary minimum electric force, which is much higher than the electric forces measured at or near the maximum of conductivity.

It may be pointed out at first that this calculation is based on the assumption that the electric force in the positive column of the high frequency discharge is the same at any point of the column, which supposition is by no means proved or even probable. But supposing that the above-mentioned procedure of measurement really gives the electric force in the positive column, not merely the mean value of it, a more comprehensive calculation gives a result, which differs slightly but not unimportantly from the result of Brasefield.

If E_0 is the amplitude of the electric force and f the frequency of oscillation, then the following equation is valid:

$$m\ddot{x} = eE_0 \sin 2\pi ft. \tag{1}$$

Integration of Equation (1) gives

$$\dot{x} = -\frac{e}{m}\frac{E_0}{2\pi f}\cos 2\pi ft + C. \tag{2}$$

If at the time zero, the electron has the velocity v_0 in the initial direction of the electric field[4] then

$$C = v_0 + \frac{e}{m}\frac{E_0}{2\pi f}.$$

The velocity of the electron in the direction of the field is then given by Equation (3):[5]

$$\dot{x} = \frac{e}{m}\frac{E_0}{2\pi f}(1 - \cos 2\pi ft) + v_0. \tag{3}$$

The maximum velocity in the direction of the field will be obtained when $t = 1/2f$ and is given by

$$v_{max} = \frac{e}{m}\frac{E_0}{\pi f} + v_0. \tag{4}$$

[4] By the direction of the electric field that direction is meant, in which the e.m.f. accelerates an electron.

[5] Brasefield gives the equation:

$$\dot{x} = \frac{e}{m}\frac{E_0}{2\pi f}\cdot[\cos\delta - \cos(2\pi ft + \delta)]$$

where δ is a phase constant depending on the value of E at the instant the velocity of the electrons is zero. Brasefield's equation includes therefore only those electrons which, at the time zero, have no velocity or a velocity contrary to the initial direction of the acceleration and smaller than the maximum velocity obtainable in half a cycle by the acceleration produced by the electric field. Equation (3) on the contrary includes electrons of all directions and velocities.

The total maximum velocity of the electron is the velocity in the resulting direction of the electron. If this direction forms an angle θ with the direction of the electric force, then the total maximum velocity V_{max} will be given by

$$V_{max} = \frac{1}{\cos\theta}\left(\frac{e}{m}\frac{E_0}{\pi f} + v_0\right). \tag{4a}$$

The real velocity V of the electron at any moment is the essential element in all processess of exciting or ionizing gas molecules. For the following discussion, however, it will be sufficient to regard only the velocities in, or contrary to, the direction of the electric field. To simplify matters, Eq. (4) instead of (4a) will therefore be used from now on.

The essential difference between the result of this calculation and that given by Brasefield is that, to the velocity an electron may obtain in half a cycle the velocity of the electron at the beginning of the half cycle must be added, with the right sign of course. To calculate the electric force necessary to give to an electron the ionizing velocity v_i, we must use

$$E_0 = \frac{v_i - v_0}{e} m\pi f. \tag{5}$$

Now the electric forces measured by Brasefield demand —near the maximum of conductivity at least—velocities v_0 which are not small compared with v_i. That means that electrons of nearly sufficient velocity must be present at the beginning of half a cycle. How can such electrons be produced? This can easily be seen, if one remembers that an electron will make elastic impacts with gas molecules before it has obtained the excitation energy.[6] By these elastic impacts it will lose insignificant amounts of energy only, but the direction of its motion will be changed. To simplify the discussion only those impacts will be regarded, for which an electron will after the impact have a component of velocity v' in the direction contrary to that before the impact.

Let us consider now an electron which, at the time zero, has the velocity zero. After half a cycle it will have obtained the velocity v_{max}. Now this electron may have an elastic impact and may immediately after the impact have the velocity v' in the direction contrary to its direction before the impact. As v' is a part of its former velocity, we may define v' by

$$v' = v_{max}/n. \tag{6}$$

The next half cycle will give to this electron the velocity v''

$$v'' = V_{max} + v' = V_{max}(1 + 1/n). \tag{7}$$

[6] Here purposely no correct discrimination is made between the possibility for an electron to get excitation and that to get ionization energy because the difference of these energies is small compared with the difference between one of these energies and the maximum energy obtainable by the e.m.f. in half a cycle. The excitation energy is of primary importance too; especially in those cases in which metastable states are produced and ionization effected by successive impacts.

As this may happen several times and the various n must not be large compared with unity, one easily sees that, as a result of elastic impacts, an electron may obtain a multiple of the maximum velocity obtainable in half a cycle.

This effect of the elastic impacts on the electronic velocities will be efficient especially at gas pressures for which the path of an electron during half a cycle is comparable with the mean free path of the electron. The path of an electron with the velocity v_0 at the time zero between $t=0$ and $t=1/2f$ has been calculated[3] by integration of Equation (3) to be

$$x = \frac{v_0}{2f} + \frac{e}{m}\,\frac{E_0}{4\pi f^2}\,. \tag{8}$$

The gas pressures at which x will be comparable with the mean free path of an electron can thus easily be calculated. The result gives pressures of the same order of magnitude as the optimum pressures measured.[7]

From Eq. (8) one sees that Equation (7) is not quite correct, because if an electron of the velocity zero at the time zero has made an impact with a gas molecule after $t=1/2f$ then the electron will after the impact meet a gas molecule before the second half cycle is finished. The velocity of the electron immediately before the second impact will therefore be smaller than $v'+v_{max}$. A correct equation can be obtained without difficulty, but even without doing so it can easily be seen that matters are much too complicated to allow more than a very rough calculation of the critical order of magnitudes.

In determining the conductivity not only the electrons with excitation or ionization energy are of importance, but the positive ions and the slower electrons too. In an earlier work A. v. Hippel[8] has shown that the energy which positive ions may periodically acquire in the alternating electric field of a high frequency discharge, is to be neglected compared with the ionizing energy. He has also directed attention to the fact that positive ions oscillate with only very small amplitudes, which at the optimum pressures measured by Brasefield may be neglected in comparison with the mean free path. This means that, if positive ions have once been produced, the chance of their getting lost from the discharge is relatively small when no static electric field is present. A small loss of ions on the other hand means a high degree of ionization and a high conductivity. The degree of ionization is limited by recombination and molecular diffusion to the glass walls and to a large extent probably by the static field due to the potential of the glass walls. By elastic impacts electrons will not only get a component of velocity parallel to the direction of the alternating electric force but also normal to it. As this velocity will not be altered by the electric force and as the mobility of the electrons is large a steady current of electrons should be directed to the glass walls and produce there a negative charge. A short time after the beginning of the discharge a stationary state will be reached and a static electric force will be produced.

[7] See also Charles J. Brasefield, Phys. Rev. 35, 1073 (1930).
[8] A. v. Hippel, Ann. d. Phys. (4) 87, 1035 (1928).

This static field will enlarge the loss of positive ions and produce a deformation of the electric field of the alternating e.m.f. Hence the supposition that the electric force in the positive column is the same at any point of the column cannot be right and any calculation based on this assumption will not give correct, but at the best only approximate results. This is another reason that the small measured mean values of the electric force in the positive column do not call for the conclusion that electrons of excitation energy cannot be produced in the high frequency discharge at the maximum of conductivity.

Another important factor in the conductivity is introduced by the oscillation of the slower electrons in the alternating electric field. Their importance for the mechanism of the high frequency discharge at low pressures was pointed out first by F. Kirchner.[9] The motion of these oscillating electrons is given by[5]

$$m\ddot{x} = eE_0 \cos 2\pi ft \tag{9}$$

and the path in a quarter of a cycle; i.e., the amplitude of oscillation; is given by

$$x' = \frac{e}{m} \frac{E_0}{4\pi^2 f^2} . \tag{10}$$

By comparison of Eq. (10) with Eq. (8) it can be seen that the optimum pressure for the oscillating electrons has not quite the same value as for the non-oscillating electrons, but that it is of the same order of magnitude. The importance of the oscillating electrons for the conductivity of the discharge lies, as is known, in the fact, pointed out by Kirchner, that by oscillating in the field these electrons will remain in the discharge.

Those electrons which at the time zero have no velocity or a velocity in the direction of their acceleration in the initial half cycle, will not oscillate in the discharge, but go in one direction only (of course without taking account of the effect of impacts). During half a cycle, they will be accelerated, during the next half they will be retarded by the alternating e.m.f. but they will always go forward. At very low pressures where the mean free path of the electrons cannot be neglected compared with the separation of the electrodes, such non-oscillating electrons produced near the electrodes may thus reach the positive column and their part in the excitation or ionizing processes in the positive column may perhaps not be neglected.

In conclusion it may be said, that the surprisingly small mean values of the electric force measured in the positive column of high frequency discharges near the maximum of conductivity do not at all force one to assume that electrons of excitation energy cannot be produced in the positive column of these discharges.

[9] F. Kirchner, Ann. d. Physik (4) **77**, 287 (1925).

THE ELECTRICAL STATE OF THE SUN

By Ross Gunn
Naval Research Laboratory, Washington, D.C.

(Received March 13, 1931)

Abstract

The magnetic field due to the rotation of our galaxy is calculated, and it is shown (a) that electricity cannot be annihilated in the sun or stars; (b) that the net electrical charge on the sun or a typical star cannot exceed 1 coulomb. The electric fields, space charge and potentials of the solar atmosphere are calculated from data relating to the solar anomalous rotation and numerical values given. The negative surface charge on the sun is calculated to be of the order of 10^9 e.m.u. The problem of the maintenance of the solar electric field is touched upon.

SYSTEMATIC observation of the solar surface by Mount Wilson astronomers and others has shown that many solar phenomena are of such a nature that they can be attributed to electrical and magnetic effects. The magnitude and distribution of the solar magnetic field has been determined by a laborious analysis of Zeeman spectra[1] and sufficient data accumulated to show that the solar magnetic field is not unlike that of the earth, save for its radial limitation. In 1915 an attempt was also made by Hale and Babcock[2] to determine the electric fields by measurements of the Stark effect but they could not detect fields smaller than 100 volts per centimeter and were only able to set an upper limit to the suspected electric field. Investigators have generally stated that the electrical fields in the emitting layers of the sun were negligibly small due to the high electrical conductivity and important effects arising from such electric fields were therefore absent. In the following discussion we shall endeavor to indicate the importance of the electric field and give numerical values for the electrical constants of the sun, insofar as they apply to obvious solar problems.

Separation of Charge Inside the Sun

In an important paper A. Pannekoek[3] noted that in any highly ionized gaseous region acted on by gravitational forces and in thermal equilibrium, the lighter ions diffused upward until their separation produced an electric field which opposed further separation. It is readily shown that the volume charge ρ_v expressed in e.m.u., resulting from the separation, is given by

$$\rho_v = \gamma d\mu/c^2 e \tag{1}$$

where γ is the gravitational constant, d is the density of the ionized matter,

[1] Hale, Astrophys. Jour. **38,** 31(1913); Hale, Seares, Van Maanen and Ellerman, Astrophys. Jour. **47,** 1 (1918).

[2] Hale and Babcock, Proc. Nat. Acad. **1,** 123 (1915).

[3] A. Pannekoek, Bull. Astro. Inst. Netherlands #19 (1922).

μ the mean mass of the molecules, c the velocity of light, and e the electronic charge expressed in *e.m.u.* Using data appropriate to the sun and Eq. (1) we find that the total positive volume charge inside the sun amounts to 33 e.m.u. or 330 coulombs. In another place we shall show that a negative charge of equal magnitude probably resides on the solar surface.

When the temperature is non-uniform the more mobile ions in a conductor diffuse toward cooler regions and in the equilibrium state, an electrical field is set up which prevents further diffusion. The space charge ρ_i existing when equilibrium has been attained is given (in the one dimensional case) by

$$\rho_i = -\frac{k}{8\pi c^2 e}\frac{d^2T}{dr^2} \tag{2}$$

where k is the Boltzmann constant, r the space coordinate and T the absolute temperature. Application to the interior of the sun at the present time will not be attempted for little is known about the internal solar temperature. If we follow the star models considered by Eddington[4] the temperatures are so related to gravitational forces that the space charge due to non-uniform temperatures will be of the same order of magnitude as the space charge due to gravitational forces. If, on the other hand, we should adopt Milne's[5] star model which suggests central temperatures of the order of 10^{11} degrees, it is evident that the interior space charge is likely to be large.

Annihilation of Electricity

Attempts to account for the earth's atmospheric electric current have led several writers to assume that electricity is annihilated at some definite but slow rate. Simpson[6] suggested that electricity might be generated spontaneously while Swann[7] assumed that positive electricity died constantly inside the earth but neither writer suggested where the required energy for the transformation might originate. Anderson[8] supplied the theoretical deficiency and assumed that the loss of the protonic mass supplied the necessary energy to annihilate the protonic charge. Thus he postulated a subatomic transformation in which the mass of one proton vanished for each protonic charge annihilated. Evidently if the energy corresponding to a given transformation is known then the lost mass and electrical charge can be immediately calculated. Anderson's calculations indicated that the sun was throwing off negative electricity at a rate of 4×10^{16} e.m.u. per second. This tremendous negative charge was assumed to dissipate itself through all space and finally be lost. In many respects Anderson's hypothesis is interesting in spite of the objections which will occur to the atomic physicist. We proceed to show, however, that in stars the annihilation of electricity is not probable unless the released ions leave our universe in a highly specialized and improbable manner.

[4] Eddington, Internal Constitution of the Stars (1926).
[5] E. A. Milne, Monthly Notices **91**, 4 (1930).
[6] C. G. Simpson, Monthly Weather Rev. **44**, 121 (1916).
[7] Swann, Jour. Franklin Inst. **201**, 143 (1926).
[8] W. Anderson, Zeits. f. Physik **42**, 475 (1927).

The system of stars embraced by the Milky Way stretches far out into space and forms our galactic system. The motions of the stars in this system, their masses, radiation, numbers and distribution are known and if electrical charges are constantly given off by each member of the galactic system, observable magnetic effects should be measured on the earth. We will assume that when ions are thrown off by a star the ion preserves its angular momentum about the gravitational center of the galaxy as it finds its way to outer space. Thus the systematic motion of the stars about the center of the galactic system is shared by the electricity which has been thrown off by them.

The systematic motion constitutes an electrical convention current and will produce a magnetic field. In the present connection we need only the order of magnitude of the effect and a rough calculation which directs attention to the physics of the problem will readily serve. Let us suppose that the entire negative charge in the space outside the stars but inside the galaxy, is compressed into a ring of radius equal to the mean radius of the system. Then the magnetic field H at the center of the system is

$$H = 2\pi Q\omega \tag{3}$$

where Q is the total free charge and ω is the mean angular velocity about the center of the system. The earth is not at the center of the system but it is difficult to see how its position and motion could change the value of the magnetic field at the earth by more than an order of magnitude.

The angular motion of our galaxy is known from astronomical data and Q is determined by calculating from the total radiation of the galactic system, the rate of release of negative electricity. We must note further that the time the released electricity remains in the system proper must be at least as great as the time it would take light to traverse the path. Thus

$$Q \geqq Ir/c \tag{4}$$

where I is the total current thrown off by all stars of the galaxy as calculated by Anderson's hypothesis, r is the mean radius of the galactic system and c the velocity of light. The mean star of the galaxy has a mass 1.6 that of the sun and there are roughly 10^{10} of them,[9] so that we may assume that the total current I of the system is 10^{10} that of the sun or 10^{26} e.m.u.[10] Taking $r = 10^3$ parsecs, $\omega = 10^{-13}$ rad/sec and combining Eq. (4) with Eq. (3) we find that the magnetic field at the center of the galaxy is of the order of 10^{25} gauss.

Such a large magnetic field seems absurd and we conclude that observation demands either that the charges which leave a star, leave in a very special manner, or else that annihilation of positive charge in stars does not occur. The evidence is such that we believe Anderson's and other similar hypotheses must be abandoned.

Net Solar Charge

An upper limit may be set for the net charge which the sun may carry if we are willing to assume that the sun is a star typical of the average star of

[9] Russell, Dugan and Stewart, Astronomy (1927).

[10] R. Gunn, Phys. Rev. **32**, 133 (1928).

our galaxy. Magneticians have been collecting precise data on the variations of terrestrial magnetism for a great many years but there is no evidence of which we are aware that suggests that there may be an extra-terrestrial magnetic field which would be observed to have a period of a siderial day. Certainly such a field would have been found if it was as great as 10^{-3} gauss and probably a field much smaller would be noticed. We may then assume that if a galactic magnetic field exists its value H is probably less than 10^{-3} gauss.

If the stars of our galaxy (of which the sun is typical) carry free electrical charges, then certainly their ordered motion in our galaxy will give rise to a magnetic field. In Eq. (3) we substitute for Q the product of the total number of stars n, by q the mean charge on each, and write the inequality

$$q \leqq H/2\pi\omega n. \tag{5}$$

Substituting the appropriate numerical values in Eq. (5) we find that the mean charge on each star of our galaxy cannot be greater than 0.1 e.m.u. or one coulomb. In the present case there is no question regarding the motion of the charges for they are attached to the stars. When we reflect that the total surface charge of the earth is of the order 10^5 coulombs we see that stars are neutral to a high degree of approximation. We note in passing that measurements show the earth is probably neutral as a whole. These considerations lead us to assume that the sun as a whole is electrically neutral.

Solar Atmospheric Electricity

The highly ionized regions of the solar surface which can be observed are known to be regions of low pressure and the ion free paths are therefore very long. An early paper[11] showed that when ions execute long free paths in crossed electric and magnetic fields, ions of both kinds were swept in a direction perpendicular to both the electric and magnetic fields with a velocity which depended only on the relative magnitude of the crossed fields. This effect is of the nature of a mass motion and is of great importance because it connects directly the easily observable mechanical motions of an ionized region with the magnitudes of the impressed electric and magnetic fields. In a series of papers[11] the above electromechanical effect was shown to account quantitatively for the observed anomalous solar rotation, if the sun possessed an atmospheric electric field which was strikingly similar to the field observed on the earth.

The superposed drift velocity $\boldsymbol{u}$ of an ionized atmosphere is given by

$$\boldsymbol{u} = \frac{\boldsymbol{E} \times \boldsymbol{B}}{B^2[1 + (R/\lambda)^2]} \tag{6}$$

where $\boldsymbol{E}$ and $\boldsymbol{B}$ are the electric and magnetic fields respectively, R the radius of the spiral generated by an ion as it is constrained to move about the impressed magnetic fields and λ is the mean free path. We calculate R from

[11] R. Gunn, Phys. Rev. **35,** 635 (1930); **36,** 1251 (1930); **37,** 283 (1931).

$$R = \frac{mv^1}{Be} = \frac{(2mkT)^{1/2}}{Be} \tag{7}$$

where m is the mass of the ion, v^1 the component of its velocity perpendicular to the magnetic field B, and e the ionic charge in e.m.u. In the atmospheric levels of the sun which we can see, λ is large compared to R and if we agree for simplicity to consider only the motions at the solar equator, Eq. (6) takes the simpler scalar form.

$$E = Bu \tag{8}$$

where E is now the radially inward electric field, B the northward magnetic field and u the eastward atmospheric ion drift measured with reference to the surface of the sun proper. The eastward superposed drift u is readily determined from

$$u = u_0 - a\omega \sin \phi \tag{9}$$

where u_0 is the measured velocity of the observed point whose colatitude is ϕ, a is the solar radius and ω is the angular velocity calculated from the rotation of the sun's magnetic pole. The magnetic field B can be measured directly by the Zeeman effect, so that E can always be calculated for all observed levels. The drift velocity u is known to change with altitude, solar activity and to be subject to large local fluctuations. As we have seen elsewhere[11] the fluctuations are probably due to variations in E rather than B.

In a typical region of the reversing layer the magnetic field is observed to be 25 gauss and the difference of velocity of the surface proper and that actually measured or u is 5×10^4 cm/sec. By aid of Eq. (8) we find the electric field in this region is 0.013 volts/cm. Similarly where the magnetic field is 55 gauss the electric field is 0.027 volts/cm. Now the difference in altitude between these two points is roughly 8×10^6 cm, according to Mt. Wilson data, and we can estimate the volume charge by a one dimensional Poisson's equation. Thus

$$\rho_a = -\frac{u}{4\pi c^2}\frac{dB}{dr} \tag{10}$$

where ρ_a is the atmospheric volume charge in e.m.u. and the other quantities are those defined before. From Eq. (10) and the foregoing observational data we find that over a small interval the space charge in the solar reversing layer is $+1.66\times10^{-23}$ e.m.u./cm^3 or on the average there is one singly charged free positive ion per liter.

The space charge increases rapidly as we go deeper and deeper into the sun and if the magnetic field and drift velocity were known at all levels the surface charge and total atmospheric charge could be determined. The solar astronomical data giving the intensity of the magnetic field as a function of the altitude are not very reliable on account of the difficulties of measurement and there is even sharp disagreement as to the scale of altitudes in the reversing layer. In an earlier paper[11] a semi-empirical relation was employed to

represent the magnetic field as a function of altitude and the constants so chosen as to fit observation over a limited range. Precise analysis requires appeal to direct observational data for it is unlikely that the radial distribution of the magnetic field is as simple as our assumed formula indicates. We will assume that the magnetic field at any level in the solar atmosphere is given[11] approximately by

$$B = B_0 \exp\left[-\frac{zHg(r-a)}{2kT}\right] \tag{11}$$

where B_0 is the magnetic field of the sun at the "surface proper," z the mean atomic weight of the atmospheric ions, g the acceleration due to gravity, H the mass of the hydrogen atom and $(r-a)$ the altitude above the sun. Relation (10) becomes by aid of Eq. (11)

$$\rho_a = \frac{uzHgB}{8\pi c^2 kT} \tag{12}$$

so that the total atmospheric volume charge in a prism 1 cm² in cross-section is given by

$$\int_a^\infty \rho_a dr = uB_0/4\pi c^2 \tag{13}$$

and since on the whole the sun is neutral and there is no external electric field it follows that the surface charge on the sun proper is equal and opposite to the positive space charge. Following earlier work[12] we use 12,000 gauss for B_0 and calculate the total positive charge in a prism 1 cm² extending from the sun outward and get $+5.3\times10^{-14}$ e.m.u. The surface charge is equal and opposite. The total negative surface charge of the sun is therefore 3×10^9 e.m.u.

We can use Eq. (11) to determine the potential difference between the surface proper and free space if we combine it with Eq. (8) and integrate.[11] Let ϕ_1 be the potential difference, then

$$-\phi_1 = \int_a^\infty E dr = u\int_a^\infty B dr \tag{14}$$

which by aid of Eq. (10) becomes

$$\phi_1 = \frac{2uB_1kT}{zHg} \tag{15}$$

where B_1 corresponds to a level where the atmospheric electrical conductivity begins to drop off rapidly due to the solar magnetic field[11,12] and it amounts to about 280 gauss.[11] Substitution of the approximate values in Eq. (15) shows that the sun proper is negative with respect to free space by 1.5×10^6 volts. The foregoing values, calculated by aid of semi-empirical formula cannot be expected to be precise for we have made the assumption that the equatorial

[12] R. Gunn, Phys. Rev. **33**, 614 (1929); **34**, 1621 (1929).

drift velocity was the same constant at all altitudes. In the region of the reversing layer where the constants were made to fit the known points the equations are more reliable.

Maintenance of the Solar Electric Field

The electrical conductivity of the solar atmosphere is high even in the reversing layer where the magnetic field greatly reduces the mobility of the ions.[10] It is readily shown that the solar atmosphere would discharge itself in 10^{-10} seconds if no mechanism was provided to maintain the current. We are therefore faced with precisely the same problem that has puzzled physicists for years in connection with the earth's electric charge. As in the case of the earth we may now assert that the sun is neutral to a high degree of approximation and we may further maintain that electricity does not continuously leave the sun. These restrictions narrow down the investigation to fairly definite problems and several have been examined keeping always in mind that the mechanism of replenishment should also be capable of modification to fit the earth. Even though the mechanism in the sun must be quite simple compared to that on the earth, no definite conclusion has been reached. The extreme variability of the electric field as indicated by the atmospheric motions suggest that local conditions may affect the field greatly somewhat in the manner that an electrical storm disturbs the earth's local electrical state. Young[13] had the idea long ago that the solar atmosphere "rained" condensed metallic particles and brought charges down with them. While the idea is tempting because of present ideas regarding the maintenance of the earth's charge it has several weak points and cannot be made quantitative. It has been shown[11] that the electrical energy dissipated in the solar atmosphere is an appreciable fraction of the total radiated energy and any mechanism which will account for the field must be a moderately efficient one.

Conclusion

Our study has shown that the rather artificial postulate of the annihilation of charge is inconsistent with observation and that to a high degree of approximation the sun is electrically neutral. Our calculations show that the separation of charge in the solar atmosphere is considerable and that the resulting distribution of electric field is remarkably similar to that observed on the earth. In a typical equatorial region of the reversing layer the electric field is radially inward and amounts to 0.015 volts/cm, a value far too small to be detected by measurements of the Stark effect. In the present paper the fields have been calculated from data derived from the observed solar atmospheric motions. In a forthcoming paper the electric fields will be calculated from certain spectroscopic data and the values obtained shown to be consistent with the present estimates.

[13] Young, The Sun.

SURFACE TENSION OF MERCURY

By Marie Kernaghan, R.S.C.J.
Department of Physics, The Saint Louis University

(Received March 9, 1931)

Abstract

Consistent values for the surface tension of mercury in a high vacuum (air pressure less than 1.2×10^{-5} mm Hg throughout the period of experimentation), ranging from 438.4 ± 0.3 dynes per cm at 12.5°C to 423.9 ± 0.6 dynes per cm at 67°C, have been found by a modified flat-drop method. In evaluating them Worthington's equation

$$\sigma=\frac{(K-k)^2\rho}{2}\cdot\frac{1.641\,L}{1.641\,L+(K-k)}$$

was used. The temperature gradient, determined from the best mean straight line through the experimental points, is 0.3015 dyne per cm per degree. Hence the average value of k, in the E tv"s relation, was found to be 1.82. Reproduction of concordant results at intervals during a period of four months affords ample evidence of the thorough outgassing of the apparatus and is attributed to the great care used in securing relative perfection of details.

Introduction

WITHIN the last decade many publications (between one and two on an annual average) have been concerned with the surface tension of mercury[1–21] and the greater number have dealt with its measurement in a vacuum. Hogness[9] and later Bircumshaw[2] have given excellent summaries of

[1] L. L. Bircumshaw, Phil. Mag. **2,** 341–350 (1926).
[2] L. L. Bircumshaw, Phil. Mag. **6,** 510–525 (1928).
[3] R. C. Brown, Phil. Mag. **6,** 1044–1055 (1928).
[4] R. S. Burdon and M. L. Oliphant, Trans. Faraday Soc. **23,** 205–213 (1927).
[5] S. G. Cook, Phys. Rev. **34,** 513–520 (1929).
[6] W. D. Harkins and E. H. Grafton, J. Am. Chem. Soc. **42,** 2534–2538 (1920).
[7] W. D. Harkins and W. W. Ewing, J. Am. Chem. Soc. **42,** 2539–2547 (1920).
[8] J. Hartman, Phys. Rev. **20,** 728–744 (1922).
[9] T. R. Hogness, J. Am. Chem. Soc. **43,** II, 1621–1628 (1921).
[10] T. Iredale, Phil. Mag. **45,** 1088–1100 (1923).
[11] T. Iredale, Phil. Mag. **48,** 177–193 (1924).
[12] T. Iredale, Phil. Mag. **49,** 603–627 (1925).
[13] M. L. Oliphant, Phil. Mag. **6,** 422–433 (1928).
[14] E. Perucca, Atti. Acc. Torino **57,** 81 (1921).
[15] E. Perucca, Atti. Acc. Torino **57,** 541 (1922).
[16] E. Perucca, Phil. Mag. **7,** 418–419 (1929).
[17] M. J. Popesco, Comptes Rendus **172,** 1474–1476 (1921).
[18] M. J. Popesco, Comptes Rendus **175,** 148–149 (1922).
[19] M. J. Popesco, Ann. de Physique **3,** 402–464 (1925).
[20] T. W. Richards and S. Boyer, J. Am. Chem. Soc. **43,** I, 274–294 (1921).
[21] Sauerwald and Drath, Zeits. Anorg. Chem. **154,** 79 (1926).

the work done in that line since 1898. Hence another summary just now is unnecessary. Suffice it to say that in spite of the great variety of methods painstakingly tried by eminent experimenters, the final results continue to be discordant even in single experiments, the values obtained ranging from "340 to 575 dynes per cm."[9] The true value of the surface tension of mercury cannot be as erratic as the above quoted discordant values would make it. Since the modified flat-drop method, used in finding the surface tension of sodium in a vacuum,[22] gave perfectly consistent results, it was decided to try it out on mercury. Some of its marked advantages are: a high degree of accuracy, perfect control of temperature conditions, facility in the production of fresh and uncontaminated surfaces, possibility of maintaining a high vacuum during a long interval of time, and independence of the contact angle.

Apparatus

The apparatus (Fig. 1) though similar in general outline to that used in the experiment on sodium,[22] differed in several details. The chief difference lay in the shape and size of the surface tension chamber *C* (Fig. 1). It was

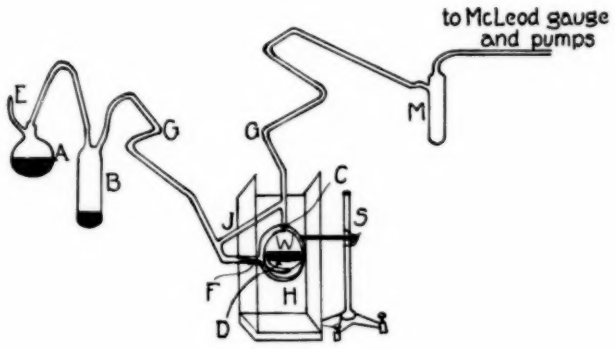

Fig. 1. Diagram of apparatus.

arranged in a horizontal position and though shorter it was wider and more roomy than the first. The plane circular glass window *W* (made to order by the Corning Glass Company) was fused into the end of the tube in preference to the side, in such a way as to render the entire disk optically available. The shallow cup *D* in which the flat drop of mercury was formed was ground with fine emery until all clip scars had disappeared. While similar in general appearance to the cup used for sodium it was wider (average outer diameter 6.04 cm) and deeper (maximum depth 1.2 cm). The difference existing between the various diameters was not more than 0.02 cm. As in the case of sodium, the mercury was introduced into the cup by means of a thick-walled capillary tube *F* which served to prevent too rapid introduction and consequent surging back and forth of the liquid. The tube *J* necessary for outgassing purposes prevented an accumulation of pressure behind the cup. To

[22] F. E. Poindexter and M. Kernaghan, Phys. Rev. **33**, 837–843 (1929).

procure a fine levelling adjustment at any time during the course of the experiment the cup chamber was tightly clamped and exteriorly cemented to a levelling stand S; and coiled tubes G one on either side of C were inserted into the apparatus. The presence of the flask M was merely an added precaution against contamination resulting from any possible overflow of mercury from the McLeod gauge. The entire piece of apparatus, including the McLeod gauge, was constructed of Pyrex glass, having only glass seals throughout.

Redistilled mercury was well shaken with chromic acid solution and then thoroughly rinsed with distilled water. It was next distilled in a current of air, then in a vacuum. This whole process was gone through twice before admitting it into the flask A. After sealing off E and thoroughly outgassing the apparatus the mercury was carefully distilled in a vacuum with a hand burner into the reservoir B from which it was distilled into the cup D as needed. The surface tension chamber was sufficiently roomy to allow the cup to be emptied and refilled without disturbing the apparatus.

The heater of the sodium experiment,[22] adjusted to suit the modification of the cup chamber, was used, hence the temperature conditions were those of the former experiment and hence within one degree of correct values. A frosted glass window arranged in the back panel of the heater made it possible to illuminate the drop from without and thereby get a sharp focus along the meniscus. Once this arrangement was perfected there was no difficulty in determining the exact top of the drop.

The combination of travelling microscope and dividing engine, used as a measuring device in the sodium experiment, was again employed. But instead of locating a number of points on the meniscus of the drop and then graphing the curve, it was decided to use a small carbon filament lamp for locating the top of the meniscus. It was mounted in a manner similar to that described by Richards and Boyer[20] and used by Iredale,[12] Cook,[5] and others. The small lighted lamp, attached to the telescope some distance behind it and on a level with it, was reflected from a spot on the maximum horizontal diameter as a tiny star which could be brought easily to a focus on the cross hairs. The vertical distance from the maximum horizontal diameter to the top of the drop ($K-k$ in Table I) could then be found by direct measurement. The diameter of the drop was measured directly by means of the dividing engine.

Data and Results

A summary of the results obtained from readings taken at intervals during a period of more than four months is given in Table I. The temperatures below 41° (second column) were room temperature in degrees centigrade. The number of separate readings of K (the top of the drop) and of k (the location of the star), from which $K-k$ was in each case determined, may be found in the third column. The values for the density quoted in column 4 have been taken from the Smithsonian Physical Tables.[23] For each set of

[23] Smithsonian Tables, Handbook of Chemistry and Physics, Thirteenth Edition, p. 746 (1928).

TABLE I. *Surface tension of mercury in a vacuum.*

No.	Temp. C	No. of Trials	Density ρ	Radius L cm	$K-k$ cm	Uncorrected σ dynes	Corrected σ dynes	Date
1	12.5°	11	13.5646	2.87	0.2639	462.9±0.3	438.4±0.3	Nov. 26, 1930
2	14.°	20	13.5610	2.87	0.2638	462.4±0.3	437.9±0.3	Nov. 28, 1930
3	18.3°	15	13.5504	2.87	0.2635	461.0±0.3	436.6±0.3	Nov. 26, 1930
4	20.°	9	13.5462	2.87	0.2634	460.5±0.3	436.1±0.3	Nov. 28, 1930
5	21.°	9	13.5438	2.87	0.2633	460.1±0.3	435.7±0.3	Nov. 29, 1930
6	21.5°	15	13.5425	2.87	0.2633	460.0±0.3	435.7±0.3	Nov. 30, 1930
7	22.5°	15	13.5400	2.92	0.2632	459.6±0.2	435.7±0.2	Nov. 2, 1930
8	23.1°	13	13.5389	2.87	0.2630	458.9±0.3	434.6±0.3	Nov. 30, 1930
9	23.5°	11	13.5377	2.87	0.2629	458.5±0.3	434.2±0.3	Nov. 27, 1930
10	23.5°	10	13.5377	2.87	0.2630	458.8±0.6	434.5±0.6	Nov. 30, 1930
11	24.°	10	13.5364	2.87	0.2628	458.1±0.3	433.8±0.3	Nov. 27, 1930
12	25.1°	9	13.5337	2.91	0.2631	459.05±0.2	435.1±0.2	Oct. 12, 1930
13	25.2°	9	13.5335	2.92	0.2631	459.03±0.2	435.1±0.2	Oct. 11, 1930
14	25.8°	9	13.5320	2.91	0.2632	459.3±0.2	435.4±0.2	Oct. 11, 1930
15	26°	8	13.5315	2.84	0.2630	458.6±0.3	434.3±0.3	Sept. 25, 1930
16	28°	10	13.5266	2.84	0.2628	457.8±0.3	433.5±0.3	Sept. 25, 1930
17	31°	11	13.5193	2.89	0.2624	456.1±0.3	432.2±0.3	July 31, 1930
18	31°	12	13.5193	2.89	0.2624	456.1±0.3	432.2±0.3	Aug. 1, 1930
19	32.3°	10	13.5161	2.86	0.2624	456.0±0.3	431.9±0.3	July 29, 1930
20	32.3°	24	13.5161	2.86	0.2624	456.0±0.3	431.9±0.3	July 29, 1930
21	33°	9	13.5144	2.89	0.2624	455.95±0.3	432.1±0.3	July 30, 1930
22	33.3°	12	13.5136	2.85	0.2623	455.6±0.3	431.5±0.3	Aug. 5, 1930
23	34°	10	13.5119	2.91	0.2622	455.2±0.3	431.5±0.3	July 27, 1930
24	34.8°	10	13.5100	2.85	0.2622	455.1±0.2	431.0±0.2	Aug. 6, 1930
25	35°	10	13.5095	2.91	0.2621	454.8±0.2	431.1±0.2	July 26, 1930
26	35°	10	13.5095	2.91	0.2622	455.1±0.3	431.4±0.3	July 27, 1930
27	35°	9	13.5095	2.85	0.2621	454.8±0.3	430.7±0.3	Aug. 4, 1930
28	41°	12	13.4949	2.91	0.2619	453.6±0.2	429.9±0.2	Aug. 1, 1930
29	43°	8	13.4900	2.87	0.2618	453.1±0.3	429.0±0.3	Nov. 30, 1930
30	44°	9	13.4875	2.87	0.2617	452.6±0.3	428.6±0.3	Nov. 30, 1930
31	47.5°	7	13.4790	2.85	0.2616	452.0±0.3	428.1±0.3	Aug. 2, 1930
32	48°	13	13.4778	2.92	0.2615	451.6±0.3	428.1±0.3	July 27, 1930
33	48°	11	13.4778	2.92	0.2616	451.96±0.3	428.4±0.3	Aug. 1, 1930
34	48°	9	13.4778	2.85	0.2615	451.6±0.3	427.7±0.3	Aug. 5, 1930
35	49.5°	10	13.4741	2.85	0.2614	451.2±0.3	427.2±0.3	Aug. 6, 1930
36	54°	10	13.4632	2.85	0.2613	450.4±0.3	426.5±0.3	Aug. 2, 1930
37	57.5°	11	13.4547	2.85	0.2612	449.8±0.4	425.9±0.4	Aug. 6, 1930
38	64°	9	13.4389	2.85	0.2609	448.2±0.5	424.5±0.5	Aug. 2, 1930
39	67°	10	13.4317	2.84	0.2608	447.7±0.6	423.9±0.6	Aug. 2, 1930

readings two values for the surface tension are given. That under uncorrected value (seventh column) was found by means of Quincke's simple formula[24]

$$\sigma = \tfrac{1}{2}h^2\rho \cdot 980 \tag{1}$$

(where σ and ρ are surface tension and density respectively; 980 cm per sec^2 is the value of the acceleration of gravity in Saint Louis.) The corrected values of σ (eighth column) were determined according to Worthington's equaton[25]

$$\sigma = \frac{(K-k)^2\rho}{2} + 2\sigma(K-k)\left\{\frac{1}{b} - \frac{1}{3.282L}\right\} \tag{2}$$

[24] G. Quincke, Ann. d. Physik, **105**, 1–48 (1858); **139**, 1–89 (1870); **160**, 337–374 (1877).
[25] A. M. Worthington, Phil. Mag. **20**, 51–66 (1885).

(where $(K-k)=h=$distance from vertex to maximum horizontal diameter; $b=$radius of curvature at the vertex and $L=$maximum horizontal radius).

According to Worthington[25] for values of L greater than 2 cm the term $1/b$ is negligible. Therefore since in this experiment the minimum value of L was 2.84 cm it was at all times sufficiently large to justify the omission of $1/b$ from the equation, which consequently reduces to the form

$$\sigma = \frac{(K-k)^2\rho}{2} \cdot \frac{1.641L}{1.641L + (K-k)} \times 980. \qquad (3)$$

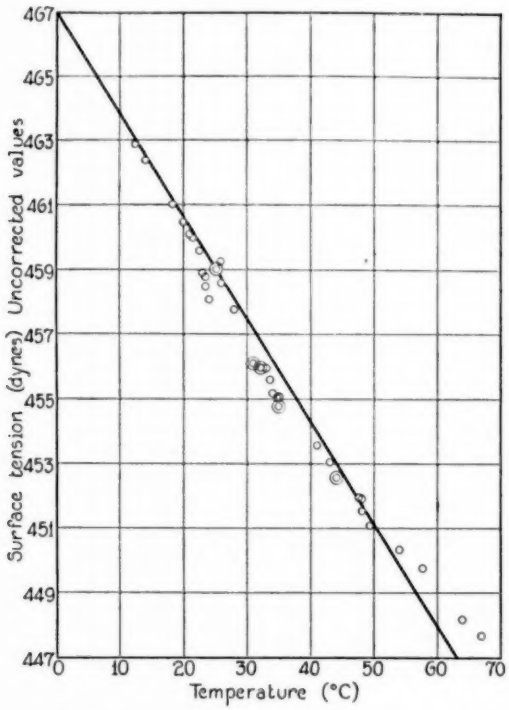

Fig. 2. Surface tension of mercury as function of temperature.

Hence to correct values computed from equation (1) we have only to multiply the result obtained by the correction factor

$$\left(1 + \frac{K-k}{1.641L}\right)^{-1}$$

Since there was scarcely any appreciable variation in the size of the drops used, the correction factor reduced to either 1/1.055 or 1/1.056.

From the two surface-tension, temperature graphs (Figs. 2 and 3) it is evident that temperature variations gradually decrease as temperature increases. However, for values of T lower than 65°C the deviation of experimental points from a straight line is slight. Hence from the best mean straight line through the experimental points (Fig. 3) σ at 0° and at 63° was

judged to be 442 and 423 dynes per cm, respectively. Hence the temperature gradient is 0.3015 dyne per cm per degree.

Upon differentiating with respect to temperature, the Eötvös relation $\sigma v^{2/3} = k(T_c - T)$ we get,

$$v^{2/3}\left(\frac{d\sigma}{dT}\right)_v + \frac{2}{3}\sigma v^{-1/3}\left(\frac{dv}{dT}\right)_\sigma = -k \tag{4}$$

(σ, v, T represent surface tension, volume of a gram atom, temperature respectively. T_c and k are constants.)

The Eötvös constant, k, was found at 20°C by substituting in Eq. (4) for $(d\sigma/dT)_v$ and for σ experimental values, and for v and $(dv/dT)_\sigma$ values

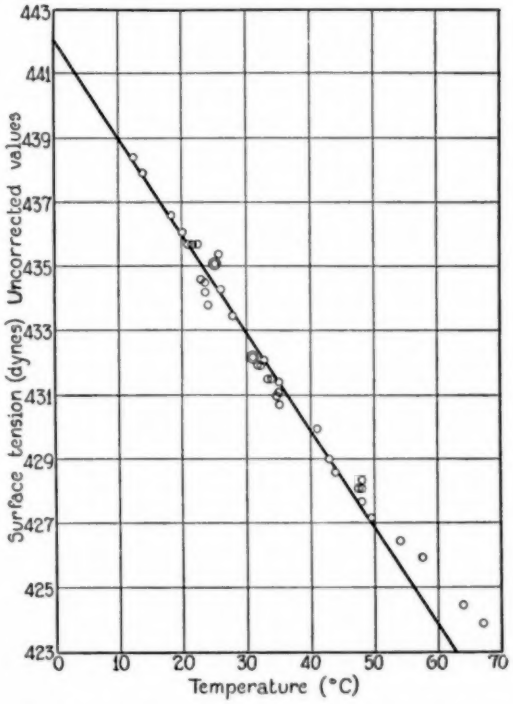

Fig. 3. Surface tension of mercury as function of temperature.

calculated from data given in the Smithsonian Physical Tables, as quoted in the thirteenth edition of Handbook of Chemistry and Physics.[23] The value found is 1.82.

Discussion

Every possible precaution was taken to procure absolute cleanliness. Boiling hot chromic acid solution was used to cleanse not only the entire glass apparatus (including the still used for distilling the mercury in a current of air), but also the beakers and the bottles into which the mercury was poured at any stage of experimentation. Several consecutive days were devoted to a thorough outgassing of the apparatus. During periods of four or

five hours each, while the pump was running, the entire apparatus was kept at a high temperature by means of the heater and a hand burner. The thoroughness of the process was proven by the fact that the McLeod gauge registered stiction (a gas pressure less than 1.2×10^{-5} mm Hg) except when filtered air was purposely admitted into the apparatus. Occasionally over night the pressure rose to 4.6×10^{-5} mm Hg, but then the apparatus was again outgassed. No readings were recorded except when the McLeod gauge registered stiction.

The main purpose of this experiment was to get consistent values for the surface tension of mercury in a vacuum hence no perfection of detail that might lead to a higher order of accuracy was overlooked. To eliminate vibration of the mercury drop a special wall table was constructed. The difficulty experienced by Cook[5] in determining the exact position of K (the top of the drop) was obviated by keeping the drop enclosed in the heater, even when working at room temperature, and by illuminating it from without. As previously mentioned, for all readings recorded the top showed as a sharp dark line. The small lamp used for determining the point of vertical tangency was set at the same level as the center of the objective of the travelling microscope, by means of a reading telescope. The utmost care was used to keep it in that exact position for it was noticed that the least deviation from it caused a considerable difference in the readings of K and k. The same is true of the level position of the travelling microscope and the dividing engine.

A tenths thermometer, calibrated by comparison with a standard thermometer was throughout immersed in the heater to the same depth and at the same angle of inclination. Stem correction was, however, found to be negligible for temperatures lower than 70°C, i.e., for temperatures used in this experiment.

No set of readings was recorded until all details were brought to relative perfection. On the other hand no set of readings was discarded after that point had been reached, except in cases of fluctuating temperature.

On two different occasions a set of readings was taken in a vacuum (15 and 16; 19 and 20, Table I) the dish was partially emptied by violent shaking, filtered air was admitted and the apparatus was allowed to stand for a while. When again pumped to stiction the change in surface tension was merely that to be expected from variation in temperature.

Popesco[17,18,19] Iredale[12] and Cook[5] have determined the surface tension of mercury in a vacuum by the flat-drop method. However, the experiments of the first two differed from this experiment in some important details—to mention only a few: the method of forming the drops was essentially different; both used wax seals. Iredale was himself conscious that "the experimental conditions would be very much improved if such adhesives could be done away with." (reference 12, page 607) Both worked on drops too small (Popesco's was about 3.6 cm in diameter; and Iredale's ranged from 1.2 cm to 1.5 cm in diameter) to be considered perfectly flat. The values obtained by Iredale from eleven consecutive drops, at a temperature of 19.5°C, vary from 430 to 472 dynes per cm. Cook's flat-drop method is essentially the same as

the one used in this experiment. But he has quoted only one value found for the surface tension of mercury in a vacuum; and that value seems abnormally high even though in the author's words "the measurements were very carefully checked." (reference 5, page 517). The apparatus of this experiment was as completely outgassed as his, but not once was a value any where near as high as his obtained. His readings of K and k were taken with a cathetometer the vernier of which "reads directly to 0.02 mm and under the microscope can be estimated to 0.01 mm" (reference 5, page 516). The travelling microscope used in this experiment records to 0.002 mm.

The dates given in the last column of Table I show how well conditions were reproduced. In turn the consistent values obtained seem to point to the fact that, more than a new theory, we need a high vacuum, uncontaminted surface and utmost care in manipulation.

This work was suggested by and carried on under the guidance of Doctor F. E. Poindexter in the laboratories of Maryville, Corporate College of Saint Louis University. I wish to thank him for his generous cooperation. I wish to thank both him and Rev. Professor James I. Shannon for their many helpful and encouraging suggestions. Thanks are also due to Brother A. Zeller for his kindness in rearranging the heater to fit the remodelled apparatus.

CORRECTED VALUES FOR THE COEFFICIENT OF RECOMBINATION OF GASEOUS IONS

By Overton Luhr and Norris E. Bradbury
Physical Laboratory, University of California

(Received March 9, 1931)

Abstract

Previously published values of the coefficient of recombination are found to be twelve percent too high because of the distortion of the field between the plates of the ionization chamber. Corrected values which may be used for the purpose of calculation are given as follows: Air, $(1.23 \pm 0.1) \times 10^{-6}$; O_2, $(1.32 \pm 0.1) \times 10^{-6}$; N_2 and A, $(1.06 \pm 0.1) \times 10^{-6}$; H_2, $(0.28 \pm 0.05) \times 10^{-6}$.

RECENTLY one of the writers[1,2] has published results of research on the recombination of ions produced by x-rays in a number of gases. It was found that the coefficient of recombination given by $\alpha = (1/t)(1/n - 1/n_0)$, the integrated form of the equation $dn/dt = -\alpha n^2$ is not a constant, but varies with the age of the ions. It was assumed that the high initial values of α and rapid drop at short time intervals (up to 0.05 to 0.1 seconds after the formation of the ions) is due to non-random distribution, and that the later more gradual drop is due to the loading up of the ion with impurities and subsequent selective recombination, producing abnormally low values of α at long time intervals up to one or two seconds. On the assumption that normal conditions were most closely approximated between the ages of 0.05 and 0.1 seconds, so-called "absolute values" were set which would be useful for purposes of calculation. Hydrogen is the only gas which did not exhibit any change in the value of α with time.

In all the results heretofore published it was assumed that the volume of ionization swept out by the electric field was the total geometrical volume contained between the plates of the ionization chamber. In planning for further work with the same apparatus, it has been found that, despite the guard ring surrounding the upper plate, there is an error of about twelve percent in this assumption. Owing to the proximity of the grounded walls of the chanber, the field is not uniform between the plates, the lines of force curving slightly towards the walls. (See Fig. 1.) The magnitude of the error was obtained by plotting the equipotential lines for a cross-section model of the chamber, making use of a telephone buzzer and probe points in a conducting solution. On drawing the lines of force, which are perpendicular to the equipotential lines, it was found that the volume swept out by the field was about twelve percent smaller than the assumed geometrical volume. In this connection it is interesting to note that under conditions where grounded

[1] O. Luhr, Phys. Rev. **35,** 1394 (1930).
[2] O. Luhr, Phys. Rev. **36,** 24 (1930).

walls are within a few centimeters of the plates of the ionization chamber, the guard ring would have to be approximately equal in width to the distance between the plates to obtain a uniform field.

In calculating the coefficient of recombination, n, the number of ions of either sign per cm^3 is found by dividing the total number of ions swept to the upper plate by the volume. Hence the equation is of the form $\alpha=(V/t)(1/N-1/N_0)$. As the volume was actually twelve percent smaller than that assumed in the previous results, all values of α should be reduced by a cor-

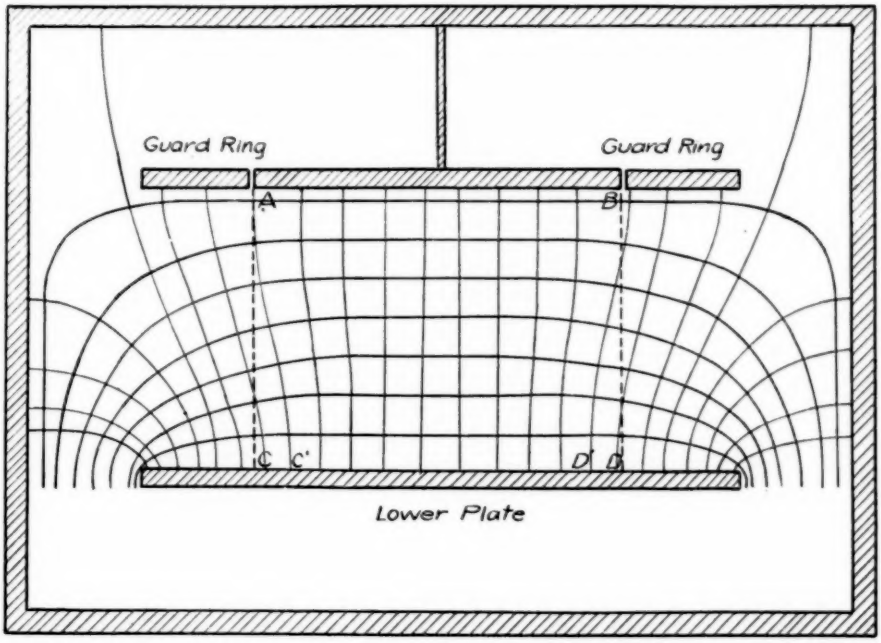

Fig. 1. Cross section of the ionization chamber drawn to scale showing equipotential lines and lines of force when a potential is applied to the lower plate. $ABCD$ is the geometrical volume, while $ABC'D'$ shows the actual volume of ionization swept to the upper plate by the field.

responding amount. This error is not as serious as it might seem offhand since the curves will retain their same form, which after all is the most important result of the experiments as apparently there is no absolute value for the coefficient. The so-called "absolute values" which may be useful for purpose of calculation are now set as given in Table I.

TABLE I. *Corrected values of the coefficient of recombination.*

Gas	Coefficient of Recombination
O_2	$(1.32\pm0.1)\times10^{-6}$
N_2	$(1.06\pm0.1)\times10^{-6}$
A	$(1.06\pm0.1)\times10^{-6}$
H_2	$(0.28\pm0.05)\times10^{-6}$
Air	$(1.23\pm0.1)\times10^{-6}$

It must be understood that the possible error of plus or minus one-tenth indicated in these results is not an experimental error, but represents a portion of the curves between ages of 0.05 and 0.1 seconds. The experimental error is probably not more than two or three percent for all of the gases except hydrogen. The writers take pleasure in expressing their gratitude to Professor R. B. Brode whose critical suggestion led to the present revision of the values of α, and once more to Professor Leonard B. Loeb under whose able direction the whole research has been accomplished.

LETTERS TO THE EDITOR

Prompt publication of brief reports of important discoveries in physics may be secured by addressing them to this department. Closing dates for this department are, for the first issue of the month, the twenty-eighth of the preceding month; for the second issue, the thirteenth of the month. The Board of Editors does not hold itself responsible for the opinions expressed by the correspondents.

An Attempt to Measure the Energy of the Cosmic Electrons by Magnetic Deflection

An attempt has been made to measure the energy of the cosmic electrons with an apparatus based on Bothe and Kolhörster's[1] coincidence principle making use of Geiger-Müller tube-counters. A description of the method has previously been given.[2]

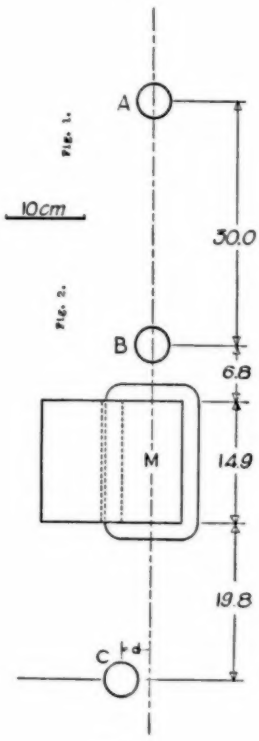

Fig. 1.

The arrangement is schematically shown in Fig. 1. A and B represent two tube-counters, viewed end-on, which serve to define a beam of the particles, M is a closed-core "magnet" which furnishes the deflecting magnetic field (produced directly in the iron), and C is a third counter which serves to analyse the beam which has passed through the magnet. An electrical vacuum tube system records on an impulse counter only triply coincident discharges of the three counters, events which are assumed to indicate the passage of an electron through the apparatus.

The principal experiment consisted in making counts of the triple coincidences for various displacements (d) of the analysing counter with the magnet unmagnetized and with it successively magnetized to a magnetic induction of 17,000 in either direction. The results are shown in the curve of Fig. 2. The values are believed to be reliable to about 8 percent (the statistical error is about 4 percent) with the exception of the points at the central position and those at 4 cm north which were studied more carefully and should not be in error by more than about 4 percent. The shape of the curve is about what is expected from the geometry of the arrangement, assuming rectilinear passage of the ionizing particle, and the count at the 10 cm displacement represents that due to chance coincidences. It is seen that within the present limits of error no deflection exists. This result is of interest because if the assumptions on which the operation of this apparatus is based are correct the energy of the particles is very high. On making what appears to be the correct assumption that the force on an electron in the iron is given by $(e/c)[v\times B]$

[1] W. Bothe and W. Kolhörster, Zeits. f. Physik **56**, 751 (1929).

[2] Phys. Rev. **35**, 1125 (1930). Experiments with the present method have been independently made by Rossi, Rend. Acc. dei Lincei **2**, 478 (1930).

where B is the magnetic induction, a deflection of 2.2 cm measured at the analyser is expected for electrons of energy 10^9 e-volts. It is seen from the curve that an easily observable change in count should be produced by such a deflection, particularly at the most favorable displacement of about 4 cm. Accordingly, with the reservation mentioned above, it appears that the energy of the majority of the cosmic electrons is greater than about 2×10^9 e-volts. The possibility that these particles may be protons or heavier nuclei should also be considered. This seems unlikely on various grounds, but even if the particles were protons we can conclude that the energy must be greater than about 10^9 e-volts.

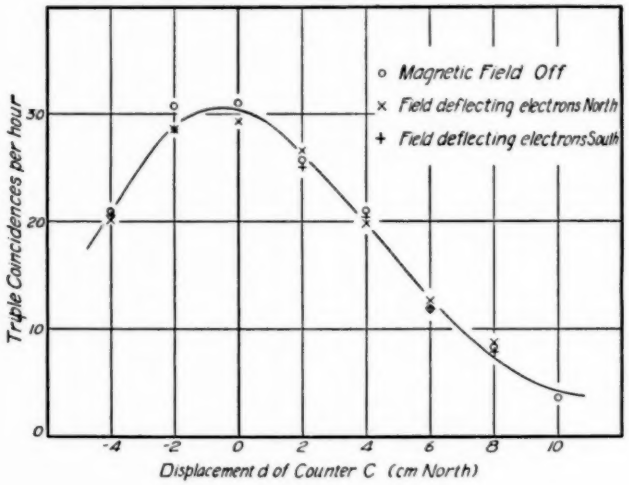

Fig. 2.

There is, however, a difficulty with the assumption of electrons of such high energies, which comes from a consideration of the process by which they are absorbed. From the usual theory of multiple scattering it is found that the path of such a particle should be nearly rectilinear until it has lost a large fraction of its energy, so that absorption must be principally due to a gradual loss of energy by the production of ions along the path. Accordingly, since the cosmic radiation (assumed electronic) is known to follow an exponential absorption law, we should expect to find at any point electrons with a definite distribution of velocities ranging from zero to some maximum. In fact, if the Thomson absorption law is still valid for these high energies, it is found, by using the known absorption coefficient for the cosmic radiation, that a considerable fraction of the electrons should have energies ranging from zero to a few hundred million e-volts (about 30 percent between zero and 2×10^8 e-volts). Were this the case, an effect of the magnetic field should have been observed. Consequently, if we wish to interpret this experiment to mean that the energy of the bulk of the electrons is as great as indicated above it is necessary to find a method of absorption for very penetrating electrons which gives considerably greater absorption than that expected on the ordinary theory. A possibility in this direction which should be investigated is a consideration of nuclear effects which are negligible when treating the absorption of electrons of low energy but which might be expected to become important when dealing with electrons of such large penetrating power.

It should be mentioned that absorption measurements have been made with this apparatus by taking counts with the magnet in position and with it withdrawn from the beam. In agreement with the result of Bothe and Kolhörster, the observed absorption is nearly the same as the value calculated for these conditions from the absorption coefficients obtained by the electroscope measurements.

It is also necessary to be sure that the coincidences are actually produced by a corpuscular radiation and not by a γ-type radiation. This question has been investigated by Bothe

and Kolhörster[1] both experimentally and theoretically, with the result that they do not find it possible to ascribe the coincidence effects to a γ-type radiation unless some new phenomenon is postulated. In view of our present result it would seem desirable to reexamine this question. On the experimental side a possibility in this direction would be to look for a definite correlation between coincidences in tube-counter and tracks in a suitably disposed cloud expansion apparatus. Such an experiment appears feasible and is in progress.

In view of the foregoing considerations and also on account of certain difficulties[3] with the assumption of a corpuscular nature for the cosmic radiation, it would seem that a definite conclusion with regard to the significance of the present experiment must await further study.

A part of this work was done at the California Institute through the kindness of the members of the administration of that institution.

L. M. MOTT-SMITH
Department of Physics,
The Rice Institute,
Houston, Texas,
March 25, 1931.

[3] See R. A. Millikan and **G. H.** Cameron, Phys. Rev. **37,** 235 (1931)

Transmission of Gases from 20 to 33μ

In a letter to this section Dickinson and West[1] reported a Raman shift for liquid sulfur dioxide of 524.3 cm^{-1}. Bailey, Cassie and Angus[2] interpret this as a combination band. I have found the transmission of a four inch layer of this gas for the 20.75μ quartz reststrahlen to be only 7 percent. Such strong absorption would seem more likely to be associated with a fundamental band.

The transmissions of several gases have been determined in the spectral region 20–33μ and the results are given in Table I. These values are for a layer of gas four inches thick at atmospheric pressure and are probably correct to 2 percent.

TABLE I.

Gas	Reststrahlen Wave-length:	20.75μ	22.9μ	27.3μ	29.4μ	32.8μ
SO_2		7	58	100	99	96
NH_3		65	95	84	79	63
H_2S		96	98	93	89	82
N_2O		86	100	100	100	100
C_2H_2		95	100	100	98	97

JOHN STRONG
National Research Fellow,
California Institute of Technology,
Pasadena, California,
March 25, 1931.

[1] Roscoe G. Dickinson and S. Stewart West, Phys. Rev. **35,** 1126 (1930).

[2] C. R. Bailey, A. B. D. Cassie and W. R. Angus, Roy. Soc. Proc. **A130,** 133 (1930).

A Preliminary Report of the Application of the Photoelectric Cell to the Reading of Minima in a Magneto-Optic Method of Analysis

It has been found that chemical compounds in solution, when traversed by polarized light and subjected to particular types of transient magnetic fields, are characterized under certain conditions by the scale readings of the minima of light intensity produced, by means of which a compound may be detected when present in a concentration as low as about 1 part in 10^{11} (Allison and Murphy, Journal the American Chemical Society **52,** 3796 (1930); Physical Review **36,** 1097 (1930)). These results have been interpreted upon the hypothesis of differential time lags in the Faraday effect. Inasmuch as the results thus far reported were obtained by visual observations only, the importance of devising some objective means of reading the minima has long been recognized. We have recently suc-

ceeded in building a photoelectric cell circuit which indicates the presence of the minima by the deflection of a galvanometer. The method of current amplification is similar to that described by DuBridge (Physical Review **37,** 392 (1931)), two FP-54 Pliotron tubes being employed together with other tubes for additional amplification. We have as yet had opportunity to take observations with the photoelectric cell upon only a few of the compounds which have been studied visually, but those selected are representative and their metallic elements contain isotopes. We used concentrations ranging from about 1 part in 10^{14} to 1 part in 10^{2}. Our results, which confirm those based on visual observations, may be summarized as follows.

(a) The photoelectric cell reads minima at the exact points of the scale at which they have been observed visually.

(b) The photoelectric cell is able to detect a compound when present in an amount as small as about 1 part in 10.[12]

(c) The photoelectric cell, in addition to detecting minima corresponding to the number of isotopes of the metallic element of the compound, indicates by the galvanometer deflections the relative abundance of the isotopes. This indication, however, is a rough one and does not as yet yield quantitative estimates of precision.

(d) The photoelectric cell registers but very slight differences in the blackness of the minima with changes in concentrations over wide limits, a result in agreement with visual observations.

Alabama Polytechnic Institute,
Department of Physics,
March 21, 1931.

FRED ALLISON
J. H. CHRISTENSEN
GEORGE V. WALDO

A New Source of Active Nitrogen

It has been possible for the first time to produce the afterglow of active nitrogen in an uncondensed discharge. The discharge was produced by a 25000 volt 1 KW Thordarssen transformer at pressures ranging from 0.1 mm to about 5 mm. Although a tremendous number of discharges of the same type in the same gas have been observed by the writer during the past four years, this is the first time that the afterglow associated with active nitrogen has been obtained. The afterglow was as strong as those obtained with the usual sources of active nitrogen, namely, condensed discharges and electrodeless ring discharges. The spectrum of the glow was observed with a direct vision spectroscope and also photographed and it consists of the usual sharp selection of the first positive bands of nitrogen as obtained in the ordinary afterglow. If there are any differences between this and other glows then more photographs may bring them out. The glow was obtained in two different tubes, each time however only after about two weeks running of the tubes at almost a no-discharge vacuum, i.e., at about 0.001 mm pressure. While other factors may have an effect, the long running of the tube certainly indicates that the condition of the walls is an important factor in the production of the glow.

A few very interesting points about the glow will be mentioned, which will help to emphasize the unusual nature of the phenomenon. For example, the exciting discharge itself possesses a spectrum which could readily be taken for an afterglow spectrum. The β bands of nitric oxide and the violet cyanogen bands, both of which are usually observed in nitrogen afterglows and but seldom in electric discharges, were both present in the exciting discharge. These, and the first positive bands of nitrogen comprised most of the radiation of the exciting discharge in the visible and the first positive bands also showed a structure similar to the one observed in active nitrogen. The second positive bands of nitrogen, which are strong in almost any type of nitrogen discharge and which are unusually strong in the condensed discharge, were almost completely missing from the exciting discharge in the present experiments. Just one remark will be made regarding the significance of the nature of the exciting discharge in these experiments. The writer has at various times assigned the weak radiations of the aurora spectrum to the first positive bands of nitrogen and has explained them as arising in processes similar to those that take place in active nitrogen. This assignment always raised the embarrassing question in the writer's mind as to the nature of an electric discharge in which the spectrum is so much like that of an

afterglow or a chemiluminescence phenomenon. This question has now been answered and one can say that as far as the first positive bands of nitrogen are concerned there is added spectroscopic evidence that the auroral displays are electric discharges at low pressures. That the discharge conditions in the upper atmosphere are unusual can be seen by the consideration that the upper atmosphere is really a discharge tube without walls. In view of some recent attempts to explain the aurora the present experiments should merit some attention. In another communication more will be said about some experiments in which other spectroscopic features of the aurora are pointed out and studied.

JOSEPH KAPLAN

Department of Physics,
University of California at
Los Angeles, California,
March 24, 1931.

The Zeeman Effect and Uncoupling Phenomena in Helium Bands

Weizel[1] has calculated the energies due to the uncoupling of the electronic angular momentum from the electric axis in light molecules. He predicts that such uncoupling should, if present, be greater for large values of the total quantum number, n, for large values of the difference between the orbital angular momentum quantum number of the series electron, l, and its projection on the electric axis, λ, and for large values of the rotational quantum number, K. For the helium molecule, rigid coupling of l to the molecular axis, so that λ is a true quantum number, should correspond to Hund's case b'. For large rotational energies the coupling should be destroyed and the molecule correspond to Hund's case d'. Since this uncoupling is not expected to be abrupt, many levels should correspond to cases intermediate between b' and d'. The energy of a case b' molecule in a magnetic field of strength H is well known to be

$$\Delta E=\frac{\mu_1 H M\Lambda^2}{K(K+1)}$$

where M is the magnetic quantum number and $\Lambda=\lambda$ for the present case. The corresponding relation for case d' can be calculated in the same manner as for the above case. The relation is

$$\Delta E=\frac{\mu_1 H M[K(K+1)+L(L+1)-R(R+1)]}{2K(K+1)}$$

where R is the rotational quantum number, and K the quantized resultant of l and R. It is evident that the Zeeman effect should afford a means to determine the degree of conformity to the limiting cases and indicate the presence or absence of uncoupling phenomena. Information may be drawn from partially resolved patterns by applying the intensity relations for the components of a spectral line given by Honl[2] and Kronig.[3] Harvey[4] has pointed out that unusual widths of the helium band lines in a magnetic field can be interpreted as indicative of uncoupling phenomena in certain states of this molecule. To check the above predictions quantitatively, an extensive investigation of the Zeeman effect in the ortho-helium bands has been carried out.

The spectrum has been photographed in the second and third orders of a 21-foot grating affording a dispersion of 1.31A per mm in the second order with field strengths up to 30,500 gauss. Measurable Zeeman pattern have been obtained for at least six lines of the bands $2p\pi^3\Pi^{(0)}-4s\sigma^3\Sigma^{(0)}$, $2s\sigma^3\Sigma^{(0)}-3p\pi^3\Pi^{(0)}$, $2s\sigma^3\Sigma^{(0)}-4p\pi^3\Pi^{(0)}$, $2p\pi^3\Pi^{(0)}-4d\delta^3\Delta^{(0)}$, $2p\pi^3\Pi^{(0)}-3d\delta^3\Delta^{(0)}$, $2p\pi^3\Pi^{(0)}-4d\pi^3\Pi^{(0)}$, $2p\pi^3\Pi^{(0)}-3d\pi^3\Pi^{(0)}$, $2p\pi^3\Pi^{(0)}-4d\sigma^3\Sigma^{(0)}$, and $2p\pi^3\Pi^{(0)}-3d\sigma^3\Sigma^{(0)}$. In agreement with previous investigators, the first three above mentioned bands correspond rigorously to case b' predictions. Departure from case b' appears in the band $2p\pi^3\Pi^{(0)}-4d\delta^3\Delta^{(0)}$ at values of K greater than 9. Evidence of uncoupling in the band $2p\pi^3\Pi^{(0)}-4d\pi^3\Pi^{(0)}$ is shown by departure from case b' patterns for all values of K greater than 2 and a gradual approach to case d' predictions as K increases to 14. Similar evidence of uncoupling is found in the band $2p\pi^3\Pi^{(0)}-4d\sigma^3\Sigma^{(0)}$ for values of K greater than one. The approach to case d' patterns is more rapid in this band than in the others mentioned above. In the last two mentioned bands the rate of uncoupling is somewhat more rapid than for

[1] W. Weizel, Zeits f. Physik **54,** 321 (1929).
[2] H. Honl, Zeits. f. Physik **31,** 340 (1926).
[3] R. de L. Kronig, Zeits. f. Physik **31,** 885 (1926).
[4] A. Harvey, Proc. Roy Soc. **A126,** 583 (1930).

the bands of the same electronic transition but of total quantum number 3.

It may, therefore, be stated that Zeeman patterns of the ortho-helium bands confirm the idea that the peculiarities of some of these bands, in particular those with large values of n and with l greater than λ for the series electron, can be explained by a gradual uncoupling of l from the molecular axis with increasing rotation. The Zeeman patterns offer a new means of following the progress of the uncoupling.

A complete report of data and results will be presented at a later date.

JOHN S. MILLIS

Lawrence College,
Appleton, Wisconsin,
March 18, 1931.

The Alleged Production of Adsorbed Films on Tungsten by Active Nitrogen

Pure molecular nitrogen has no effect on the thermionic emission from tungsten. The decrease in emission that occurs if a discharge is passed through the nitrogen with voltages above about 20 has been attributed to the formation of a film of adsorbed nitrogen.[1] Kenty and Turner found that the accommodation coefficient for heat conduction from the tungsten surface by nitrogen was increased about 20 percent by this treatment.

More recent experiments in this laboratory have shown that the film produced on the tungsten by active nitrogen is an *oxygen* film. The active nitrogen, coming into contact with the walls of the tube and the surfaces of electrodes, decomposes adsorbed water vapor or metallic oxides which are almost always present and thus drives oxygen (probably atomic) into the gas phase, whence it reacts with the filament. With great care to avoid oxygen and with the bulb cooled in liquid air, active nitrogen does not produce any adsorbed film which alters the electron emission or the accommodation coefficient, but instead it is able to remove any oxygen film already present.

A similar evolution of oxygen from well baked out glass surfaces occurs when neon metastable atoms strike the walls of a discharge tube.

The detailed description of these experiments will soon be submitted to the Journal of the American Chemical Society for publication.

IRVING LANGMUIR

Research Laboratory,
General Electric Company,
Schenectady, New York,
March 24, 1931.

[1] I. Langmuir, Phys. Rev. **2,** 460–72 (1913); Phys. Zeit. **15,** 523 (1914); J. Amer. Chem. Soc. **38,** 2279 (1916); C. Kenty and L. A. Turner, Phys. Rev. **32,** 799–811 (1928).

Partial Absorption of X-Rays

Ray,[1] Majumdar,[2] and Bhargava and Mukerjie[3] have found evidence that a quantum of x-rays may, in passing through matter, give *only a part* of its energy to a bound electron and continue in its original direction with diminished frequency. These authors do not give detailed information regarding their experiments, but Ray reproduces spectrograms which clearly show the lines which he ascribes to *partially absorbed* x-rays. Ray estimates the intensity of these lines to be between 1/400 and 1/500 of that of the parent line.

[1] B. B. Ray, Nature **125,** 746 and 856 (1930); **126,** 399 (1930); Zeits. f. Phys. **66,** 261 (1930).

[2] R. C. Majumdar, Nature **127,** 92 (1931).

[3] S. Bhargava and J. B. Mukerjie, Nature **127,** 273 and 305 (1931).

Cork[4] and Lindsay[5] have tried to produce these modified lines, but with negative results. Cork claims to have been able to detect lines, if present, of 1/1000 to 1/3000 of the intensity of the parent line. Lindsay reproduces photometric curves of the K-spectrum of copper taken through a carbon absorbing screen which show definitely the presence of the $K\alpha_{3,4}$ satellite of copper, known to have about 1/400 the intensity of the α_1 line, but no trace of a modified line.

We have tried to find lines corresponding to the partial absorption of the $K\alpha$ doublet of molybdenum by aluminum, but without success. We used the spectrometer and calcite

[4] J. M. Cork, Comptes Rendus **192,** 153 (1931).

[5] G. A. Lindsay, Nature **127,** 305 (1931).

crystal recently described by us.[6] The source of x-rays was a water-cooled Coolidge tube with molybdenum target, operated at about 60 KV peak potential and 12–13 ma current. The first slit was about 16.8 cm from the crystal and 0.04 mm wide. The second slit was 4.5 cm from the crystal and wide enough to permit the full beam from the first slit to fall on the crystal. The photographic plate was placed normal to the direct beam at such a distance from the crystal that the $K\alpha_1$ line of molybdenum was in focus. The absorbing screen consisted of powdered "alumina" (obtained from the General Electric Co. of Schenectady) pressed between two sheets of "celophane" about 0.02 mm thick and was placed close to the second slit, between it and the tube. In some cases the screen was about 1 mm thick and in others about half that thickness. During exposures the crystal was rotated back and forth through an angle of about 52.5′ around a position at which it should reflect the modified lines due to absorption in aluminum. The rotation was produced by means of a cam designed to give the crystal approximately constant angular velocity between turning points. The mean position about which the crystal rotated was slightly different for different plates. The exposures for the modified lines lasted for about 15 hr., and then short exposures were taken to record the central image and the $K\alpha$ and $K\beta$ lines of molybdenum on both sides of the latter.

All the plates showed a band of continuous spectrum corresponding in position and width to the range of rotation of the crystal. The band on each plate had a structure which was probably due to irregularities in the cam since the structure remained fixed with respect to the band when the position of the latter on the plate was changed. No lines were found as definite as those appearing on Ray's photographs.

Since the bands of continuous spectrum were quite dark, the modified lines may have been obscured. We are planning to eliminate the continuous spectrum as much as possible by introducing a crystal between the first slit and the x-ray tube.

D. Cooksey
C. D. Cooksey

Sloane Physics Laboratory,
Yale University,
March 18, 1931.

[6] C. D. and D. Cooksey, Phys. Rev. **36**, 85 (1930).

The Absorption Spectrum of Bromine

In the absorption spectrum of bromine vapor at room temperature with columns of vapor long enough (two to four meters) to bring out the progressions of the visible band system arising from the fifth and sixth vibrational states of the normal level a number of new bands appear in the region 6400A to 7500A. These can be classified into five rapidly converging progressions of which three can be followed nearly to the point of convergence. Assigning $v''=1$ to the lowest observed progression the G'' differences agree well with those for the "main" system, and the point of convergence agrees with the assumption that these bands constitute a new system the upper level of which leads to dissociation into two atoms in the $^2P_{1\,1/2}$ state. This level may thus be a member of the case $c^3\Pi$ multiplet predicted by Mulliken.[1] The dispersion employed (first order of a 3 m. concave grating giving 5.4A/mm) was not sufficient to determine the character of the bands, which should consist of Q branches only, if the new level is Mulliken's 0_u^- level.

The vibrational isotope effect has not been definitely located so that the v' numbering, on which calculations of the constants given in the accompanying table are based, is arbitrary. This table shows also the constants resulting from a re-examination of the main system in which the isotope effect has been observed for a number of bands in the $v''=0$, 1, and 2 progressions. These measurements indicate that Kuhn's[2] v' numbering should be increased by four. This is in addition to a further correction of $+5$ to be made for v' greater than Kuhn's 11, which resulted from an incorrect assignment of bands.[3] The $\Delta G:v$ curves for the upper level of the main system and of the extreme red system show points of

[1] R. S. Mulliken, Phys. Rev. **36**, 699, 1440 (1930).

[2] H. Kuhn, Zeits. f. Physik **39**, 77 (1926).

[3] R. T. Birge, I.C.T. **V**, 411 (1929).

inflection[4] at about 65 percent of the dissociation energy, and only observations at points lower than these have been used in making least squares calculations of the constants given in Table I. The ground level of the molecule is denoted by A, the upper level of the main system by B, and of the extreme red system by C.

TABLE I. *Molecular constants of bromine.*

Electronic Level	ν_e cm^{-1}	ω_e	$\omega_e x_e$	D (volts)	Dissociation products
A	0	323.86	1.150		
B	15,910.5	165.39	1.579	0.464	$^2P_{1\frac{1}{2}}+{}^2P_{\frac{3}{2}}$
C	14,841.4	115.69	3.395	0.144	$^2P_{1\frac{1}{2}}+{}^2P_{1\frac{1}{2}}$

From the measurements of Bodenstein[5] on the dissociation equilibrium an estimate of the moment of inertia of bromine has been made by means of the Gibson-Heitler equation, the mean value of I'' from observations at the ten highest temperatures being 445×10^{-40} C.G.S. and the average deviation from the mean 5.6×10^{-40}. With this value of I the equation gives ΔF° 298.1 = 38,600 cal. for the reaction $Br_2(g)=2Br_g$. The heat of dissociation deduced from the equilibrium measurements is in excellent agreement with the spectroscopically determined value, 1.962 volts.

Bands which may correspond to the extreme red system of bromine have been found in the infrared absorption spectrum of iodine (vapor pressure 1 atmosphere, in a 1 m tube at 185°C) between 8000A and 9000A. These have not yet been analysed. An account of them will be given at a later time as well as detailed results for bromine. Further experiments with a view to determining the character of the new bromine bands and the isotope effect are being undertaken.

WELDON G. BROWN

Department of Chemistry,
University of California,
Berkeley, California.

[4] R. T. Birge, Trans. Faraday Soc. **XXV**, 707 (1929).

[5] M. Bodenstein, Zeit. f. Elektrochemie **22**, 327 (1916).

BOOK REVIEWS

Applications of Interferometry. W. EWART WILLIAMS. Pp. viii+104, diagrams 43. E. P. Dutton and Company, New York. Price $.85.

This is as complete a treatment of the subject as could reasonably be presented in a monograph. As the author says in his preface, it is not possible to include in such a book all the applications which can be made of interferometry. Certainly the selection made is representative and interesting.

Perhaps the most prominent feature of the work is the classification of interference phenomena into two groups: first, those in which a division of wave front is accomplished as in Young's interference experiment, second, those in which there is a division of amplitude as in the Michelson interferometer. For a monograph devoted largely to technical applications it contains a considerable amount of theory, with simplifications which enable a technical man, not extensively trained in mathematical theory, to understand what is meant without too much additional reading. Particularly lucid are the description of Michelson's apparatus for the measurements of stellar diameters and the chapter on multiple beams, in which the Fabry-Perot interferometer, the Lummer plate, and similar instruments are described.

A good bibliography is given at the end of each chapter. It is unfortunate that the abbreviations of the journal references are not more consistent. For instance, on page 45, Annales de Chimie et de Physique is abbreviated in three different ways. The book is free from technical errors, and the diagrams are good. It should make a very substantial addition to the reference material for teachers and students of optics, and persons engaged in other divisions of scientific work.

GEORGE S. MONK

Matter and Radiation, with particular reference to the detection and uses of the infrared rays. JOHN BUCKINGHAM. Pp. 144, figs. 15. Oxford University Press, London, 1930. Price $3.00.

This book summarizes in a semi-popular way, the many interesting discoveries concerning matter and radiation that have been made in the last century. In particular, the complete electromagnetic spectrum is discussed in connection with the recent theories of atomic structure. It is pointed out that the powerfully destructive rays one occasionally reads about in the newspapers are the result of imagination, or at least enormous exaggeration. While the text is usually accurate, there are a few blunders and inaccuracies. Occasionally, but not always, these are evidently introduced for simplicity or for effect. Thus the miracle of the shortest light path would lose some of its effectiveness if it were also pointed out that sometimes light chooses the longest path. One also finds the naïve statement that x-rays readily pass through matter because their wave-lengths are smaller than the holes between the atoms. However, while it occasionally falls short of scientific accuracy, the book makes very interesting reading.

JOSEPH VALASEK

A Treatise on Light. R. A. HOUSTOUN. Pp. 494, 6th Edition, Longmans, Green and Company, New York, 1930. Price $4.00.

The sixth edition of this much used text book is not greatly different from the preceding editions. There seem to be no changes in the first two "parts" of the book, viz.: (I) Geometrical Optics and (II) Physical Optics. In part III, Spectroscopy and Photometry, the most important changes are the addition of three paragraphs dealing with the elements of the Bohr theory of spectral series, resonance potentials, and band spectra. It seems unfortunate that the treatment of the Zeeman effect was not changed so as to introduce the idea of the Larmor precession. In part IV, mathematical theory, the principal changes are the introduction of Einstein's proof of Planck's Law of radiation and a restatement of the status of the relativity principle. In the "Notes" on recent advances is a notice of the Raman effect. Houstoun's *Light* has the virtue of giving a little information about a great many subjects. That is also its weakness, along with the lack of any adequate number of references to sources of fuller information.

T. TOWNSEND SMITH

PROCEEDINGS

OF THE

AMERICAN PHYSICAL SOCIETY

MINUTES OF THE NEW YORK MEETING, FEBRUARY 26–28, 1931
JOINT MEETING WITH THE OPTICAL SOCIETY OF AMERICA

The 169th regular meeting of the American Physical Society was held in New York City on Thursday, Friday and Saturday, February 26–28, 1931, as a joint meeting with the Optical Society of America. The presiding officers at the sessions of the Physical Society were Dr. W. F. G. Swann, President of the Society, Dr. Paul D. Foote, Vice-president and Professor R. C. Gibbs. All sessions were held at Columbia University.

The joint session with the Optical Society of America was held on Friday afternoon at 2:30 o'clock in the McMillin Theater of Columbia University. This session was a Symposium on "Physical Problems Related to the Biological Effects of Radiant Energy." The President of the Optical Society, Dr. L. A. Jones presided. The invited papers were as follows: "Some Physiological Effects of Light," by Brian O'Brien, Institute of Optics, University of Rochester; "The Spectra and Anti-Rachitic Potency of Various 'Therapeutic' Lamps," by Harvey B. Lemon, University of Chicago; and "Methods of Measuring Radiant Energy," by Harold W. Webb, Columbia University. The attendance was between four and five hundred.

The Optical Society held its sessions at the Museum of Science and Industry Thursday morning and afternoon, occupied with papers on "Color". Their regular Friday morning and Saturday morning and afternoon sessions were held in the Physics Laboratory of Columbia University.

On Friday evening the Society joined with the Optical Society for dinner at the Hotel Commodore after which they attended the Color Exhibition at the Museum of Science and Industry. This dinner was attended by 175 guests.

Meeting of the Council. At its meeting on Thursday, Feburary 26, 1931, Professor Albert Einstein was unanimously elected to Honorary Membership in the Society.

The Council accepted the cordial invitation of Union College and the General Electric Company to hold the summer meeting in Schenectady in September. It was decided that this meeting should be of an informal nature much like the one held last year in Ithaca. A one-half day session of this meeting is to be devoted to papers on Faraday and Henry commemorating their notable work in the field of electromagnetic induction. The Council furthermore accepted the invitations extended by Harvard University and the Massachusetts Institute of Technology to hold the meeting of the Society in February, 1932 in Cambridge.

The Treasurer reported the receipt on January 29, 1931 of a contribution of $1,425.42 to meet the deficit of the Physical Review as of December 31, 1930 and moved that the thanks of the Council be expressed to the Chemical Foundation for this contribution.

The Council elected four persons to fellowship, one hundred and nineteen persons were transferred from membership to fellowship and twenty-five were elected to membership. *Elected to Fellowship:* G. H. Dieke, Rudolf Ladenburg, Leo J. Peters and Max von Laue.

Transferred from Membership to Fellowship: Fred Allison, Donald H. Andrews, Alice H. Armstrong, Edward J. Baldes, Russell S. Bartlett, J. W. Beams, J. A. Bearden, Ralph D. Bennett, F. Russell Bichowsky, Francis Bitter, Oswald Blackwood, Walker Bleakney, C. Boeckner, Joseph C. Boyce, Charles J. Brasefield, A. Keith Brewer, Ferdinand Brickwedde, James B. Brinsmade, W. G. Brombacher, Detlev W. Bronk, S. Leroy Brown, Andrew B. Bryan, Perry Byerly, Thoedore W. Case, Andrew Christy, George L. Clark, Kenneth S. Cole, J. R. Collins, Richard T. Cox, Donald Cooksey, William H. Crew, Leo H. Dawson, David M. Dennision, Elmer Dershem, Jane M. Dewey, Leo A. DuBridge, Jesse W. M. DuMond, Theodore Dunham Jr., James M. Eglin, Frederick E. Fowle, John G. Frayne, James B. Friauf, William F. Giauque, George Glockler, Frank Gray, Grover R. Greenslade, Ross Gunn, Otto Halpern, William R. Ham, Arthur C. Hardy, L. Grant Hector, Edward L. Hill, Maurice L. Huggins, Elmer Hutchisson, Sydney B. Ingram, Lewis V. Judson, J. C. Karcher, Sebastian Karrer, E. Lee Kinsey, Dewey D. Knowles, Lewis R. Koller, Frank C. Kracek, Victor K. LaMer, R. M. Langer, Karl Lark-Horovitz, Charles C. Lauritsen, Victor F. Lenzen, H. H. Lester, Noel C. Little, Walter A. MacNair, Louis R. Maxwell, Helen A. Messenger, Louallen F. Miller, Allan C. G. Mitchell, Philip M. Morse, L. L. Nettleton, J. Rud Nielsen, Wayne B. Nottingham, Christian Nusbaum, Paul S. Olmstead, A. R. Olpin, Lars Onsager, Dimitry E. Olshevsky, John M. Ort, Frederic Palmer Jr., I. I. Rabi, Hubert H. Race, N. Rashevsky, Howard P. Robertson, Vladimir Rojansky, Duane Roller, Edward O. Salant, William Schriever, Nadiashda Galli-Shohat, Francis G. Slack, William W. Sleator, Sinclair Smith, Ambrose H. Stang, F. W. Stevens, John B. Taylor, James D. Tear, Lewi Tonks, Alva Turner, M. A. Tuve, J. T. Tykociner, D. S. Villars, G. R. Wait, Warren Weaver, Lars A. Welo, T. Russell Wilkins, Robert C. Williamson, Thomas A. Wilson, Enos E.Witmer, Jay W. Woodrow, Winthrop R. Wright, Oliver R. Wulf, Ralph W. G. Wyckoff, Otto J. Zobel and Vladimir Zworykin.

Elected to Membership: B. C. Adkerson, R. H. Bacon, L. J. Buttolph, Jessie Y. Cann, Samuel L. Case, T. C. Chow, H. M. Evjen, Isidor Fankuchen, Louis W. Gardner, Maria Goeppert-Mayer, Harold W. Harkness, Francis E. Haworth, Nathan Howitt, Lorenz D. Huff, George B. Lamb, K. O. Lee, Charles F. Lucks, John C. Melcher, Harry B. Mulkey, Edward J. Murphy, H. V. Neher, Filmer S. C. Northrop, Robert W. Perry, William B. Plum and James G. Potter.

The titles and abstracts of papers presented before the Optical Society

of America will be found the Proceedings of that Society, published in the Journal of the Optical Society.

The regular scientific program of the American Physical Society consisted of 49 papers, numbers 5, 6, 8 and 35 were read by title. The abstracts of these papers are given in the following pages. An **Author Index** will be found at the end.

W. L. SEVERINGHAUS, *Secretary*

ABSTRACTS

1. Water vapor absorption spectrum in the near infrared. E. D. MCALISTER, *Division of Radiation and Organisms, Smithsonian Institution, and* H. J. UNGER, *University of Oregon.*—The 1.13, 1.38 and 1.45μ water vapor bands have been obtained with a self recording spectrograph using an effective slit width of 6A. The fine structure of the 1.13 and 1.45μ bands has been revealed for the first time and several lines have been added to the 1.38μ band. Forty lines appear in the 1.1μ region and eighty-five in the 1.4μ region. A comparison of these bands with similar ones due to atmospheric absorption in the solar spectrum identifies several superimposed solar lines. Regularities in frequency and intensity are lacking, due to the fact that a 6A slit is much too coarse to reveal the true structure of these bands.

2. Transmission of radiation through fog. S. HERBERT ANDERSON, *Signal Corps Laboratories.*—A laboratory method for the production of fog was developed in which the processes of formation of natural fogs were closely simulated. Transmission of radiation through this laboratory-made fog was measured for a range of wave-lengths from 3000A to 26,000A. A wide range of fog densities was used corresponding to natural fogs in which the visibility varies from 5 meters to 500 meters. A minimum transmission was found in the visible spectrum, the position of the minimum being a function of particle size. From λ_{min} to $\lambda = 26{,}000$A the transmission increased, likewise from λ_{min} to $\lambda = 3000$A. The transmissions obtained have been used to test King's equation $I = I_0 e^{-(a+b\lambda^{-4})}$. This equation if found *not* to hold for transmission of radiation through fog, contrary to the conclusion reached by Granath and Hulburt (Phys. Rev. **34,** 140, 1929). The discrepancy is probably due, (1) to the difference in particle size, (2) the width of the bands in the infra-red used by Granath and Hulburt, (3) to the absorption of water vapor, the effect of which was eliminated in this work but not in Granath and Hulburt's.

3. The absorption spectrum of blood and its relation to rickets. R. C. GIBBS, J. R. JOHNSON AND C. V. SHAPIRO, *Cornell University.*—The ultraviolet absorption spectra of solutions, obtained by haemolyzing the red blood cells of healthy and rachitic rats, have been found to be identical. This result is contrary to that reported by Suhrmann and his co-workers, Phys. Zeits. **30,** 959 (1929), whose curves for the two sets of animals show a difference in intensity, which increases in the direction of shorter wave-lengths. Calculations based on Rayleigh's law of light scattering indicate that this difference can be attributed to the presence of an excess of a disperse phase in the solution whose absorption is the more intense. Experimental verification of this hypothesis has been obtained by measuring the absorption of one of our solutions after it had been centrifuged to remove most of the suspended matter. The new curve so obtained is less intense than the original and the difference increases toward shorter wave-lengths, in close accordance with the Rayleigh law. This evidence points to a physical cause for the variation reported by Suhrmann and renders unnecessary his improbable assumption of a chemical change in the haemoglobin. The discrepancy between his results and ours may be accounted for by assuming either that there are two types of rickets, possibly brought on by different diets, or else that the variation reported by him, especially in view of its physical origin, is due to some cause, not necessarily associated with rickets.

4. Energy distribution in the lunar ultraviolet spectrum. BRIAN O'BRIEN AND E. DICKERMAN O'BRIEN, *Institute Optics, University of Rochester, N. Y.*—The energy distribution in the ultraviolet spectrum of sunlight reflected from the full moon has been measured from λ4400A to

λ3020A, by the method previously applied to direct sunlight. (Phys. Rev. **36**, 381 (1930)). Uniformity of slit illumination was secured by an astigmatic telephoto combination of quartz provided with rectangular stops, the measured spectral energy distribution being an average across a lunar diameter. Transmission coefficients and ozone content of the earth's atmosphere were obtained directly. The amount of ozone at night has been found to differ only slightly from the day values obtained on succeeding days in agreement with Chalonge and Götz (Gerl. Beit. z. Geophys. **24**, 20) (1929)). By comparison with direct sunlight the reflection coefficients for the moon's surface have been calculated throughout the above spectral region. No pronounced maxima or minima of reflecting power have been found within this range of wave-lengths. A test of some delicacy is thus provided, with negative results, for very small amounts of ozone (and hence oxygen) surrounding the moon.

5. Raman spectra of some organic halides. CLAUD EDWIN CLEETON AND R. T. DUFFORD, *The University of Missouri.*—Raman spectra obtained by helium excitation from nineteen organic compounds, several of which have not been studied previously, are reported and discussed. It has been found by one of the writers (C. E. C.) that in the cases of many simple organic halides the observed frequencies can be expressed as harmonics or combinations of four fundamentals (five in the cyclic compounds), two of which are not found in the Raman spectra, and are lower than predicted by any theory available, and hence may prove to be illusory; but the scheme does serve to point out certain regularities in these spectra. The bearing of such theory as is available is discussed.

6. Raman spectra and a slight asymmetry of the carbon and nitrogen atoms. R. T. DUFFORD, *The University of Missouri.*—The interpretation of the Raman spectra of the simpler organic halides and other related compounds is discussed; it is shown that most of the observed frequencies can be associated with vibrations of pairs or groups of atoms as predicted by theory, except that, in order to explain the multiplicity of certain lines, it seems necessary to assume a slight dissymmetry—i.e., a lack of equality of the valance bonds—of the carbon atom. Similar but less extensive evidence seems to indicate that the three valences of nitrogen are also not quite equally strong.

7. Vibrational quantum analysis of the ultraviolet SO_2 and CS_2 absorption bands. WILLIAM W. WATSON AND ALLAN E. PARKER, *Yale University.*—Analysis of spectrograms taken with a Hilger E-1 spectrograph shows that the SO_2 bands may be represented by the formula

$$\nu = 30586 + \{[381.1(v_1'+\tfrac{1}{2}) + 6.22(v_1'+\tfrac{1}{2})^2 - 0.223(v_1'+\tfrac{1}{2})^3] - [1381(v_1''+\tfrac{1}{2}) - 20(v_1''+\tfrac{1}{2})^2]\}$$
$$+ \{[436.7(v_2'+\tfrac{1}{2}) + 2.94(v_2'+\tfrac{1}{2})^2 - 0.199(v_2'+\tfrac{1}{2})^3] - [1157(v_2''+\tfrac{1}{2}) - 12.5\ (v_2''+\tfrac{1}{2})^2]\}$$

Noteworthy points are: positive quadratic term of the upper state levels, agreement with two of the fundamental frequencies determined by Raman and infrared analysis, no evidence for the 606 cm^{-1} deformation frequency, and the existence of various addition series as given by the double formula. Apparently a triplet electronic level is involved. High dispersion plates do not resolve the rotational fine structure. Most of the bands of the CS_2 system are given by

$$\nu = 28880 + 215(v_1'+\tfrac{1}{2}) - 802(v_1''+\tfrac{1}{2}) + 270(v_2'+\tfrac{1}{2}) - 1466(v_2''+\tfrac{1}{2})$$

the anharmonic coefficients being nearly negligible. There is slight evidence for a deformation frequency of 208 cm^{-1} in the ground state. Series of addition bands are found as for SO_2. The Raman frequency 655 cm^{-1} is the difference between the 1466 cm^{-1} and 802 cm^{-1} fundamental frequencies.

8. Paschen-Back effect and hyperfine structure in the spectrum of bismuth III. J. B. GREEN, *Ohio State University.*—A study of the spectrum of Bi in a field of 34000 gauss yields interesting data with respect to the hyperfine structure of Bi III. In particular, the line 4561, classified by McLennan as $^2P_{1/2}{}^2S_{1/2}$ gives 2.52 cm^{-1} for the ^2S separation, and 0.53 cm^{-1} for the $^2P_{1/2}$ separation. Several "forbidden" components appear on the plates. The line 3695, classified as $^2P_{3/2}{}^2S_{1/2}$ seems to indicate that the $^2P_{3/2}$ separation is much smaller.

9. Hyperfine structure in Bi II and Bi III. R. A. FISHER AND S. GOUDSMIT, *University of Michigan.*—The hyperfine structure of several lines in Bi II and III has been determined. The

results form a partial confirmation of the classification given by McLennan, McLay and Crawford (Proc. Roy. Soc. **A129,** 579 (1930)). It is possible to derive the hyperfine splitting for a number of levels. Together with the data on Bi I they form useful material for theoretical investigation. Bismuth is at present the only element for which hyperfine structure depending upon other than a single *s* electron is known for several levels.

10. Difficulties in the theory of hyperfine structure. S. GOUDSMIT, *University of Michigan.*—Sum rules and formulae for the hyperfine separations of the levels are derived for complicated configurations. The observed hyperfine structure of neutral and ionized bismuth, shows large deviations from the theoretical expressions. The nature of the discrepancies suggests that the present theory of the interaction between a single electron and nuclear spin is incomplete.

11. The theory of complex spectra II. E. U. CONDON AND G. H. SHORTLEY, *Princeton University.*—Formulas for the relations between the energies of multiplets arising from the same electron configuration for all two-electron configurations up to f^2 and several cases of three-electron configurations have been worked out following Slater's method. A systematic comparison of the known data with this first-order perturbation theory shows only rough agreement in most cases although in a few there is excellent agreement. The theory predicts the observed alternation in the relative position of singlet and triplet through *S*, *P*, *D*, *F*, etc. in the *pd* and *pf* triads and the *dd* and *df* pentads. For the d^2 configuration it was found that good fits are obtained except for the ^1S which theory indicates is much higher than the ^1S which spectroscopists assign to this configuration. The same is probably true for ^2S in d^2s.

12. The determination of heats of dissociation from predissociation spectra. LOUIS A. TURNER, *Princeton University.*—Two distinct types of predissociation spectra are known. In one the broadening of the lines begins suddenly at a definite wave-length, in the other it sets in gradually. Consideration of various possible relationships of potential energy curves suggests that the one or the other type occurs according to whether the curves for the two states concerned intersect below or above the energy of dissociation in the perturbing state, respectively. Accurate values of heats of dissociation can be obtained only from predissociation spectra of the first type. The others give merely upper limits. A predissociation of each kind is observed in the spectrum of NO_2 and the numerical relationships are in accord with the theory.

13. The inverse-cube central force field in quantum mechanics. G. H. SHORTLEY, *Princeton University.*—The problem of the motion of a particle in an inverse-cube central force field is fully treated by quantum mechanics and the results compared with the classical theory. Taking the effective radial potential energy as $(M^2/2\mu - S)/r^2$, one gets good correspondences between the quantum mechanical and classical solutions except for *S* between $l(l+1)\,h^2/8\pi^2\mu$ and $(l+\frac{1}{2})^2h^2/8\pi^2\mu$, where one gets a peculiar absence of oscillations in the ψ-function near the origin and somewhat poor agreements in regard to the radial probability functions. This is interesting in view of the uncertainty as to which value to compare with the classical angular momentum. However, the correspondence in allowed energies is complete only if the value $l(l+1)$ is taken. Solutions are found corresponding to the six classical types of orbits, with no quantization whatever. The solutions involve Bessel functions of both real and imaginary order with both real and imaginary arguments.

14. van der Waals' forces of helium and the stability of a small energy helium molecule. HENRY MARGENAU. *Yale University.*—Hopfield (Astrophys. J. LXXII, 133 (1930)) has recently postulated the existence of a He molecule of very low energy of binding. Theoretical evidence for the existence of such a molecule will here be given. The work consists of two parts. (1) A general method is outlined by which van der Waals' forces can be calculated without the knowledge of wave functions. Main features are: The expression for the interaction energy of 2 atoms in their lowest state is written in terms of the dispersion *f*-values, which are shown to be derivable with good approximation, by the aid of the "Summensatz" of Thomas and Kuhn, from the relative intensities of the resonance lines and the polarizability. The method is applicable to atoms (and molecules) more complex than He. Results for He:

$$\Delta_2 E = 11.58/R^6 \times 10^{-61} \text{ ergs}, \quad R > R_0.$$

(2) From the potential energy curve given by this expression and $\Delta_2 E = +\infty$ for $R < R_0$, R_0 being taken as 2.33×10^{-8}cm, the vibrational states for the resulting molecule are computed. Results: Minimum of potential energy $= -10^{-14}$ ergs; the molecule has but one vibrational state of energy about 3.3×10^{-16} ergs $= 0.2$ millivolts, which is in qualitative agreement with Hopfield's predictions

15. Group theory and the electric circuit. NATHAN HOWITT, *Naval Research Laboratory Bellevue, D. C.* (*Introduced by Elias Klein*).—The paper shows that electrical networks consisting of inductances, resistances, and capacitances form a group with the impedance function as an absolute invariant. That is, to a given impedance function there corresponds an infinite number of networks, any one of which can be obtained from any other by a special linear transformation of the instantaneous mesh currents and charges of the network. In this manner one may arrive at the complete infinite set of networks equivalent to a given network of any number of meshes. This is done by writing down the three fundamental quadratic forms of the network. Then a linear affine transformation of the instantaneous mesh currents and charges of the network results in the formation of new quadratic forms, the matrices of the coefficients of which represent a member of the group, i.e., an equivalent network. Instead of performing the substitutions, the three matrix multiplications $C'AC$ are used, one for each quadratic form, where A represents the original matrix, C the transformation matrix, and C' its conjugate. It may be possible to extend this theory to include continuous systems where the quadratic forms become integrals or infinite series and one deals with infinite matrices and infinite transformations.

16. Magnetic lag at low flux densities. L. W. MCKEEHAN, *Yale University.*—Energy losses in alternating magnetization are often compared by assuming that H and B vary sinusoidally, B lagging by an angle ϵ. At low flux densities ϵ is not fully accounted for by calculated eddy current and hysteresis terms if each branch of the hysteresis loop is assumed parabolic with least slope equal to that at the origin of the normal magnetization curve. The residue, ϵ_n, is a true magnetic lag. No explanation for it has hitherto been offered. It is now pointed out that Barkhausen discontinuities involve a magnetic lag which may suffice to explain the existence of ϵ_n. For example, 600 equal discontinuities per half cycle would suffice if $\epsilon_n = 10^{-3}$. The necessary mean magnitude of these discontinuities is improbably great unless it is principally strained regions which are affected by weak applied fields. If Jordan, Zeits. f. techn. Physik **11**, 2–8 (1930), is right in supposing that ϵ_n is independent of H_{max} over the small range in which it can be measured with any precision, the average magnitude of the discontinuities would have to vary directly with H_{max} throughout this range. This is not inconsistent with the parabolic form of (smoothed) magnetization curves at low flux densities.

17. Ferromagnetism of dilute solid solutions. FRANCIS BITTER, *Westinghouse Elec. & Mfg. Co., East Pittsburgh.*—Since the atoms of the solvent are known to move about in the solute it is possible to consider annealed and aged solutions as systems in thermodynamic equilibrium. It is shown that the strains set up by the atoms of solvent in the solute do not produce long range forces. There are, then, no long range repulsive forces tending to produce a microscopically uniform distribution. Under these circumstances the fluctuations in density of the solute will be at least as large as those in a perfect gas, and may become much larger (as large as those giving rise to opalescence, for instance). Local concentrations or rarifications of impurities may play an important part in determining magnetic properties through the inhomogeneities and strains they set up. For instance, in the iron-carbon diagram, the observed magnetic transformation of Austenite at 770°C would necessitate a drastic revision of ideas about ferromagnetisms if it were granted that Austenite is a solid solution of carbon in γ-iron. If, however, it is assumed that Austenite contains small inclusions of α-iron where there are local rarifications of carbon concentration, the difficulty disappears. Whether Austenite contains α-iron at 770°C should be determined by x-ray investigations. It is further suggested that the magnetic properties of dilute solutions of ferromagnetic substances in other metals are largely determined by local concentrations of ferromagnetic atoms.

18. Capillary rise in sands of uniform spherical grains. W. O. SMITH, PAUL D. FOOTE, AND P. F. BUSANG, *Gulf Research Laboratory, Pittsburgh.*—Uniform spheres packed in regular

array form a non-cylindrical cyclic capillary, characterized by a maximum and minimum capillary rise with intermediate positions of possible equilibrium. In practice spheres may be packed to a variety of porosities P thus requiring a mixture of regular and irregular piling arranged in a very distorted pattern. However the meniscus is also distorted to conform in a general way with the distortions of the lattice. Accordingly positions of maximum and minimum rise may be expected. The meniscus for maximum rise tends to pass through the plane of centers of neighboring spheres. Slight deviations from this condition due to the rise at sphere contacts are shown to be of minor importance. Any piling may be treated statistically as a hexagonal array with a spacing $2r+d$ where d is computed to give the observed porosity. In such a system three types of cell occur with a definite frequency, and these cell types are assumed present in the meniscus with the same frequency distribution. Hence it is possible to evaluate $pr/a=\rho ghr/\sigma$ where p=perimeter, r=grain radius, a=area of pore opening, g=accelation of gravity, σ=surface tension, ρ=density and h=capillary rise. The final formula so derived reduces to

$$\frac{pr}{a}=\frac{\rho ghr}{\sigma}=\frac{2}{\frac{0.9590}{(1-P)^{2/3}}-1}$$

This agreed with experiments made with several sizes of grains, porosities, and liquids. The minimum rises were also determined but a satisfactory interpretation in terms of a model has not been effected.

19. The variation of the thermal boundary layer of a miniature airfoil. MERIT SCOTT, *Guggenheim Research Physicist, Cornell University.*—By mounting thin, narrow conducting strips parallel to the span of an airfoil, and flush with its surface, it is possible, experimentally, to measure a thermal dissipation coefficient, p_c, associated with a particular location on the lifting surface, as well as its variation with velocity and angle of attack, α. Such measurements have been accomplished with a velocity range of 12 to 24 m/sec and for angles of attack varying from $-40°$ to $+35°$. It is found that p_c, independent of position on the surface, is a linear function of the velocity at the strip. Curves, showing its variation with angle of attack, present definite maxima and minima, characteristics which bear no direct correspondence to the velocity at the strip. It was to be expected that the variation of p_c, at a given location, with angle of attack would be of the same character as its variation with position along the chord. This is experimentally verified. Theoretical considerations suggest converting this coefficient to boundary layer thickness, B, and interpreting this thickness as identical with the viscous boundary layer. The measurements have been extended over the wide range of angle of attack so that the relation of these quantities to the useful range of the airfoil might be studied.

20. The variation of C_p of oxygen and nitrogen with pressure at 26° and 60°C. E. J. WORKMAN, *National Research Fellow, Bartol Research Foundation.*—By the use of improved apparatus of the type previously described by the author (Phys. Rev. **36**, 1083 (1930)) the ratio of C_p at a pressure p to C_p for the same gas at a pressure of one atmosphere is determined. Oxygen and nitrogen gas have been studied at 20 and 60°C in the pressure range 10 to 130 Kg per cm². Values of the ratio as measured may be inferred from smooth curves drawn through the points plotted from the data in the table below, where the pressure is given in Kg/cm².

Oxygen, 26°C		Oxygen, 60°C		Nitrogen, 26°C		Nitrogen, 60°C	
Pressure Kg/cm²	Ratio $C_p's$	Pressure Kg/cm²	Ratio $C_p's$	Pressure Kg/cm²	Ratio $C_p's$	Pressure Kg/cm²	Ratio $C_p's$
1	1	1	1	1	1	1	1
30	1.052⁰	30	1.035⁵	30	1.044³	30	1.032⁴
60	1.106⁵	60	1.076⁸	60	1.090⁰	60	1.066⁵
90	1.163⁵	90	1.116³	90	1.133²	90	1.099⁰
130	1.241⁰	130	1.168⁰	130	1.186³	130	1.139⁰

21. Some Physiological Effects of Light. BRIAN O'BRIEN, *Institute of Applied Optics, University of Rochester.* Invited paper

22. The Spectra and Anti-Rachitic Potency of Various "Therapeutic" Lamps. HARVEY B. LEMON, *University of Chicago.* Invited paper.

23. Methods of Measuring Radiant Energy. HAROLD W. WEBB, *Columbia University* Invited paper.

24. X-ray measurements of the elastic deformation of metals. WILLIAM P. JESSE, *The General Electric Company.*—The metal wire to be tested lies along the axis of a precision x-ray camera. A series of photographs is taken with various loads on the wire. On the photograph only the lines are measured where the resolving power is a maximum, i.e., where the incident angle θ is almost 90°. As the load on the wire increases, these high order lines shift in the direction indicating smaller grating spaces. This shift measures the contraction of the crystal lattice in a direction perpendicular to the direction of stress. For duralumin wire this contraction is in approximate agreement with the value calculated from the macroscopic Young's modulus and Poisson's ratio for the material. Similar results have been obtained with steel piano wire.

25. A new x-ray tube based on the "transparent target" principle. DIMITRY E. OLSHEVSKY. *Yale University.*—A new "transparent target" x-ray tube is described in which the portion of x-rays transmitted through the target is utilized. It is found that by using a properly designed, thick, double layer target in contradistinction to the thin single layer targets used by Owen and by Coolidge satisfactory heat dissipation may be secured at comparatively little sacrifice due to absorption. The new tube has a target made of a thick layer of low atomic number metal, backing a thin layer of high atomic number metal, in thermal contact with the former. A simplified theory of heat dissipation from the cathode spot is developed and a table is given, showing merits of various target materials as functions of wave-length. Important advantages of the tube over the conventional Campbell-Swinton arrangement are: proximity of the cathode spot to the outer surface of the tube and the possibility of utilizing x-rays in the direction of the initial electron beam. As applied to crystallographic purposes, vertical beam models were built in which the first slit of the spectrograph is defined by a hole drilled in the body of the tube immediately behind the target. This arrangement permits higher intensities at the second slit on account of a shorter slit distance from the cathode spot. Both slits are made integral with the tube, the whole arrangement possessing complete symmetry around the vertical axis. This vertical design, with the beam directed upwards, complete shielding of the tube proper and high tension leads concealed in a grounded table, contributes to the safety and comfort of work and is valuable for x-ray studies involving the liquid state. Special tubes based upon the new principle may prove of value for medical purposes.

26. New K series x-ray lines. WILLIAM DUANE, *Harvard University.*—K series x-rays have been examined by means of a Bragg spectrometer, the Moseley photographic method being employed. The incident ray and that reflected by the crystal to the photographic plate through distances of 4725 mm passed through long metal tubes, exhausted of air in order to reduce the absorption. The K_β doublet lines of molybdenum ($\Delta\lambda = 0.00056$A), examined by photometric curves, appear separated 0.88 mm. No third line lies in the immediate neighborhood of the β doublet. Between the γ line and the short wave-length limit of the series appears a marked blackening that represents several lines close together. They are not in the position of a line reported by Leide. The new lines may be due to 0 electrons falling into the K level, but a better explanation is, perhaps, that the lines are produced by falls into the K level of conductivity electrons which may from time to time lie in outer atomic energy levels. Several photographs produced by long exposures show a fainter single line, roughly halfway between the β_2 and the γ lines. It does not correspond to a known x-ray line of any chemical element reflected in the first or second order.

27. Electron diffraction by a silver crystal. H. E. FARNSWORTH, *Brown University.*—A previous investigation of electron diffraction by a copper crystal, for normal incidence on a (100) face (Phys. Rev. **35**, 1131 (1930)) revealed a series of weak beams requiring unit refractive

index, in addition to the more intense beams requiring refractive indexes greater than unity. These weak beams are in most cases so close in voltage to the main beams that they appear as components or satellites of them. A similar series of measurements for two silver crystals shows, in general, the same to be true for silver, although certain beams have more complex structures containing additional components. In many cases the different components are extraordinarily sharp and intense. These results for low-velocity electrons suggest a complex variation of the inner potential near the surface of the metal.

28. Radiation from low speed electron bombardment of metals. F. L. MOHLER AND C. BOECKNER, *Bureau of Standards.*—A small probe surface at a positive potential in a discharge may draw a current of many amperes per cm² with the potential gradient limited to a thin sheath over the surface. Under such conditions a continuous spectrum is emitted by metal surfaces in caesium, potassium, and helium discharges. With a copper probe at 7 volts in caesium vapor, the intensity J remains of the same magnitude between 6200A and 2400A with a minimum at 5800 and a maximum at 3800. Below 4 volts the spectrum has a high frequency limit in this range (3000A for copper at 2.15 volts). On the assumption that this is analogous to a continuous x-ray spectrum, observed limits indicate work functions of 1.95 for Cu, 2.1 for Ag, 1.45 for W (all in caesium vapor). The absolute intensity (except for Ag) agrees within a factor of 2 with values computed from the theoretical equation for intensity of the continuous x-ray spectrum. Efficiency for Cu at 7 volts is estimated as 3×10^{-7}. Comparison with published data on photoelectric effect of radiation from electron bombardment of metals indicates that the magnitude of effects below 10 volts can be explained by this continuous spectrum.

29. The distribution of electricity near the surface of contact of two conductors. A. T. WATERMAN, *Yale University.*—Two dissimilar metals are postulated in contact along an infinite plane, and the equilibrium distribution of electricity is sought in a direction perpendicular to this plane on the basis of Sommerfeld's electron theory using Poisson's equation and the Boltzmann principle. The problem is solved under the assumptions that the potential and the electric intensity are continuous across the boundary, and that the P.D. between points in the two metals far from the boundary is equal to the contact P.D. In general, if the normal concentration of conducting electrons is assumed to be one per atom the electrons in both metals remain in the degenerate state, though their concentration may vary from normal by 30 to 50 percent at the boundary. In this case the distribution is unaffected by temperature. In this special case of a pair of metals with high contact P.D., such as Cs and W, the electrons near the boundary in the more electropositive metal are reduced to the classical state and the distribution is a function of temperature. The possible bearing of these results upon the properties of thin metallic films is discussed.

30. An estimation of patch sizes on a thoriated tungsten filament. LEON B. LINFORD, *National Research Fellow, Princeton University.*—It is well known that coated filaments fail to follow Schottky's equation for thermionic emission in strong accelerating fields. Becker and Mueller (Phys. Rev. **31,** 341 (1928)) showed that the emission from thoriated tungsten is what would be expected if the surface fields were much larger than image fields at distances greater than 10^{-5} cm from the surface. These fields were confirmed by the author using the photoelectric method (Phys. Rev. **36,** 1100 (1930)). One explanation assumes that these large fields are due to a non-uniform surface distribution of positive ions. If these patches are assumed to be square and of dimension b, arranged checkerboard fashion with a contact potential difference V_0 between adjacent patches, the field above the center of a more positive area can be calculated. Using two values of the observed ion field the size of the patches was found to be about 2×10^{-4} cm, with about 0.5 volts contact potential difference V_0. The sum of the field produced by such a charge distribution and the image field was within experimental error of the observed field. From the surface field, and the threshold at a known accelerating field, the work function at zero field was found to be 2.7 volts or 1.8 volts less than that of pure tungsten.

31. Some thermionic properties of barium films absorbed on tungsten. HERBERT NELSON, *RCA Radiotron Company, Harrison, New Jersey* (*Introduced by G. R. Shaw*)—The activity and the change in contact potential difference have been studied as a function of the thickness of

the barium film. The velocity distribution of the electrons, the effect of non-uniformities in the film, and the effect of field intensity on the activity have also been studied. The experimental tube was constructed such that the measurements could be made on a small area of the filament in order that errors due to lead losses, non-uniformities, and voltage drop along the filament might be minimized. A vacuum tube electrometer was used in measuring the electron currents. The experimental results obtained by Eglin were confirmed, i.e., the activity of the composite surface was found to increase with the thickness of the barium film until an optimum thickness was reached after which further deposit caused the activity to decrease. A relation such as derived by Richardson was found to exist between the thermionic constants and the contact potential difference. The distribution of velocities of the emitted electrons were found to be Maxwellian for all thicknesses of the barium film. The presence of non-uniformities in the emitting surface had the effect of decreasing the slope of the Maxwellian distribution curve.

32. Time changes in oxide-coated filaments. E. F. LOWRY AND W. T. MILLIS, *Westinghouse Electric and Mfg. Co., East Pittsburgh.*—The oscillograph is made use of in studying time changes in the electron emission of oxide-coated filaments. The decay of emission with time while drawing current is compared with rate of recovery when instantaneous measurements are made. It is found that similar phenomena, though of much less magnitude, occur when thoriated tungsten or bariated filaments are used. It has also been found that this fading effect is not a universal characteristic of oxide filaments though it is present in greater or less amount in the majority of instances. Oscillograph methods have also been employed in studying oxide emission at normal operating temperature.

33. Grid current required by hot-cathode, grid controlled mercury arcs before discharge. W. B. NOTTINGHAM, *Bartol Research Foundation.*—The hot-cathode, grid-controlled mercury arc or "thyratron" has been described by A. W. Hull, (G. E. Rev. **32,** 213 and 390 (1929)). Although the thyratron has been called "an electrostatically controlled arc rectifier," a definite grid current is required in the grid or control circuit. With a d.c. plate potential, this grid current, before the discharge begins may have any value from 6×10^{-3} amp. to -10^{-7} amp. depending on the type of thyratron, the plate potential and the mercury condensation temperature. In certain cases, the temperature enters so drastically that a change in ambient temperature of only a few degrees can cause the thyratron to fail to operate. With 60 cycle a.c. plate and grid potentials, experiment seems to show that 0.001 second is required to set up conduction in the thyratron. A time lag of this amount was unexpected. A comparison of the "phase shift" and "critical potential" methods of controlling a thyratron with photoelectric currents showed that for extremely small light intensities, the critical potential method is the more sensitive, although for greater light intensities the phase-shift method is perhaps more reliable. Satisfactory operation using either method of control was obtained with 10^{-8} amp. photoelectric current (approx. 3×10^{-4} lumen). The measurements were made on General Electric FG-17; FG-27 and FG-67 thyratrons.

34. A further study of galvanoluminescence. ROY RICHARD SULLIVAN WITH R. T. DUFFORD, *Bell Telephone Laboratories and The University of Missouri.*—Previous work by one of the writers has been checked and extended in several directions. The glow surrounding aluminum anodes was studied in several new solutions, as well as those already described. Several-fold larger efficiencies have been obtained by using water-cooled electrodes. Study of the glow seems to be against the theory of a gas film covering the electrode; the spectrum of the glow is a typical luminescence spectrum, and the brightness and efficiency lie in the same range as for other luminescent reactions under study in this laboratory. In many cases, the law of increase of brightness with voltage seems to have closely the same form as for a tungsten filament. The spectrum of the sparkles which appear at higher voltages is, however, a bright-line spectrum; the two strongest lines coincide with the strongest lines in the spark spectrum of aluminum. The glow surrounding various metals in ether solutions of Grignard reagents and of $MgBr_2\cdot 2(C_2H_5)_2O$ has been studied, giving the highest efficiencies so far found in this type of luminescence. Systematic differences between chemical groups of metals are found. The work was done at the University of Missouri.

35. Intensities of the magnetic and electric illumination components in the electrodeless discharge. CHAS. T. KNIPP, *University of Illinois.*—Recent theory (J. T. Tykociner and J. Kunz, Chicago Meeting, American Physical Society, November 1930, paper No. 5) indicates that a considerable portion, perhaps even 80 or 90 percent of the illumination in the electrodeless discharge is due to the electrostatic field. A discharge vessel was constructed experimentally to test this point. Obstructions were set in it with the idea that each type of discharge would cast its own shadow. With the most favorable conditions for a discharge passing due wholly to the magnetic field, shadows were obtained in the plane of the exciting coil which extended one-third way around the tube, while there were no indications of shadows at right angles, i.e., in the direction of the electrostatic field. By placing a band conductor to the right and to the left of the medial line, and removing the energizing coil entirely, a powerful electrostatic field was produced and shadows in this direction were now readily obtained, but the characteristic ring discharge was gone. Hence it appears, when conditions are favorable for the formation of *ring discharges*, that the intensity of the attending illumination is in part, if not entirely, due to carriers moving in the plane of the energizing coil. This result seems to support the calculations of Sir J. J. Thomson.

36. High frequency behavior of a plasma. LEWI TONKS, *General Electric Company, Schenectady, N. Y.*—Earlier work on spontaneous short-wave oscillations in a low-pressure mercury arc plasma (Phys. Rev. **33,** 195 (1929)) has been extended to forced oscillations by experiments similar to those of H. Gutton (Ann. de Physique **13,** 62 (1930)). Theory gives $K=1-\nu_e^2/\nu^2$, where ν is the impressed, ν_e $(=8980\ (N_e)^{1/2})$ the plasma-electron frequency, for the specific inductive capacity of a plasma. The unit cube thus behaves like a tuned shunt circuit $C=1/4\pi$, $L=m_e/N_e e^2$. This disagrees with Gutton's conclusion. A modified Mossotti theory requires that a cylindrical plasma between plane condenser plates show shunt resonance when $\nu_e=(2)^{1/2}\nu$. With a constant impressed frequency, the positive column of a Hg arc always resonated at two values of arc current (ionization density) and sometimes at three, due possibly, to the non-uniformity of the plasma cross-section. The two main resonance densities were roughly in the ratio 2 to 5 and lay above and below the theoretical value. The variation with frequency was $\nu_e \propto \nu^{1.1}$ cf. $\nu^{1.0}$ theoretically. Above resonance $(\nu_e > (2)^{1/2}\nu)$ the variation of K with ν_e as given above was confirmed.

37. Oscillations and travelling striations in an argon discharge tube. T. C. CHOW, *Princeton University.* (*Introduced by* H. D. SMYTH).—Oscillations of audible frequencies in an argon discharge tube with a long positive column were observed in a pressure range 0.06 to 4.2 mm Hg. The amplitude of the fluctuation of voltage across discharge tube is of the order of magnitude of 10 volts. Only in a certain portion of that pressure range distinct travelling striations were observed. The flash frequency, defined as the number of striations passing across a certain cross-section per second was approximately equal to the frequency heard in a telephone receiver attached to the circuit. It was found to depend on conditions in the circuit, such as current, external resistance, inductance, capacity, and filament current. The space potentials in the tube were also found to fluctuate. Tonks and Langmuir have described a kind of electric sound waves, possible if a certain condition involving electron temperature and concentration and the wave-length of the sound waves is satisfied. This condition was satisfied in our experiment. From their expression for the velocity of electric sound waves and the experimentally determined flash frequencies a set of wave-lengths were calculated most of which are integral or half-integral multiples of the length of the discharge tube.

38. The fall of potential in condensed discharges. J. C. STREET, *University of Virginia.*—The fall of potential in the initial stages of discharges has been studied by utilizing the well-known fact that an electric pulse on a wire when reflected from an open end of the wire has its maximum potential doubled at reflection, provided the length of the pulse is not greater than twice that of the wire. Transient electric pulses produced by the condensed discharge under investigation traveled along two parallel, symmetrical, straight wires to their open ends where they were reflected. The maximum potential across the open ends was measured as a function of the length of wire from the spark gap by two independent methods and was found to de-

crease when the lead wires became a few meters in length. From this curve the rate of potential fall can be obtained directly by electric circuit theory. In the case of static sparks at atmospheric pressure, where the potential was slowly applied, a comparatively slow fall of potential (6% in 2×10^{-8} sec.) was obtained at the beginning, but a very rapid (94% to $1/e$ of value in 2×10^{-8} sec.) fall later. This result is in fair agreement with the results obtained by Rogowski and Klemperer (Archiv. f. Electrot. **24,** 127 (1930)) using a different method. When the pressure in the spark gap was decreased the rate of fall of potential in the initial stages was decreased. The method gives an easy way of studying the fall of potential in various kinds of discharges and is free from certain objections inherent in other methods. Such measurements, aside from giving information concerning the electrical breakdown itself, are desirable for a complete understanding of the operation of Kerr cells and cathode-ray oscillographs.

39. The Kerr electro-optical effect in gases. E. C. STEVENSON AND J. W. BEAMS, *University of Virginia.*—The electric double refraction or Kerr electrooptical effect in CO_2 has been studied as a function of the density and the temperature. The method previously reported (Phys. Rev. **35,** 1440 (1930) and O.S.A. program Oct. 31, 1930) has been refined so that the temperature of the Kerr cell can be set and maintained to 0.05°C. The average deviation of the Kerr constant per molecule was found to be less than 2 percent throughout the density range from 0.08 to 0.18 grams per cubic centimeter when the temperature, electric field, and wave-length band (4700A to 4300A) were kept constant. Holding the density, electric field and wave-length fixed the Kerr constant per molecule was observed to increase with decreasing temperature. Our preliminary results show that this increase was approximately 10 percent for a temperature change from 45°C to 20°C which is in rough agreement with what might be expected from theory.

40. On the correlation of radio reception with the position of the Moon in the observer's sky. HARLAN T. STETSON, *Ohio Wesleyan University.*—Observations of the intensities of radio reception at the Perkins Observatory and elsewhere have been utilized for a study of correlation of signal strengths with cosmic phenomena. Papers already published by the writer and by Greenleaf W. Pickard call attention to apparent change in the altitude of the Kennelly-Heaviside layer with the change in solar activity. The same data have now been utilized in an investigation of the possible relation between the intensity of signal strength and the position of the moon with respect to the observer, on the assumption that the moon is at a different electrical potential from that of the earth. The result of the observations indicates that the height of the Kennelly-Heaviside layer is substantially decreased by the presence of the moon above the horizon, and elevated as the moon passes underneath the observer. A plausible explanation follows on the assumption that the moon is negatively charged with respect to the earth. The form of the curve showing correlation between the moon's altitude and the intensity of radio reception suggests an electronic tide which follows a hypothetical equipotential surface in the electrostatic field of the earth-moon system.

41. Optical dispersion of helium. HENRY MARGENAU, *Yale University.*—The numbers of dispersion electrons (f-values) for helium calculated from Hopfield's intensity data by the semi-empirical method outlined in the author's first paper in this bulletin are used to construct an optical dispersion formula. Attention is to be called to the fact that transition matrices, computed from intensities of emission lines, are subject to considerable error. Nevertheless, the dispersion formula thus obtained, in which none of the constants are adjusted in the usual fashion, shows satisfactory agreement with the experimental data on the refractive index.—The theory of molecular forces is extended to a calculation of dissociation potentials and vibrational levels of the molecules Hg-rare gas, observed by Oldenberg.

42. Intensities in the ultraviolet spectrum of mercury. E. D. MCALISTER, *Division of Radiation and Organisms, Smithsonian Institution.*—The intensities of the major spectral lines in the region 2000 to 4000A from a mercury vacuum arc have been measured. A quartz double monochrometer and vacuum thermocouple were employed. The effective slit width was 2A

at 2100A increasing to 12A at 4000A. The 2537 line gave a deflection of 50 mm with a 4A slit width. The intensities of the first four "sharp" triplets are quite close to the theoretical 1–3–5 rule.

43. Application of spinor analysis to the Maxwell and Dirac equations. OTTO LAPORTE AND GEORGE E. UHLENBECK, *University of Michigan.* With the spinor analysis developed by B. Van der Waerden (Gött. Nach. 1929, p. 100), which comprises all representations of the Lorentz group, even those not contained in ordinary tensor calculus, one is able to write all derivations and equations in an *automatically covariant form.* For the convenient translation into spinor language of Maxwell equations, it becomes important to introduce three self dual tensors, one representing the electromagnetic field, one corresponding go the Hertzian vector, and one representing a kind of current potential. These correspond to symmetric spinors of the 2nd rank. Many spinor equations thus become simpler than the corresponding tensorial equations, especially the expression for the stress energy tensor. From the 1st order Dirac equations in spinor form, as given by v.d. Waerden, we derived the 2nd order equations, which agree with the Gordon-Klein form but for a correction term which again contains the self dual field tensor. Further the expression for the current was obtained, and its decomposition into conduction and polarization currents, and finally both Maxwell and Dirac equations were derived from a spinorial variation principle, analogous to the results of Gordon and Darwin.

44. Stereoscopic three dimensional models showing the electron's motion in the Stark effect. R. W. WOOD, *Johns Hopkins University.* By means of multiple exposures with a stereoscopic camera of a rotating wire frame representing the curved quadrangle formed by the intersection of the parabolic coordinates of the Epstein-Schwarzchild treatment of the Stark effect, within which quadrangle the electron is progressively advanced along a properly curved wire, the orbital motion within the anchor-ring is very clearly brought out. The pictures when viewed with a stereoscope show the anchor-ring as a wire cage within which the precessing orbit appears as a white dotted line. The change in orientation and eccentricity of the orbit, with the constancy of the distance of the electric center from the YZ plane (field parallel to X) are easily seen. Photographs are shown illustrating various assignments of the quantum numbers n_1 and n_2.

45. Improved technique for Raman effect. R. W. WOOD, *Johns Hopkins University.*—For excitation by the mercury arc I find that the highest efficiency is obtained with a Hanovia quartz arc (220 volts) in a metal housing with a narrow rectangular aperture just over the horizontal burner. After much experimenting with filters, I have found that two only are needed, except in special cases. A solution is made of about 1.5 grams of suphate of quinine in 500 cc of water, acidulated with a little sulphuric acid. This is contained in a glass tube 2 inches in diameter and 12 inches in length which acts as a cylindrical lens, when mounted just above the burner. Photochemical change can be nearly prevented by a thin sheet of Corning noviol glass, transparent to 4046A and opaque to 3650A. The yellowing of the quinine is due almost entirely to the 3650 group of lines. A space of about 1 cm is left between the noviol plate and the aperture in the lamp housing for a stray draught of air from a fan. A concave reflector of polished aluminum is placed over the tube containing the liquid under investigation, which is mounted above and in contact with the filter tube. This arrangement is two or three times as efficient as any arrangement for absorbing 4046 by glass filters. The Zeiss filter, if heavy enough to reduce 4046 to one percent of its value, reduces 4358 to one third of its value. Quinine is perfectly transparent to 4358. For excitation by 4046, the 4358 line is removed by a solution of iodine in carbon tetrachloride. A saturated solution diluted to about 1:15 with CCl_4 will practically suppress 4358, when contained in a tube 1.75 inches in diameter. A 1:30 dilution will suppress all modified lines due to 4358, but the unmodified group comes out fairly strong. A 1:10 or even a 1:5 dilution can be used but with the latter concentration 4046 is considerably weakened. The iodine tube is used with the noviol glass plate below it. The cooling can be increased by mounting a flat plate in such a position as to concentrate the air draught into the gap between the top of the lamp and the noviol glass plate.

46. The masses of O^{17}. HAROLD C. UREY, *Columbia University.*—Blackett (Proc. Roy Soc. **107A,** 359) and Harkins and his co-workers (Zeits. f Physik **50,** 97; Phys. Rev. **35,** 809 (1930)) have given the velocities of the nuclei involved in the transmutation reaction $N^{14}+He^4 \rightarrow O^{17}+H^1$ and these together with the rest masses of N^{14}, He^4 and H^1 of Aston permit a calculation of the rest mass of the O^{17} atom by assuming the conservation of mass and energy. The atomic weight of O^{17} calculated from 8 sets of data available varies from 17.00133 to 17.00502 ($O^{16}=16$). The absolute value is not certain to this number of significant figures since Aston's values are not so certain but the uncertainty due to the probable errors in the rest masses of N^{14}, He^4 and H^1 is the same for all 8 cases and the differences must be accounted for in some other way. The discrepancies are far greater than the probable errors in Blackett's measurements. The most probable reason for them appears to be that O^{17} atoms with different masses and energies are produced and that the different values are due to different energy levels of the O^{17} nucleus. Then, the gram atomic rest mass of the O^{17} atom in the normal nuclear state is equal to or less than $17.00133 \pm \backsim 0.0028$, i.e. the smallest value observed.

47. Regularities in an emission spectrum of CO_2. H. D. SMYTH AND T. C. CHOW, *Princeton University.*—About a year ago Smyth and Arnott did some work on the excitation of the band spectrum of nitrogen by an electron beam. The method used seemed to offer two advantages for the study of the spectra of polyatomic gases, namely small chance for dissociation and a somewhat simplified spectrum. The method has been applied to CO_2 and spectra obtained showing hardly a trace of CO bands. The spectrum obtained is nearly identical with that measured by Fox, Duffendack and Barker. With their data, supplemented by preliminary measurements of our own plates, we have found a divergent set of 14 vibration terms given by $\nu = 1101.7n + 1.7n^2$ taking the lowest as zero. These combine with three higher doublet terms which are probably part of another vibration set and appear to converge strongly. Referred to the lowest of the first set as zero they are, taking the lower of each pair, 31,953.1, 34,833.0 and 37,455.1 wave-number units. The upper member is 167 wave-numbers higher in each case. Though it is impossible to be certain which is the higher and which the lower of these two sets of levels, either choice gives one set of levels divergent over the range studied.

48. Absorption of iodine lines by atoms from optically dissociated molecules. LOUIS A. TURNER AND E. W. SAMSON, *Princeton University.*—Great improvement over former results (Phys. Rev. **31,** 983 (1928)) has been obtained by use of (1) a vacuum spectrograph, (2) argon at 5 cm pressure in the absorption cell, to retard diffusion of atoms to the walls, (3) a source giving fine unreversed lines (pressure 0.003 mm, excitation by short wave oscillator, outside electrodes). The absorption cell contained I_2 at a pressure of 0.03 mm and was illuminated by full light from a 13 ampere carbon arc. The only three lines in the region investigated ($\lambda > 1630$) which result from combination with the $^2P_{1\frac{1}{2}}$ ground term, viz. 1830, 1782, and 1642 are all strongly absorbed upon illumination of the absorption cell. Six others from combination with $^2P_{\frac{1}{2}}$ are not absorbed.

49. Hyperfine structure in the copper spectrum. A. G. SHENSTONE, *Princeton University*—As a result of recent observations of hyperfine structure in the copper spectrum, it can be stated that the nuclear moment is almost certainly $1\frac{1}{2}$. Several lines for which the upper state is d^9s, $s^4\ D_{2\frac{1}{2}}$ have four rather widely spaced components and all other lines from that level are wide, though unresolved by the apparatus available. The term d^9s, $s^4\ D_{\frac{1}{2}}$ has two components. Lines due to the other two members of this term do not appear in the source at all. This is probably due to the Auger effect; and, if so, it is the first observation of that effect in an atomic spectrum. Back's observation of the resonance lines and Wali-Mohammad's observation of the $d^9s^2\ ^2D_{1\frac{1}{2}}$ lines can be reconciled with the nuclear moment $1\frac{1}{2}$. Silver shows no hyperfine structure.

AUTHOR INDEX

Anderson, S. Herbert—No. 2

Beams, J. W.—see Stevenson
Bitter, Francis—No. 17
Boeckner, C.—see Mohler
Busang, P. F.—see Smith

Chow, T. C.—see Smyth
——— No. 37
Cleeton, Claud E. and R. T. Dufford—No. 5
Condon, E. U. and G. H. Shortley—No. 11

Duane, William—No. 26
Dufford, R. T.—see Sullivan
——— see Cleeton
——— No. 6

Farnsworth, H. E.—No. 27
Fisher, R. A. and S. Goudsmit—No. 9
Foote, Paul D.—see Smith

Gibbs, R. C., J. R. Johnson and C. V. Shapiro—No. 3
Goudsmit, S.—No. 10
——— see Fisher
Green, J. B.—No. 8

Howitt, Nathan—No. 15

Jesse, William P.—No. 24
Johnson, J. R.—see Gibbs

Knipp, Charles T.—No. 35

Laporte, Otto and George E. Uhlenbeck—No. 43
Lemon, Harvey B.—No. 22
Linford, Leon B.—No. 30
Lowry, E. F. and W. T. Millis—No. 43

McAlister, E. D.—No. 42
——— and H. J. Unger—No. 1
McKeehan, L. W.—No. 16
Margenau, Henry—No. 14, 1
Miller, W. T.—see Lowry
Mohler, F. S. and C. Boeckner—No. 28

Nelson, Herbert—No. 31
Nottingham, W. B.—No. 33

O'Brien, Brian—No. 21
———**and E. Dickerman O'Brien**—No. 4
Olshevysky, Dimitry E.—No. 25

Parker, Allan E.—see Watson

Samson, E. W.—see Turner
Scott, Merit—No. 19
Shapiro, C. V.—see Gibbs
Shenstone, A. G.—No. 49
Shortley, G. H.—see Condon
——— No. 13
Smith, W. O., Paul D. Foote and P. F. Busang—No. 18
Smyth, H. D. and T. C. Chow—No. 47
Stetson, Harlan T.—No. 40
Stevenson, E. C. and J. W. Beams—No. 39
Street, J. C.—No. 38
Sullivan, Roy R. and R. T. Dufford—No. 34

Tonks, Lewi—No. 36
Turner, Louis A.—No. 12
——— **and E. W. Samson**—No. 48

Uhlenbeck, George E.—see Laporte
Unger, H. J.—see McAlister
Urey, Harold C.—No. 46

Waterman, A. T.—No. 29
Watson, William W. and Allan E. Parker—No. 7
Webb, Harold W.—No. 23
Wood, R. W.—Nos. 44, 45
Workman, E. J.—No. 20